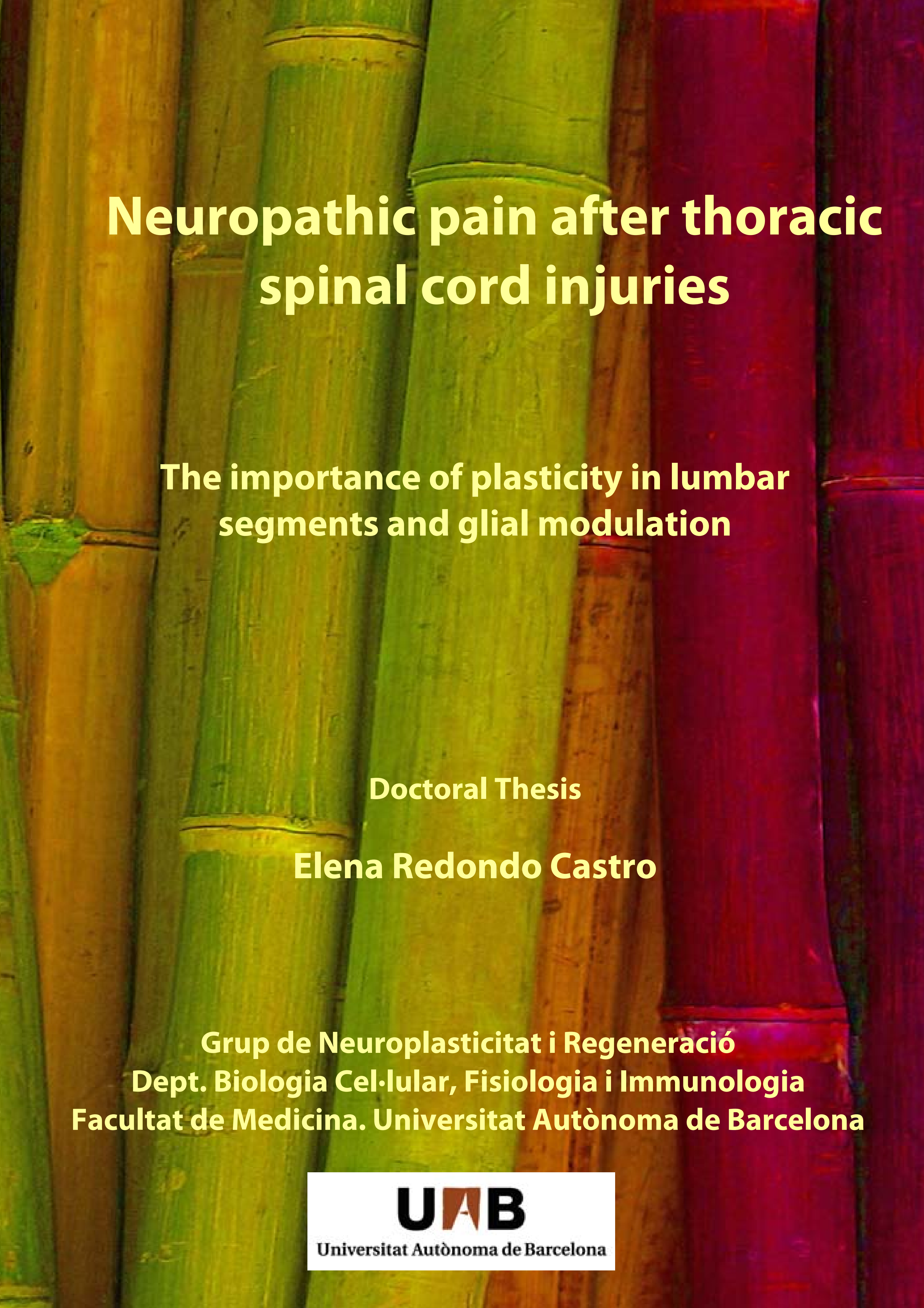

Neuropathic pain after thoracic spinal cord injuries

The importance of plasticity in lumbar segments and glial modulation

Doctoral Thesis

Elena Redondo Castro

Grup de Neuroplasticitat i Regeneració
Dept. Biologia Cel·lular, Fisiologia i Immunologia
Facultat de Medicina. Universitat Autònoma de Barcelona

UAB
Universitat Autònoma de Barcelona

Neuropathic pain after thoracic spinal cord injuries

The importance of plasticity in lumbar segments and glial modulation

Memòria de la Tesi Doctoral presentada per **Elena Redondo Castro** per a optar al grau de Doctora en Neurociències per la Universitat Autònoma de Barcelona.

Aquesta tesi doctoral ha estat realitzada dins el programa de Doctorat en Neurociències i sota la direcció del **Dr. Guillermo García Alías i el Dr. Xavier Navarro Acebes**.

Director de Tesi

Director de Tesi

Dr. Guillermo García Alías

Dr. Xavier Navarro Acebes

Doctoranda

Elena Redondo Castro

Bellaterra, gener del 2013.

Unitat de Fisiologia Mèdica. Departament de Biologia Cel·lular, Fisiologia i Immunologia. Facultat de Medicina.

Universitat Autònoma de Barcelona

Index

Page

Introduction

I – Anatomy of the spinal cord

The mammalian central nervous system is constituted by the brain and the spinal cord. Whereas the brain is localized inside the skull, the spinal cord is hosted inside the vertebral column. It starts at the foramen magnum, at the base of the skull, connected to the brainstem. It is protected by the spinal meninges and by the vertebrae, and ends at the first lumbar vertebra, although rootlets emanating from each segment continue down until reaching the correct exit point from the vertebral column. Along all its length, spinal nerves exit the spinal cord, constituting the dorsal and ventral roots (conveying sensory and motor information, respectively). In a transverse section of the spinal cord it can be distinguished the gray matter, with an H shape, and the white matter, surrounding it. The gray matter is mainly occupied by neuronal cell bodies and the white matter by axonal fibers traveling along the spinal cord (Fig.1).

Organization of the gray matter

The gray matter of the spinal cord is placed at the center, and is full of neuronal cell bodies, as well as other cell components. It is organized in several regions called laminae, classified by Rexed. Functionally it can be divided in the dorsal, medial and ventral horn, Whereas the dorsal interneurons are involved in sensory input, medial are related to autonomic functions and ventral are involved in modulating descending motor control. Below there is a brief description of each lamina (Zigmond et al., 1999; Afifi and Bergman, 2005; Purves et al., 2008; Anderson et al., 2009):

- **Laminae I and II** receive sensory information from nociceptors and convey this information to the thalamus and to deeper laminae. Projection neurons from small afferents in the anterolateral system arrive to lamina I, whilst interneurons receiving inputs from small diameter afferents are located in lamina II, where they integrate forward and feedback inputs related with pain transmission. These laminae are also known as marginal zone and substantia gelatinosa, respectively.
- **Laminae III and IV** are more related to the reception of tactile information. Neurons in this area receive contacts from Aβ fibers and from neurons in laminae IV, V and VI. They mainly

act as interneurons and propiospinal interneurons. From these areas, also known as nucleus propius, arise some ascending projections to the thalamus via the spinothalamic tract.

- **Lamina V** contains neurons that contact to outer laminae (II). It receives afferent inputs from Aβ and C axons, mainly in wide dynamic range neurons (WDR), which respond in front of noxious and innocuous stimuli with different firing patterns. In this lamina nociceptive information from the periphery and from the guts is also received. From this lamina projections arise to the thalamus and the brainstem through the spinothalamic tract. They also receive descending rubrospinal and corticospinal connections.
- **Lamina VI** is where proprioceptive connections coming from the muscle spindles arrive and where the spinocerebelar tract is originated. Descending brainstem connections are also received here. This lamina is especially large in the cervical and lumbar enlargements, and it contains numerous propiospinal interneurons, mainly related to the spinal reflex circuitry.
- **Lamina VII** is the intermediate area of the spinal cord, full of interneurons that communicate the dorsal and the ventral horn. Neurons placed in this area receive contacts from laminae II to VI and from visceral afferent fibers. These cells mainly act as relay points in the transmission of visceral information.
- **Lamina VIII**, in the ventral horn, receives vestibulospinal and reticulospinal descending fibers, and its motor interneurons modulate the motor activity through gamma-motoneurons, which innervate the intrafusal muscle fibers. Its size is reduced in the cervical and lumbar enlargements, since the motoneuron pools from lamina IX are larger there.
- **Lamina IX** is mainly occupied by columns of alfa motoneurons, as well as by smaller motoneurons (β and γ). It is especially large in the cervical and lumbar enlargements, since it hosts all the motoneurons responsible for limbs muscle control. The big alfa motoneurons launch their axons by the ventral roots to innervate the extrafusal fibers of skeletal muscle and the small gamma motoneurons innervate the intrafusal fibers.
- **Lamina X** is placed around the central canal and hosts neurons which project to the contralateral side of the spinal cord. It is also known as central gray matter.

Organization of the white matter

The white matter is composed by short and long axons, in addition to glial cells. It is organized in regions (dorsal, ventral and lateral) which allocate the ascending (sensory) and descending (motor) tracts, as well as some local pathways restricted to the spinal cord itself. A few differences are found between the tract organization of the spinal cord in different species ranging from rodents, cats, primates and humans. In fact, one of the major differences is the location of the corticospinal tract: while in humans is placed in the lateral and ventral funiculi, rats present an important dorsal component of the corticospinal tract (Anderson et al., 2009, Fig1).

The ascending tracts arise from primary neurons whose somas are in the dorsal root ganglia or from interneurons in the dorsal horn, and convey sensory information to higher areas of the central nervous system. Below there are described the most important tracts for this work, the dorsal columns and the spinothalamic tract. Apart from these, there are several other tracts, such as the spinoreticular, the spinomesencephalic, the spinoparabrachial, the spinohipothalamic, the spinocervical and the spinovestibular, and the spinocerebellar and cuneocerebellar tracts.

In the dorsal funiculus, the cuneatus and gracilis fasciculi conform the **dorsal columns** tracts, which transmit signals of touch, vibration and position. The dorsal columns contain the ascending central axons of primary afferents (direct dorsal column pathway) and also axons coming from postsynaptic dorsal column neurons (second order dorsal column pathway). The dorsal columns are somatotopically organized, with axons of the lower limb placed at the medial side and those from more rostral segments progressively placed more lateral.

The **spinothalamic tract (STT)**, placed in the lateral and ventrolateral regions brings nociception, temperature, pressure and gross touch information to the somatosensory region of the thalamus. The ventral STT transmits mainly crude touch and pressure sensation. The lateral STT is focused on transmitting pain and temperature information. While the dorsal part of the STT is more related to the discrimination and the conscious perception of pain, the ventrolateral tracts are more related to the gross information regarding pain. There is somatotopic organization of the axons, with the fibers entering from rostral segments being placed in the medial part of the tract, and the caudal segments in the lateral part.

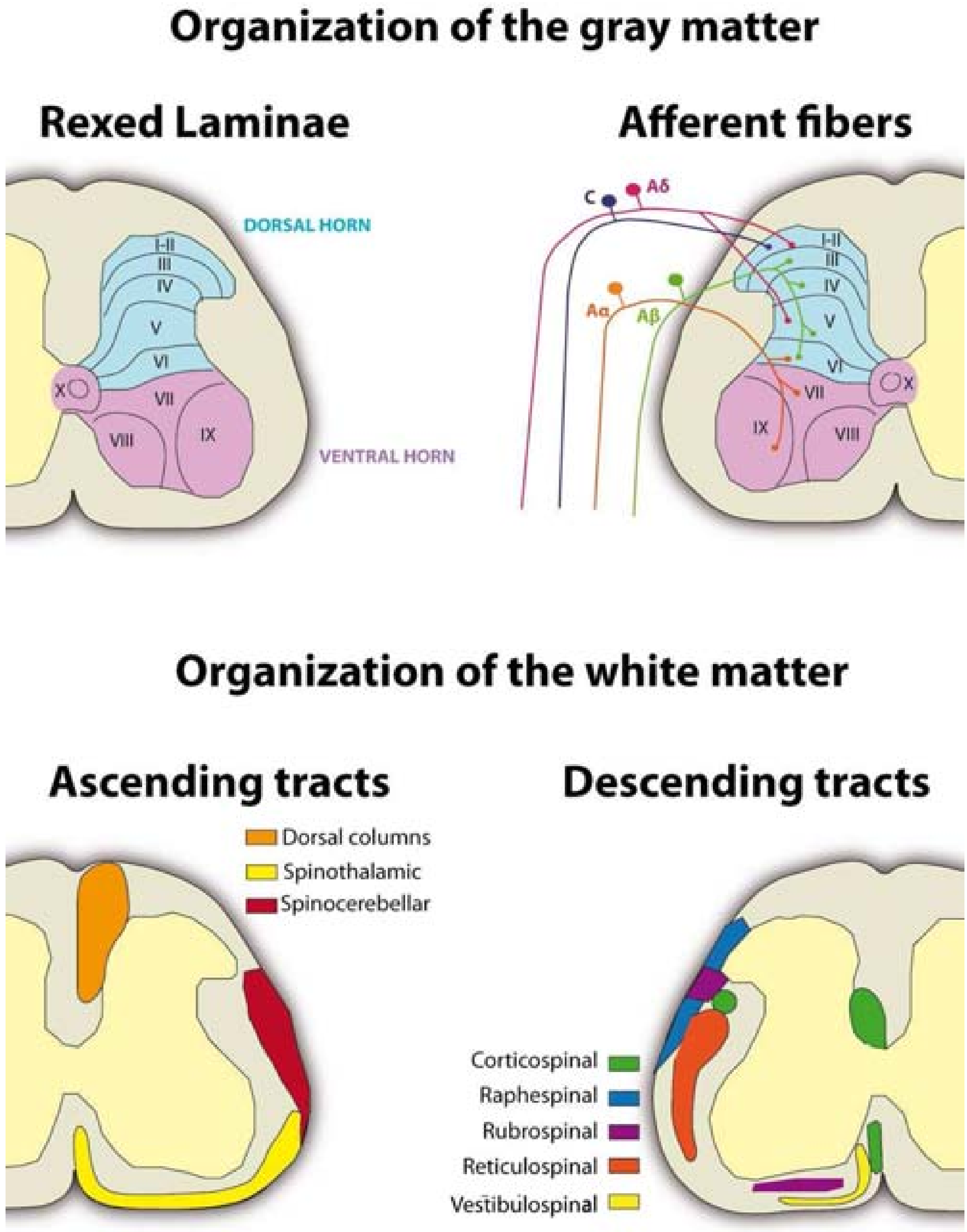

Fig. 1: Schematic diagram of the organization of the gray and white matter of the spinal cord.

The descending tracts arise from different structures in the cortex and the brainstem, and reach different areas of the spinal cord. Their main function is to control motor functions, such as posture, balance, muscular tone, locomotion and skilled movements. The main tracts are the corticospinal and the rubrospinal, in the dorsal funiculus (rat) or in the lateral funiculus (human), and convey information about conscious movement. The reticulospinal and vestibulospinal tracts (together with the ventral corticospinal tracts) mediate control of balance and posture.

The **corticospinal tract** (**CST**) is the most known from all the descending tracts, and its major bundle is placed in a dorsal position in rodents but not in humans, in which is placed in the lateral funiculus. This tract decussates at the pyramids of the medulla, and travels along the spinal cord until reaching intermediate and basal lamina of the dorsal horn (laminae III-VII) in most mammals, although some ending connections have been described in other laminae.

The **rubrospinal tract** influences general locomotion, but it is thought to play a cooperative role with corticospinal tract in many animals, thus adding the control of skilled motor tasks. It is also known that in case of injury in the CST, the rubrospinal tract could partially supply its function. Not all the rubrospinal fibers decussate, and some travel until reaching the motoneurons in lamina IX. In humans, the corticospinal and rubrospinal tracts merge in the **descending lateral system**, focused in controlling fine movements of the distal parts of the limbs.

On the other hand, the vestibulospinal, reticulospinal and tectospinal tracts constitute the **descending medial system**. In this system, neurons are placed in the brainstem and their axons travel in the medial part of the ventral funiculus. Their main functions are related to the control of posture and locomotion. The major function of the **reticulospinal tracts** is related to the preparation and modulation of some movements, as well as postural control and modulation of sensory and autonomic functions. The **vestibulospinal tracts** are supposed to initiate the coordinated activity in the limbs and the trunk in order to maintain postural control. The **raphespinal tract** has neuromodulatory effects on motor function, as well as modulatory effects in some autonomic functions and in the perception of pain. The **tectospinal tract** originates in the superior colicullus where inputs from the retina as well as somatosensory and auditory information are received. Its main function is to mediate reflex postural movements in response to visual and auditory stimuli.

Spinal circuits:

The spinal cord is something more that bundles of axons conveying ascending and descending information. Several circuits have already been described to be placed in concrete regions of the spinal cord, together with local interneuron circuits. Although circuits can be modulated by brain inputs, most can work independently of them. This explains why a decerebrated animal can, in certain circumstances, maintain some behaviours such as scratching, walking, breathing or swimming. Spinal networks are also responsible for posture control, tonus and reflexes.

One example is the locomotion circuit, orchestrated by the central pattern generators (CPGs) placed in the cervical and lumbar segments. They coordinate extensor and flexor muscles to generate rhythmic patterns of movements, and using the afferent inputs to adequate the gait to the environment. Spinal interneurons are usually involved, adding complexity and flexibility to the circuits (Edgerton et al., 2008). Some other functions, as reaching and grasping were thought to be organized only in the cortex, but recently it has been described also a spinal contribution (Alstermark and Isa, 2012). A network of spinal interneurons and motorneurons has also been described to be involved in respiratory functions in certain pathological conditions (Lane, 2011). All these circuits can function without the supraspinal inputs that normally modulate them, and for this reason, even injured spinal cords preserve some functionality below the injury site.

II - Spinal cord injury

A traumatic spinal cord injury (SCI) is a devastating and unexpected event that usually conditions the rest of the life of those who suffer it. The first spinal cord injuries were documented more than two thousand years ago, but it was not until 50 years ago that the prognosis and the life span of those who suffered it have really improved. Nowadays the treatments and the medical care has evolved, and patients present a life span very close to those without it, despite the loss of functionality below the lesion site, the appearance of secondary complications, and the consequent reduction in quality of life. Researchers and clinicians are working together in order to improve the present therapies to improve the quality of life of these patients as well as to reduce as much as possible the secondary deficits such as paralysis, spasticity, pain, sensory loss, and autonomic dysfunctions.

Epidemiological data about spinal cord injury

The most common causes of SCI are car accidents (50%) and fallings (20-30%), followed by work and sport accidents (4-11%), and violence injuries (1%). Less frequently, SCI can occur for medical causes such as tumors, vascular diseases and infections. The incidence is higher in young people (16-30 years), especially in men (4:1 ratio of male: female). Considering only the developed countries, SCIs present an incidence of 12 to 58 cases per million habitants, depending on the study.

In Spain there are each year around 800-1000 new cases, and it is calculated that around 25.000 people are living with a SCI. The incidence in Spain is around 24 injuries per million habitants and year, and it maintains the global ratio of male and females, as well as the main factors causing them (Herruzo-Cabrera et al., 1993). Regarding traumatic SCIs, a slow but constant decrease has been recorded in Spain in new cases of spinal cord traumas, presenting every year a mean decrease of 3.5%. In fact, the rate of new SCIs is lower in Spain than in other European countries.

SCIs represent a high economical cost, calculated in 2007 as more than 150 millions euros only for injuries derived from car crashes, and almost 400 millions for injuries caused by other factors, only in Spain. Some secondary costs are not included in these figures, such as additional medical care (ambulance and transport services, psychological and social attention, etc) and lavour costs regarding the loss of productivity, which enormously increase these numbers.

Consequences and classification of spinal cord injuries

When the spinal cord is damaged all its functions can be compromised below the lesion site. The usual consequences are total or partial loss of movement (tetraplegia or paraplegia), sensation (anesthesia or hypoesthesia), and autonomic deficits (sexual dysfunction, loss of control of the sphincters, etc). Despite the evident loss of sensation below the injury site, SCI usually course with pain, being this one of the most devastating symptoms, which severely affects the quality of life of the patient.

Different factors account for the magnitude of final deficits and consequences of a traumatic SCI, such as the level of the spinal cord, the severity (partial or complete), as well as the type of injury (contusion, compression, section …). The severity of the lesion is evaluated attending an international classification: *Standards for Neurological Classification of Spinal Cord Injury,* elaborated by the American Spinal Injury Association (ASIA) and the International Spinal Cord Society (ISCOS) (Marino et al., 2003). The neurological level is defined as the last unaffected segment (in sensory, motor and autonomic terms). This scale indicates the neurological level as well as if the lesion is complete or not (it is incomplete if there is still some partial preservation of function below the level site). In any case, due to the poor regenerative capacities of the adult central nervous system in mammals, most of the consequences are permanent.

Amongst traumatic SCIs, there are some different mechanical insults, such as contusion, compression, hemisection or complete transection. Although sharing many physiopathological mechanisms, these different lesions present some intrinsic features and therefore can produce deficits of different severity. The contusion injury is the most frequent and implies the contusion itself as well as secondary lesions such as the impact of fractured bones. This is the kind of lesion that most frequently occurs in car crashes (the most common cause of SCIs), and consequently is the one that presents more animal models trying to mimic their pathological features.

Physiopathology of traumatic spinal cord injuries: primary and secondary injury

There are several animal models reproducing features occurring after a SCI. Despite intrinsic differences, animal injury models are quite similar to human injuries, so they are a really useful research tool and will be further discussed in this thesis. Below the main features occurring after a contusive SCI are presented (Fig. 2):

- **Time course**

The events following a traumatic SCI are divided in two phases. The first is known as the **primary injury**, characterized by the mechanical trauma and the subsequent hemorrhage, edema, axonal and neuronal necrosis, as well as an important edema. This phase is located in the site where the impact has taken place, and is uncontrollable and unpredictable, since it depends on the trauma itself. In human injuries, it usually implies the fracture of bones and disk displacement within the spinal canal. Little can be done to reduce or modulate the events occurring in this phase. The initial trauma causes a transitory state called **spinal shock** in which all the spinal functions and reflexes are abolished. The main cause is the transient disruption of ionic homeostasis. Potassium ions shift from the intracellular to the extracellular space, provoking the interruption of the generation of action potentials. The spinal shock varies its duration depending on the species, and although most related to the primary injury, it prolongs with events occurring in the secondary injury phase.

From hours to days after the initial trauma, a range of secondary cellular and molecular events occur, constituting the **secondary injury**. In this phase, the lesion is not restricted to the injury site itself but tends to expand rostral and caudally to the lesion, increasing the affected area and the cell death of neurons and glial cells.

There are several physiopathological mechanisms acting simultaneously and usually forming synergies during the secondary phase, such as changes in the ion homeostasis and ion channels, changes in neurotransmitters and release of excitatory aminoacids, production of reactive species of oxygen, mitochondrial dysfunction, lipid peroxidation, and cell death. Despite being the main responsible for the deficits occurring after the injury, the secondary phase presents possibilities of modulation, so any therapy or treatment aimed at reducing any of its components may reduce also the negative consequences of the SCI.

- **Ischemia and vascular alterations**

The initial impact causes vascular disruption and hemorrhage, edema and thrombosis (Tator and Fehlings, 1991). In order to counteract this massive effect, several vasoactive factors are released, such as thromboxanes, leukotrienes, platelet aggregation factors, serotonin and endogenous opioids. These agents lead to hypoperfusion, hypoxia and hypoglycemia. In addition, there are also some problems regarding autoregulation, microcirculation and loss of neurogenic tone in the vessels. For all this reasons, after an SCI there is an important ischemia that specially affects the gray matter, since it normally receives more blood than the white matter. Although this situation is transitory, the reperfusion implies the production of reactive oxygen species, exacerbating the damage already caused by the ischemia. Moreover, the ischemia also leads to cell death, which acts as an initiator of signaling cascades that will eventually expand the area of tissue damage.

Problems regarding the normal blood supply cause a decrease in the supply of oxygen to the tissue. This anoxia increases the anabolic metabolism, leading to the production of acidic products such as lactic acid. These molecules reduce the pH of the injured tissue, and affect the ATP levels, which would eventually affect ion pumps and therefore ion homeostasis.

- **Excitotoxicity**

One of the consequences of the disruption of cell membranes, by the primary cell death and the ischemia, is the massive release of glutamate into the extracellular space, together with a global alteration of ion equilibrium. Increased concentrations of glutamate provoke persistent neuronal depolarization, which will lead to excitotoxic cell death. The initial activation of AMPA receptors is followed by the activation of sodium voltage-dependent channels, which results in sodium influx followed also by chloride influx and the entrance of water. NMDA receptors are also activated by the persistent presence of glutamate, leading to an excess of the calcium influx, which can stimulate several intracellular mechanisms that become detrimental for cell survival. Taken together, these changes produce osmotic cell lysis, as well as the consequent release of cell contents into the extracellular medium, therefore enhancing apoptotic and necrotic actions.

- **Oxidative stress**

After the SCI there is also an increase in the formation of free radicals and reactive oxygen species (ROS), in part secondary to the activation of glutamate mediated intracellular pathways. This activation leads to an increase in intracellular calcium, COX2 and prostaglandins synthesis, and obviously to the formation of ROS. These compounds are highly oxidizing and cause the oxidation of lipids, proteins and DNA, leading to metabolic dysfunction, as well as to neuronal and glial death. They can also enhance the already existent excitotoxicity by impairing glutamate uptake by astrocytes (Rao et al., 2003), as well as by modulating the action of several proteins and enzymes. Their action on lipid peroxidation also contributes to cell membrane disruption, contributing again to cell death and generation of more ROS; then promoting a positive feedback that can expand the secondary damage from the epicenter of the injury to rostral and caudal regions. Another source of ROS is provided by leukocytes that invade the spinal parenchyma after the SCI, as well as activated microglia and astrocytes. It has also been proposed that ROS contribute to hyperexcitability by mechanisms barely known, but that could include modulation of glial reactivity or second messenger systems (Hulsebosch et al., 2009).

- **Inflammation**

SCIs include an important inflammatory component, starting just after the injury, and involving both cellular and humoral components. After the initial trauma, neutrophils rapidly infiltrate into the tissue (Yang et al., 2004; Fleming et al., 2006), where they produce ROS and promote the release of lysosomal enzymes and phagocytosis. The damaged endothelial cells secrete proinflammatory cytokines such as IL-1 TNFα and IFNγ, contributing to the recruitment of blood and immune cells. During the first hour after the SCI, the resident microglia become activated and begin to proliferate. This population shifts to a more phagocytic phenotype, and starts to release proinflamatory cytokines in the area of the lesion, affecting neurons, astrocytes and other glial cells. Inflammatory signaling cascades promote the recruitment of more immune cells within the first hours, and contribute to extend tissue damage. Nevertheless, this inflammation has also a positive effect on cleaning the area of rests of dead cells and myelin debriss. Macrophages do this task, and can be detected within the injured spinal segments during the first week and until some months after the injury. Macrophages also produce inflammatory mediators such as cytokines, interleukins and prostaglandins that cause cell death, demyelination and the formation of ROS. Macrophages are also known to produce some neuroprotective molecules, and contribute to the restoration of the tissue functions after the injury.

Together with the inflammatory cells arriving to the injured area, resident glial cells also play an important role after the SCI. The microglial populations become reactive, proliferative and phagocytic after the lesion, and release inflammatory mediators. The astrocytes, the most abundant cells in the CNS, play an essential role in maintaining the homeostasis in the nervous tissue. A few hours after the SCI they become activated, and last in this state for months or even years. They are the main responsible of filling the empty spaces caused by cell death as well as to form the glial scar, and act as buffers of glutamate, in order to reduce their increased concentrations. Moreover, they secrete some proinflammatory cytokines (IL-1, IL-6, IL-10, MCP-1, TNF-α, etc.), contributing to the maintenance of the inflammatory process. Although the inflammatory response is necessary to heal the injured tissue, inflammation is one of the most detrimental features of the SCI, and a lot of efforts are being done to modulate its evolution.

- **Cavity formation and inhibitory environment**

One of the typical features of the spinal cord contusions is the formation of a cystic cavity in the epicenter, although it can be extended rostrally and caudally. This cavity is filled at the beginning with cellular debris, rests of injured axons, inflammatory cells and astrocytes, but it is progressively replaced by liquid as the immune cells scavenge the debris and the myelin. The cavity is tightly surrounded by reactive astrocytes and condroitin sulphate proteoglycans, although it can include also fibroblasts, microglial cells and oligodendrocytes. The glial scar is one element designated to limit the expansion of the lesion to the intact tissue, but it also constitutes an important barrier for the regeneration of the spared axons.

Together with the glial scar and the cavity, the presence of inhibitors of neuronal growth also difficults the regeneration of the neural elements after the SCI. The three more potent inhibitors are Nogo, myelin-associated glycoprotein (MAG) and oligodendrocyte myelin glycoprotein (OMgp), all of them associated to myelin.

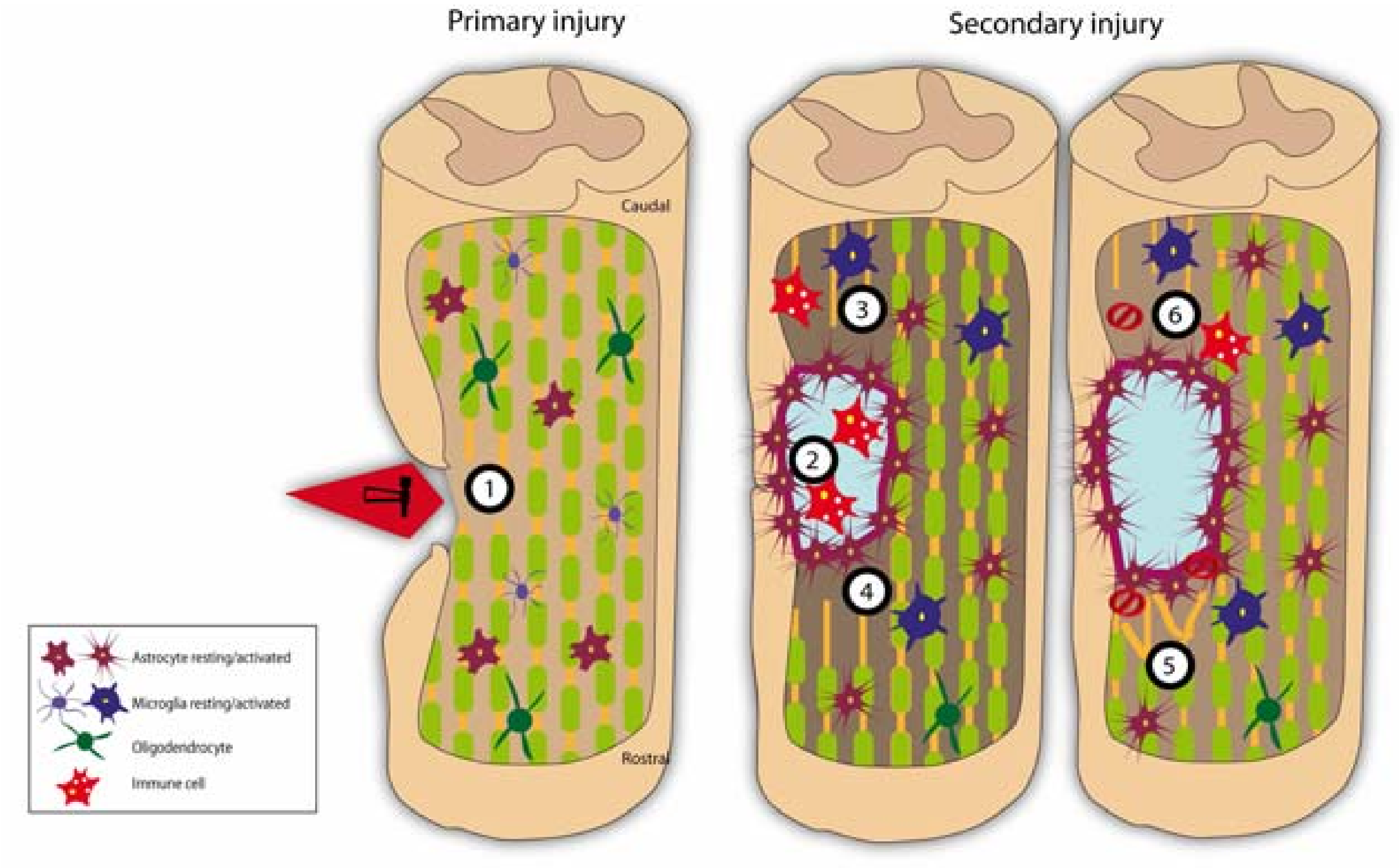

Fig. 2: Pathophysiology of a traumatic SCI: 1: Contusion; physical disruption of spinal tracts, cell death of neurons and oligodendrocytes; breakdown of the blood brain barrier. 2: Infiltration of immune cells to remove cell and myelin debriss, initial formation of a cavity surrounded by glial scar and full of death cells and immune cells. 3: Degeneration of caudal segments of the injured axons, as well as demyelination of axons partially alterated. Activation of glial populations and infiltration of inflamatory cells in the surrounding tissue. 4: Changes in ion concentrations, release of excitatory aminoacids and proinflammatory mediators. 5: Final stablishment of the cavity, and progressive normalization of aminoacid levels; spared axons can sprout. 6: The glial scar is full of inhibitory cues that difficult the regeneration across the injury site. Progressive reduction in glial reactivity and inflammation. Adapted from (Ronsyn et al., 2008)

III. Physiology of pain

Pain is a physiological experience, designed to alert us from potential damages to our body, so it has a clear protective role. When the pain circuits are correctly working they aware us from external (abnormal heating, pinch stimuli, etc) or internal stimuli (cardiac ischemia) that would potentially hurt the tissues. Ideally, the sensation we perceive should be unpleasant enough so it cannot be ignored, and the sensation should continue as long as the stimulus is present. Different types of "normal" pain can be distinguished depending on their origin and characteristics: acute (or pricking), chronic (or burning) and continuous or visceral.

The inflammatory pain is that pain related to inflammation affecting peripheral tissues that are supplied with nociceptive fibers. The neuropathic pain would be then that caused by a lesion or dysfunction in the central or peripheral nervous tissue. Although the neuropathic pain can be sometimes accompanied by inflammatory processes, it is important to distinguish the two kind of pain, since their processes and mechanisms can differ (Graeber and Christie, 2012)

Nociceptors and nociceptive fibers

There are two main types of nerve fibers conveying pain information: C fibers and Aδ fibers, (table 1). In both cases, the stimuli can come from the skin, muscle and joint tissues or certain visceral structures. They do not present a clear ending receptor structure, and are commonly identified as free nerve endings.

Aδ fibers are thinly myelinated, so they can conduct a *fast pain* signal, at 5-30 m/s. In this case, Aδ nociceptive fibers convey nociceptive information as well as information coming from intense mechanical or thermal stimulation. This fast pain has been reported as the *first pain*, the initial painful and sharp sensation just after the contact with the noxious stimuli (Fig.3).

C fibers are related with a *slow pain*, since these unmyelinated fibers conduct impulses at less than 2 m/s, normally regarding thermal, mechanical and chemical stimuli. Most act as **polimodal nociceptors**, although a proportion seems to be sensitive only to mechanical or thermal stimuli. This slow pain is also called *second pain,* and evokes a diffuse and long lasting painful sensation, more diffuse and prolonged than the pain evoked by the Aδ fibers.

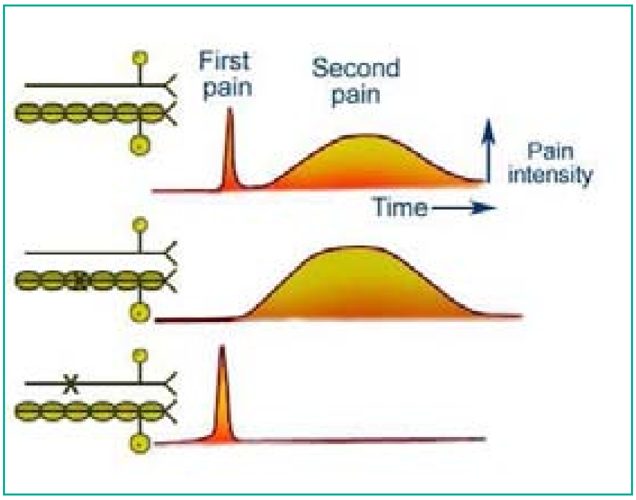

Fig 3: First and second pain are transmitted by myelinated and unmyelinated fibers, respectively.

Fiber	**Myelin**	**Diameter (µm)**	**Velocity (m/s)**	**Function**
Aα	Yes	13-20	80-120	Proprioception of skeletal muscle.
Aβ	Yes	6-12	35-75	Touch, mechanoreceptors.
Aδ	**Yes**	**1-5**	**5-30**	**Pain. mechanical and thermal stimulation.**
C	**no**	**0.2-1.5**	**0.5-2**	**Pain.**

Table 1: Primary afferent axons arriving to the spinal cord.

The transduction of the nociceptive information starts in the periphery, where a stimulus is able to activate the nociceptor endings, by stretching or bending the nociceptor surface or by promoting the activation of ion channels present in its membrane. At the site of injury some algenous substances are released, such as proteases, bradikinin, ATP, and potassium ions.

Due to the variety of stimuli that can elicit nociceptive signaling (thermal, mechanical and chemical stimuli), different specifics receptors have been described. Both Aδ and C fibers present the vanilloid receptors or transient receptor potential (TRPV) receptors, which respond to heat and capsaicin. There are several TRPV receptors, differing in the range of temperature that activates them. They resemble voltage gated ion channels, presenting six transmembrane domains and a central pore which allows an influx of sodium and calcium that initiates the generation of action potentials. These action potentials are transmitted to the spinal cord, where the signals will be integrated and transmitted to other areas.

Ascending pain pathways

The nociceptive information arriving from the periphery travels along the peripheral axonal branch of primary nociceptive neurons, whose soma are located in the dorsal root ganglia, and the central axon entering into the spinal cord by the dorsal roots. After the dorsal root entry, they travel within the zone of Lissauer, in which axons move up or down a pair of segments before entering the gray matter of the dorsal horn, in a region called substantia gelatinosa. Central nociceptive terminals contact to second order neurons mainly placed in laminae I and II (pure nociceptive), and V (mixed nociceptive and mecanosensory). Sensory fibers that are peptidergic terminate mostly in laminae I and outer II, and a few in lamina V; those that are non-peptidergic (labeled by binding lectin IB4) terminate mostly in the middle third of lamina II. The main neurotransmitter involved in these first relays is glutamate, but also substance P, acting as cotransmitter in peptidergic nociceptors, and important to experience moderate to intense pain.

From the second order neuron the thermal and nociceptive information crosses the midline and ascends to the brain in the spinothalamic tract. This decussation occurs at the spinal level and in two or three segments all the fibers are in the contralateral side. The ascending axons travel through the medulla, the pons and the midbrain without synapsing, until reaching the thalamus. From here, the information is conveyed to the primary somatosensory cortex. This route is followed in order to transmit the gross information of pain, the essential information for the brain to note stimuli that threaten the integrity of the body. This route is called the spinothalamic pathway, part of the **anterolateral system** (Fig.4).

Axons from the second order spinal neurons make relays on different structures and nucleus, in order to mediate different aspects of the sensory and behavioral response to pain. One of these aspects is the sensory discrimination of pain (location, intensity and quality). The main responsible of this discrimination is the thalamus, in particular the ventral posterior lateral (VPL) nucleus. Another aspect is the affective or motivational, more related with the emotion that pain provokes in the individual who is suffering it (unpleasant feeling, fear, anxiety and secondary autonomic reactions). In this case the information travels by the spinoreticular and spinomesencephalic tracts, reaching several structures, such as the reticular formation, the superior colliculus, periaqueductal gray matter, hypothalamus and amygdala. In addition to this, another group of neurons constituting the anterior spinothalamic tract, reach another structure in the thalamus, the midline thalamic nuclei, that will later connect with the anterior cingulate cortex and the insular cortex.

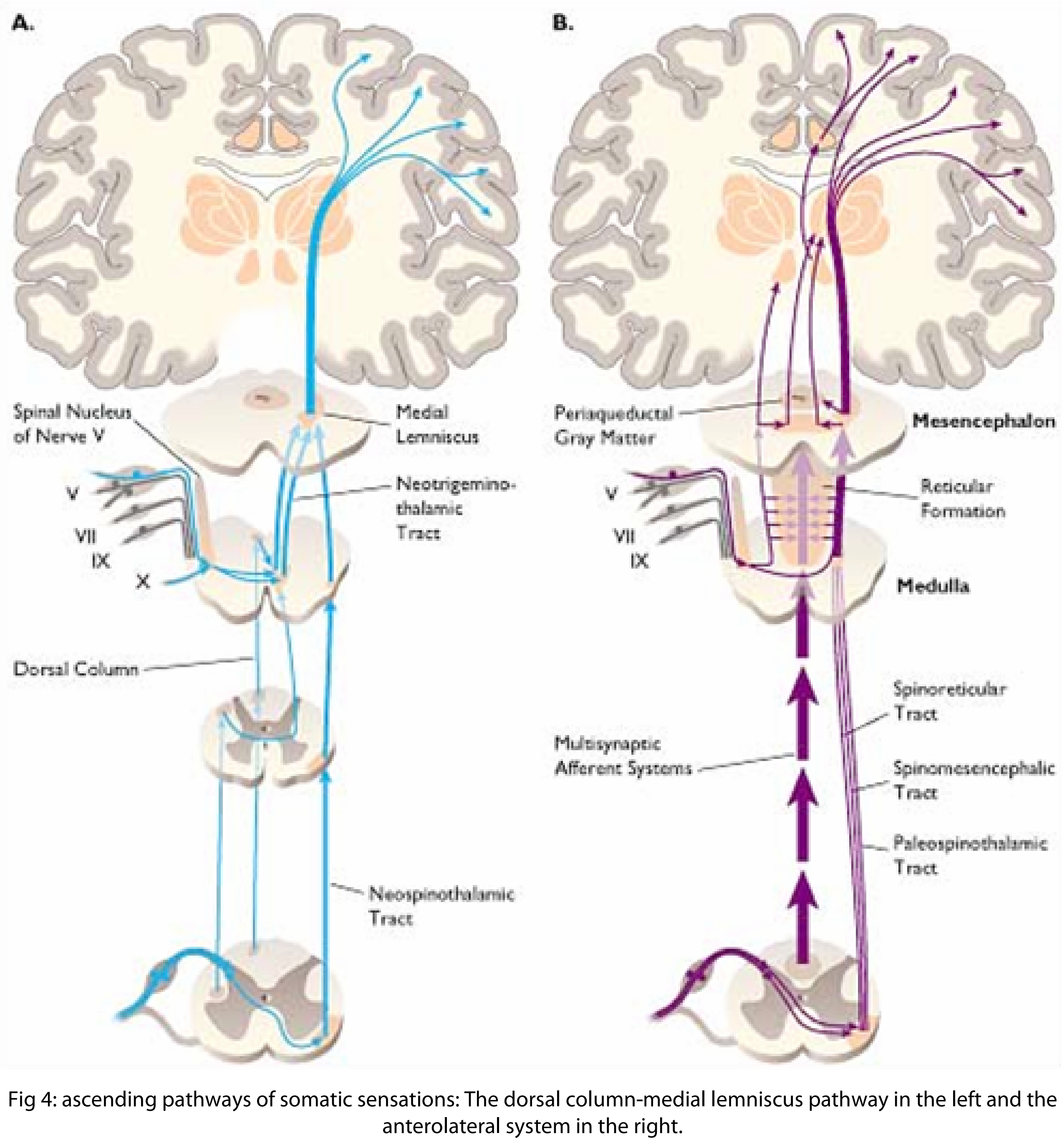

Fig 4: ascending pathways of somatic sensations: The dorsal column-medial lemniscus pathway in the left and the anterolateral system in the right.

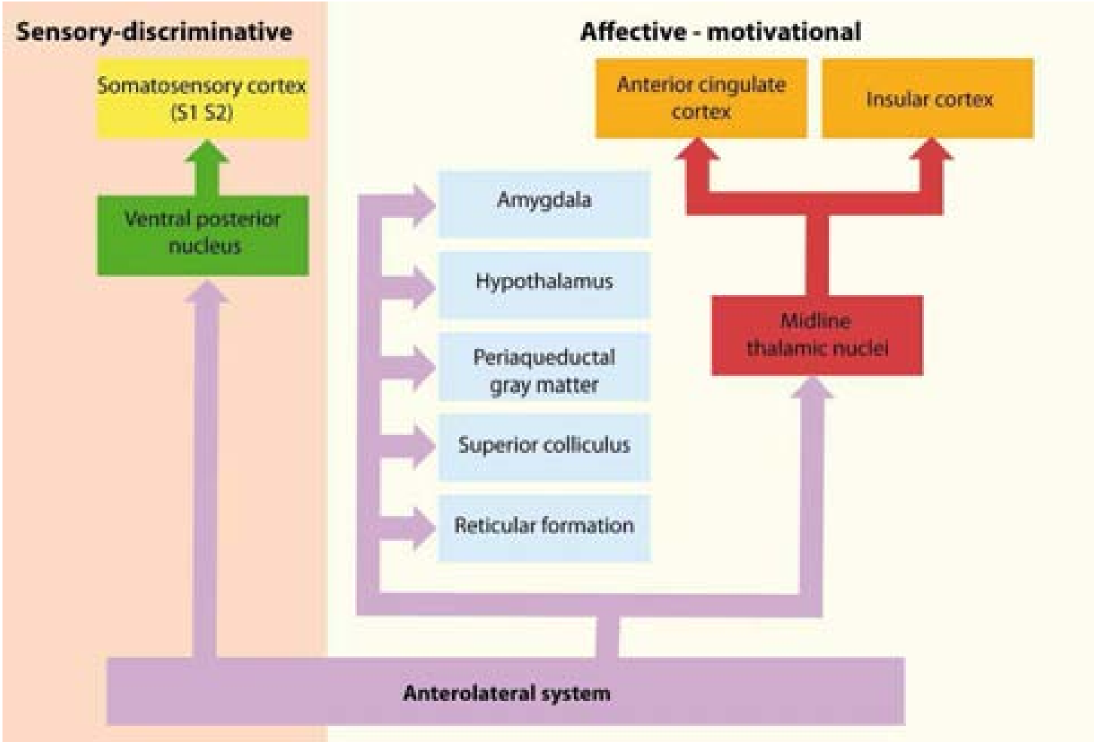

Fig. 5: Different aspects of pain. Adapted from Purves.

Apart from the anterolateral system, another fraction of information entering from the peripheria travels along the dorsal columns, which will provide more qualitative information of the stimulus that is reaching the nociceptive signaling system. This route is used essentially by the mechanoreceptive afferents, which provide information about touch, vibration and proprioception, and is known as the **dorsal column-medial lemniscus system**. This information travels directly by the central axons of primary sensory neurons in the dorsal columns ipsilateral to the site of entrance until the dorsal column nuclei in the medulla, where it decussates to reach the thalamus in the contralateral side and later on the cortex. This system is also related to the discriminative aspects of pain (Fig.5).

Descending control of pain

Once the nociceptive information arrives to the higher level centers, it is integrated in order to elicit a complex physiological response in front of the noxious stimuli, and also modulated in order to reduce the intensity of the painful sensation. The main mechanisms for pain modulation conform the descending pathway (Fig.6). One of the most important regions is the periaqueductual gray matter (PAG) in the midbrain, but there are other regions in the brainstem also involved in this process: parabrachial nucleus, medullary reticular formation, locus coeruleus and raphe nuclei. These centers use noradrenaline, serotonin, dopamine, histamine and acetylcholine to exert both excitatory and inhibitory effects on different sets of neurons in the dorsal horn. Then, they can act on synaptic terminals of nociceptive afferents, interneurons (excitatory and inhibitory), synaptic terminals of other descending pathways, and projection neurons. These contacts do not only act inhibiting the transmission of nociceptive information but also modulating it, as well as controlling the balance between excitation and inhibition in the spinal cord.

The main action of the PAG is to modulate nociceptive signalling in the dorsal horn by secreting endogenous opioids (enkephalins, endorphins and dinorphins) on the dendrites of nociceptive neurons and WDR neurons, causing the hiperpolarization of the second order neurons that implies its partial inactivation. They also release glycine on the terminals of primary afferents (Aβ and C fibers), inducing a presynaptic inhibition that reduces the release of neurotransmitters on the second order neurons. Finally, the secretion of glutamate from the PAG excites the GABAergic interneurons in lamina II of the dorsal horn. This promotes the release of GABA on the second order neurons, hyperpolarizing them and therefore inhibiting them.

The PAG also causes the depolarization of serotoninergic neurons in the raphe magnocellular nucleus (RMN), which project to second order neurons in the dorsal horn via the raphespinal tract. The binding of serotonin to receptors 5-HT_1 and 5-HT_2 induces an increase in the conductance of potassium and therefore the hyperpolarization of the second order nociceptive neurons. It also interacts with 5-HT_3 receptors in the dendrites of GABAergic interneurons in lamina II, inducing the release of GABA and the inhibition of second order neurons. Something similar happens when PAG neurons secrete glutamate on the locus coeruleus neurons. Once depolarized, these neurons release noradrenaline, which causes hyperpolarization of the nociceptive second order neurons by binding to α-adrenergic receptors.

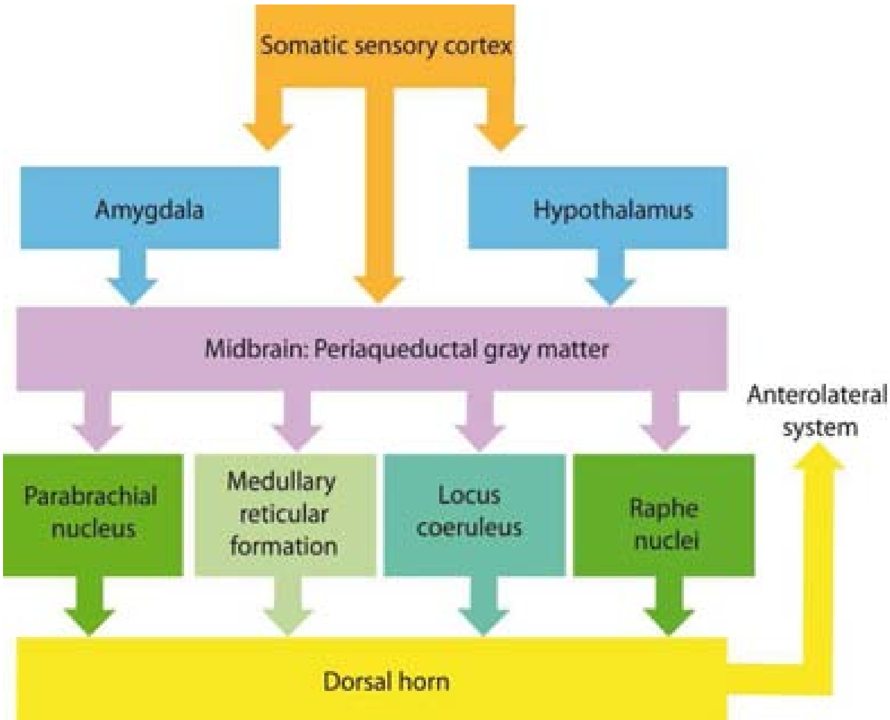

Fig. 6: Descending control of pain. Adapted from Purves.

Local circuits within the dorsal horn also play a role in modulating the nociceptive system. One of these systems was proposed by Wall and Melzack, and called the “gate theory of pain” (Melzack and Wall, 1965), which actually is included under the afferent regulatory system of pain. This theory says that the activation of mechanoceptors (Aβ fibers) can act on local interneurons to inhibit the transmission of information from C fibers to the dorsal horn projection neurons. This would explain how a mechanical stimulus such as scratching can temporarily give relief from pain in the same area.

Similarly, it has also been described a mechanism by which pain can inhibit pain. This phenomenon is called diffuse noxious inhibitory control (DNIC), or heterotopic noxious conditioning stimulation (HCNS) if strictly referred to human assays (Sprenger et al., 2011), and implies a spinal-medullary-spinal pathway. DNIC systems permit a spinal neuron to be inhibited by a nociceptive stimulation applied in another part of the body (outside its receptive field), thus inhibiting the pain sensation after the application of a remote pain stimulation. WDR neurons and trigeminal nociceptive neurons play a key role in this phenomenon, which is subjected to regulation by serotoninergic pathways, and probably by opioids (Cervero, 2006). DNIC effects are usually contralateral and extrasegmental, and highly depend on the intensity of the stimulus. DNIC mechanisms are important since they may reflect alterations in the function of central descending inhibitory systems that could be potentially involved in chronic pain. In fact, research based on the use of DNIC has shown interesting results, since dysfunctions in DNIC were found in chronic pain conditions such as fibromyalgia or irritable bowel syndrome (van Wijk and Veldhuijzen, 2010).

Other elements are also involved in pain regulation, such as the endogenous opioids. Several brainstem regions, most of them conforming the descending system of pain control, are susceptible to the action of these molecules, provoking an important analgesic effect. Endogenous opioids are classified in three groups, called enkephalins, endorphins and dynorphins, which present different distribution along the nociceptive system. Enkephalins, for example, can be released by local neurons on the dorsal horn, then impeding the release of neurotransmitters from the terminals onto the projection neurons, and therefore diminishing their level of activity. This local circuit can also be the target of other descending inhibitory projections, therefore constituting a powerful control mechanism of the amount of nociceptive information able to reach superior centers. Endorphins are released in pain states within some brain regions, but they can also provide tonic analgesic effect in the dorsal horn. Dynorphins have been described to increase after neural injuries, and are related to the development of thermal hyperalgesia by acting on the NMDA receptors and driving to spinal sensitization (Ossipov et al., 2000).

IV – Neuropathic pain after spinal cord injury

Pain is defined by the IASP (International Association for the Study of Pain) as "*an unpleasant sensory and emotional experience associated with actual or potential tissue damage, or described in terms of such damage*". Neuropathic pain (NP) can also be defined as that pain provoked by a lesion or a dysfuntion in the nervous system.

Although sharing features with other kinds of pain (inflammatory or cancer pain), NP presents some particular characteristics. Nociceptive and inflammatory pain can be both symptoms of peripheral tissue injury, and present a clear defensive, beneficial component, whereas NP is a symptom of neurological disease or injury, either affecting the peripheral or the central nervous system (Cervero, 2009), and instead of a defensive component it is considered as a maladaptive response. NP can be defined as central or peripheral depending on the site of the neural injury. Then, SCI may cause a syndrome of central NP, since the lesion affects the CNS. In the case of central pain syndromes, a taxonomy has already been established, in which pain is classified as below-level or at-level pain (Michaelis, 1970; Siddall et al., 1997). Below-level pain is the pain that arises from dermatomes below the segmental level of the injury site, and at-level pain is that pain felt in dermatomes surrounding the injury site. Although above-level pain is also sometimes described (placed in dermatomes above the injury site), this kind of manifestation is not as usual as the other two types after a SCI.

Epidemiology and characteristics of pain after SCI

Neuropathic pain may appear from weeks to months after the injury, with usual onset in the first 6 months in humans (Widerstrom-Noga et al., 2001a), and affects around 70-80% of SCI patients (Siddall and Finnerup, 2006; Soler et al., 2007; Hulsebosch et al., 2009). It is one of the most devastating consequences of a SCI, having a great impact on the quality of life of the patient, since dealing with pain can difficult daily issues as sleep, work, exercise and housework (Widerstrom-Noga et al., 2001b). In fact, SCI patients suffering from NP present fatigue, anxiety and sadness, as well as a high rate of depression and suicide (Soler et al., 2007). The pain felt by SCI patients is usually described as a severe painful sensation, and greatly influences their mood and daily activities. For these reasons it is essential to count on effective treatments, since even a small reduction in the pain intensity can be important. Unfortunately, at least one third of the cases are refractory to most pharmacological treatments.

One of the characteristics than can be used to distinguish nociceptive pain from NP is the quality of the pain: nociceptive pain usually is referred as *aching*, whilst NP is usually *burning* or *shooting*. When assessing pain in humans, there is plenty of descriptors than can be used and help the clinicians: sharp, shocking, burning, pressing, shooting, pricking, pulsating, crushing, cramping, dull, electric, radiating, stabbing, cold, penetrating, stinging, etc. It is also important to assess the **severity** of the pain that do not necessarily correspond to the **intensity** reported by the patient. The onset, extension and continuity of the pain should be also assessed (Widerstrom-Noga et al., 2001a). Although NP can be located in every part of the body, the back appears to be one of the most painful areas, followed by thighs, legs and feet, since are reported as painful areas in half of the patients (Widerstrom-Noga et al., 2001a).

NP can be **spontaneous**, if it appears without any noxious stimulus, or **evoked**, when a stimulus is eliciting the painful response. The response to an evoked noxious stimulus is usually abnormal in a NP state, and we can refer to **hyperalgesia** (when the response is exaggerated to the evoked noxious stimulus) or to **allodynia** (when an innocuous stimulus causes a painful response) (Fig. 7). It is important to take into consideration that sometimes NP can be considered as pathological since it does not correspond to a real threatening stimulus or to a potential damage. In fact, whilst normal pain is something important and necessary for the survival of the individual, NP usually does not follow this principle.

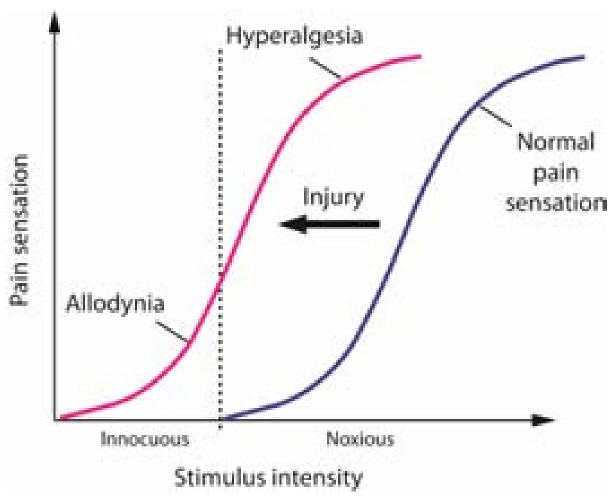

Fig. 7: shift in the normal response to innocuous and noxious stimulus after an injury.

Mechanisms of neuropathic pain after a SCI

It is widely accepted that the appearance and maintenance of neuropathic pain after SCI is a secondary injury feature. Several distinct mechanisms have been described as contributors to the development of NP after central injuries. After a SCI, all of them may act simultaneously, and it is dificult to unravel if some mechanisms are more responsible than others in the appearance of pain. In any case, it is important to know them all to provide new therapies and treatments focused to each of them. In addition, it is essential to distinguish the role of injured segments (those close to the injury site) from the intact segments of the spinal cord, not directly affected by the injury but which also suffer functional changes. Despite minor changes, the peripheral components of the nociceptive system are usually unaffected by a SCI, therefore central mechanisms must account for the enhancement in the nociceptive transmission pathway. The most important central changes are briefly explained below.

- **Dorsal horn hyperexcitability and central sensitization**

Several injury features, such as the release of massive amounts of excitatory amino acids and proinflammatory mediators, induce hyperresponsiveness in the neurons of the dorsal horn. This includes a shift in the neurons which respond to noxious stimulus, increase in the spontaneous background activity, and alterations in sodium channels and currents (Hulsebosch et al., 2009). It has been also reported that a proportion of inhibitory interneurons die after the injury, therefore contributing to the loss of inhibition in the dorsal horn, as well as reduction of inhibitory transmitters content in the surviving interneurons and downregulation of their receptors (Costigan, 2000).

A specific element of the hyperexcitability is the **central sensititzation**. By definition, sensitization is an increase in the response to a determined stimulus, and therefore it may happen at any place of the nociceptive system (Baranauskas and Nistri, 1998). Although peripheral nociceptors are known to increase their responsiveness under certain conditions, it is though that the main sensitization takes place in the spinal cord (Woolf, 1983), and for this reason this phenomenon is usually called central sensitization. Central sensitization is the expression of an increase in excitability of neurons in the spinal cord (Woolf, 1983). This can be seen at a single cell level as a change in the receptive field, a reduction in the thresholds, or as an increase in the response and the recruitment of new inputs. This is translated into an abnormal or increased sensitivity to external inputs, as well as the spread to uninjured sites, a phenomenon also known as secondary hyperalgesia. Sensitization may be due to different situations: increased sensitivity, loss of inhibitory control, increase in responsiveness, changes in the surrounding circuits (activation of silent synapses, deafferentation), changes in ion channels that alter membrane properties, receptor plasticity, or alteration in membrane transporters (Baranauskas and Nistri, 1998; Hulsebosch et al., 2009).

At the molecular level, central sensitization shares some characteristics with long-term potentiation (LTP), since both phenomena have an early activity-dependent phase followed by a secondary phase which implies synthesis of new proteins (for example, cytokines). Moreover, in both cases the NMDA receptors are at the beginning of the cascade of molecular events, which include activation of adenyl cyclases, PKA, PKC, CaMK, which will produce the phosphorilation and activation of different MAPKs (ERK1/2, p38, c-jun N terminal kinase). These kinases would later act on different transcription factors to modulate the gene expression (for review see (Hulsebosch et al., 2009). In all the steps of this cascade, the increase in calcium influx after the injury is present, activating different signaling pathways.

Central sensitization includes a secondary phase that implies synthesis of some cytokines and chemokines. Cytokines are intercellular communication proteins, and their binding to receptors causes the activation or the expression of some surface molecules and membrane receptors, and the activation or differentiation of some cell types. They are usually secreted by immune and some neural cells, and are closely related to inflammatory processes. Some of the most important cytokines are the interleukins, usually synthesized by leucocytes, and that can act as proinflammatory (IL-1, IL-6, IL-8…) or antiinflammatory mediators (IL-2, IL-4, IL-10…). Proinflammatory cytokines are considered as pro-algesic molecules, since they can contribute to the depolarization of nociceptive neurons as well as to the sensitization of receptors (White et al., 2005). Chemokines are cytokines with chemotactic functions for the migration and recruitment of immune cells to the injury site. All of them act coupled to G receptors, and their production and secretion are usually related to inflammatory processes, since their concentrations are very low in normal conditions. After a SCI, their production and the expression of their receptors is upregulated and maintained, contributing to the maintenance of inflammatory processes as well as hyperexcitability states and persistent pain states. These molecular cascades are usually under the action of TNFα (White et al., 2005; Moalem and Tracey, 2006). TNF-α acts sensitizing Aδ and C fibers receptors. Together with IL-1β, it promotes the expression of NFKB, which will promote the synthesis and release of more inflammatory mediators.

- **Glial activation**

In the last years, glia has received more attention and nowadays it is thought to be involved in pathological pain states (Watkins et al., 2001). The dysfunction of neurons is not the only cause of NP, and despite the beneficial properties of microglia and astroglia in the lesion site just after the injury, they can become pathologically activated and contribute to NP (Watkins et al., 2001; Hains and Waxman, 2006; Scholz and Woolf, 2007; Gwak and Hulsebosch, 2009).

Microglia seems to be more related to the initial phase of persistent NP, the induction, while astroglia is more related to the maintenance of NP (Hains and Waxman, 2006; Inoue and Tsuda, 2009). Several mechanisms can account for this induction, including the release of cytokines, chemokines and prostaglandines, as well as the interaction with neurons in the synapses and the endocannabinoid pathway (Graeber and Christie, 2012).

Microglia becomes quickly activated after the injury, since they have a very low threshold of activation and respond to a wide range of disease or damage stimuli (Scholz and Woolf, 2007; Graeber and Christie, 2012). In normal conditions, microglial cells act sensing the microenvironment, especially near the synaptic areas, so they act as a tissue alarm system. Once activated, microglia display a clear change in morphology, as well as in expression profile. The expression and release of some modulatory molecules led to the concept that microglia form part of inflammatory processes in the CNS, called neuroinflammation. Microglia can become activated by differents pathways, some of them mediated by inflammatory mediators such as chemokines and cytokines:

a) **Fractalkine**, CX3CL1**:** fracktalkine is expressed by neurons and its receptors are placed in glial cells (Lindia et al., 2005). It is considered a neuron-to-glia signal released from damaged neurons, binding to glia to induce its activation (Watkins et al., 2001). Fractalkine is a transmembrane protein that requires proteolytic cleavage of cathepsin to be released. Cathepsin is produced and released by microglia (Clark et al., 2009).
b) **Interferon gamma**, IFN-γ: its receptor is considered a key element in promoting the adquisition of an activared state in microglia that drives neuropathic pain (Inoue and Tsuda, 2012).

c) **Monocyte chemoattractant protein-1**, MCP1 or CCL2: chemokines mediate the communication between microglia and neurons, and are known to increase nociception. MCP1 is released in an activity dependent manner from the central terminals of primary sensory neurons (Thacker et al., 2009) and from astrocytes. It can be induced by TNF-α and IL1 released by activated microglia, hence regulating the excitability of dorsal horn neurons. In fact, the binding of MCP1 to its receptor reduces the inhibitory effects of GABA, facilitating depolarization (Zhang and De Koninck, 2006), and therefore contributing to pain states.
d) **Prostaglandin E2,** PGE2**:** can be secreted by microglia in remote regions of the lesion, and promotes hyperexcitability in the dorsal horn neurons (Hulsebosch et al., 2009). Their actions are mediated by the postsynaptic inhibition of glycinergic receptors, and the direct depolarization of some neurons in the inner lamina of the dorsal horn. It can also modulate the synaptic transmission by promoting the increase of glutamate in the synaptic cleft and the reduction of the inhibitory effects of glycine (Ma and Quirion, 2008). The communication between neurons and activated glia mediated by PGE2 is considered as a tonic influence in NP, more related to chronic than acute pain.

Another form to activate microglia is by acting on the **toll-like receptor 4** (TLR4). This activation is related to the production of prostaglandins and TNF-α. Another receptor involved is the **purinergic receptor P2X4** (P2X receptor, ligand-gated ion channel 4). The P2X4 receptor is expressed by activated microglia and mediates an increase in calcium and the activation of p38 kinase. This activation induces the synthesis and release of BDNF, a protein used in the communication between microglia and neurons that can cause a shift in the neuronal anion gradient that would underlie NP.

Endocannabinoids are also related with microglia activation and pain. The cannabinoid type 1 receptor (CBR1) is highly expressed in neurons and at low levels in microglia. CBR2 is also expressed by microglia, as well as other uncommon or abnormal cannabinoid receptors. CBR2 is especially upregulated in activated microglia, and it is related to an increase in proliferation and chemotaxis and to a reduction in the release of pronociceptive mediators, such as free radicals and TNF-α (for a review see (Graeber and Christie, 2012). Regarding the function of these receptors in NP, it is thought that endocannabinoids act on CBR1 at inhibitory synapses reducing aberrant excitatory activity, whereas CBR2 activation on microglia would produce a reduction in the release of nociceptive mediators.

Together with the microglia, the **astroglia** also play essential roles in the maintenance of chronic NP. Activated astrocytes release cytokines and chemokines which would act enhancing and perpetuating persistent pain states in the spinal cord. It is assumed that microglia presents a fast activation after injuries, and that astroglia progressively replaces microglia. Astrocytes contribute to pain maintenance possibly by a PGE2 mediated pathway, as well as by changing the expression of IL-18R, GLT1, and ERKs. The JAK-STAT3 pathway is also activated in microglia, and it is related to the activation of astrocytes and to some pain symptoms. Astrocytes can perpetuate pain states by secreting inflammatory mediators, such as TNF-α, IL-1β, IL-6 and NO (Vallejo et al., 2010).

It is important to note that populations of glia are initially activated in the areas surrounding the lesion, but with time, all the inflammatory mediators as well as other signaling molecules diffuse and contribute to the extension of the area affected by the lesion changes. This can also contribute to the remote activation of glia in regions away from the injury site, such as other regions of the spinal cord, or even supraspinal centers. (Watkins et al., 2001; Zhao et al., 2007; Gwak and Hulsebosch, 2009; Carlton et al., 2009). This remote activation is another mechanism contributing to chronic NP and plastic changes in spinal circuits after the lesion.

- **Loss of descending inhibition**

The spinal cord lesion disrupts spinal tracts, as those descending from modulatory centers of pain such as the periaqueductal gray matter, the raphe magnocellular nucleus and the locus coeruleus. In normal conditions, these tracts, placed in the dorsal part of the spinal cord, modulate the ascending nociceptive pathways. After a SCI, their inhibitory and modulatory functions are seriously compromised. Although descending tracts provide both excitatory and inhibitory inputs, after a SCI the loss of the inhibitory inputs becomes especially important, since the injury itself causes a high excitability. The final balance between excitation and inhibition in the spinal cord is clearly biased to excitation. This can contribute to the appearance of clinical signs such as spasticity, hyperreflexia and NP.

- **Disinhibition and plasticity**

Apart from the loss of descending inhibition, another feature contributing to the hyperexcitablity in the spinal cord after SCI is **disinhibition**. This can occur because of the death of inhibitory interneurons caused by the excitoxicity of the lesion, the reduction in the release of inhibitory neurotransmitters from surviving interneurons, or the reduction in the expression of inhibitory transmitter receptors (Costigan and Woolf, 2000; Meisner et al., 2010). Another important change to take into account is the important **plasticity** and **reorganization** properties of the spinal circuits, that imply functional changes of different elements. The dorsal horn is organized in laminae; lamina I-II only receive nociceptive inputs in normal conditions, and lamina III and IV only inputs related to touch and temperature. After an injury, this clear organization can be lost, as some Aβ fibers arriving to lamina III-IV can produce aberrant sprouting and reach outer laminae. This may imply that some innocuous, tactile information will be processed abnormally in a nociceptive territory, constituting a potential mechanism for allodynia (Costigan and Woolf, 2000).

Silent circuits and synapses in normal conditions can also become activated after an SCI, as has been shown to occur after peripheral nerve injuries (Koerber et al., 2006). Another plasticity phenomenon is the disinhibition itself, that can be produced by a shift in the properties of some inhibitory receptors (for example the loss of inhibitory function in GABA receptors, in relation with a shift in the function of chloride transporters NKCC and KCC) (Pitcher and Cervero, 2010).

Neural plasticity occurring after a SCI is also detectable in reflex circuits, which are usually used as an indirect measure of central hyperexcitability. Electrophysiological changes caused by the lesion and by following plastic reorganization can produce the appearance of hyperreflexia and an increase in wind-up responses, that can eventually lead to spasticity and NP. It has been also reported that SCI induces plastic changes in supraspinal structures such as the cortex and the thalamus (Hains et al., 2005; Zhao et al., 2007), favoring the shift from inhibition to excitation of the descending modulatory pathways.

V- Pharmacological treatment of neuropathic pain

Nowadays there are plenty of options more or less useful to treat NP, as well as some other secondary consequences of SCI. Drugs aimed to treat NP may interfere with pain processing and modulation, and this can be achieved by different pharmacological treatments (Sindrup et al., 2006). Pain conditions are diverse, and not all the drugs are useful for all of them (table 2). The first line of treatment for NP was the use of antidepressants and anticonvulsants, drugs designed for treating other pathological entities. Later on, other drugs have been incorporated, such as NMDA antagonists, cannabinoids and anaesthetics (lidocaine). Finding the right treatment for NP syndromes is essential but difficult. Since pain is usually debilitating and worsens the quality of life of those who suffer it, it is necessary to count on effective treatments with few side effects. Unfortunately, there are few treatments really useful, and NP is usually referred as refractory to common treatments. From these conditions, some of the most common are the spinal cord injury pain, multiple sclerosis pain, complex regional pain syndrome (CRPS), nerve injury pain, painful polyneuropathy and postamputation pain.

Below there is a summary of the main groups of drugs used in the treatment of NP syndromes.

- **Tryciclic antidepressants (TCA):** their main functions are the inhibition of the presynaptic reuptake of noradrenaline and serotonine, the postsynaptic blockade of NMDA and α-adrenergic receptors, as well as the blockade of sodium and calcium channels. The main action of TCA is based on its effect on monoamines, and therefore enhancing endogenous pain modulation. Amitryptiline is the most used TCA, which exerts a positive effect on NP by its action as a noradrenaline reuptake inhibitor (Jain, 2008).
- **Anticonvulsants**: their main action is by increasing GABA mediated inhibition, although they also exert functions on ion channels and neurotransmitters (excitatory and inhibitory). Some drugs are designed to normalize membrane potentials and reduce hyperexcitability, such as carbamazepine, oxcarbazepine and phenytoin. Their action is aimed to block sodium channels, but some new blockers have been recently designed, and are supposed to act more specifically, such as lamotrigine (acts on the slow inactivated conformation of the channel), gabapentine and pregabaline (they block the influx of calcium ions to reduce the release of neurotransmitters; this action is originated by their binding to the α2γ-subunit). This causes reduction in the release of glutamate and substance P, contributing to the

decrease of hyperexcitability. Other drugs potentiate GABA actions, as topiramate, which blocks sodium and calcium channels and blocks glutamate receptors. Similarly, valproate increases the release and decreases the degradation of GABA, also enhancing their functions. Some other drugs included in this class are the benzodiazepines.

- **Opioids**: opioids that are useful for NP are oxycodone, with combined actions on μ- and K - opioid receptor, and tramadol that acts on μ-receptors and also has monoaminergic effects, inducing the release of serotonin and inhibiting the presynaptic reuptake of noradrenaline (Raffa et al., 1992). Despite their efficacy is similar to that attributed to gabapentine and pregabalin, opioids are rarely used as first-line treatment due to their side effects, and problems with tolerance during long term treatments (Jain, 2008; Finnerup et al., 2010a).
- New drugs have emerged in the last years, such as topical lidocaine or capsaicin, TRPV agonists and antagonists or intradermal application of botulinum toxin (Finnerup et al., 2010b). Some NMDA receptor agonists, such as ketamine, have been also tried. Unfortunately, their use is limited because of their numerous side effects (Jain, 2008).

	Pain condition	Useful drugs
Peripheral pain	Painful diabetic neuropathy	TCAs and selective noradrenaline and serotinin reuptake inhibitors (SSNRIs)
	CRPS	None
	Nerve injury pain	Amitriptyline (TCA), topical lidocaine and topical capsaicine
	Painful neuropathy	TCAs, gabapentine, pregabaline, lamotrigine, tramadol, oxycodone
	Postherpetic neuralgia	TCAs, gabapentine, pregabaline, lamotrigine, tramadol, oxycodone, morphine, lidocaine
	Postamputation pain and phantom limb pain	Gabapentine, lamotrigine, pregabaline, carbamazepine
Central pain	SCI pain	Gabapentine, lamotrigine
	Multiple sclerosis	Cannabinoids

Table 2: Table of drugs with pain-relieving effects: Modified from Sindrup et al. (2006).

Although it is difficult to choose the right drug for each condition, gabapentine might be considered the first-line treatment for post-SCI pain, together with anticonvulsants and TCAs. Nevertheless, the combination of different drugs acting on different mechanisms is a common strategy, especially in patients who do not respond to treatments of one single drug, or in cases of only partial efficacy. It is also important to take into account the possible contraindications in each patient as well as the possible side effects of each treatment. These features are summarized in table 3.

Drug	Major contraindication	Side effects
TCA	Cardiac complications and epilepsy	Dry mouth, constipation, sweating, dizziness, somnolence, palpitations, and urine retention.
Gabapentine and pregabaline	None	Somnolence, ataxia, dizziness, headache, nausea, vomiting, peripheral edema.
Lamotrigine	Uremia	Somnolence, headache, nausea, double vision, vomiting, ataxia, dizziness.
Tramadol	None	Nausea, vomiting, constipation, dizziness, somnolence, sweating, dry mouth, headache.
Oxycodone	None	Somnolence, nausea, vomiting, constipation, dizziness.
Carbamazepine Oxcarbamazepine	Cardiac disturbances, liver disease	Somnolence, ataxia, dizziness, double vision, erythema, fluid retention.

Table 3: major contraindications and side effects of drugs used in the treatment of neuropathic pain. Modified from Sindrup et al. (2006).

In the last years, and as more mechanisms are discovered to be involved in the generation and maintenance of NP, more options are raising. Some of them are focused in the modulation of the neuroinflammation (Iannotti et al., 2011; Esposito et al., 2012), as well as in the modulation of molecular targets (David and Lacroix, 2003; Ji and Suter, 2007; Gao et al., 2009). Together with these new advances, there is a huge field of research based on complementary treatments, based on the use of grafts of different cell types to promote neuroprotection and plasticity (Karimi-Abdolrezaee et al., 2010; Wagner et al., 1998), as well as some other experimental treatments, such as the use of chondroitinase or trophic factors (Pezet and

McMahon, 2006; Deng et al., 2011), aimed to promote plasticity of the spinal nociceptive circuits (Xia et al., 2008; García-Alías et al., 2009). In any case, it is also important to complement any pharmacological, biochemical or cellular therapy with rehabilitation therapies (Fouad and Tetzlaff, 2011).

There are also some not pharmacological therapies that can be used in patients suffering from neuropathic pain after an SCI. Some of them are based on transcranial stimulation or deep brain stimulation (Prévinaire et al., 2009; Plow et al., 2012). Some other complimentary therapies are based in cognitive experiments that include virtual reality devices and movement imaginery (Soler et al., 2010).

VI – Animal models for the study of central neuropathic pain after spinal cord injury.

Animal models are an essential tool to study the physiopathological events and the mechanisms underlying all the consequences of a SCI, including the appearance and maintenance of NP. Several species have been used to study these events such as rat, mouse, cats, dogs, monkeys and even turtles, although every species implies some pros and cons. For instance, while cats are very used for locomotion studies, rodents as mouse and rat are the election when studying neuroinflammation.

It is important to note that the terms “pain” and “nociception” are slightly different, and this is especially important to have into account when working with animals. ***Pain*** refers to the feeling or the sensation, the aversive and emotional reaction to a sensation coming from some part of the body. ***Nociception*** is the sensory process that provides the signals to trigger pain. Due to its emotional and conscious components, analysis of pain is usually restricted to humans, so the term nociception would be in fact more appropriate for animal models. Nevertheless, and for convenience, *pain* is also used when using animal models, but always with the semantic difference in mind.

Another important limitation of animal studies is the difficulty to interpret the deficits appearing after a SCI as well as the symptoms of pain. Similarly, it is evident that the locomotion systems are affected after a SCI, but the symptoms differ between humans and animals: while a thoracic injury can imply a persistent paraplegia in a human, the recovery seems much better in rodents, mainly because the biomechanical differences of their skeleton, which allows better restoration of locomotion reflex circuits. Moreover, algesimetry tests in animals become much more complex than in humans, since humans can express what are they feeling and where, and describe the sensations in understandable terms. For these reasons, it is important to understand that animal models do not completely mimic a human lesion and its consequences, but they are equally useful since they can reproduce most of the acute and long-term physipathological events occurring after spinal trauma, and can provide very important information for future treatments and therapies.

Spinal cord injury models

There are several spinal cord injury models, aimed to study different aspects of the lesions. Below there is a brief overview of the most useful models, representing different lesions, depending of the cause of the injury.

- **Contusion models:**

The contusion models are the ones who better mimic the human features after a contusive lesion (Yezierski, 2005; Gwak et al., 2012), which is the most frequent type (usually for car crashes and falls). Also known as acute compression injuries, they are caused when a force is applied to the spinal parenchyma, causing a disruption of the spinal tissues. The main difference between animal and human lesions is that in animal models usually a laminectomy is performed before applying the impact, so the bones cannot break uncontrollably and can not give unpredictable lesions. This could add an additional and undesired effect of variability to the model.

The first contusion model was used for Allen in 1911, who applied a falling weight from a determined distance to the exposed spinal cord of dogs. This was the first attempt to get a quantifiable and reproducible lesions, and was known as the "**weight drop**" model (García-Alías et al., 2010). From that moment, many devices have been used in order to perform the contusions (Fig. 8), and nowadays not only the mass of the weight and the height can be measured. New devices include software programs that can record the velocity of the impact, the exact time of dwelling, as well as the displacement suffered for the spinal cord and the real force applied. These devices are produced by different manufacturers, and although displaying some slight differences, all of them are based in the same principles. The most used are the Infinite Horizon Impactor (monitorized impact, it records real force applied, velocity and displacement of the spinal tissue, (Cao et al., 2005)), the LISA contusion device (it uses laser for a major precision of the displacement measurement, (Zhang et al., 2008), and the NYU-MASCIS (a monitorized version of the original weight drop, (Kerr et al., 2010; Agrawal et al., 2010)).

Contusions into the spinal cord cause permanent sensorymotor deficits, although locomotion and functional outcomes tend to recover with time until theu reach a plateau. Sensory defficits are more difficult to resolve, so most of them are permanent. Some of the main pathophysiological events accurring after the SCI are the excitotoxicity, ischemia, and pathological glial activation, appart from the formaton of a cystic cavity in the epicenter.

This model has widely been used to study pain and sensory outcomes, functional recovery as well as some promising therapies, such as cell therapies.

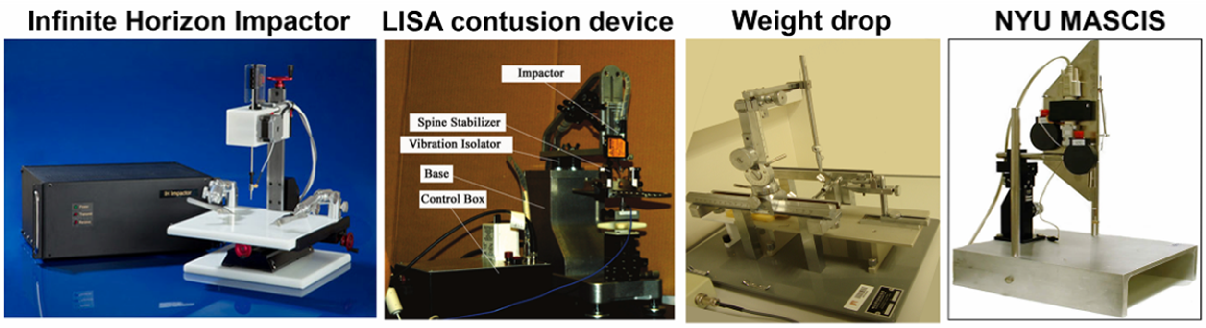

Fig. 8: images from some of the most used devices to perform SCI.

- **Compression models:**

In these models the pressure on the spinal cord is applied continuously in a time period. The first descriptions appeared around 60 years ago (Tarlov and Klinger, 1954), and as it is also a closed lesion, located inside the vertebral channel, represents a good tool to reproduce some of the human SCI.

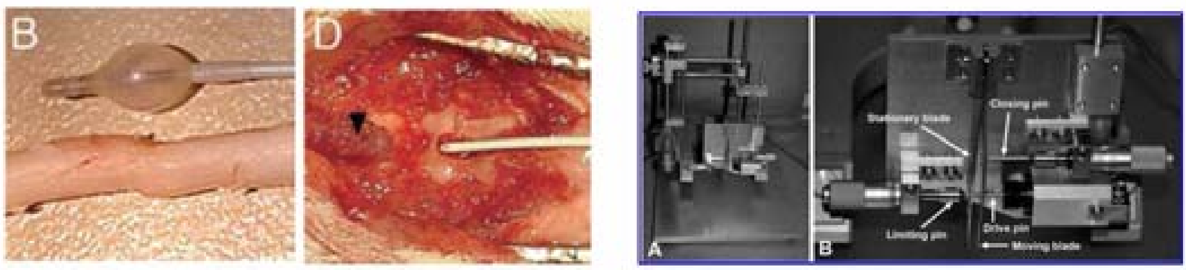

Fig. 9: The first image depicts the ballon used to perform the spinal compression, filled with liquid. Note the similar diameter of the filled balloon and the spinal cord of a rat. In the second pannel, image of a catheter entering the subdural space just. On the right, a mechanical device to perform compressions by using aneurism clips. Images obtained from Lonjon et al. (2010) and Semler et al. (2011).

The compressive models normally use an inflatable balloon (Fig.9) placed in the extradural space which can be filled with air or liquid by the researcher (Lonjon et al., 2010; Amemori et al., 2010; Yazdani et al., 2012). Volumes used can differ, but in animal models it normally ranges from 10 to 50µl, for 1 to 10 minutes. As an example, a balloon filled with 15 µl for 5 minutes induces total paraplegia (the first 2-4 days) in adult rats, followed by partial recovery. It also provokes bladder control dysfunction, cavities within the spinal parenchyma, a robust and long lasting hypersensitivity, and even abolishment of propioception (Hama and Sagen, 2007; Lonjon et al., 2010; Amemori et al., 2010; Densmore et al., 2010). In this type of injury, locomotor and autonomic recovery presents a good correlation with the balloon inflation volume, whilst sensory and reflex outcomes were independent of the lesion severity.

A similar approach is the use of aneurism clips, which can produce different severities of injury depending on the applied pressure or on the time of application (Pinzón et al., 2008; Esposito et al., 2012). Clip compression leads to the development of evoked pain. The effects in different nerve types present temporal and spatial differences, and in some cases are worst and longer lasting than in complete injuries (Kalous et al., 2009)

There is also a third compression model, based on the prolonged application of a weight into the spinal cord surface, a procedure very similar to the contusion (Swartz et al., 2009).

The main physiopathological events after a spinal cord compression are the excitotoxicity, the ischemia, incomplete axonal loss, cell death and several elements of metabolic failure in the gray matter (Hama and Sagen, 2007; Lonjon et al., 2010; Amemori et al., 2010). Compression injuries have also been used to study the effectivity of cell therapies (Amemori et al., 2010; Yazdani et al., 2012).

- **Section models:**

These models can include complete or partial section models, normally performed by surgical methods (scissors, blades). The complete section is especially useful to study local spinal systems, independently from descending influences; in fact, it can be used as an isolation mechanism somehow. Complete sections of the spinal cord are not frequent in human injuries, but the animal models can be used to study some features of the injuries (Tillakaratne et al., 2000; Guízar-Sahagún et al., 2004).

Apart from the complete lesion, there is a wide variety of options when applying partial lesions. These lesions can be restricted to one specific tract (dorsal column tract, for example), or to only one side of the cord (hemisections, HS), etc. Depending on which part is sectioned, the functional deficits would also differ. They can be also used to study the function of concrete nucleus or tracts in the spinal cord, so their utility is really high, especially in descriptive and anatomical studies.

Transverse hemisection has been widely used in studies focused in pain and functional deficits. Hemisection models present some advantages when compared to other models, such as the possibility to control the number and the type of injured fibers and the clear differentiation between injured and intact sides. Moreover, it is a reproducible model, with little variability between individuals (Kim, 2003), and specially sensitive for detecting unilateral differences in locomotor function.

Regarding functional outcomes, HS injuries cause an early paralysis in ipsilateral hindlimbs just after the injury, but animals can recover normal and almost coordinated locomotion by the day 14^{th} after the injury, although recovery presents a plateau in the third week (Gwak and Hulsebosch, 2009).

Pain responses after HS can include cold and mechanical allodynia in both hindlimbs (Kim, 2003; Gwak and Hulsebosch, 2009). This fact relays in the preservation of several contralateral ascending pathways which convey nociceptive information to unilateral and bilateral supraspinal centers of pain (spinothalamic, spinocervicothalamic, spinoreticular and short propiospinal tracts). Moreover, this bilateral and non localized expression of pain syndromes may indicate the existence of common generator mechanisms of NP, such as bilateral astrocytic and microglial activation, which eventually lead to hyperexcitability of WDR neurons, even in caudal segments. In HS animals it has also been described an increase in CGRP expression colocalized with GAP43 protein in laminae III and IV, suggesting that there are growing neurites doing sprouting into not appropiate laminae, which could be the basis of allodynia (Kim et al., 2005)

Mechanical allodynia symptoms start just after the injury in the contralateral side, but it takes few days to appear in the ipsilateral site. Contrarily, cold allodynia is developed simultaneously in both sides, and it appears just one day after the injury (Gwak and Hulsebosch, 2009). These symptoms are long lasting (6 months), although they tend to recover normal values. Hemisection lesions in humans (Brown-Sequard syndrome) account only for a 2% of SCI, and normally develop with a bilateral below-level pain (Kim, 2003).

Complete sections or transections are also used as a SCI model. It is normally used as an extreme condition with a total loss of connectivity with upper centers. Nevertheless, a severe lesion implyes sometimes a total paralysis, which difficults the assessment of functional and pain outcomes (Densmore et al., 2010). It has also been used to study the local reflex circuits and recovery without the descending influence of superior centers (Basso et al., 1996).

- **Other models:**

Other models can mimic specific features occurring after an SCI, not necessarily the trauma. These models can be focused on the vascular damage, the excitotoxicity, the production of free radicals, or any of the events occurring after a spinal cord injury. Although these mechanisms do not reproduce the human lesions, are really important to unravel the specific mechanisms underlying the events occurring after the human traumas.

Objectives

In order to be able to design better therapies and treatments directed to improve the quality of life of patients as well as to reduce as much as possible the maintenance of neuropathic pain, it is essential to have a better knowledge of all the processes happening in the spinal cord after an injury. With this aim, we established the following general objectives that would be divided in specific objectives in further sections of this thesis.

1. Characterization of the functional deficits and the appearance of neuropathic pain in different models of spinal cord injury in the rat.

2. Quantitative evaluation of functional deficits after different SCIs, especially focused in the locomotion and nociception.

3. Description of the plastic and functional changes occurring at distal segments of the spinal cord injury.

4. Study of the efficacy of pharmacological treatments to alleviate neuropathic pain responses based on the modulation of glial cell reactivity.

Methods and procedures

Laboratory animals

Adult female Sprague Dawley rats (8 weeks old; 250-300 grams) were used in this thesis. They were housed with free access to food and water at a room temperature of 22±2ºC under a 12:12 light-dark cycles. Injured animals were frequently evaluated (daily during the first week, and weekly therafter) in order to detect signs of suffering, such as loss of weight, changes in the hair or in the response to manipulation, as well as the appearance of exudates around the nose and the eyes. All experimental procedures were approved by the Ethics Committee of the Universitat Autònoma de Barcelona, and followed the European Communities Council Directive 86/609/EEC.

Surgical procedures

In this thesis different types of spinal cord lesions of different severities have been chosen in order to obtain differential information of each model regarding neuropathic pain and the plastic changes occurring after injury.

Rats were anesthetized with sodium pentobarbital in the first experiments (50mg/kg, intraperitoneal) or later with a mixture of ketamine/xylacine (90-10mg/kg, intraperitoneal). After a subcutaneous injection of buprenorphine (0.05mg/kg) near the incision site, the animals were placed on a warming pad to maintain the body temperature. The back of the rats was shaved and disinfected with povidone iodine solution, and vaseline was placed on the eyes to avoid dehydratation.

A surgical scalpel was used to make a longitudinal incision in the back (around 5cm), and muscle and adipose tissue was gently removed in order to expose the vertebral spinous processes. By identifying the medial dorsal spinal artery, which enters into the spinal channel between T5-T6, the T8-T9 vertebrae were identified and subjected to dorsal laminectomy with a fine rongeur. Once exposed, the spinal cord was subjected to a different model of injury as described below (Fig.10):

- **Spinal cord contusion**: Once the laminectomy is performed, and ensuring that there are no lateral pieces of bone that could disturb the contusion, the animal was placed on the impactor device (Infinite Horizon Impactor, Precision Scientific Instruments; Lexington, UK). Vertebral processes of T7 and T10 vertebrae were clamped with forceps to maintain the spinal column straight, and the contusive tip was placed over the middle of the spinal cord, at 4mm of height. Then, the contusion force was set in the software, which records the real force, the displacement suffered by the spinal cord tissue and the velocity at which the impact took place. In this work we have used forces of 100, 150 or 200kdyn in order to have a gradation in severity of the lesion.

- **Spinal hemisection**: after the laminectomy, a fine surgical tweezer was used to lift up the meninges. With the meninges slightly elevated, a small longitudinal incision was done in the dura with the help of a sharp needle. Then a partial section of the right spinal cord was done by means of small spring scissors. Special care was taken to avoid the lesion affecting the two sides of the spinal cord. To ensure the total hemisection, a sharp needle was introduced several times in order to ensure that all the fibers were completely cut.
- **Complete spinal section**: was performed similarly to the spinal hemisection, but in this case a total section of the spinal cord was made with the spring scissors. The dura was previously cut and subjected in order to avoid the swelling of the tissue. A sharp needle was also used in this surgical procedure, in order to ensure again the complete disruption of the spinal cord tracts.

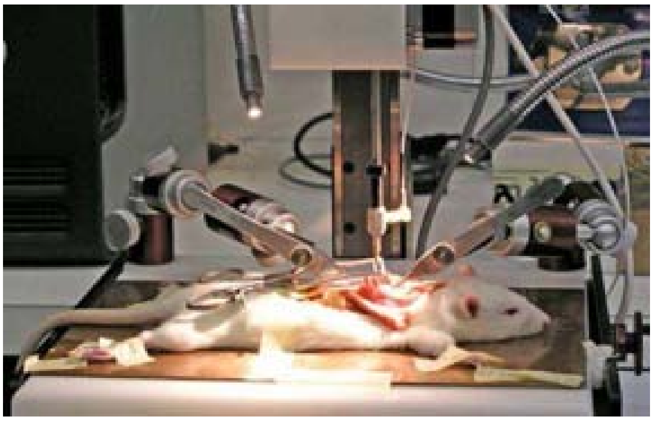

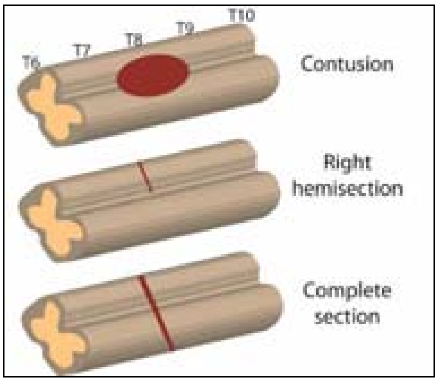

Fig 10: Left pannel: Image taken during a surgery, just before the contusion. Vertebraes T7 and T10 are clamped with forceps, while placed under the impactor device. Right pannel: schematic representation of the different injuries used in this thesis.

During the surgery, blood loss was limited as much as possible as well as the loss of body temperature, and bupivacaine was added as a local anesthetic. After finishing the lesion, the wound was sutured with silk sutures (5/0) in the muscle plain and with surgical staples in the skin. The dorsal skin was disinfected again with povidone iodine, animals were rehydrated (5-10ml of saline solution i.p.), and kept in a warm environment until fully recovery from the anesthesia.

Since the spinal injuries provoke a spinal shock that affect autonomic functions, bladders were emptied twice a day until reflex voiding was reestablished. Amoxicilin was given in the drinking water for one week to prevent postoperative infections. This treatment was continued if any sign of infection was detected in the daily revision of the animals.

It is important to consider that each type of lesion is more suitable for a determined purpose. The hemisection and the complete section represent good models to study some fringe features: while the complete section implies total disconnection with higher centers, the hemisection lesion supposes a minor affectation in most functions, since they show slightly minor deficits, although they can be similar to the ones present in a mild contusion injury. For this reason, hemisection animals were used in locomotion studies together with animals of different contusions (see chapter 2 of the results section).

Once the different consequences of the injuries were evaluated (spared tissue, painful responses, locomotion, etc), the milder contusion lesion (100kdyn) was used to test pharmacological treatments, since they are more versatile than the more severe ones, and slight differences are more easily observable than in animals severely injured. Nevertheless, the severe contusion injuries are more convenient in other kind of treatments, such as cell therapies, in which the best results are obtained in this kind of lesions.

Drug treatment

- **Glibenclamide**: this drug was directly administered after the contusion by means of an Hamilton syringe coupled to an automatic injector and using a glass capillary. One microgram dissolved in saline solution was injected in two injection points (1µl per point, at 0.5µg/µl). The injection was performed around two millimeters rostral and caudal to the epicenter of the lesion, and injected at low speed (2µl/min). The injection was done at 1mm of depth, and close to the midline, avoiding damage to blood vessels. After each injection, the capillary was maintained inside the cord parenchyma for a few minutes in order to avoid fluid spilling. Since glibenclamide can cause hypoglycemia, special care was given to the treated animals. As a precaution, rehydration after the surgery was done with saline solution and glucose.

- **Ibuprofen**: ibuprofen was started 30 minutes after the spinal cord contusion and administered twice daily since then (approximately every 12 hours). Ibuprofen was delivered subcutaneously at 60mg/kg, prepared in saline solution, and varying the injection site in order to avoid skin damage. The group of control animals were injected with saline solution, using a similar volume than in ibuprofen treated animals. The treatment was prolonged until the end of the follow-up (42dpo).

- **Combined group (GB+IBU):** just after the SCI, animals were injected with glibenclamide, as described above (intraparenchyma). The treatment with ibuprofen was started one week after, so it did not interfere with glibenclamide initial action. The dose and the protocol of administration was the same than for ibuprofen alone treatment.

Functional evaluation

- **Open field locomotor test:** Locomotor hindlimb function and recovery was assessed using the Basso, Beattie and Bresnahan (BBB) rating scale (Basso et al., 1995). Briefly, the BBB testing scale consists of an ordinal scale from 0 points (no discernable hind limb movement) to 21 points (consistent, coordinated gait with parallel paw placement of the hindlimb and consistent trunk stability (Table 4). For measuring locomotor recovery, one animal at a time was allowed to move freely inside a circular plastic tray (90 cm diameter x 24 cm wall height) for 5 minutes, and two examiners observed the hindlimbs movements of the rat. The final score of each animal was the mean value of both examiners. This test is performed at 3dpo and weekly thereafter until the end of the follow-up. It is also usually used as an internal control of the correct performance of the lesion, so animals with abnormal scorings due to problems with the surgery can be discarded at an early time.

- **Beam test:** For this test, a dark tunnel was designed (tunnel dimensions: 7 cm width, 13 cm height, 40 cm length) to allow the animals walking along an elevated beam (2.5 cm width, 2 cm height, 2 mm separated from the ground to allow the placement of a paper sheet). The hindpaw plantar surfaces were inked while the animal was gently subjected with a cotton cloth by the researcher. Then, the rat walked along the beam so only the missteps were recorded by ink prints on the paper placed under the beam. Three consecutive runs were performed, and the left and right missteps done in the first 30 cm were counted in each run. The mean of the three values was considered as the result for the animal in each testing day.

- **Inclined/graded plane test:** This test measures the ability of the animals to maintain their position in an inclined plane for at least five seconds. The angle of the surface is progressively increased, until recording the maximum angle supported by the animal that is scored as the outcome measure. A minimum of three trials are done to obtain the average value for each animal and day.

- **Digigait**: the Digigait system consists in a running belt coupled to a high speed camera that record videos from the bottom of the animals running on the belt. It is important to train animals in the running belt, by doing short trials at increasing speeds. A minimum of 9-10 regular steps must be recorded for each animal. The system includes a software that recognizes and digitizes every paw, depicting the sequence of steps. The same software is able to measure around 30 different gait parameters, if the gait sequence recorded is good enough. Coordination measurements can also be performed. Animals with spinal cord injury can walk in an irregular manner and not following a straight direction. This can cause problems with the recognition of the paws, that makes it difficult to correct further measurements. For this reason, some easy programming macros were done, in order to extract the length of every step and the sequence of alternation. Using correctly all the obtained data, different types of coordination and step patterns can be quantified.

- **Walking track and foot print analysis:** this is a useful technique to assess the recovery of locomotor function and changes in the normal gait posture, adapting the original technique set to study sciatic nerve lesions. The plantar surface of the rat paws was painted with red ink for forepaws and blue ink for hindpaws, and the rat left to walk along a corridor of 40 x 8 x 10 cm with a white paper on the base. Distances between forepaw prints (forelimb stance width) and between hindpaw prints (hindlimb stance width) were measured with a precision device in order to assess the base of support.

Fig 11: Representative images from different functional tests used in this thesis.

Table of BBB scores

0	No observable hind limb (HL) movement
1	Slight movement of one or two joints, usually hip and/or knee
2	Extensive movement of one joint **or** extensive movement of one joint ***and*** slight movement of one other joint
3	Extensive movement of two joints
4	Slight movement of all three joints
5	Slight movement of two joints **and** extensive movement of the third
6	Extensive movement of two joints **and** extensive movement of the third
7	Extensive movement of all three joints of the hind limb
8	Sweeping with no weight support **or** plantar placement of the paw with no weight support
9	Plantar placement of the paw with weight support in stance only (when stationary) **or** occasional, frequent, or consistent weight supported dorsal stepping and no plantar stepping.
10	Occasional weight supported plantar steps, no forelimb (FL)-HL coordination
11	Frequent to consistent weight supported plantar steps **and** no FL-HL coordination
12	Frequent to consistent weight supported plantar steps **and** occasional FL-HL coordination
13	Frequent to consistent weight supported plantar steps **and** frequent FL-HL coordination
14	Consistent weight supported plantar steps, consistent FL-HL coordination; **and** predominant paw position during locomotion is rotated (internally or externally) when it makes initial contact with the surface as well as just before it is lifted off at the end of stance **or** frequent plantar stepping, consistent FL-HL coordination, and occasional dorsal stepping
15	Consistent plantar stepping and consistent FL-HL coordination; **and** no toe clearance or occasional toe clearance during forward limb advancement; predominant paw position is parallel to the body at initial contact
16	Consistent plantar stepping and consistent FL-HL coordination during gait; **and** toe clearance occurs frequently during forward limb advancement; predominant paw position is parallel at initial contact and rotated at lift off
17	Consistent plantar stepping and consistent FL-HL coordination during gait; **and** toe clearance occurs frequently during forward limb advancement; predominant paw position is parallel at initial contact and lift off
18	Consistent plantar stepping and consistent FL-HL coordination during gait; **and** toe clearance occurs consistently during forward limb advancement; predominant paw position is parallel at initial contact and rotated at lift off
19	Consistent plantar stepping and consistent FL-HL coordination during gait; **and** toe clearance occurs consistently during forward limb advancement; predominant paw position is parallel at initial contact and lift off; and tail is down part or all of the time
20	Consistent plantar stepping and consistent coordinated gait; consistent toe clearance; predominant paw position is parallel at initial contact and lift off; tail consistently up; **and** trunk instability
21	Consistent plantar stepping and coordinated gait, consistent toe clearance, predominant paw position is parallel throughout stance, consistent trunk stability, tail consistently up. Normal locomotion.

Table 4: Scores used in the open field locomotion test.

Algesimetry tests

- **Mechanical algesimetry: electronic Von Frey**

Mechanical nociceptive thresholds of the hindpaws were determined using an electronic von Frey unit (Bioseb, Chaville, France). Rats were placed into a plastic box with an elevated metallic fine-grid surface, and acclimated to the test chamber for 20 minutes. From the bottom of the box, a metal tip attached to the sensor was applied directly to the glabrous surface of both hindpaws. The force applied (in grams) until the withdrawal of the paw was measured, being the value for the test the mean of at least three trials separated by 5 min resting periods. The maximal force was limited to 35 grams to avoid skin damage. Tests were performed if the animals had a BBB score higher than 8, indicating the ability to support their weight with the hindlimbs.

- **Mechanical algesimetry: Randall- Selitto test**

The Randall-Selitto test (Digital Paw Pressure Meter, IITC Life Science, Woodland Hills, CA) was performed in all animals in order to have algesimetric data also from complete section animals (and therefore with BBB score lower than 8). Before the test, each animal received some minutes of handling to get used to the manipulation; then it was placed into a soft cotton cloth and carefully immobilized with the same hand used to hold the tested paw. The test consisted of the application of an increasing mechanical force, in which the tip of the device was applied onto the medial portion of the plantar or the dorsal surface of both fore and hind paws until a withdrawal response resulted. The maximum force applied was limited to 250 g to avoid skin damage. This measurement can be done in all animals, independently of their locomotor performance, since they do not need to stand their own weight with the hindpaws (Santos-Nogueira et al., 2011).

- **Thermal algesimetry: Plantar test**

Thermal nociceptive sensitivity was evaluated using a thermal plantar algesimeter (Ugo Basile, Comerio, Italy). Animals were acclimated in a plexiglas testing chamber for 20 minutes. A movable light of a projection lamp (150W) was focused directly onto the plantar surface of the right and left hindpaws. The time to withdrawal of the heated paw (withdrawal latency) was measured through a time-meter coupled with infrared detectors directed to the plantar surface. The maximal time of stimulation was limited to 20 seconds to avoid skin damage. The value for each test was the mean of three trials separated by 5 min resting periods (Hargreaves et al., 1988). Tests were performed in rats with a BBB score higher than 8.

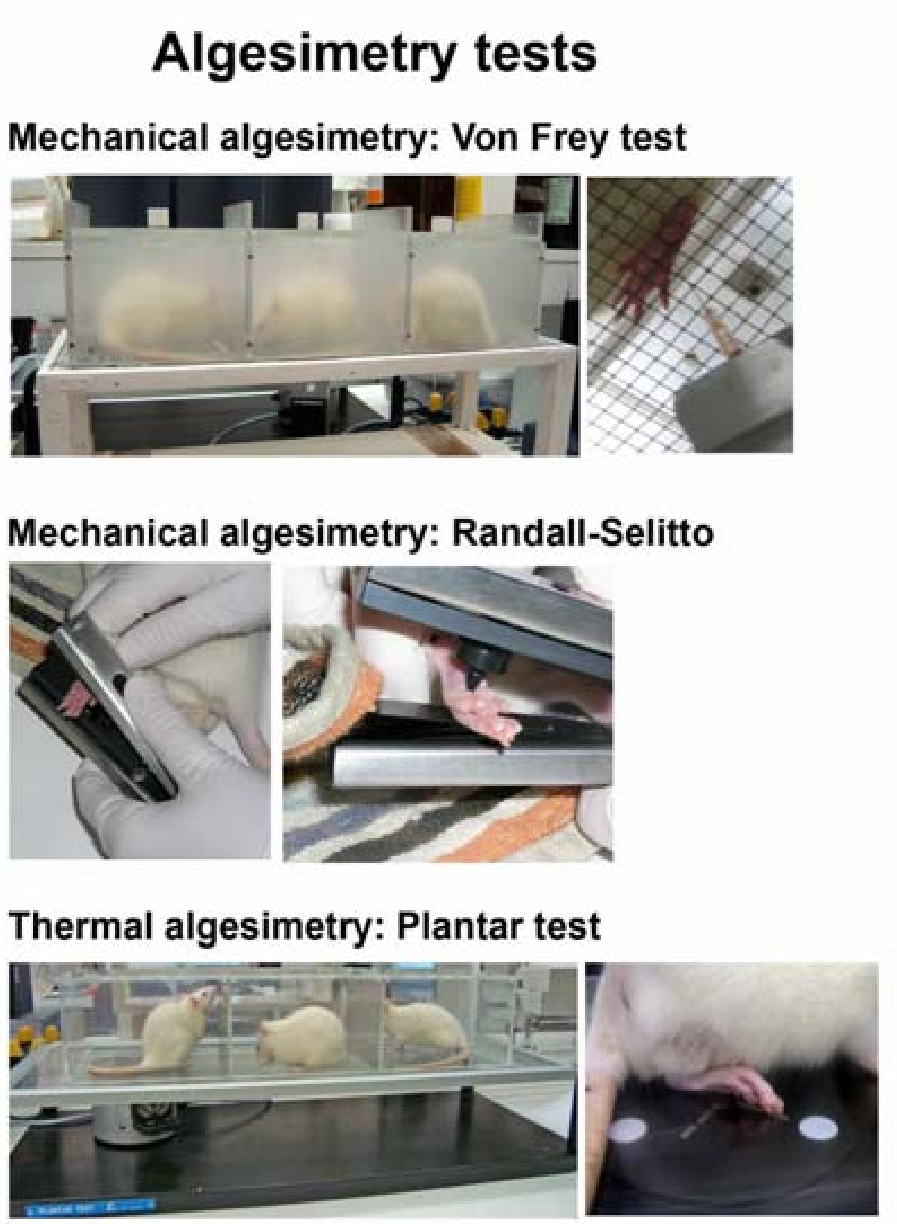

Fig. 12: Top pannel: mechanical algesimetry testing session. A sharp filament is pressed on the plantar surface of the animal through a grid surface. Middle pannel: Randall-Selitto device position in a testing session. Bottom pannel: Thermal algesimetry testing session. A radiant heat focus is placed under the hindpaws until the animal withdraw it.

Electrophysiology

Animals were anaesthetized with pentobarbital (30 mg/kg, i.p.; testing took around 30 minutes, so no additional anaesthetic dosages were required) and placed prone over a warmed flat coil controlled by a hot water circulating pump to maintain body temperature.

- **Peripheral nerve conduction**: Single electrical pulses (100 µs duration at supramaximal intensity) were delivered by monopolar needles (27G) inserted close to the sciatic notch. The compound muscle action potentials (**CMAP**) were recorded from the tibialis anterior and from the plantar interosseus muscles, by means of an active electrode inserted on the belly of the muscle and the reference electrode at the fourth toe (Valero-Cabré and Navarro, 2001; Valero-Cabré, et al., 2004). The responses with the highest amplitude were selected and used for analysis (Fig.13). The degree of hyperreflexia was calculated as the ratio between the maximal amplitude of the H wave and that of the M wave (Valero-Cabré and Navarro, 2001). Values from both hindlimbs of each animal were averaged.

- **Motor evoked potentials (MEPs)** were elicited by transcranial electrical stimulation, using two monopolar needle electrodes placed subcutaneously over the skull, the anode over the sensorimotor cortex and the cathode on the hard palate (García-Alías et al., 2006). Single rectangular pulses of 25 mA and 100 µs width, were delivered at 1 or 9 Hz, the optimal pulse rate to elicit the brainstem component (bs-MEP) and the cortical component (c-MEP), respectively. Recording electrodes (monopolar needles, 28 G) were placed in the tibialis anterior muscle. The muscle responses were displayed in an oscilloscope to measure the amplitude and latency of each component.

- **Somatosensory evoked potentials (SSEPs):** were evoked by electrical pulses of 6 mA and 100 µs of duration, delivered at 6 Hz to the tibial nerve at the ankle, and recorded by needle electrodes placed subcutaneously on the skull (same sites as stimulation needles for MEPs). Up to 256 responses were averaged on-line; the peak latency and the peak-to-peak amplitude were measured for N15, N20 and N30 waves (Valero-Cabré et al., 2004), referenced here as N1, N2 and N3 waves. SSEPs were repeated three times with minutes between trials, and the responses with the highest amplitude were selected and used for analysis.

In all cases, signals were amplified, filtered (bandpass 1Hz-5KHz), and displayed on an oscilloscope (Sapphire 4ME, Vickers).

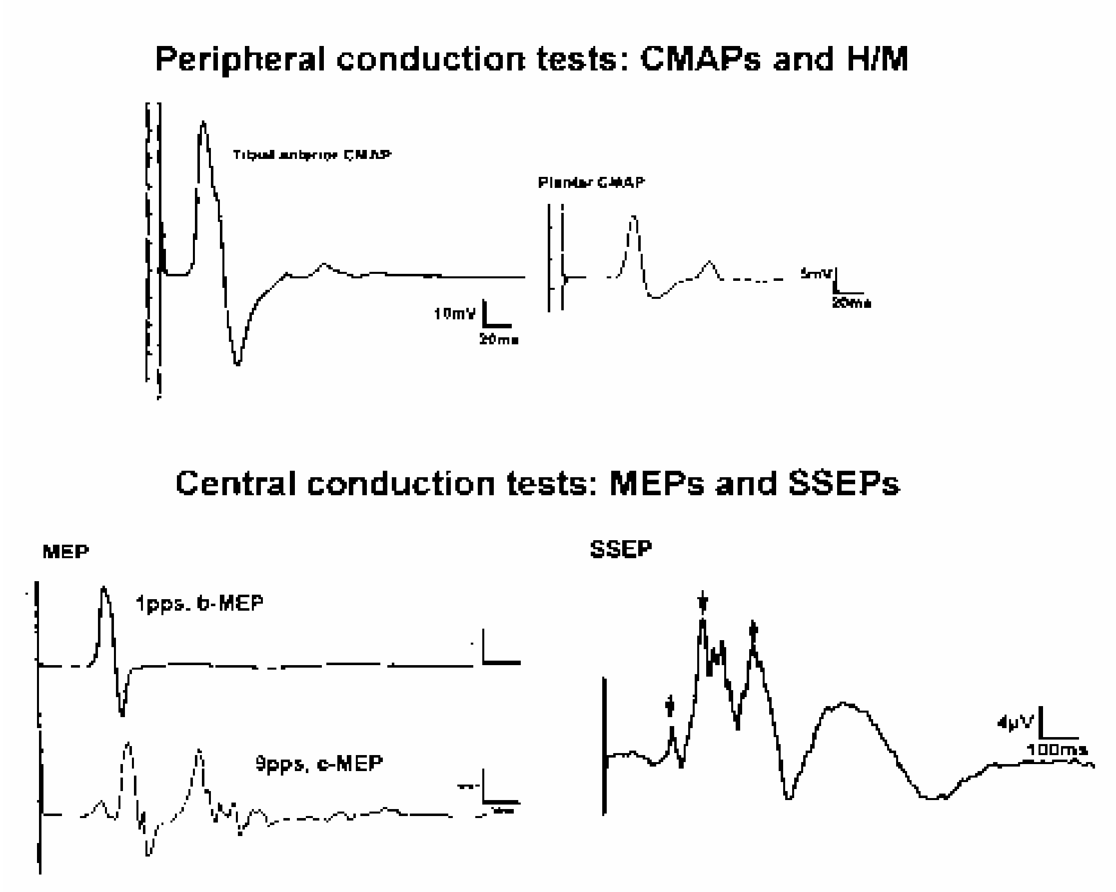

Fig. 13: Representative recordings obtained from intact animals. In the upper panels CMAPs of the tibialis anterior and the plantar muscles. The H wave, used as an indicator of hyperreflexia is especially evident in the plantar recordings. Lower pannels, recordings of MEPs from the tibialis anterior muscle, and SSEPs recorded on the skull, near to the somatosensory cortex (arrows indicate the three main components).

- **Wind-up responses:** were recorded from the tibialis anterior muscle using a modified protocol (Solano et al., 2003; Redondo Castro et al., 2011). Trains of repetitive electrical stimulation (16 pulses at 1 Hz, 1 ms width and 30 mA) were applied by means of monopolar needle electrodes, being the cathode inserted near the medial plantar nerve in the right paw and the anode between the fourth and fifth toes of the same paw. Electrical stimuli were supplied by a Grass S44 stimulator using an isolation unit (PSIU6; Grass Instruments Co., USA). For recording, the active needle electrode was placed in the tibialis anterior muscle, the reference electrode in the tendon at the ankle, and a ground electrode at the base of the tail. Responses were amplified 100 times with a Grass P511 amplifier, fed into a PowerLab/16SP system and recorded with Chart software (ADInstruments Ltd.). In each session, electromyographic wind-up responses were recorded (Fig. 14) and analyzed to measure the area under the curve (AUC) of each response, using Chart software and the RMS and Noise extension that determines the power content of a signal.

Data obtained from wind-up recordings can be expressed in different ways. The mean total activity is the mean increment achieved from the 2nd to the 16th stimuli when rectified for the first response; this representation is useful to see the general amplification. The second is the measure of the AUC of the first stimuli, as an indicator of the central excitability of the spinal cord before the train of repetitive stimuli (Redondo Castro et al., 2011). Some other measurements can include the maximal response, the slope achieved in the first five responses, etc. Each representation is useful to quantify different features of excitability (basal excitability, gain, …).

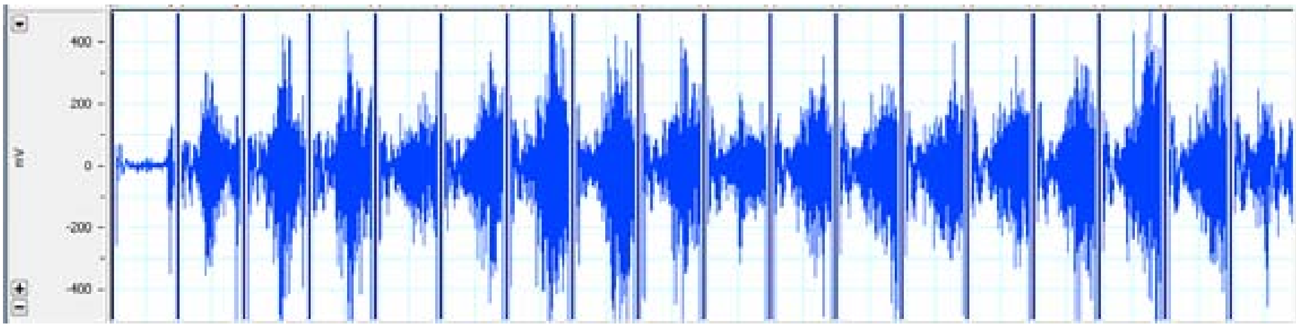

Fig. 14: representative recording of wind-up responses of an injured animal. The first response is very small, but after the second stimulus responses become increased respect the first.

- **Withdrawal reflexes** were measured using the same preparation as for wind-up responses. In this case reflexes were measured by delivering single electrical stimuli of 50 mA, 1 ms, using the same setting used in wind-up recordings. Measurements of the AUC of the C-fiber mediated response during the first second of the response were made to assess the intensity of the withdrawal reflex response (Valero-Cabré et al., 2004), although in some animals responses were longer lasting. Measurements included the AUC of the response in the first second, since is a simple way to normalize all the recordings, but also the total activity, the maximum amplitude or the duration of the response can be quantified (Fig. 15).

Fig. 15: representative recording of a withdrawal reflex recorded in the tibialis anterior muscle.

Retrograde labeling

At the end of the follow up, some animals were anesthetized with pentobarbital (40 mg/kg). The right hindlimb was gently shaved and disinfected with povidone-iodine. A small incision was done in the skin above the tibialis anterior muscle, and 5µl of 0.5% cholera toxin subunit B (CTB, List Biological Laboratories, CA) were injected, using a Hamilton syringe (10µl, serie 700) coupled with a 30G needle, in the proximal third of the muscle, close to the entrance of the peroneal nerve branch. The total injected volume was distributed in two or three injection sites to avoid muscle damage, and after every injection the needle was left in place for 20 seconds and then slowly removed to avoid leaking out of the tissue. The skin was closed with 2/0 silk thread and disinfected, and animals were rehydrated with saline solution. Five days later, animals were perfused in order to detect the motoneuron pools from the tibialis anterior muscle.

Perfusion and tissue harvesting

Transcardiac perfusion with 4% paraformaldehyde in phosphate-buffered saline was carried out in anesthetized rats at the end of the follow-up period. A T7-T10 spinal cord segment around the lesion epicenter was removed, post-fixed overnight and cryoprotected in 30% sucrose. The thoracic spinal cord segments were embedded in TissueTek and serially cut (30 µm thickness) in the transverse plane in a cryostat. Lumbar segments L1-L6 were also removed, embedded and cut at 20 µm thickness. Sections were collected onto gelatin-coated glass slides to further histological procedures.

Immunohistochemistry

Standard immunohistochemical protocols were followed for labeling different cells or molecules of interest in the study. Primary antibodies are listed in table 5; all of them were incubated with the samples overnight at 4ºC or for 1h at room temperature. Secondary antibodies were used always at room temperature for 2 hours, and protected from light. Cy3 anti mouse/rabbit secondary antibody (1:200, Jackson Immunoresearch, UK) was used for GFAP and Iba1 single immunohistochemistry, whereas for double immunodetections Alexa Fluor 488 or 594 were used (1:200, Invitrogen).

Antigen	Dilution	Manufacturer
Cholera toxin B subunit	1:5000	List biological laboratories
Choline acetyl transferase (ChAT)	1:50	Millipore
ED1 (CD68)	1:200	Serotec
Glutamic acid decarboxylase (GAD)	1:1000	Abcam
Gephyrin	1:300	Abcam
Glial fibrilary acidic protein (GFAP)	1:1000	Sigma
Isolectin B4 (ib4)	1:1000	Vector
Ionized calcium binding adaptor molecule 1 (Iba1)	1:1000	Wako
Calcitonin gene related peptide (CGRP)	1:500	Abcam
Serotonin	1:5000	Ultraclone

Table 5: Primary antibodies used in this thesis, the optimal dilution and the manufacturer.

Mixed glial cultures

Glial cell cultures were prepared from 1 day-old Sprague Dawley rats. Animals were decapitated and cortices immediately dissected out. After meninges and blood vessels were removed, the tissue was minced and incubated for 10 min at 37°C in Ca^{2+}-free Krebs-Ringer buffer containing 0.0025% trypsin. Cells were then mechanically triturated through a glass pipette and filtered through a 40-µm nylon mesh in the presence of 0.52 mg/ml soybean trypsin inhibitor and 170 IU/ml DNAse. After centrifugation (500g), the cells were stained with Trypan Blue exclusion dye, counted in a Neubauer chamber, and then resuspended (300000 cells/ml) in 90% DMEM, 10% FBS, 20 U/ml penicillin, and 20 mg /ml streptomycin. Cells were incubated at 37°C in a humidified atmosphere of 5% CO_2 and 95% air and used after 9-11 days in vitro; media replaced every 5-7 days. Microglial cells were separated from the mixed culture (astrocytes and microglia) by shaking the flasks during 3-4 hours at 300 rpm. Floating cells (microglia) were pelleted and subcultured at 100,000 cells/ml on mixed glial-conditioned medium.

In order to artificially activate microglia, LPS (10ng/ml) or a spinal cord lesion extract (100µg protein/ml) were added for 24h. **Lesion extracts** were obtained from injured spinal cords harvested 7 days after a 100kdyn spinal cord contusion. Fresh tissue was obtained from the lesion site (around 1cm) and frozen with liquid nitrogen. Samples were rinsed with liquid nitrogen a few times while being mechanically disgregated with a mortar and a pestle. Then the frozen particles were resuspended in DMEM media supplemented with a cocktail of inhibitors of proteases and disgregated. Finally, samples were sonicated for 5 minutes and centrifugated (15000 rcf, 5 minutes). Quantification of the protein content was done with the BCA method.

Glibenclamide and Ibuprofen were also addedd to the cultures, 24h after the addition of the activators, in order to study their effects directly on activated microglia.

Results

Results in this thesis are divided in four chapters. The first chapter is dedicated to the initial characterization and validation of the spinal cord injury model. We made special emphasis on the study of the development and establishment of neuropathic pain responses, as well as in changes in spinal excitability. Two publications are included in this first chapter, focused in the pain responses and in the spinal reflexes.

The next chapters deal with changes occuring below the lesion site, such as functional defficits regarding locomotion, which are fully described and quantified in the publication included in the second chapter. The third chapter includes a comprehensive review of the different elements altered in the lumbar segments after a thoracic spinal cord injury. Peripheral nerve preservation was also assessed in this chapter, which includes two publications.

Finally, the last chapter is dedicated to pharmacological strategies for the treatment of neuropathic pain responses, based on glial activity. This chapter also includes two publications. Different chapters are defined in the scheme below, and the number of publications included in each one is indicated by the sheet symbols.

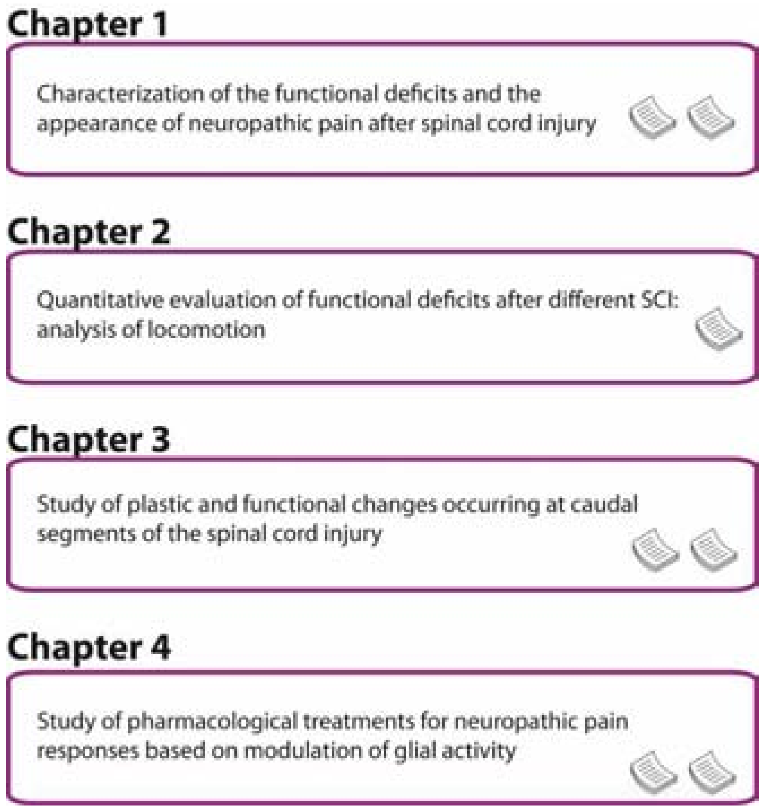

1

Characterization of the functional deficits and the appearance of neuropathic pain in different models of spinal cord injury

Specific objectives

The general objective of this chapter was the characterization of the functional deficits and the appearance of neuropathic pain in different models of spinal cord injury. This objective was divided in the following specific objectives:

1. Establishment of the model conditions in order to produce reproducible and accurate spinal cord contusions.

2. Assessment of the appearance of symptoms of chronic neuropathic pain in lesions of different severities. Characterization of pain responses to mechanical and thermal stimuli using different methods

3. Histological study of the injury site and of the glial response.

4. Characterization of electrophysiological changes occurring after SCI, with particular interest on withdrawal reflexes and wind-up responses that reflect the state of spinal excitability.

Introduction

This chapter is focused to the characterization of the spinal cord contusion model. For this reason we performed contusions of different severities, in order to evaluate differences in the nociceptive responses, the functional and electrophysiological (wind-up responses) outcomes, and the histological features (spared tissue and glial reactivity). All the contusions were performed using the Infinite Horizon Impactor device, which is linked to a software that records the parameters of the contusion, such as tissue displacement, velocity of the impact, and real force applied in the contusion.

The results are divided in two blocks, being the first aimed to characterize the appearance of thermal and mechanical hyperalgesia after different severities (100, 150 and 200kdyn) of spinal cord contusion. NP is one of the consequences that frequently occur after SCI, and can affect dermatomes below and above the injury site, as well as dermatomes of the injury site itself. Since the most common syndrome is the below-level pain, we assessed hyperalgesia in the hindlimbs. This extensive study permits to detect the onset and the maintenance of hyperalgesia up to two months of follow up. This part of the work was lately expanded with another method of pain assessment, the Randall-Selitto test. This test was applied in animals suffering different contusion severities and animals with complete section, and provided data regarding neuropathic pain above and below the level of the injury. This test was especially useful since most algesimetry tests are focused in the mesure of NP in the plantar surface of the hindlimb, so animals need to stand supporting their own weight. This excludes severe contusion and complete section animals from the customary tests. Moreover, the Randall-Selitto test can also be applied in dorsal as well as in plantar surface of the paws.

Finally, this study was complemented with the histological measurement of the lesion, and with electrophysiological outcomes, such as the assessment of withdrawal reflexes and wind-up responses that reflect the state of neuronal excitability in the spinal cord.

Characterization of the spinal cord contusion model

Validation of the injury model

In order to validate the SCI by contusion, we recorded the applied force and the tissue displacements to confirm that we were producing different but reproducible lesions. The velocity of the impact was also recorded, although it is known not to be an essential factor when determining the severity of the injury (Zhang et al., 2008).

The mean force applied was 103.5 ± 1.64 kdyn in the 100kdyn group, 155.67 ± 1.39 kdyn in the 150kdyn group and 232.56 ± 16.85kdyn in the 200kdyn group. These values were not significantly different from the expected forces. The displacements were 741.91 ± 26.74 in the 100kdyn group, 1071.67 ± 41.15 in the 150 kdyn group and 1433.50 ± 84.50 in the 200 kdyn group. For both parameters, statistical significance was achieved in all the comparisons between groups ($p<0.001$), indicating that the induced lesions were different between them. The two parameters kept a close relation with the severity of the functional deficits observed, as the BBB scores reflected (see table of scores in *Methods and Procedures* section). Thus, animals receiving a higher force suffered a larger displacement, and this produced more functional loss. While the animals receiving a mild lesion (100kdyn) presented good limb coordination at the end of the follow up, animals receiving a severe contusion (200kdyn) showed consistent weight support with the hindlimbs but the plantar stepping was not consistent, neither the coordination (Fig. 16). The functional deficits were proportional to the severity of the lesion.

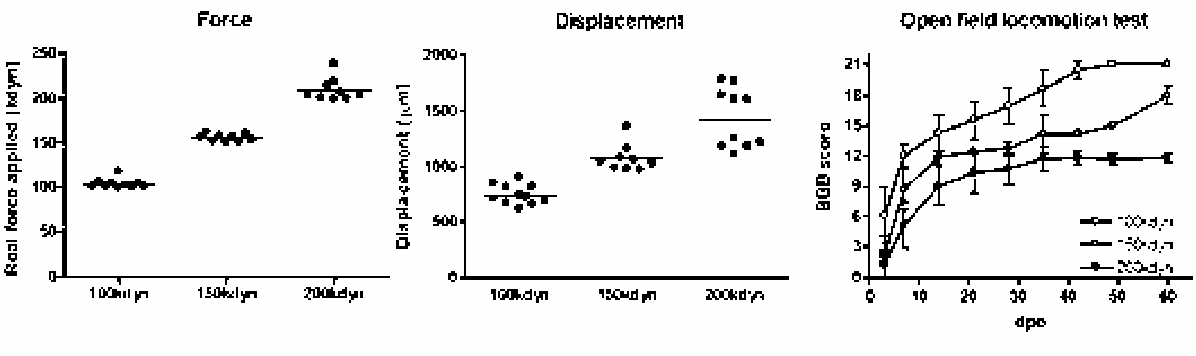

Fig. 16: Validation of the injury. Plots show the real force applied in each contusion and the displacement suffered by the spinal cord. Open field locomotion test results are also shown, indicating higher score in animals with milder lesions.

Appearance and maintenance of signs of neuropathic pain

Algesimetry tests were performed weekly to detect the appearance of symptoms of NP. Since the stimulus starts from the innocuous intensity, paw withdrawal response at low levels of stimulus intensity allow the detection of thermal and mechanical **hyperalgesia**. Because of the setting of the standard thermal and mechanical algesimetry tests used, only animals which can stand their own weight on the hindpaws were tested.

All the injured animals display a fast decrease in the mechanical and thermal thresholds when compared to values from intact animals. This reduction was detected in the first test sessions and was maintained until the end of the follow-up. It is interesting to note that all the injured groups displayed a similar reduction in the thresholds, independently of the severity of the injury they received (Fig.17).

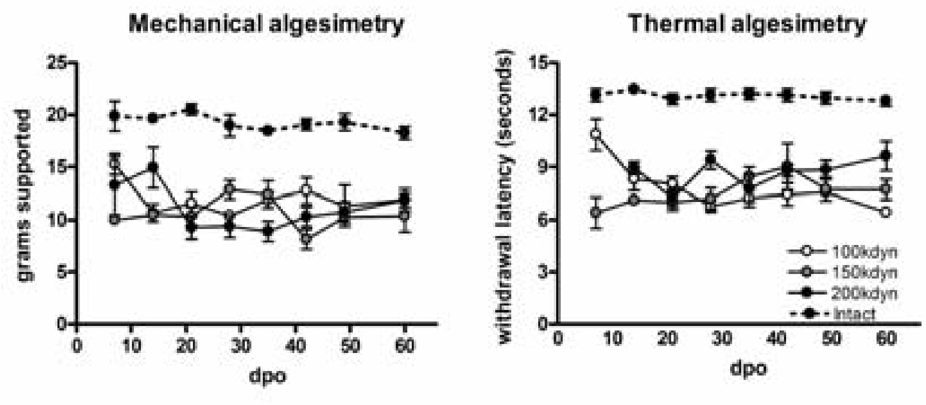

Fig. 17: Results of the algesimetry tests performed using mechanical and thermal stimuli. Results indicate that hyperalgesia occurs very early after the contusion and is mantained until at least the first two months. All the injured groups displayed a similar reduction in nociceptive thresholds despite the different severity applied in the SCI.

Cavity formation and glial reactivity

At the end of the follow up, animals were perfused and the spinal cords removed. Thin sections of 30µm thickness were serially cut, and an immunolabelling for the detection of GFAP was performed. This protein is upregulated in the activation of astrocytes, and after SCI permits the detection of the astrocytes surrounding the cavity and forming the glial scar, so it becomes a reliable method to measure the cavity as well as the tissue sparing. Both parameters keep a close relation to the severity of the injury, so they can also be used to validate the reproducibility of the model. In all groups, a clear cavity was observed at the epicenter of the injury, and was expanded rostrally and caudally for some millimeters (Fig.18).

The measurements of the preserved tissue indicated that the higher the force applied the higher the loss of tissue. Differences were especially clear in the epicenter, where 100kdyn animals only had a 64% of the tissue spared, a 50% in the 150kdyn group and a 40% in the

200kdyn, being these values significantly different in comparisons between groups. In order to gain more data about the progression of the formation of the cavity, some animals were perfused at 35 days, and their cavities were compared with cavities from injured spinal cords harvested 60 days after SCI. Measurements of the spared tissue were performed and no significant differences were found between the two time points, indicating that the cavity is already constituted at 35 dpo (data not shown).

The values obtained from the histological and functional assessments were correlated with the parameters of the contusion, but not with the results regarding hyperalgesia. This was the start of a new line of research focused on the plasticity of the spinal cord, since the study was displaced from the injury site to remote regions, such as the lumbar region, particularly to segments corresponding to L4 and L5, where the sensitivity of the hindlimbs is collected into the spinal cord.

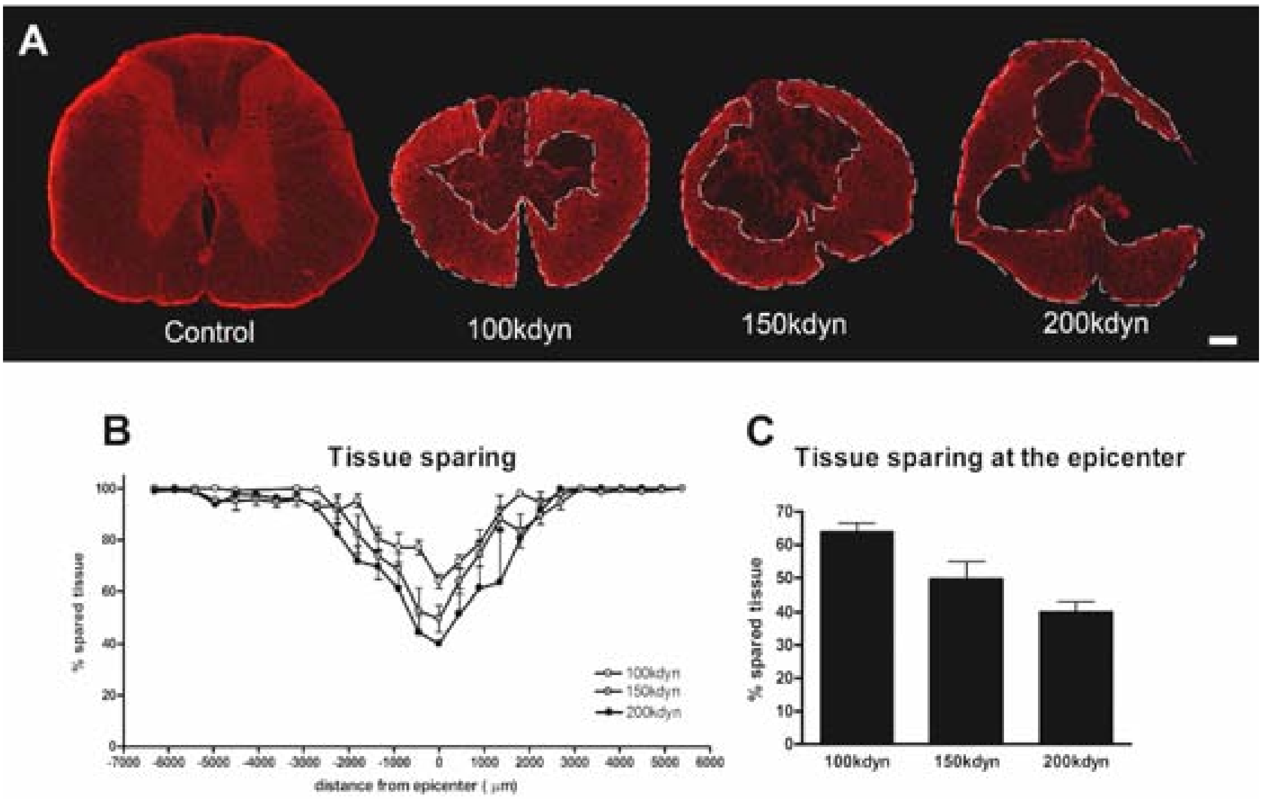

Fig. 18: Histological assessment of the contusion SCIs. A) Representative images depicting the epicenter of SCI at different severities of contusion. Scale bar: 200μm. Measurements of the tissue sparing along the spinal cord (B) and at the epicenter (C).

The glial reactivity was assessed in spinal cord samples from the injury site as well as from the lumbar region (Fig. 19). Microglia was evaluated by means of immunohistochemistry against

Iba1 and astrocytes by means of immunohistochemistry against GFAP. Both markers were over expressed in the injured animals, in almost all the gray matter. In both populations, cells displayed morphological changes that corresponded to a reactive state. These changes were visible at the injury site as well as in the lumbar segments, and were persistent in time. Measurements were performed in the dorsal horn of the lumbar regions, using a ROI (region of interest) that included the medial part of the superficial laminae. Measurements indicated an increase between 200-300% in the integrated density when compared to intact samples. This increase was detected at 35 and at 60 days post injury, confirming the persistent activation of both glial cell populations.

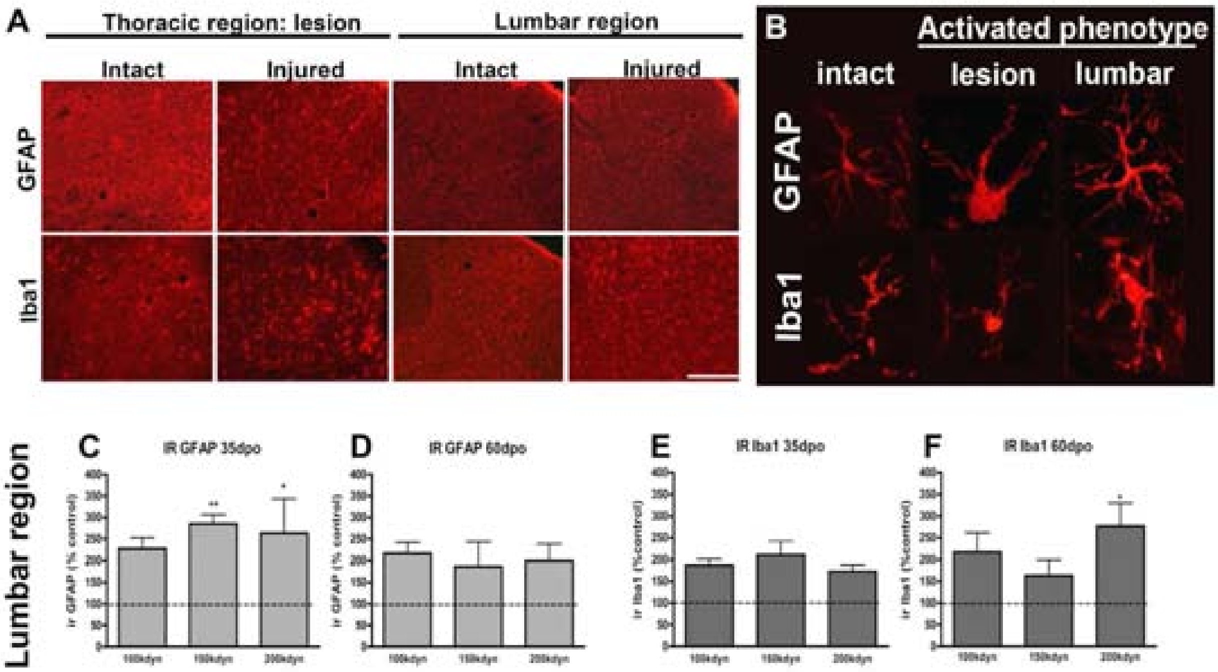

Fig. 19: A) Representative images from intact and injured rats, depicting the glial reactivity in the injury site as well as in the lumbar region. Scale bar: 100µm. B) Details of the morphology of microglial and astroglial cells. Activated phenotypes were observed in the lesion area as well as in remote regions. C-F) Quantification of the glial immunoreactivity in the dorsal horn of the lumbar segments. Data is expressed as mean ± SEM; statistical significance: *, p<0.05 vs. intact animals; **, p<0.01 vs. intact animals.

The histological measurements do not display a direct correlation neither with the parameters of injury severity, nor with the functional outcomes, but were more coherent with the algesimetric results.

Wind-up responses and withdrawal reflexes

Spinal cord injuries also cause electrophysiological changes in the spinal cord. Those can include spasticity, hyperreflexia, increased responses or hyperexcitability. From all of them, the ones more relevant to the study of neuropathic pain are those related to the nociceptive withdrawal reflex. In fact, sometimes they are used as indicators of hyperexcitability of the spinal circuits, and may play a role in some mechanisms of the NP. Reflexes are elaborated in front a sensory and noxious stimuli, and although some supraspinal input is always given, it is not fully necessary. Reflexes can be modulated by central hyperexcitability states as well as changes in the descending connections (Clarke and Harris, 2004).

In our models spinal reflexes were evaluated in the lumbar region, segments not directly affected by the injury, but that could have suffered some plastic changes after the injury. We used the neural circuits of withdrawal reflexes to assess the central hyperexcitability, and in order to find some alteration that may be involved in the generation of neuropathic pain symptoms. Using the same circuit but this time providing a repetitive stimulation, wind-up responses were also measured, since they can be directly involved in the generation of abnormal pain signals (Fig. 20).

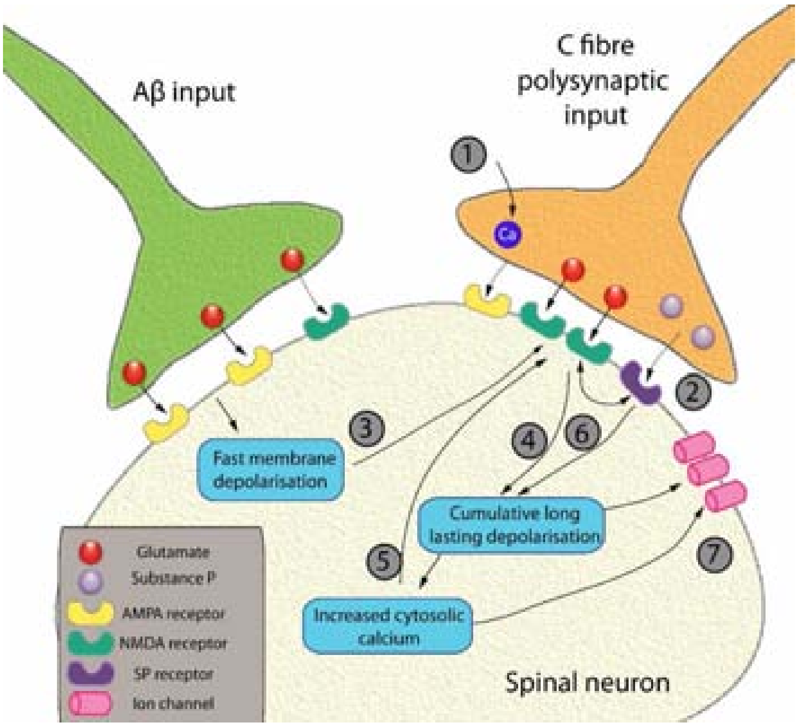

Fig. 20: Schematic representation of wind-up generation: (1) Increase of intracellular calcium in the presynaptic terminal leads to the increase in the release of amino acids and substance P (2). This causes the activation of AMPa receptors and a fasst membrane depolarization (3). This permits the removal of the magnesium blockade in NMDA receptors. The activation of NMDA and Nk1 receptors (4) causes a long lasting depolarization, implying an increase in the intracellular calcium in the spinal neuron. The increase is translated into a boosting of the receptor activity in the membrane (5,6), facilitating the generation of action potentials and therefore the generation of wind-up phenomenon. Adapted from Herrero et al., 2000.

Publication

Randall-Selitto test: A new approach for the detection of neuropathic pain after spinal cord injury

E. Santos-Nogueira*, E.Redondo Castro*, R.Mancuso*, X.Navarro

Journal of Neurotrauma, 2011; 8:1-8

* These authors contributed equally to this work.

JOURNAL OF NEUROTRAUMA 29:898–904 (March 20, 2012)

DOI: 10.1089/neu.2010.1700

Randall-Selitto Test: A New Approach for the Detection of Neuropathic Pain after Spinal Cord Injury

Eva Santos-Nogueira,* Elena Redondo Castro,* Renzo Mancuso,* and Xavier Navarro

Abstract

In this work we assess the usefulness of the Randall-Selitto test as a method to detect and quantify neuropathic pain responses in rats subjected to different spinal cord injuries. The mechanical nociceptive thresholds were significantly reduced during follow-up after spinal cord contusion or transection. Our results demonstrate that the Randall-Selitto test allows the detection of neuropathic pain both in forepaws and hindpaws, as well as in dorsal and plantar surfaces. Moreover, it does not require weight support capacity, so it can be used at early time points after the injury. This is the first time that this method has been used to describe the changes in nociceptive thresholds that take place after spinal cord injuries of different severities over time.

Key words: hyperalgesia; neuropathic pain; Randall-Selitto test; spinal cord injury; withdrawal threshold

Introduction

Spinal cord injury (SCI) causes loss of motor, sensory, and autonomic functions below the lesion level, in addition to plastic changes in neural circuits below and above the injury site that may trigger positive symptoms such as spasticity and neuropathic pain. Neuropathic pain is a major cause of disability, and interferes with functional recovery and patient's quality of life (Soler et al., 2007; Widerstrom-Noga et al., 2001). Based on the body areas where symptoms appear in relation to the site of the injury, neuropathic pain is classified as above-level, below-level, or at-level pain (Siddall et al., 1997). Animal models, such as the spinal cord contusion that parallels the injury characteristics described in most traumatic human SCI, have been demonstrated to induce mechanical and thermal allodynia in forelimbs (above-level), "girdling" (at-level), and in hindlimbs (below-level) (Hulsebosch et al., 2000).

Different techniques have been used to quantify and assess the development of neuropathic pain after SCI in animal models (Christensen et al., 1996; Christensen and Hulsebosch, 1997). Some of the most commonly used tests, in particular the Von Frey filaments (Detloff et al., 2010; Hogan et al., 2004; Le Bars et al., 2001) and the electronic Von Frey aesthesiometer (Liu et al., 2008), are designed for the detection of cutaneous mechanical hyperalgesia by applying mechanical stimuli to the plantar surfaces of the hindpaws. The Randall-Selitto test (Randall and Selitto, 1957), intended to serve as a tool to assess the effect of analgesic agents on the response thresholds to mechanical pressure stimulation, has been used by a number of investigators to evaluate inflammatory painful responses (Anseloni et al., 2003; Bujalska and Gumulka, 2001; Khasar et al., 1998; Lee et al., 2001). An electronic device based on the Randall-Selitto principle, which allows testing pain in a quantitative manner by pressuring different areas of the animal's body, has been developed. This test can be applied in both plantar and dorsal surfaces of forelimbs and hindlimbs of awake animals independent of their weight support ability, thus allowing the evaluation at early time points after injury. Moreover, this test can be considered a complement to cutaneous mechanical hyperalgesic tests since the Randall-Selitto test also evaluates nociceptive responses to deep mechanical stimuli.

The purpose of this study is to evaluate the potential of customary algesimetry tests, specifically the Randall-Selitto algesimetry test, to detect and quantify above- and below-level neuropathic pain in animals subjected to SCI of different severities. Since an important problem regarding pain assessment techniques is the high variability obtained in intra-individual measurements (Hogan et al., 2004), we analyze the repeatability of the technique with the aim of validating the obtained data. The results show that the Randall-Selitto technique is a reliable and repeatable method to detect and quantify below-level and above-level neuropathic pain in a rat model of

Group of Neuroplasticity and Regeneration, Institute of Neurosciences and Department of Cell Biology, Physiology and Immunology, Universitat Autònoma de Barcelon, and Centro de Investigación Biomédica en Red sobre Enfermedades Neurodegenerativas (CIBERNED), Bellaterra, Spain.

*These authors contributed equally to this work.

SCI. Moreover, it can be used to distinguish different kinds of SCIs, such as spinal cord contusion from complete section.

Methods

Laboratory animals

Adult female Sprague-Dawley rats (250–300 g body weight) were used. The animals were kept in standard laboratory conditions with 12 h light/dark periods at a temperature of 22±2°C and supplied with dry rat food and drinking water *ad libitum*. A total of 43 animals were used to perform all experiments: 33 for the algesimetry assay (25 injured and eight control intact animals, see below section on surgical procedure) and 10 for the repeatability analysis (see section on Randall-Selitto test). All experimental protocols were approved by the Ethics Committee of our institution, and followed the European Communities Council Directive 86/609/EEC.

Surgical procedure

Operations were performed under deep pentobarbital anesthesia (50 mg/kg i.p., Sigma, St. Louis, MO) and after subcutaneous injection of buprenorfine (0.05 mg/kg, Buprex, Schering-Plough, Kenilworth, NJ) near the incision site. The dorsum of the animal was shaved and disinfected with povidone iodine. A longitudinal midline incision was made through the skin and fascia, and paravertebral muscle insertions were gently removed along T8–T10 vertebral bodies. A T8 selective laminectomy was then practiced to expose the spinal cord, which was subjected to different injuries. In two groups of rats, the spinal cord was contused using the Infinite Horizon Impactor device (Precision Scientific Instruments, Lexington, UK), applying a fixed force of 100 kilodynes (group 100 kdyn, $n=8$) or 200 kdyn (group 200 kdyn, $n=8$). The actual force used to produce the injury was recorded, as well as the resultant displacement of the spinal cord. In a third group, the spinal cord was completely transected by means of a sharp scalpel at T8 vertebral level (complete section group, $n=9$). To ensure that the injury transected the whole spinal cord, both stumps were gently lifted away and repositioned back into the vertebral channel. In all surgeries, the wound was sutured with 5/0 silk thread in the muscular plane and small surgical clips in the skin plane to disinfect. Animals were kept in a warm environment until full recovery from anesthesia. Bladders were expressed twice a day until reflex voiding of the bladder was re-established.

Functional assessment

Locomotor hind paw function after injuries was assessed in an open field using the Basso, Beattie, and Bresnahan (BBB) rating scale (Basso et al., 1995). Briefly, the BBB testing scale scores locomotor ability from 0 points (no discernable hind paw movement) to 21 points (coordinated gait with parallel hind paw placement and consistent trunk stability). Scores from 0 to 8 indicate isolated movements in the three joints (hip, knee, and ankle). Scores 9 to 13 indicate the return of paw placement and coordinated movements with the forelimbs, whereas scores 14 to 21 indicate the return of consistent coordination, toe clearance during stepping, predominant parallel paw position, trunk stability, and elevation of the tail. Locomotor recovery was evaluated one animal at a time in an open enclosure of 90 cm diameter×24 cm wall height, allowing individuals to move freely for 5 min. Hind paw movements were observed by two examiners and the average score was used as the recorded value. The locomotor test was performed weekly up to 42 days post-operation.

Randall-Selitto test

Description. The nociceptive withdrawal threshold was assessed by using the Randall-Selitto electronic algesimeter (IITC 2500 Digital Paw Pressure Meter, IITC Life Science, Woodland Hills, CA). Before the test, each animal received 5 min of handling to get used to manipulation; then it was placed into a soft cotton cloth and carefully immobilized with the same hand used to hold the tested paw. The test consisted of the application of an increasing mechanical force, in which the tip of the device was applied onto the medial portion of the plantar or the dorsal surfaces of both fore and hind paws until a withdrawal response resulted (Fig. 1). The point of

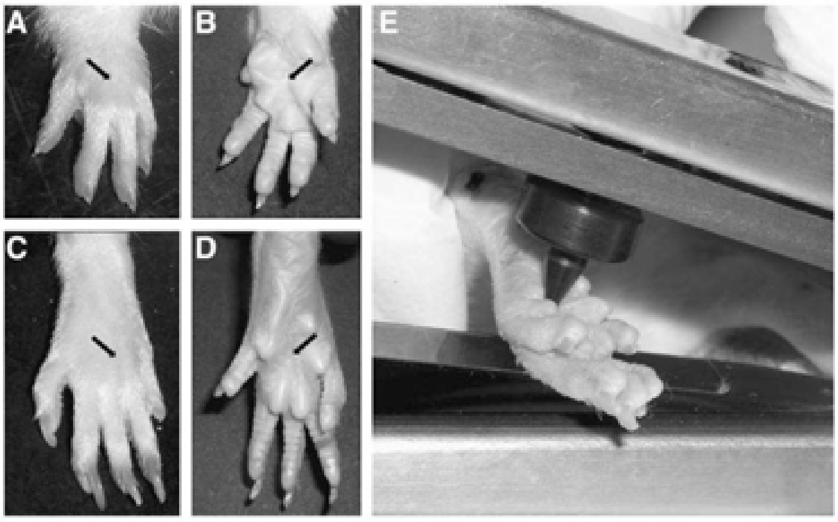

FIG. 1. Dorsal and plantar surfaces of fore (**A, B**) and hind paws (**C, D**), with black arrows indicating the point of application of the mechanical stimuli in the Randall-Selitto test. (**E**) Application of the tip of the Randall-Selitto probe during a test.

application was marked with ink in order to maintain the location over repeated trials. The maximum force applied was limited to 250 g to avoid skin damage. Measurements in the skin of the dorsal and lateral parts of the trunk were also performed to assess at-level neuropathic pain after SCI, with a maximum force of 350 g (400 g is the maximum reliable measurement suggested by the manufacturer). Because no response from the animals was observed in the trunk sites, the device used did not seem sensitive enough to detect pain response at this level; therefore, no further reference will be made regarding at-level pain testing.

Repeatability of technique. Repeatability quantifies the proportion of the total variance in multiple measurements of a trait that is due to differences among individuals. It is traditionally estimated using the intra-class correlation coefficient (Sokal and Rohlf, 1995), which is derived from one-way analysis of variance (ANOVA). It is understood that if repeated measurements of a given individual are very similar relative to the differences among individuals, then repeatability is high, and there may be little practical reason to obtain multiple measurements. If measurements within individuals are highly variable, then repeatability is low and a gain in precision is achieved by taking multiple measurements of individuals.

We estimated both intra- and inter-day repeatability from a sample of 10 control rats as follows. The Randall-Selitto test was performed once on each individual and, after an entire round on all individuals, it was repeated again on the same day for up to five times (the harmonic mean was 3.4). The observer was blind with respect to the results from previous measurements. The whole experimental protocol was repeated after one week. Intra-day repeatability was estimated as the intra-class correlation. Inter-day repeatability can also be estimated using the intra-class correlation coefficient from the averages of each rat on each day. However, this coefficient is very sensitive to changes in the average values of traits through time (Bulmer, 1985); for this reason, we first tested for average differences, which were very similar in magnitude for the different body parts (fore paw plantar surface, fore paw dorsal surface, hind paw plantar surface, and hind paw dorsal surface) in the one-week period.

Experimental assays. The potential use of the Randall-Selitto test to detect and quantify neuropathic pain in rats subjected to SCI was evaluated using the three groups of animals described in the surgical procedure section (100 kdyn contusion, 200 kdyn contusion, and complete section) plus a control group ($n = 8$; these animals were an independent sample to that used in the repeatability test). The Randall-Selitto test was performed on days 14, 28, and 42 after injury, and the order of stimulated sites was randomly assigned on each day. Because the estimated repeatability of the test was relatively low (see section on Results), the average of the measurements was used as the estimated value for neuropathic pain detection in a repeated-measures design ANOVA (see below section on neuropathic pain detection).

Statistical analysis

Side differences. Possible differences between right and left paws were assessed using conventional two-way ANOVA with individuals as a random factor and side as a fixed effect. Control and injured groups were analyzed separately at each time interval, and non-significant side differences were detected after correcting for multiple testing by using a sequential Bonferroni test. We therefore pooled right and left paw measurements to simplify statistical analyses.

Neuropathic pain detection. Since preliminary tests detected a positive correlation between the averages and standard deviations of the different groups, analyses were done after log-transforming the data (taking natural logarithms of each one of the repeated measurements for each individual on each day). Data analysis was performed with a multifactorial repeated-measurement ANOVA, considering the injury group and the body part as independent variables. To control for type I errors, post-hoc Bonferroni paired comparisons were performed when statistical significance ($p < 0.05$) was detected. The statistical software packages Statistica, v. 9 (StatSoft Inc., Tulsa, OH) and SPSS v. 15 (SPSS Inc., Chicago, IL) were used for statistical analyses.

Results

Spinal cord injury parameters and functional recovery

We estimated the accuracy of the actual force applied and the displacement suffered by the spinal cord in the two contusion injuries of 100 and 200 kdyn, since they are the main variables in the contusion technique (Cao et al., 2005; Scheff et al., 2003; Zhang et al., 2008). Animals from the 100 kdyn group received a mean impact force of 104.9 ± 2.08 kdyn, which is not statistically different from 100 ($p > 0.05$), whereas animals from the 200 kdyn group received a mean of 209.14 ± 3.61 kdyn ($p > 0.05$). The displacements suffered by the spinal cord averaged 807.63 ± 47.57 μm and 1468.71 ± 89.35 μm for the 100 kdyn and 200 kdyn groups, respectively. Therefore, the different forces applied lead to lesions of different severity.

The severity of the SCI is directly related to the functional recovery (Zhang et al., 2008). Functional recovery, assessed by the evaluation of voluntary locomotion (BBB test), is plotted in Figure 2. In animals from the 100 kdyn group the BBB score increased from 10.89 ± 0.31 one week after surgery to 16.0 ± 0.65 at the end of the study, when the rats displayed plantar stepping and consistent coordination, frequent toe clearance and rotated position of the paws at lift off. In the 200 kdyn group the BBB score averaged 4.82 ± 0.98 after one week and 10.07 ± 0.47 at six weeks; animals displayed occasional weight support and plantar stepping but no coordination between fore and hindlimbs. The average BBB scores were clearly different between these two groups (Fig. 2), but their rate of recovery was similar (that is, an average increase of 5.11 points from day 7 to day 42 in the 100 kdyn group, and 5.25 points in the 200 kdyn group). Animals with complete section had a mean score of ~1 point throughout the follow-up, indicating paralysis of the hind paws, with only some slight movements of one or two joints, most likely of reflex origin.

Repeatability

Individual differences were significantly repeatable (intra-class correlation coefficients) based on the individual

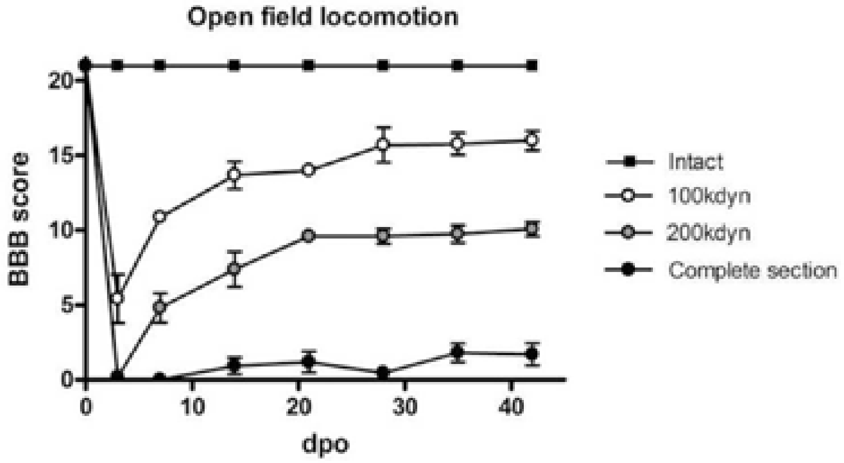

FIG. 2. Open field locomotion assessed by the BBB scale in the four groups of rats tested. All groups are significantly different ($p<0.05$) from day 7 to the end of the follow-up.

ANOVAs. The repeatability tended to be highest for plantar fore and hind paw testing (Table 1). As an average, individuals accounted for 41.4% and 21.0% of the intra-day variance and 38.2% and 28.9% of the inter-day variance for plantar and dorsal surfaces, respectively.

Neuropathic pain responses

When analyzing results from intact animals we found that thresholds found with the Randall-Selitto test were quite similar between fore- and hindlimbs. Paw dorsal surfaces were more sensitive to mechanical stimuli than plantar surfaces, so the mean threshold values were about 60% lower in the former (Table 2).

Table 2 shows the absolute values of the pain withdrawal threshold resulting from the application of the Randall-Selitto probe for each group of SCI rats on day of follow-up. Evidences of neuropathic pain were detected in all injury groups on nearly all the follow-up days compared to the control group. For the hindlimb, the decrease in the withdrawal threshold was comparatively greater when testing the plantar than the dorsal skin. The two groups with contusion injury (100 and 200 kdyn) showed roughly constant reduction of nociceptive threshold throughout the study, which was more marked, although not significantly, in the 200 kdyn group (Fig. 3). The complete section group displayed the highest pain response 2 weeks after surgery; its mechanical nociceptive threshold was statistically lower compared to the 100 kdyn group, but it tended to increase 4 weeks after surgery. Interestingly, Randall-Selitto tests performed on the forelimb also revealed a significant reduction in nociceptive thresholds, indicative of mechanical hyperalgesia following SCI. In this case, the reduction was similar and stable for 100 and 200 kdyn contusion groups during the study, whereas for the complete section group the thresholds were reduced 1 week after lesion but tended to reverse to normal values 4 weeks thereafter (Fig. 3).

Regarding the manifestation of neuropathic pain in different body areas with respect to the SCI site, values for the plantar surfaces showed that 100 and 200 kdyn groups presented significantly reduced mechanical nociceptive thresholds at both above- and below-level injury, while the complete section group presented more marked below- but not above-level pain.

Discussion

One of the main problems when studying neuropathic pain in animal models is the low availability of versatile techniques; hence most of them focus on the detection of pain in the hind paws. Hyperalgesic manifestations have already been described after traumatic lesions of the spinal cord (Christensen and Hulsebosch, 1997; Christensen et al., 1996). The Randall-Selitto test appears to be a useful method for

TABLE 1. CORRELATION MATRIX OF REPEATABILITY (INTRA-CLASS CORRELATION) FOR NOCICEPTIVE WITHDRAWAL THRESHOLD USING THE RANDALL-SELITTO TEST

	Plantar fore paw		*Dorsal fore paw*		*Plantar hind paw*		*Dorsal hind paw*	
	Day 1	*Day 2*	*Day 1*	*Day 2*	*Day 1*	*Day 2*	*Day 1*	*Day 2*
Day 1	<u>0.471</u> (0.002)	0.509 (0.048)	0.307 (0.035)	0.578 (0.026)	<u>0.417</u> (0.005)	0.254 (0.215)	0.047 (0.346)	0 (0.910)*
Day 2		0.405 (0.009)		0.255 (0.058)		0.363 (0.009)		0.230 (0.078)

For each body part, the diagonal values are the intra-day repeatability and the upper diagonal values are the inter-day repeatability (numbers in parentheses represent significance level from the one-way ANOVA). Repeatability underlined is significant ($p<0.05$) after correcting for multiple testing using Bonferroni test.

*The between-rats estimated variance from the ANOVA method was negative.

TABLE 2. SUPPORTED PRESSURE (IN GRAMS) IN FORE- AND HINDLIMBS AFTER SCI IN RATS SUBMITTED TO CONTUSION OR COMPLETE SECTION AT 14, 28, AND 42 DAYS POST-SURGERY

			100 kdyn			*200 kdyn*			*Complete section*		
	Day	*Control*	*14*	*28*	*42*	*14*	*28*	*42*	*14*	*28*	*42*
Forelimb	Plantar	170.3±12.5	117.3±9.65	116.8±12.7	128.2±12.0	105.9±16.1	124.8±13.0	117.12±16.2	116.3±14.3	162.2±14.5	176.7±7.5
	Dorsal	113.8±7.1	76.7±3.5	83.1±5.8	71.7±4.8	73.4±4.7	87.4±7.2	77.1±3.7	69.9±6.9	98.9±4.2	89.8±10.9
Hindlimb	Plantar	172.9±17.7	89.9±5.3	90.8±5.7	88.2±3.9	69.3±7.1	79.0±6.2	63.6±6.4	57.5±10.2	65.6±3.0	53.3±3.1
	Dorsal	97.6±8.6	73.9±5.6	81.2±5.3	73.3±2.4	57.6±5.5	57.3±5.5	51.2±5.5	50.0±6.6	53.5±2.5	46.3±4.0

Values are shown as mean±SEM. Values for control animals are shown as the mean of the three testing times. $n=8$–9 per group.

studying neuropathic pain conditions affecting both the fore- and hindlimbs, and thus responses corresponding to above and below the segmental level of the lesion. The test does not require the weight support ability of the animal, can be performed at early time points after the injury, and introduces the possibility of studying the dorsal surface area of the paws. In this study, we demonstrate the usefulness of the Randall-Selitto test to detect and quantify the appearance of neuropathic pain after SCI of different severities.

When focusing on the hindlimb responses, measurements obtained from rats after contusion injuries (100 and 200 kdyn) presented similarly reduced nociceptive thresholds compared to those of intact animals. No significant differences were detected between lesion groups, indicating that the severity of the SCI does not necessarily correspond to the degree of neuropathic pain signs (Redondo Castro et al., 2011; Zhang et al., 2008). Nonetheless, in the hindlimb measurements there is a tendency toward greater reduction in pain withdrawal threshold as the severity of the lesion increases, although without statistical significance. Other studies reported that a more severe lesion induced more pain (Knerlich-Lukoschus et al., 2008).

Regarding the side of the paw, the application of the pointed pressure on the dorsal surface caused less reduction in withdrawal threshold than when testing the plantar surface, as previously reported (Kauppila et al., 1998). The differences between plantar and dorsal surfaces may be due to intrinsic differences, since plantar thresholds were higher than dorsal thresholds in intact animals, probably because plantar stepping confers more resistance to the plantar skin. The hairy skin of the dorsum of the paw is thinner and presents a higher density of mechanoreceptors than the glabrous plantar skin (except in the plantar pads) (Verdú and Navarro, 1997). It is well-known that in conditions causing central sensitization (as in the case of SCI), not only nociceptors but also low threshold mechanoreceptors need a lower intensity of stimulation to elicit sensory responses (Cervero and Laird, 1996).

In examining the forelimb measurements in the contused animals, there were also reduced mechanical nociceptive thresholds compared to intact animals. These differences were maintained during the entire follow-up, thus indicating the appearance of above-level neuropathic pain after SCI (Carlton et al., 2009; Hulsebosch et al., 2009). On the other hand, animals with complete spinal cord section showed hyperreactive responses at 2 weeks after injury but not at later times, indicating normal nociception in the forelimbs. The difference in responses points to differences in plastic changes taking place at cord segments cranial to the lesion between incomplete and complete SCI. The maintenance over time of forelimb mechanical hyperalgesia in the contusion rats in contrast to the normalization in the complete section group may suggest that hyperexcitability in nociceptive spinal system cranial to the lesion may be sustained chronically by the persistent ascending spinothalamic pathways, which are abnormally active after SCI and have been suggested to function as a pain generator (Wasner et al., 2008). These findings may be of practical use for differentiating complete from incomplete spinal cord lesions based on the performance in the Randall-Selitto test when applied to the forelimbs.

In the case of the animals with complete section, all painful manifestations in hindlimbs should be attributed to reflex

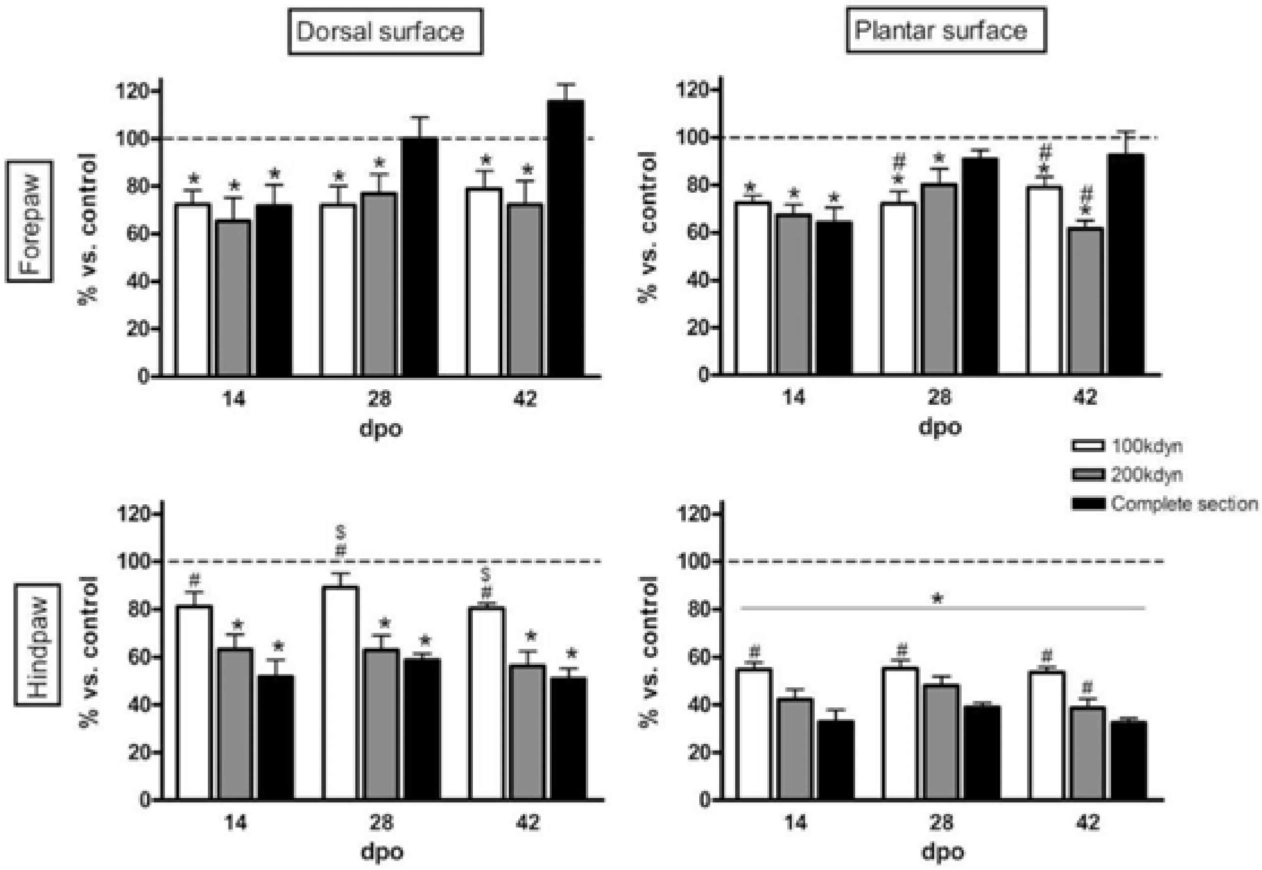

FIG. 3. Randall-Selitto measurements to assess neuropathic pain responses. Results are expressed as percentage of control values. Note that animals with spinal cord contusions show a slightly different pattern of hyperalgesic response than animals with complete transection. Dashed line represents the control values in each graph. Statistical significance: *$p < 0.05$ vs. control group; #, $p < 0.05$ vs. complete section; $, $p < 0.05$ vs. 200 kdyn.

responses, since the absence of motor and sensory evoked potentials proved that the section was complete and that no regeneration of ascending or descending pathways took place (data not shown) (Valero-Cabré et al., 2004). Thus, differences detected between contusion and section groups should be attributed to the residual ascending and descending tracts, and also the supraspinal modulation of nociceptive information (apart from the contribution of the reflex pathways), present in all cases. The distinction between abnormal pain and hyper-reflexia is rarely available in studies on the detection of neuropathic pain after SCI (Detloff et al., 2010).

When analyzing the data from the same day, the nociceptive withdrawal threshold using the Randall-Selitto test was significantly repeatable for plantar but not for dorsal surfaces (see Table 1). However, when repeatability was calculated between non-adjacent data, the associated probabilities were only sometimes significant. This marginal significance might reflect a low statistical power because only 10 individuals were used in the repeatability analysis. A recent meta-analysis using 759 estimates of repeatability suggests that 35% of the variation among individuals in behavior could be attributed to individual differences (Bell et al., 2009). The values of 41% for the intra-day and 38% for the inter-day variance for nociceptive withdrawal threshold of plantar surfaces are within the expected repeatability, which explains why pain assessment techniques are highly variable. Therefore, increasing the number of observations per individual will decrease the error around the withdrawal thresholds in this type of experiment. Moreover, the finding that higher repeatability was generally found for the plantar surfaces leads us to propose that Randall-Selitto test using only plantar surfaces is enough to provide reliable values to detect above- and below-level pain.

In conclusion, the results of this study highlight the use of the Randall-Selitto test as an adequate and sensitive method to evaluate neuropathic pain in both fore and hind paws, even at early stages, after SCI in experimental models, because it does not require animals to support their weight. Moreover, it permits the distinction of complete and incomplete spinal cord lesions. This supposes a new range of possibilities for the study of pain itself, as well as for the study of new therapies and treatments to modulate pain appearance.

Acknowledgments

This work was supported by grants from the Fundació MaratóTV3 (grant 070210), the Ministerio de Ciencia y Innovación (grant SAF2009-12495), and funds from Red de Terapia Celular (TERCEL, Instituto de Salud Carlos III) of Spain, and from FEDER. We thank Mauro Santos for his help with the statistical analysis, and Marta Morell, Abel Torres, and Samantha Dawley for their technical assistance.

Author Disclosure Statement

No competing financial interests exist.

References

Anseloni, V.C., Ennis, M., and Lidow, M.S. (2003). Optimization of the mechanical nociceptive threshold testing with the Randall-Selitto assay. J. Neurosci. Methods 131, 93–97.

Basso, D.M., Beattie, M.S., and Bresnahan, J.C. (1995). A sensitive and reliable locomotor rating scale for open field testing in rats. J. Neurotrauma 12, 1–21.

Bell, A.M., Hankison, S.J., and Laskowski, K.L. (2009). The repeatability of behaviour: a meta-analysis. Anim. Behav. 77, 771–783.

Bujalska. M., and Gumulka, W.S. (2001). Effect of cyclooxygenase and NO synthase inhibitors on antinociceptive action of acetaminophen. Pol. J. Pharmacol. 53, 341–350.

Bulmer, M.G. (1985). *The Mathematical Theory of Quantitative Genetics.* Clarendon Press: Oxford.

Cao, Q., Zhang, Y.P., Iannotti, C., DeVries, W.H., Xu, X.M., Shields, C.B., and Whittemore, S.R. (2005). Functional and electrophysiological changes after graded traumatic spinal cord injury in adult rat. Exp. Neurol. 191, Suppl 1, S3-S16.

Carlton, S.M., Du, J., Tan, H.Y., Nesic, O., Hargett, G.L., Bopp, A.C., Yamani, A., Lin, Q., Willis, W.D., and Hulsebosch, C.E. (2009). Peripheral and central sensitization in remote spinal cord regions contribute to central neuropathic pain after spinal cord injury. Pain 147, 265–276.

Cervero, F., and Laird, J.M. (1996). Mechanisms of touch-evoked pain (allodynia): a new model. Pain 68, 13–23.

Christensen, M.D., and Hulsebosch, C.E. (1997). Chronic central pain after spinal cord injury. J. Neurotrauma 14, 517–537.

Christensen, M.D., Everhart, A.W., Pickelman, J.T., and Hulsebosch, C.E. (1996). Mechanical and thermal allodynia in chronic central pain following spinal cord injury. Pain 68, 97–107.

Detloff, M.R., Clark, L.M., Hutchinson, K.J., Kloos, A.D., Fisher, L.C., and Basso, D.M. (2010). Validity of acute and chronic tactile sensory testing after spinal cord injury in rats. Exp. Neurol. 225, 366–376.

Hogan, Q., Sapunar, D., Modric-Jednacak, K., and McCallum, J.B. (2004). Detection of neuropathic pain in a rat model of peripheral nerve injury. Anesthesiology 101, 476–487.

Hulsebosch, C.E., Hains, B.C., Crown, E.D., and Carlton, S.M. (2009). Mechanisms of chronic central neuropathic pain after spinal cord injury. Brain Res. Rev. 60, 202–213.

Hulsebosch, C.E., Xu, G.Y., Perez-Polo, J.R., Westlund, K.N., Taylor, C.P., and McAdoo, D.J. (2000). Rodent model of chronic central pain after spinal cord contusion injury and effects of gabapentin. J. Neurotrauma 17, 1205–1217.

Kauppila, T., Kontinen, V.K., and Pertovaara, A. (1998). Weight bearing of the limb as a confounding factor in assessment of mechanical allodynia in rat. Pain 74, 55–59.

Khasar, S.G., Miao, F.J., Janig, W., and Levine, J.D. (1998). Vagotomy-induced enhancement of mechanical hyperalgesia in the rat is sympathoadrenal-mediated. J. Neurosci. 18, 3043–3049.

Knerlich-Lukoschus, F., Juraschek, M., Blomer, U., Lucius, R., Mehdorn, H.M., and Held-Feindt, J. (2008). Force-dependent development of neuropathic central pain and time-related CCL2/CCR2 expression after graded spinal cord contusion injuries of the rat. J. Neurotrauma 25, 427–448.

Le Bars, D., Gozariu, M., and Cadden, S.W. (2001). Animal models of nociception. Pharmacol. Rev. 53, 597–652.

Lee, E.B., Li, D.W., Hyun, J.E., Kim, I.H., and Whang, W.K. (2001). Anti-inflammatory activity of methanol extract of Kalopanax pictus bark and its fractions. J. Ethnopharmacol. 77, 197–201.

Liu, Y.M., Zhu, S.M., Wang, K.R., Feng, Z.Y., and Chen, Q.L. (2008). Effect of tramadol on immune responses and nociceptive thresholds in a rat model of incisional pain. J. Zhejiang Univ. Sci. 9, 895–902.

Randall, L.O., and Selitto, J.J. (1957). A method for measurement of analgesic activity on inflammed tissue. Arch. Int. Pharmacodyn. Ther. 111, 409–419.

Redondo Castro, E., Udina, E., Verdú, E., and Navarro, X. (2011). Longitudinal study of wind-up responses after graded spinal cord injuries in the adult rat. Restor. Neurol. Neurosci. doi: 10.3233/RNN-2011-0585

Scheff, S.W., Rabchevsky, A.G., Fugaccia, I., Main, J.A., and Lumpp, J.E., Jr. (2003). Experimental modeling of spinal cord injury: characterization of a force-defined injury device. J. Neurotrauma 20, 179–193.

Siddall, P.J., Taylor, D.A., and Cousins, M.J. (1997). Classification of pain following spinal cord injury. Spinal Cord 35, 69–75.

Sokal, R.R., and Rohlf, F.J. (1995). *Biometry,* 3rd ed. Freeman: New York.

Soler, M.D., Sauri-Ruiz, J., Curcoll-Gallemi, M.L., Benito-Penalva, J., Opisso-Salleras, E., Chamarro-Lusar, A., and Vidal-Samso, J. (2007). Characteristics of chronic neuropathic pain and their relationship with psychological well-being in spinal cord injury patients. Rev. Neurol. 44, 3–9.

Valero-Cabré, A., Forés, J., and Navarro, X. (2004). Reorganization of reflex responses mediated by different afferent sensory fibers after spinal cord transection. J. Neurophysiol. 91, 2838–2848.

Verdú, E., and Navarro, X. (1997). Comparison of immunohistochemical and functional reinnervation of skin and muscle after peripheral nerve injury. Exp. Neurol. 146, 187–198.

Wasner, G., Lee, B.B., Engel, S., and McLachlan, E. (2008). Residual spinothalamic tract pathways predict development of central pain after spinal cord injury. Brain 131, 2387–2400.

Widerstrom-Noga, E.G., Felipe-Cuervo, E., and Yezierski, R.P. (2001). Chronic pain after spinal injury: interference with sleep and daily activities. Arch. Phys. Med. Rehabil. 82, 1571–1577.

Zhang, Y.P., Burke, D.A., Shields, L.B., Chekmenev, S.Y., Dincman, T., Zhang, Y., Zheng, Y., Smith, R.R., Benton, R.L., DeVries, W.H., Hu, X., Magnuson, D.S., Whittemore, S.R., and Shields, C.B. (2008). Spinal cord contusion based on precise vertebral stabilization and tissue displacement measured by combined assessment to discriminate small functional differences. J. Neurotrauma 25, 1227–1240.

Address correspondence to:
Xavier Navarro, Ph.D.
Unitat de Fisiologia Mèdica
Facultat de Medicina
Universitat Autònoma de Barcelona
E-08193 Bellaterra
Spain

E-mail: xavier.navarro@uab.cat

Publication

Longitudinal study of wind-up responses after graded spinal cord injuries in the adult rat

E.Redondo Castro, E.Udina, E.Verdú, X.Navarro

Restorative Neurology and Neuroscience 2011; 29:115-26

Restorative Neurology and Neuroscience 29 (2011) 115–126
DOI 10.3233/RNN-2011-0585
IOS Press

Longitudinal study of wind-up responses after graded spinal cord injuries in the adult rat

Elena Redondo Castro, Esther Udina, Enrique Verdú and Xavier Navarro*
Group of Neuroplasticity and Regeneration, Institute of Neurosciences and Department of Cell Biology, Physiology and Immunology, Universitat Autònoma de Barcelona, and Centro de Investigación Biomédica en Red sobre Enfermedades Neurodegenerativas (CIBERNED), Bellaterra, Spain

Abstract. *Purpose*: The main objectives of this work were to evaluate the development of neuropathic pain after spinal cord injuries of different severities, and to assess changes in central excitability and plasticity by means of wind-up responses and withdrawal reflexes.
Methods: Two groups of rats were subjected to spinal cord contusion with forces of 100 or 200 kdyn applied at T8. Measurements of thermal and mechanical pain thresholds as well as wind-up measurements were performed weekly during two months after injury. Withdrawal reflexes were also assessed electrophysiologically.
Results: We found that animals with contusion of different severities showed a similar reduction in nociceptive thresholds. All contused animals showed increased wind-up responses compared to intact animals during the first 2 to 6 weeks post injury. The mean increase of wind-up was higher in rats with stronger spinal cord contusion. Results from the withdrawal reflexes did not correlate with nociceptive behaviors nor wind-up responses, highlighting the plasticity of spinal circuits modulation after SCI.
Conclusion: These results indicate that the graded-force spinal cord contusion model is suitable for studying central neuropathic pain, and for assessing changes in wind-up responses. Wind-up measurements can be used as a non-invasive technique to detect changes in central excitability after SCI of different severities.

Keywords: Spinal cord contusion, wind-up, below-level neuropathic pain, plasticity

1. Introduction

Spinal cord injuries (SCI) cause loss of motor, sensory and autonomic functions below the lesion level due to the discontinuity of ascending and descending spinal tracts. Plastic changes occur in segments below the injury, interfering with functional recovery and the quality of life of the patients. For example, disruption of the descending tracts produces neural hyperexcitability, leading to hyperreflexia and the so-called spastic syndrome (Lance, 1980). Plastic changes are also related to the development of chronic neuropathic pain, with a 65% prevalence in the first year after the lesion (Widerstrom-Noga et al., 2001; Soler et al., 2007).

Neuropathic pain in SCI subjects is classified as below-level or at-level pain, attending to the body areas where pain is perceived in relation to the injury site (Siddall et al., 1997). Mechanisms involved in the generation and maintenance of pain are disinhibition and central sensitization. Disinhibition is caused by death of spinal interneurons and reduction of the inhibitory tone in the spinal cord (Costigan and Woolf, 2000; Meisner et al., 2010), the loss of efficacy of endogenous opioids, and the increase in the synaptic activity of the spinal pain pathways (Woolf, 1983; White

*Corresponding author: Dr. Xavier Navarro, Unitat de Fisiologia Mèdica, Facultat de Medicina, Universitat Autònoma de Barcelona, E-08193 Bellaterra, Spain. E-mail: xavier.navarro@uab.cat.

et al., 2007). Hyperexcitability is facilitated by pain mediators secreted by immune and glial cells, eventually inducing sensitization of receptors and facilitation of neural responses to peripheral stimuli, provoking the initiation and maintenance of neuropathic pain (McMahon et al., 2005; Hains and Waxman, 2006).

To study effective therapies to overcome SCI consequences, it is important to define objective methods to evaluate the plastic changes and their modulation by different treatments. Below-level pain can be evidenced by algesimetry tests applied below the site of injury, whereas the excitability of spinal circuits can be evaluated by electrophysiological recordings of flexion/withdrawal reflexes and wind-up responses. Wind-up is a frequency-dependent increase in the excitability of spinal cord neurons when C-fibers are electrically stimulated (Mendell, 1966). It differs from other forms of synaptic plasticity such as long term potentiation, in that wind-up needs a low frequency input, its effects last only during the stimulation or some minutes later and it does not imply protein synthesis or generation of new synapses (Woolf, 1996). Wind-up has been studied in different animal models (mostly of inflammatory pain) and also in humans, and tested under different electrophysiological conditions, though there is no consensus about its pathophysiological role (for review, see Herrero et al., 2000). Although wind-up is a central manifestation, it can be studied by recording muscle activity (Gozariu et al., 1997), a more physiological preparation that allows detecting similar potentiation to that observed in dorsal horn neurons.

In this study we have evaluated below-level neuropathic pain, withdrawal reflexes and changes in wind-up responses after SCI in the rat. Injured rats showed mechanical and thermal hyperalgesia to a similar degree after mild and moderate SCI. The increase in wind-up responses, but not the increase in withdrawal reflexes, was related with the severity of the injury, indicating different modulation for both electrophysiological measurements.

2. Materials and methods

2.1. Laboratory animals

Adult female Sprague Dawley rats (8 weeks old; 250–300 grams) were housed with free access to food and water at a room temperature of 22 ± 2°C under a 12 : 12 light-dark cycles. All experimental procedures were approved by the Ethics Committee of our institution, and followed the European Communities Council Directive 86/609/EEC.

2.2. Surgical procedure

Operations were performed under pentobarbital anesthesia (50 mg/kg i.p., Sigma-Aldrich Química, Madrid), and after subcutaneous injection of buprenorphine (0.05 mg/kg, Buprex, Schering-Plough). After dorsal laminectomy at vertebrae T8-T9, the exposed subjacent spinal cord was contused using the Infinite Horizon impactor device (Precision Systems and Instrumentation, Fairfax Station, VA, USA), applying a force of 100 kilodynes (kdyn; group 100 kdyn, mild lesion, $n = 11$) or 200 kdyn (group 200 kdyn, moderate lesion, $n = 9$), as described in detail elsewhere (Scheff et al., 2003). Data from displacement and force applied was collected for each contusion to control reproducibility. Unoperated animals (intact group, $n = 8$) were used as controls. The wound was sutured with 5/0 silk thread in the muscular plane and skin closed with small surgical clips and disinfected with povidone iodine solution. Animals were kept in a warm environment until full recovery. Bladders were expressed twice a day until reflex voiding of the bladder was re-established, and amoxicillin was given in the drinking water (500 mg/l) during the first week post injury.

2.3. Functional evaluation

The locomotor hindlimb function was assessed using the Basso, Beattie and Bresnahan (BBB) rating scale (Basso et al., 1995). Briefly, the BBB testing scale consists of an ordinal scale from 0 points (no discernable hindlimb movement) to 21 points (consistent, coordinated gait with parallel paw placement of the hindlimb and consistent trunk stability). For measuring the locomotor recovery, one animal at a time was allowed to move freely inside a circular plastic tray (90 cm diameter × 24 cm wall height) for 5 minutes, and two examiners observed the hindlimb movements of the rat. The final score of each animal was the mean value given for both examiners. This test was performed at 3, 7, 14, 21, 28, 35, 42, 49 and 60 days post-operation (dpo). Only the animals that were able to support their weight with the hindlimbs (BBB-score ≥ 9)

were tested for mechanical and thermal nociceptive sensitivity (Knerlich-Lukoschus et al., 2008).

Mechanical nociceptive thresholds of the hindpaws were determined using an electronic von Frey unit (Bioseb, Chaville, France). The rats were placed into a plastic box with an elevated metallic fine-grid surface, and acclimated to the test chamber for 20 minutes. From the bottom of the box, a metal tip attached to the sensor was applied directly to the glabrous surface of both hindpaws. The force applied (in grams) until the withdrawal of the paw was measured, being the value for the test the mean of three trials separated by 5 min resting periods. The maximal force was limited to 35 grams to avoid skin damage.

Thermal nociceptive sensitivity was evaluated using a thermal plantar algesimeter (Ugo Basile, Comerio, Italy). Animals were acclimated in a plexiglas testing chamber for 20 minutes. A movable light of projection lamp (150W) was focused directly onto the plantar surface of the right and left hindpaws. The time until withdrawal of the heated paw (withdrawal latency) was measured through a time-meter coupled with infrared detectors directed to the plantar surface. The maximal time of stimulation was limited to 20 seconds to avoid skin damage. The value for each test was the mean of three trials separated by 5 min resting periods (Hargreaves et al., 1988).

2.4. *Electrophysiological recordings of wind-up*

Animals were anaesthetized with pentobarbital (40 mg/kg, i.p.; since each animal testing took ~20 minutes, no additional anaesthetic dosages were required), and placed prone over a warmed flat coil controlled by a hot water circulating pump to maintain body temperature. Wind-up evoked responses to repetitive electrical stimulation were recorded from the right tibialis anterior muscle using a protocol modified from Solano et al. (2003). Trains of repetitive electrical stimulation (1 Hz, 16 pulses, 1 ms width and 20 mA, ~0.7 times the threshold) were applied by means of monopolar needle electrodes, being the cathode inserted near the medial plantar nerve in the right paw, and the anode inserted between the fourth and fifth toes of the same paw. This configuration creates an electrical field that stimulates all sensory afferent nerve fibers in the hindpaw. The active recording needle electrode was placed in the mass of the tibialis anterior muscle, the reference electrode in the tendon at the ankle, and a ground electrode at the base of the tail. Electrical stimuli were supplied by a Grass S44 stimulator using a Grass isolation unit (PSIU6; Grass Instruments Co., USA). Responses were amplified 100 times with a Grass P511 amplifier, fed into a PowerLab/16SP system and recorded with Chart software (ADInstruments Ltd.). Electrophysiological tests were performed at 7, 14, 21, 28, 35, 42, 49 and 60 dpo.

In each session, electromyographic wind-up responses were recorded and analyzed to measure the area under the curve (AUC) of each response, by using Chart software and the RMS and Noise extension that determines the power content of a signal. We calculated the mean increase achieved from the second to the sixteenth response, using the AUC normalized by the first response, to evaluate only the increase and not the absolute value of the response. Increments were expressed as fold increase versus the first response, and values were expressed versus time or using the mean value of all the follow-up period to assess general tendencies. Another measurement of wind-up was done using the slope of the regression line obtained with the normalized AUC of the first five stimuli. In this interval the maximal response is usually reached, so this representation provides an indication of how fast is the amplification of the response.

A 200 kdyn contusion was performed in another group of animals ($n = 4$) and 14 days thereafter wind-up was measured before and after 10, 15, 20, 25 and 30 minutes of MK801 administration (0.5 mg/kg i.v., Tocris Biogen Científica, Madrid), to assess the implication of NMDA system in the generation of wind-up. Intact animals were also administered with the same drug; other intact and injured animals received only vehicle saline solution ($n = 4$ per each condition).

2.5. *Withdrawal reflexes*

Withdrawal reflexes were also measured at end point, by delivering single stimuli of 50 mA, 1ms, and using the same setting used in wind-up recordings. Several stimuli were applied, separated between them by a minimum of 30 seconds. Measurements of the AUC of the C-fiber mediated response during the first second of the response were made to assess the intensity of the withdrawal reflex response (Valero-Cabre et al., 2004), although in some animals responses were longer lasting.

2.6. Immunohistochemistry

Transcardiac perfusion with 4% paraformaldehyde in phosphate-buffered saline was carried out in anesthetized rats at 60 days after SCI. A T7-T10 spinal cord segment around the lesion epicenter was removed, post-fixed overnight and cryoprotected in 30% sucrose. The spinal cord segments were embedded in TissueTek and serially cut (30 µm thickness) in the transverse plane in a cryostat. Sections were collected onto gelatin-coated glass slides and immunostained with primary antibody against glial fibrillary acidic protein (GFAP, Sigma, 1/1000), and Cy 3 (Jackson Immunoresearch) as secondary antibody. Images of the spinal cord sections were taken at 40X. Then, the spared tissue area was measured, using Image J software (National Institutes of Health, USA), and expressed as the percentage with respect to the total area of the spinal cord section.

2.7. Statistical analysis

Data are shown as the mean ± SEM. Statistical comparisons between groups were made using ANOVA with Bonferroni *post hoc* tests (GraphPad Prism software). Differences between groups were considered statistically significant if $p < 0.05$.

3. Results

3.1. Validation of the SCI

In order to assess that our groups were receiving lesions of graded severity, the real force applied and the displacement of the spinal cord produced by the impact were monitored. In the group with 100 kdyn contusion the measured force applied averaged 103.5 ± 1.6 kdyn, and the mean displacement was 741 ± 27 µm. In the group with 200 kdyn contusion the mean force applied was 209.0 ± 4.1 kdyn and the displacement was 1434 ± 85 µm. Both parameters were significantly higher in the 200 kdyn group compared with the 100 kdyn group ($p < 0.001$).

The locomotor test was performed weekly after the day of the contusion. The animals contused with 100 kdyn force reached the maximum score of the test (21 points, normal locomotion) before the end of the follow up, whereas the group that received the 200 kdyn contusion never exceeded 12 points (meaning that animals made frequent to consistent weight supported plantar steps and occasional forelimb-hindlimb coordination); intact animals scored 21 points during all the follow-up (Fig. 1).

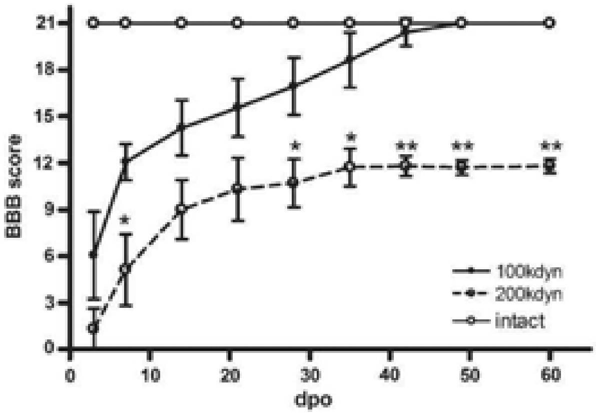

Fig. 1. Results of the open field locomotion test, scored by the BBB scale, following SCI. The two different severities in the contusion resulted in significant differences in the recovery of locomotion; whereas 100 kdyn injured animals reached normal locomotion (21 points), the 200 kdyn injured animals only reached values near 12 points (*$p < 0.05$; **$p < 0.001$ 200 kdyn vs. 100 kdyn). Intact animals presented normal locomotion (21 points) during the follow-up.

We also assessed histological differences between the groups receiving different contusion forces. The amount of spared tissue at the epicenter (defined as the section with the maximum cavity) was quantified on transverse spinal cord sections immunolabeled against GFAP (Fig. 2), in order to detect the perimeter of the cavity delimited by the glial scar. Animals with a 100 kdyn lesion showed a preservation of 63 ± 3% of the cord tissue, whereas the 200 kdyn lesion group showed only 40 ± 3% spared tissue. These values were significantly different between them ($p < 0.001$), further indicating that the two forces applied in the contusion caused lesions of different severity.

3.2. Functional evaluation of nociceptive responses

Every week after SCI, animals were subjected to mechanical and thermal algesimetry tests. All injured rats showed an increase in the sensitivity to mechanical and thermal stimuli, which was observed from the second week after injury and was maintained during all the follow-up period (Fig. 3). In the mechanical test, intact animals showed paw withdrawal thresholds around

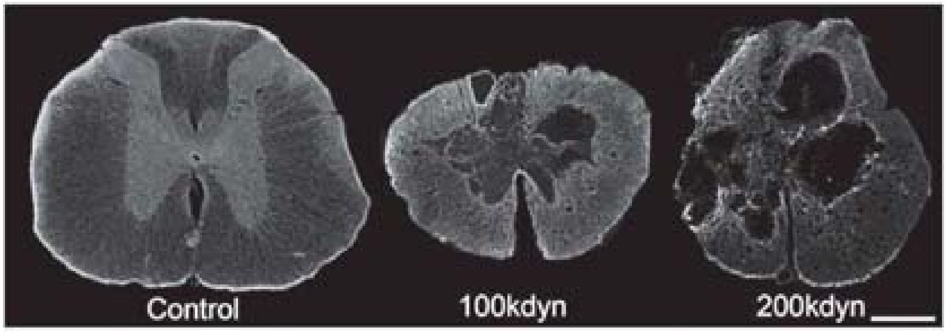

Fig. 2. Representative histological transverse sections of the contused spinal cords immunolabeled for GFAP. The different amount of spared tissue is easily observable in these images taken from the epicenter of the lesion at 2 months after injury. Sections from 100 kdyn contusion showed loss of dorsal cord tissue, while 200 kdyn contusion provoked a more spread loss of tissue. Bar: 500 μm.

19–20 g during the two months follow-up, while the injured ones had lower values around 8–12 g. The values of both groups with SCI were significantly lower than the intact animal values ($p < 0.001$), but there were no differences between injured groups. In the thermal algesimetry test, intact animals showed withdrawal latencies of 13–14 seconds, whereas in injured rats latencies were reduced to 7–8 seconds. This reduction in heat nociceptive threshold was again statistically significant compared to intact animal values ($p < 0.001$), but no differences were found between 100 kdyn and 200 kdyn injured groups. These data indicated that contusive SCI caused stable and persistent signs of neuropathic pain, to a similar degree independently of the severity of the lesion.

3.3. Electrophysiological evaluation of wind-up responses

A group of intact animals was used to obtain control values for wind-up, and was tested weekly in order to rule out any effect of repeated anesthesia and stimulation. Intact animals showed electromyographic recordings with slight wind-up effect and considerable variability between individuals. The electromyographic responses were weak, with a few motor unit spikes and small summation between responses (Fig. 4). In SCI rats the responses were much more pronounced, with intense bursts of activity beginning between the second and the fifth stimuli. This amplification reached a plateau around the fifth stimuli and was maintained until the last stimulus (16th). All the injured animals showed increased responses during the two months of follow-up. In some cases muscular activity lasted more than one minute after the last stimulus (data not shown). Such persistent activity was never observed in intact animals.

Due to the different criteria described in the literature to measure and quantify wind-up responses, we used different approaches in our study, always using the area under the curve of each response as the measure of muscular reflex activity. For convenience, all values from intact animals were unified in one single value (mean of all the test days and animals).

In a first approach, the wind-up response for each day and animal was assessed by calculating the mean AUC of the 2nd to the 16th response (normalized values). In Fig. 5A, the mean values for each group every day of testing are represented. The group of intact animals had a wind-up increase of 2.04 ± 0.03 times the first response. During the two months of follow-up, contused animals showed increased wind-up responses versus intact animals. Maximum wind-up responses were achieved at 14, 21 and 28 days in 100 kdyn contused animals (2.84 ± 0.24, 2.89 ± 0.20, 2.84 ± 0.31 times the first response, respectively), while the 200 kdyn group presented the maximum wind-up responses between days 28 and 42 post injury (4.3 ± 0.4 and 3.6 ± 0.4, respectively). The responses were significantly higher in the 200 kdyn group than in the 100 kdyn group at 28 and 42 dpo ($p < 0.001$ and $p < 0.05$ respectively). In both injured groups, wind-up responses tended to normalize during the last two weeks of follow-up (49 and 60 dpo).

Since wind-up responses did not present a clear pattern along the time after SCI, a second calculation was done using the mean increase (AUC from the 2nd to the 16th stimulus, normalized with respect to the first response) but considering now data from all the follow-up period. In this case, contused animals showed a large

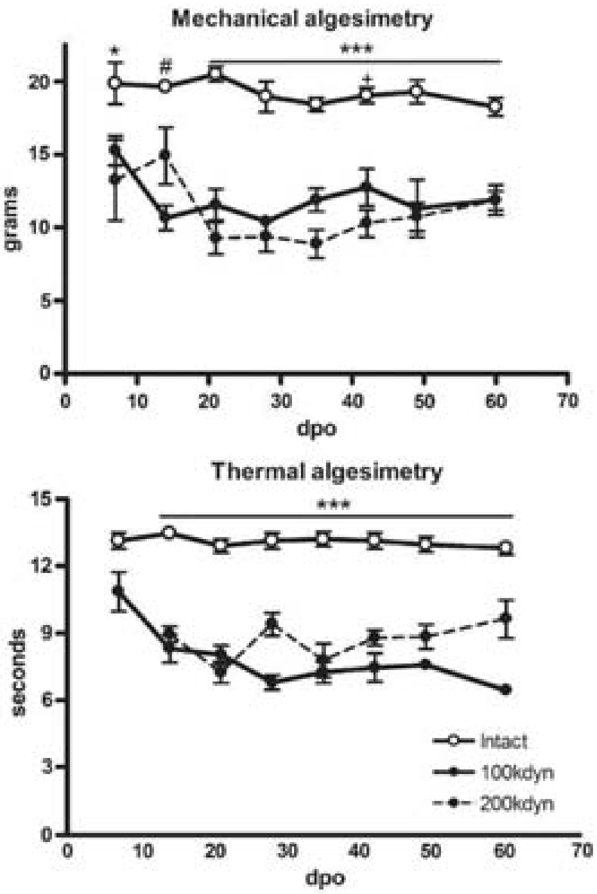

Fig. 3. Results of the algesimetry tests during follow-up after SCI. In the upper panel, results from the mechanical algesimetry tests show a decrease in the nociceptive threshold for mechanical stimuli in both groups of injured animals. In the bottom panel, results from thermal algesimetry tests show a similar trend for decrease in nociceptive thresholds. In both tests, hipersensitivity started at the first week postinjury and was maintained until the end of the 2 months follow-up. Values were significantly different from values of intact animals: $^{*}p<0.05$, 100 and 200 kdyn groups vs. intact group; $^{***}p<0.001$, 100 and 200 kdyn groups vs. intact group; $^{\#}p<0.001$ intact vs. 100 kdyn group.

wind-up facilitation, with a mean increase of 2.6 ± 0.3 in 100 kdyn rats and 3.0 ± 0.26 in 200 kdyn rats, significantly higher than the increase of 2.04 ± 0.03 times the first response in intact rats (Fig. 5B).

A third approach to evaluate wind-up responses was made by calculating the mean slope of the regression line generated for the AUC from the first five responses (Kimura and Kontani, 2008), in order to appreciate how fast the maximum facilitation was reached (usually observed in this interval). For this calculation, data were also collected from all the follow up period in order to obtain the mean slope for each group during the two first months after SCI. The slopes showed increasing values with the severity of the lesion (Fig. 5C). Slope values were 0.24 ± 0.06 for intact animals, 0.41 ± 0.05 for the 100 kdyn group, 0.53 ± 0.07 for the 200 kdyn group.

3.4. Pharmacological modulation of wind-up responses

In order to verify the mechanisms involved in the wind-up responses, pharmacological inhibition experiments were performed. We used MK801, an antagonist of NMDA receptors, to block the NMDA receptor function and to confirm its implication in the generation of wind-up responses (Davies and Lodge, 1987; Dickenson and Sullivan, 1987; Xu et al., 1995). Wind-up responses were measured in intact ($n=4$) and contused animals (200 kdyn, 14 dpo, $n=4$), before and after the administration of MK801. This drug caused a reduction of wind-up responses, with about 70% inhibition in both intact and contused animals (Fig. 6). The injection of vehicle saline solution caused no changes in wind-up responses (data not shown).

3.5. Withdrawal reflex responses

Withdrawal reflex testing can be used as an index of nociceptive responsiveness in animals (Clarke and Harris, 2004). In intact rats, stimulation of the medial plantar nerve consistently yielded a withdrawal reflex response in the ipsilateral tibialis anterior muscle, recorded as bursts of motor unit action potentials grouped in three components (Valero-Cabre et al., 2004). The third component (C3), that is dependent on activation of C afferent fibers, was detected starting at 120–135 ms after trigger, and had long duration. Withdrawal reflexes were also tested in spinal cord contused rats (Fig. 7A), which showed enhanced responses of longer duration than the controls (1 second in intact animals, 7 seconds in 100 kdyn group and 2, 3 seconds in 200 kdyn group). Measurements of the AUC during the first second of activity were done to assess facilitation in the polysynaptic spinal reflex circuit function. The mean AUC was significantly higher in rats of the 100 kdyn group than in the intact group (452.3 ± 114.9 µV·s vs 59.4 ± 26.4 µV·s, respectively, $p<0.01$) and in the 200 kdyn group (122.9 ± 34.1 µV·s) (Fig. 7B).

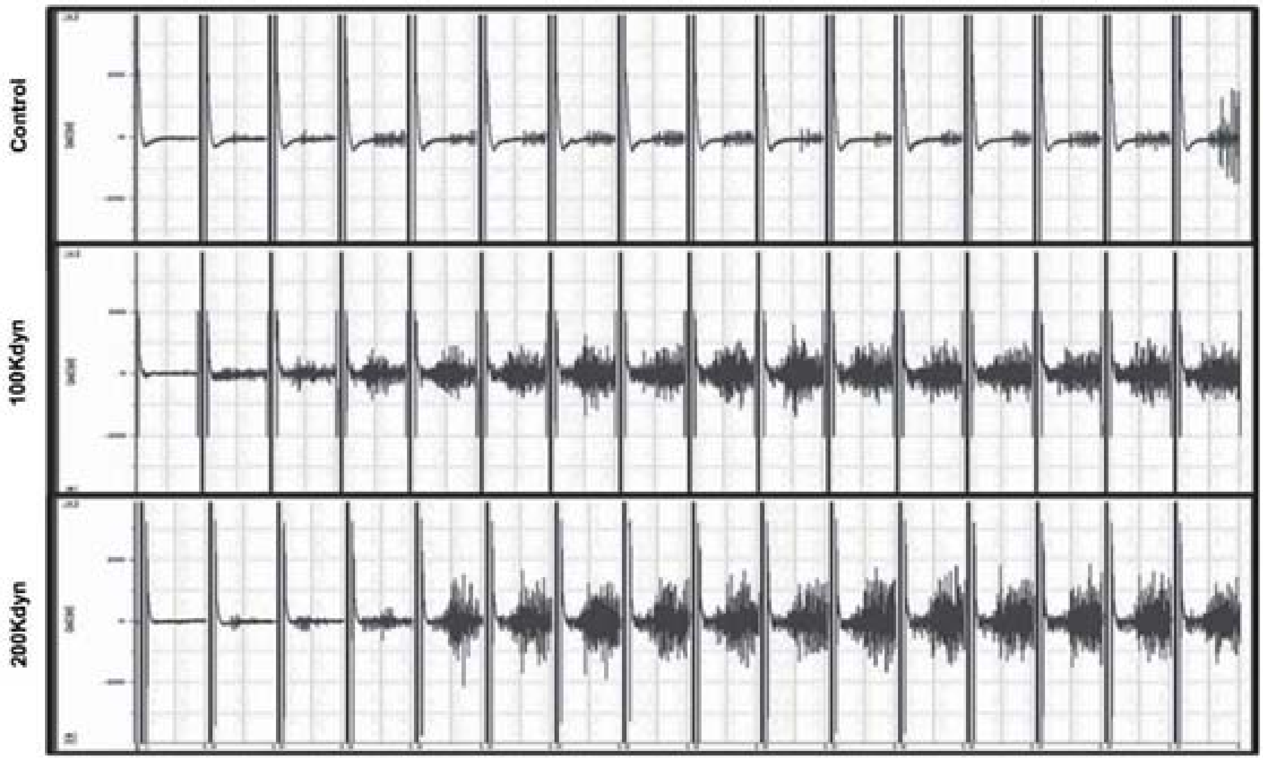

Fig. 4. Representative recordings of wind-up responses in intact and injured animals. Each vertical line indicates a new stimulus, until reaching 16 stimuli. Note that the first stimulus is subthreshold so no response is elicited. As the train of stimuli progresses, amplification occurs, especially in contused animals, that show higher responses than intact animals.

4. Discussion

The results of this study show that spinal cord injured animals have increased responses to thermal and mechanical noxious stimuli, indicative of neuropathic pain, but that this increase is independent of the severity of the lesion. Moreover, when testing the excitability of the spinal reflex circuitry, we found increased facilitation of wind-up responses in all SCI animals. The increase in wind-up responses was more marked in severe than in mild SCIs, just the opposite of withdrawal reflexes that were more increased in mild lesions. Similar to what occurs in intact animals, the wind-up phenomenon observed in SCI animals is dependent on NMDA activation. Wind-up measurements can be used as a non-invasive technique to detect central hyperexcitability, and to corroborate the existence of pain amplificators in the spinal cord after a SCI.

The spinal cord contusion model can present some variability, specially related to the displacement suffered by the spinal cord and to the real force applied (Scheff et al., 2003; Zhang et al., 2008), which influence the recovery after the contusion. For this reason, we controlled both parameters to guarantee reproducible lesions of different severity. The values for the real force applied were similar to the desired forces in both groups, and the displacements were similar to the ones described in the literature (Scheff et al., 2003; Cao et al., 2005). The severity of the lesion was also assessed functionally by means of the BBB scale of locomotor function, and histologically by evaluating the amount of spared tissue at the epicenter of the lesion. As expected, the animals receiving higher forces had more extensive loss of spinal cord tissue, and greater deficits in locomotion.

4.1. *Pain responses after SCI*

All contused animals showed increased pain responses to noxious mechanical and thermal stimuli, reflecting hyperalgesia (exaggerated response to a noxious stimulus). These manifestations had also been described after other traumatic (Christensen et al.,

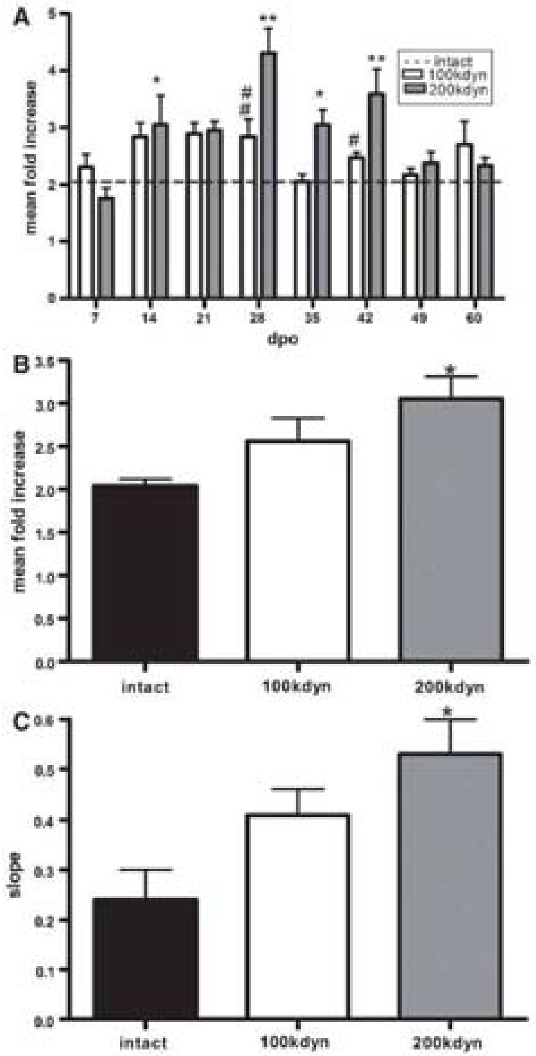

Fig. 5. Wind-up measurements. A) Longitudinal study: increase in wind-up mean fold increase during the 2 months of follow-up. In the Y axis, mean value for the increments within the 2nd and the 16th response with respect to the first one (mean fold increase); broken line represents the mean value for intact animals. Although with some variations, groups of injured animals present higher wind-up than intact animals during most of the follow-up period. $^{*}p<0.05$ vs. intact animals; $^{**}p<0.001$ vs. intact animals; $^{\#}p<0.05$ vs. 200 kdyn group; $^{\#\#}p<0.001$ vs. 200 kdyn. B) Bars represent the mean increment achieved for each group during all the follow-up period (considering all testing days, expressed as mean ± SEM). Injured animals show higher wind-up responses than intact animals, although only the value of the 200 kdyn group reaches statistical significance ($^{*}p<0.01$). These results suggest a tendency to increase the wind-up responses as the severity of the lesion increases. C) Mean slope of the regression line obtained considering the increments of AUC in the first five responses, and during the whole follow-up period (expressed as mean ± SEM). The 200 kdyn group had values significantly higher ($^{*}p<0.01$) than intact animals. The group with 100 kdyn lesion showed an increased slope, although it was not significantly different from intact animals.

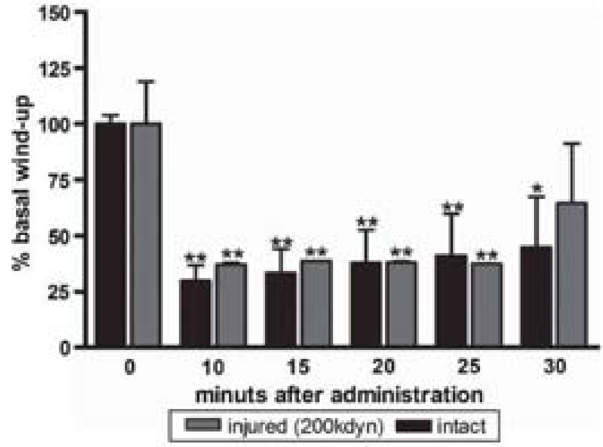

Fig. 6. Changes of wind-up responses following administration of MK801. NMDA blockade resulted in a reduction in wind-up responses (calculated using the mean AUC from 2nd to 16th normalized responses, versus basal wind-up response of each animal). This reduction was similar in intact and in contused animals, and lasted for at least 30 minutes ($^{*}p<0.05$; $^{**}p<0.01$ vs. basal wind-up values before administration of the drug).

1996; Christensen and Hulsebosch, 1997), inflammatory and excitotoxic (Yezierski, 2005) lesions of the spinal cord.

The development of neuropathic pain after SCI is related to several physiopathological mechanisms, including death of spinal inhibitory interneurons, diminishment of inhibitory neurotransmitters, changes in the receptors of the dorsal horn projecting neurons, as well as the interruption of the descending inhibitory tracts (Costigan and Woolf, 2000; Meisner et al., 2010). These tracts project from the periaqueductal gray matter (PAG) and raphe nuclei, important areas for the processing and modulation of nociception, and are located in the dorsolateral funiculus, which is the most affected part of the spinal cord by the contusion itself. This may explain why animals with different severity of lesion do not respond in a graded manner. A direct consequence of the loss of these inhibitory pathways is the activation of intraspinal mechanisms of generation and amplification of pain. In previous studies, hyperexcitability was detected in the injured spinal cord (Lenz et al., 2000), as well as changes in the expression of some sodium channels in the lumbar region of the spinal cord after a thoracic contusion (Hains et al., 2003). Local circuitry caudal to the lesion (at the lumbar segments L4-L5 collecting the sensibility of the sciatic nerve) should be preserved since it is not directly affected by the contusion. However the inflammatory

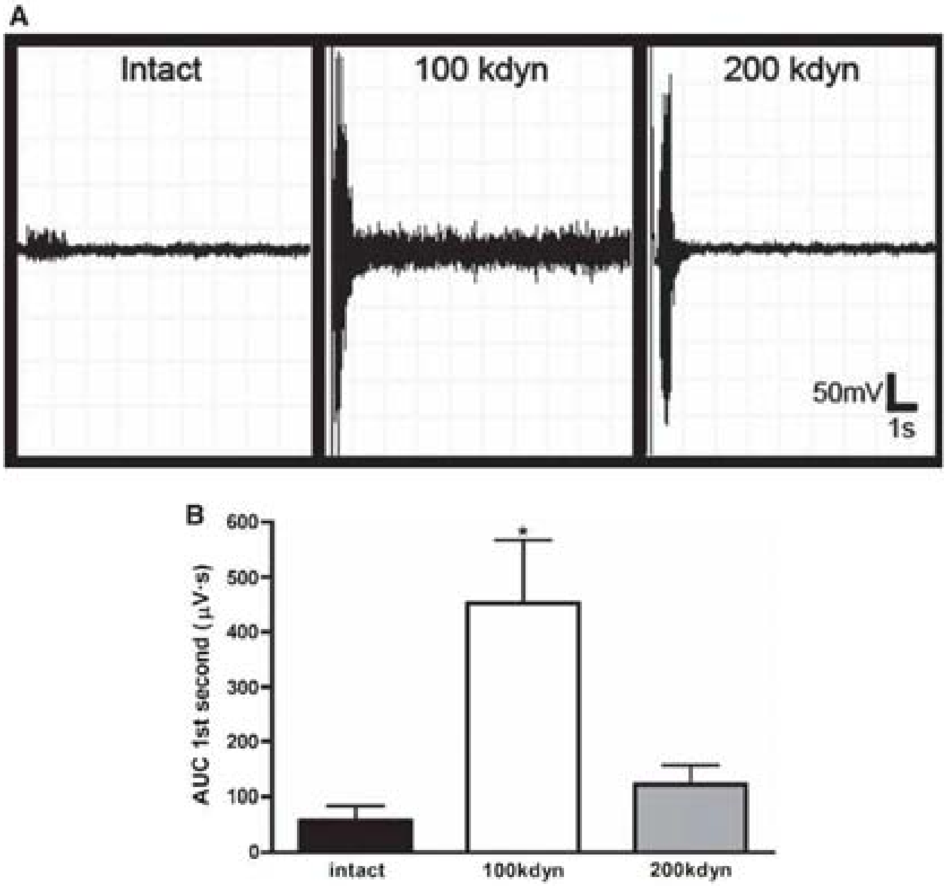

Fig. 7. A) Representative recordings of withdrawal reflexes from intact, 100 kdyn and 200 kdyn animals. B: Measurements of the area under curve of the first second of withdrawal reflex response, measured in µV·s. Animals with 100 kdyn contusion showed higher withdrawal reflexes ($^{*}p<0.01$) than intact and 200 kdyn contused animals.

process that takes place in the epicenter of the lesion is important enough to induce structural and functional changes at segments as remote as lumbar regions (Detloff et al., 2008; Abbadie et al., 2009; García-Alías et al., 2010). These changes have been related to central sensitization, for which neuronal circuits may respond inappropriately to peripheral stimuli, strengthening the response, reducing the thresholds and increasing the synaptic efficacy (Woolf, 1983; White et al., 2007).

In contrast to other reports (Knerlich-Lukoschus et al., 2008), the severity of the lesion was not proportional to the degree of hyperalgesia found in our study. Other studies have proposed that minor lesions might cause more pain, since a higher preservation of spinal tracts would enhance transmission of aberrant pain information to higher centers (Yoon et al., 2004). Even in clinically complete SCI, persistent spinothalamic tract function has been demonstrated in a majority of patients with central pain, suggesting that the partially preserved spinothalamic tract pathways might function as a 'pain generator' (Wasner et al., 2008). In the SCI model we used, superficial layers of the dorsal horn and most of the dorsal tracts are lost or non-functional at the involved thoracic segments, and the area is immersed in an inflammatory and hyperexcitable state. This pathological situation can affect the conduction of the preserved ascending nociceptive pathways through a mechanism called "activation *en passant*" (Ma and Quirion, 2008), by which normal axons would be altered when passing near to axons that are damaged or hyperexcited. On the other hand, residual spinothalamic tracts permits the conduction of nociceptive inputs, but the loss of dorsal tracts and the hyperexcitability of the system do not permit the fine discrimination, so the nociceptive response elicited by the animal is not graded to the stimulus, neither to the severity of the injury. We can not rule out the possibility that the algesimetry tests are not sensitive enough to detect differences in the intensity of neuropathic pain after severe SCI; for instance, hindlimb paresia may influence the time to withdraw the stimulated paw, although only minor movement of the paw is sufficient to stop the stimulus intensity.

4.2. *Facilitation of wind-up responses after SCI*

Despite its intrinsic variability, wind-up recordings showed some common features in all the tested animals. The response to the first stimulus was of low intensity, since no amplification had already taken place. From the second to the fifth stimulus, responses showed a marked increase, reaching the maximum response in this interval; this increased response was maintained until the last stimulus. An interesting approach to evaluate the excitability of the spinal cord after the injury is to evoke wind-up responses in electrophysiological recordings of spinal reflexes. Wind-up can be considered a form of short term potentiation, since its amplifying effects only last some minutes after the end of the stimuli. In addition, it does not imply synthesis of new proteins nor changes in synaptic components, as occurs with the long term potentiation phenomenon.

Since wind-up responses can be difficult to measure and interpret (Svendsen et al., 1999), we used different approaches to quantify wind-up changes in our study. The first representation could be useful to detect temporal patterns in wind-up responses after SCI. Although the group of 200 kdyn showed higher wind-up responses than the 100 kdyn group, the differences were only significant at some days of the follow-up. When all days are considered together, the mean increase of the succeeding responses with respect to the first response showed a trend to increase with the severity of the lesion, being the 200 kdyn group the one with highest wind-up responses. When studying the slope of the increase during the first five responses data indicated that wind-up responses were again higher in the most severe injuries, and also higher than in intact animals. This representation is useful to measure how fast the amplification is achieved and how intense it becomes. Despite the method used to measure wind-up, all contused animals showed increased wind-up responses to the same train of stimuli, indicating summation and hyperexcitability at some point of the spinal reflex pathways. This abnormal amplification mechanism may contribute to the appearance of neuropathic pain after SCI, contributing to the magnification of the response given to a noxious stimulus, and would reflect the important role of plastic changes in spinal reflex circuits after SCI.

The application of a NMDA antagonist (MK801) reduced wind-up responses in intact and contused animals, suggesting that increased wind-up responses in SCI and intact rats were highly dependent on NMDA receptors. MK801 has been used experimentally to reduce neuropathic pain and is also known to inhibit the generation of wind-up responses by inhibiting the cumulative depolarization that leads to wind-up generation (Eide, 2000; Herrero et al., 2000; You et al., 2004). It is interesting to note, however, that in some peripheral nerve lesions producing neuropathic pain, wind-up responses are not so sensitive to NMDA blocking agents (Xu et al., 1995).

4.3. *Facilitation of withdrawal reflexes*

Withdrawal reflexes have been widely used to study nociceptive responsiveness in animals. Increases in the segmental reflex responses may be consequence of the reorganization of neural circuits that takes place after SCIs (Basso, 2000). However, we found more marked withdrawal reflex responses after mild than severe SCI in our rats. Interestingly, spasticity, another sign of abnormal processing in the spinal reflex circuitry, is also more marked in incomplete compared to complete spinal cord injured subjects (Little et al., 1989; Young, 1994). In contrast to the amplitude of the withdrawal reflex, wind-up responses showed a positive tendency in relation to the contusion force applied, suggesting that the two responses are differently dysregulated after SCI. In fact, wind-up and central sensitization are not equivalent phenomena and depend on different mechanisms (Woolf, 1996). Whereas wind-up responses depend on enhanced synaptic C fiber activation and accumulative depolarization (Sivilotti et al., 1993), which supposes an increase in calcium levels, alterations in the withdrawal reflex are probably mediated by exaggerated and prolonged synaptic inputs from sensory afferents and interneurons. We cannot discard the existence of pathways that remain silent in normal conditions, but may be activated after SCI, then implicating different modulation of withdrawal reflex and wind-up responses. Moreover, facilitation of the withdrawal reflex can be partially due to amplification of afferent inputs on motoneurons below the lesion, which in turn may become hyperexcitable (for a review see Heckmann et al., 2005).

This is one of the first studies exploring the appearance and evolution of wind-up responses along time after a spinal cord contusion. Wind-up responses, measured by different approaches showed a clear facilitation after spinal contusive lesions, and they increased in relation to the severity of the injury, being the most severe injuries the ones presenting higher amplification, hence higher central hyperexcitability. Nevertheless, withdrawal reflexes were more facilitated in mild lesions, indicating the different modulation acting on the same spinal reflex circuit when applying a single or repetitive electrical stimuli, highlighting the important plasticity present in spinal segments caudal to the lesion site. This hyperexcitability, present in all contused animals, was translated into exaggerated nociceptive responses in the algesimetry tests. Our results support the importance of plastic changes in the spinal cord after SCI, demonstrated here as a facilitation in the spinal pathways that mediate wind-up responses. Moreover, wind-up measurements appears here as a useful technique to assess central hyperexcitability, therefore the presence of spinal amplificatory systems of pain.

Acknowledgments

This work was supported by grants from the Fundació MaratóTV3 (grant 070210), the Ministerio de Ciencia y Innovación (grants SAF2006-08682 and SAF2009-12495), the Instituto de Salud Carlos III (grant PI080598) and funds from Red de Terapia Celular (TERCEL) of Spain. We thank the technical assistance of Monica Espejo, Jessica Jaramillo and Marta Morell.

References

Abbadie, C., Bhangoo, S., De Koninck, Y., Malcangio, M., Melik-Parsadaniantz, S. & White F.A. (2009). Chemokines and pain mechanisms. *Brain Res Rev, 60*, 125-134.

Basso, D.M. (2000). Neuroanatomical substrates of functional recovery after experimental spinal cord injury: Implications of basic science research for human spinal cord injury. *Phys Ther, 80*(8), 808-817.

Basso, D.M., Beattie, M.S. & Bresnahan, J.C. (1995). A sensitive and reliable locomotor rating scale for open field testing in rats. *J Neurotrauma, 12*(1), 1-21.

Cao, Q., Zhang, Y.P., Iannotti, C., DeVries, W.H., Xu, X.M., Shields, C.B. & Whittemore, S.R. (2005). Functional and electrophysiological changes after graded traumatic spinal cord injury in adult rat. *Exp Neurol, 191* (Suppl 1), S3-S16.

Clarke, R.W. & Harris, J. (2004). The organization of motor responses to noxious stimuli. *Brain Res Brain Res Rev, 46*(2), 163-172.

Costigan, M. & Woolf, C.J. (2000). Pain: Molecular mechanisms. *J Pain, 1*(3 Suppl), 35-44.

Christensen, M.D., Everhart, A.W., Pickelman, J.T. & Hulsebosch, C.E. (1996). Mechanical and thermal allodynia in chronic central pain following spinal cord injury. *Pain, 68*(1), 97-107.

Christensen, M.D. & Hulsebosch, C.E. (1997). Chronic central pain after spinal cord injury. *J Neurotrauma, 14*(8), 517-537.

Davies, S.N. & Lodge, D. (1987). Evidence for involvement of N-methylaspartate receptors in 'wind-up' of class 2 neurones in the dorsal horn of the rat. *Brain Res, 424*(2), 402-406.

Dickenson, A.H. & Sullivan, A.F. (1987). Evidence for a role of the NMDA receptor in the frequency dependent potentiation of deep rat dorsal horn nociceptive neurones following C fibre stimulation. *Neuropharmacology, 26*(8), 1235-1238.

Detloff, M.R., Fisher, L.C., McGaughy, V., Longbrake, E.E., Popovich, P.G. & Basso D.M. (2008). Remote activation of microglia and pro-inflammatory cytokines predict the onset and severity of below-level neuropathic pain after spinal cord injury in rats. *Exp Neurol, 212*, 337-347.

Eide, P.K. (2000). Wind-up and the NMDA receptor complex from a clinical perspective. *Eur J Pain, 4*(1), 5-15.

García-Alías, G., Torres-Espín, A., Vallejo C. & Navarro, X. (2010). Functional involvement of the lumbar spinal cord after contusion to T8 spinal segment of the rat. *Restor Neurol Neurosci, 28*, 781-792.

Gozariu, M., Bragard, D., Willer, J.C. & Le Bars, D. (1997). Temporal summation of C-fiber afferent inputs: Competition between facilitatory and inhibitory effects on C-fiber reflex in the rat. *J Neurophysiol, 78*(6), 3165-3179.

Hains, B.C. & Waxman, S.G. (2006). Activated microglia contribute to the maintenance of chronic pain after spinal cord injury. *J Neurosci, 26*(16), 4308-4317.

Hains, B.C., Willis, W.D. & Hulsebosch, C.E. (2003). Temporal plasticity of dorsal horn somatosensory neurons after acute and chronic spinal cord hemisection in rat. *Brain Res, 970*(1-2), 238-241.

Hargreaves, K., Dubner, R., Brown, F., Flores, C. & Joris, J. (1988). A new and sensitive method for measuring thermal nociception in cutaneous hyperalgesia. *Pain, 32*(1), 77-88.

Heckmann, C.J., Gorassini, M.A. & Bennett, D.J. (2005). Persistent inward currents in motoneuron dendrites: Implications for motor output. *Muscle Nerve, 31*(2), 135-156.

Herrero, J.F., Laird, J.M. & Lopez-Garcia, J.A. (2000). Wind-up of spinal cord neurones and pain sensation: Much ado about something? *Prog Neurobiol, 61*(2), 169-203.

Kimura, S. & Kontani, H. (2008). Separate recording of A-delta and C fiber-mediated nociceptive flexor reflex responses of mouse hindlimb using electromyography and the characteristics of wind-up appearing in the responses. *J Pharmacol Sci, 108*(2), 172-178.

Knerlich-Lukoschus, F., Juraschek, M., Blomer, U., Lucius, R., Mehdorn, H.M. & Held-Feindt, J. (2008). Force-dependent development of neuropathic central pain and time-related CCL2/CCR2 expression after graded spinal cord contusion injuries of the rat. *J Neurotrauma, 25*(5), 427-448.

Lance, J.W. (1980). The control of muscle tone, reflexes, and movement: Robert Wartenberg Lecture. *Neurology, 30*(12), 1303-1313.

Lenz, F.A., Lee, J.I., Garonzik, I.M., Rowland, L.H., Dougherty, P.M. & Hua, S.E. (2000). Plasticity of pain-related neuronal activity in the human thalamus. *Prog Brain Res, 129*, 259-273.

Little, J.W., Micklesen, P., Umlauf, R. & Britell, C. (1989). Lower extremity manifestations of spasticity in chronic spinal cord injury. *Am J Phys Med Rehabil, 68*(1), 32-36.

Ma, W. & Quirion, R. (2008). Does COX2-dependent PGE2 play a role in neuropathic pain? *Neurosci Lett, 437*(3), 165-169.

McMahon, S.B., Cafferty, W.B. & Marchand, F. (2005). Immune and glial cell factors as pain mediators and modulators. *Exp Neurol, 192*(2), 444-462.

Meisner, J.G., Marsh, A.D. & Marsh, D.R. (2010). Loss of GABAergic interneurons in laminae I-III of the spinal cord dorsal horn contributes to reduced GABAergic tone and neuropathic pain after spinal cord injury. *J Neurotrauma, 27*(4), 729-737.

Mendell, L.M. (1966). Physiological properties of unmyelinated fiber projection to the spinal cord. *Exp Neurol, 16*(3), 316-332.

Scheff, S.W., Rabchevsky, A.G., Fugaccia, I., Main, J.A. & Lumpp, J.E., Jr. (2003). Experimental modeling of spinal cord injury: Characterization of a force-defined injury device. *J Neurotrauma, 20*(2), 179-193.

Siddall, P.J., Taylor, D.A. & Cousins, M.J. (1997). Classification of pain following spinal cord injury. *Spinal Cord, 35*(2), 69-75.

Sivilotti, L.G., Thompson, S.W. & Woolf, C.J. (1993). Rate of rise of the cumulative depolarization evoked by repetitive stimulation of small-caliber afferents is a predictor of action potential windup in rat spinal neurons *in vitro*. *J Neurophysiol, 69*(5), 1621-1631.

Soler, M.D., Sauri-Ruiz, J., Curcoll-Gallemi, M.L., Benito-Penalva, J., Opisso-Salleras, E., Chamarro-Lusar, A. & Vidal-Samso, J. (2007). Characteristics of chronic neuropathic pain and their relationship with psychological well-being in spinal cord injury patients. *Rev Neurol, 44*(1), 3-9.

Svendsen, F., Hole, K. & Tjolsen, A. (1999). Some problems with wind-up and its calculation. *Pain, 83*(1), 109-112.

Valero-Cabre, A., Fores, J. & Navarro, X. (2004). Reorganization of reflex responses mediated by different afferent sensory fibers after spinal cord transection. *J Neurophysiol, 91*(6), 2838-2848.

Wasner, G., Lee, B.B., Engel, S. & McLachlan, E. (2008). Residual spinothalamic tract pathways predict development of central pain after spinal cord injury. *Brain, 131*(Pt 9), 2387-2400.

White, F.A., Jung, H. & Miller, R.J. (2007). Chemokines and the pathophysiology of neuropathic pain. *Proc Natl Acad Sci U S A, 104*(51), 20151-20158.

Widerstrom-Noga, E.G., Felipe-Cuervo, E. & Yezierski, R.P. (2001). Chronic pain after spinal injury: Interference with sleep and daily activities. *Arch Phys Med Rehabil, 82*(11), 1571-1577.

Woolf, C.J. (1983). Evidence for a central component of post-injury pain hypersensitivity. *Nature, 306*(5944), 686-688.

Woolf, C.J. (1996). Windup and central sensitization are not equivalent. *Pain, 66*(2-3), 105-108.

Xu, X.J., Zhang, X., Hokfelt, T. & Wiesenfeld-Hallin, Z. (1995). Plasticity in spinal nociception after peripheral nerve section: Reduced effectiveness of the NMDA receptor antagonist MK-801 in blocking wind-up and central sensitization of the flexor reflex. *Brain Res, 670*(2), 342-346.

Yezierski, R.P. (2005). Spinal cord injury: A model of central neuropathic pain. *Neurosignals, 14*(4), 182-193.

Yoon, Y.W., Dong, H., Arends, J.J. & Jacquin, M.F. (2004). Mechanical and cold allodynia in a rat spinal cord contusion model. *Somatosens Mot Res, 21*(1), 25-31.

You, H.J., Morch, C.D. & Arendt-Nielsen, L. (2004). Electrophysiological characterization of facilitated spinal withdrawal reflex to repetitive electrical stimuli and its modulation by central glutamate receptor in spinal anesthetized rats. *Brain Res, 1009*(1-2), 110-119.

Young, R.R. (1994). Spasticity: A review. *Neurology, 44*(11 Suppl 9), S12-S20.

Zhang, Y.P., Burke, D.A., Shields, L.B., Chekmenev, S.Y., Dincman, T., Zhang, Y., Zheng, Y., Smith, R.R., Benton, R.L., DeVries, W.H., Hu, X., Magnuson, D.S., Whittemore, S.R. & Shields, C.B. (2008). Spinal cord contusion based on precise vertebral stabilization and tissue displacement measured by combined assessment to discriminate small functional differences. *J Neurotrauma, 25*(10), 1227-1240.

2

Quantitative evaluation of functional deficits after different SCI: analysis of locomotion

Specific objectives

Locomotion analysis can be done using different levels of complexity, depending on the information needed. For a simple evaluation of functional deficits between different lesions, or for ensuring a correct performance of an injury, maybe a BBB test is enough. Contrarily, in order to detect changes in spinal circuits, or to assess the efficacy of some treatments, the BBB test has limitations because it is partly subjective and does not provide enough detailed information. For this reason it is important to have available more sophisticated locomotion assays based in the study of complex features such as coordination or step patterns. For this purpose, we set some specific objectives listed below:

1. Review the most common tests to assess locomotion and functional performance after spinal cord injuries.

2. Assess changes in locomotion after SCI by simple methodologies that provide objectivity and quantitative parameters to the analysis of:

    a. interlimb coordination.
    b. basic parameters of gait.
    c. the sequence step patterns.

3. Relate the electrophysiological changes occurring after SCI of different degrees to the functional deficits.

Publication

Quantitative assessment of locomotion and interlimb coordination in rats after different spinal cord injuries

E.Redondo Castro, A. Torres-Espín, G.García-Alías, X.Navarro

Journal of Neuroscience Methods,, 2013; 213:165-178

Journal of Neuroscience Methods 213 (2013) 165–178

Contents lists available at SciVerse ScienceDirect

Journal of Neuroscience Methods

journal homepage: www.elsevier.com/locate/jneumeth

Basic Neuroscience

Quantitative assessment of locomotion and interlimb coordination in rats after different spinal cord injuries

Elena Redondo-Castro[a], Abel Torres-Espín[a], Guillermo García-Alías[b], Xavier Navarro[a,*]

[a] Group of Neuroplasticity and Regeneration, Institute of Neurosciences and Department of Cell Biology, Physiology and Immunology, Universitat Autònoma de Barcelona, and Centro de Investigación Biomédica en Red sobre Enfermedades Neurodegenerativas (CIBERNED), Bellaterra, Spain

[b] Department of Integrative Biology and Physiology, University of California Los Angeles, Los Angeles, CA 90095-1606, USA

HIGHLIGHTS

- Different spinal cord injuries cause differential functional deficits.
- A new method to quantify interlimb coordination and gait disturbances in the rat is described.
- The quantitative assessment of locomotion discriminates spinal cord injuries of different severity.
- Subjective and objective methods combined provide a full description of locomotion.

ARTICLE INFO

Article history:
Received 27 September 2012
Received in revised form
20 December 2012
Accepted 22 December 2012

Keywords:
Spinal cord injury
Functional tests
Locomotor function
Coordination

ABSTRACT

Animal models of spinal cord injury (SCI) are intended to mimic the main features of human spinal cord lesions, although sometimes it becomes a difficult task to find the right technique to discriminate the severity of the lesion as well as to assess different aspects of functional recovery. For this reason, we have used several functional methods to assess gross and fine locomotion deficits, as well as electrophysiological data to study the dysfunctions underlying the behavioral changes. Moreover, an extensive study based on the quantification of alternation and coordination parameters during gait has been done. Spinal cord injuries of varying severity (mild contusion, moderate contusion and hemisection) were performed at the thoracic level in adult rats that were followed-up for 6 weeks. Lesions resulting in similar scores in the open field test (i.e. mild contusion and hemisection) caused more marked differences in fine coordination when assessed by quantitative coordination analysis based on a digitized walking treadmill. In conclusion, gross and fine deficits can be detected using a battery of tests based on the performance of the animals during tasks of different difficulty. When used appropriately, they become useful tools to study functional recovery due to spontaneous plastic changes or to therapeutic interventions after SCI, as well as to test the effects of new therapies.

1. Introduction

The rat is widely used as a model of human spinal cord injury (SCI), specially spinal cord contusions, the type of lesion that has more clinical relevance and similarities with the lesions affecting humans (Majczyński and Sławińska, 2007). Deficits after SCI are especially noticeable below the lesion site, and affect motor and sensory systems, as well as autonomic functions. Most of the tests used to assess function after SCI are focused in assessing locomotion, especially of the hindlimbs. Several functional tests have already been described, but sometimes it is difficult to chose the right one to discriminate the deficits appearing in every injury and severity. Moreover, sometimes it is also difficult to interpret the obtained results, since animals present spontaneous improvements and compensations of their deficits after SCI, masking the real dimension of the deficits as well as the recovery. This occurs both in animals as in humans (Curt et al., 2008; Gulino et al., 2007; Majczyński and Sławińska, 2007).

Locomotion depends on a spinal network under the influence of supraspinal centers as well as the modulation of the afferent inputs (Majczyński and Sławińska, 2007). After the injury, descending motor tracts may become completely or partially disrupted, and the remaining elements of the network may adapt to the new circuitry to compensate the deficits. Most SCI imply the lesion of some white matter tracts, and depending on which are affected, the deficits can be more or less evident. For instance, while only a

* Corresponding author at: Unitat de Fisiologia Mèdica, Facultat de Medicina, Universitat Autònoma de Barcelona, E-08193 Bellaterra, Spain. Tel.: +34 935811966; fax: +34 935812986.
E-mail address: xavier.navarro@uab.cat (X. Navarro).

0165-0270/$ – see front matter © 2013 Elsevier B.V. All rights reserved.
http://dx.doi.org/10.1016/j.jneumeth.2012.12.024

few preserved ventrolateral tract fibers are needed to allow weight support and plantar paw placement, dorsal tracts are required for skilled movements and coordinated actions of the distal musculature (Drew et al., 2004; Rossignol and Frigon, 2011).

The first aim of this work is to compare the appearance of functional deficits in different SCI. To achieve this objective several techniques are used, such as the BBB scale for open field locomotion, the narrow beam, the inclined plane and the walking track analysis. These tests give subjective and semi-quantitative results, but are fast and require short training of the researcher. Adding objectivity to this kind of methods is important to promote the comparison of results between different models, different treatments and different laboratories. The second objective was to perform a detailed quantitative assessment of the main features related to gait. In this case, the methods are more complex and time-consuming, requiring good training of the researcher. We have used the recordings obtained with the Digigait system to quantify different gait parameters, coordination and alternation. Using simple programs, we provide a novel analysis of locomotion, faster and more discriminative than others reported in the literature. Moreover, the treadmill used in the Digigait system can provide a fine control of speed, avoiding the effects of changing speed in the normal free walking or running of the animals during the analysis. Finally, electrophysiological studies were performed to assess the functionality of central and peripheral circuits, in order to determine the extent of damage below the injury and the functional consequences of SCI of different severity. All these results led to an objective evaluation of locomotor performance after different SCI in the rat, which may be useful when comparing new treatments or rehabilitation techniques aimed to improve motor function and locomotion.

2. Materials and methods

2.1. Laboratory animals

Adult female Sprague Dawley rats (8 weeks old; 250–300 grams) were housed with free access to food and water, at a room temperature of 22 ± 2 °C under a 12:12 h light-dark cycle. All experimental procedures were approved by the Ethics Committee of our institution, and followed the European Communities Council Directive 86/609/EEC. Researchers involved in the different assessments were initially blinded to the injury received by the animals.

2.2. Surgical procedure

Operations were performed under pentobarbital anesthesia (50 mg/kg i.p., Sigma-Aldrich), and after subcutaneous injection of buprenorphine (0.05 mg/kg, Buprex, Schering-Plough) near the incision site. In two groups of rats, after dorsal laminectomy of T8–T9, the spinal cord was contused at the T8 level using the Infinite Horizon Impactor device (Precision Scientific Instruments, Lexington, UK), applying a force of 100 kilodynes (kdyn; group 100 kdyn, $n = 10$) or 200 kdyn (group 200 kdyn, $n = 10$). Data from displacement and real force applied were collected for each contusion. In another group of animals a hemisection was performed at T8 level using a thin scalpel to cut only the right part of the spinal cord (hemisection group, $n = 10$). To ensure that the spinal cord was completely transected in the right side, a thin needle was introduced twice until touching the ventral surface of the vertebral channel. After the injury, the wound was sutured with 5/0 silk thread in the muscular plane and small surgical clips in the skin, and disinfected with povidone iodine. Animals were rehydrated and kept in a warm environment until full recovery from anesthesia. Bladders were expressed twice a day until reflex voiding of the bladder was re-established. To prevent infection, amoxicillin (500 mg/l) was given in the drinking water for one week. No additional analgesia was administered during the follow-up.

2.3. Functional evaluation of locomotion

All animals were tested before surgery and at 42 days thereafter, except for the BBB test that was performed at 3 days post operation (dpo) and then weekly. Since preoperative values did not differ between groups, for convenience all values were considered together and represented as the control "intact group".

2.3.1. Open field locomotion test

Locomotor hindlimb function was assessed using the Basso, Beattie and Bresnahan (BBB) rating scale (Basso et al., 1995). Briefly, the BBB scale consists of an ordinal scale from 0 points (no discernable hind limb movement) to 21 points (consistent, coordinated gait with parallel paw placement of the hind limb and consistent trunk stability). For measuring locomotor recovery, one animal at a time was allowed to walk freely inside a circular plastic tray (90 cm diameter × 24 cm wall height) for 5 min, and two examiners observed the hindlimbs movements of the rat. The final score of each animal was the mean value of both examiners.

2.3.2. Inclined plane test

This test measures the ability of the animals to maintain their position in an inclined plane for at least 5 s. The angle of the surface was progressively increased (starting from a flat surface, 0°), until recording the maximum angle supported by the animal that was scored as the outcome measure. Three trials were done to obtain the average value for each animal and day.

2.3.3. Beam test

For this test, a dark tunnel was designed (tunnel dimensions: 7 cm width, 13 cm height, 40 cm length) to allow the animals walking along an elevated beam (2.5 cm width, 2 cm height, 2 mm separated from the ground to allow the placement of a paper sheet to print the inked paws). The hindpaw plantar surfaces were inked while the animal was gently subjected with a cotton cloth by the researcher. Then, the rat walked along the beam so only the missteps were recorded by ink prints on the paper placed under the beam. Three consecutive runs were performed, and the left and right missteps done in the first 30 cm were counted in each run. The mean of the three values was considered as the result for the animal in each testing day.

2.3.4. Walking track and foot print analysis

It was carried out to assess the recovery of locomotor function and changes in the normal gait posture, adapting the original technique set to study sciatic nerve lesions (De Medinaceli et al., 1982). The plantar surface of the rat paws was painted with red ink for forepaws and blue ink for hindpaws, and the rat left to walk along a corridor of 40 cm × 8 cm × 10 cm with a white paper on the base. Distances between forepaw prints (forelimb stance width) and between hindpaw prints (hindlimb stance width) were measured with a precision device in order to assess the base of support (García-Alías et al., 2010).

2.4. Analysis of locomotion using treadmill tests

Gait video images were obtained with the Digigait Imaging system (Mouse Specifics Inc., Boston, MA) as previously described (Vincelette et al., 2007). Briefly, a high-speed video camera mounted below a transparent treadmill belt captured ventral images of the animal. The images were automatically digitized at 140 frames per second, and a minimum of 7 s of continuous gait were recorded, enough to provide around 10 sequential step cycles.

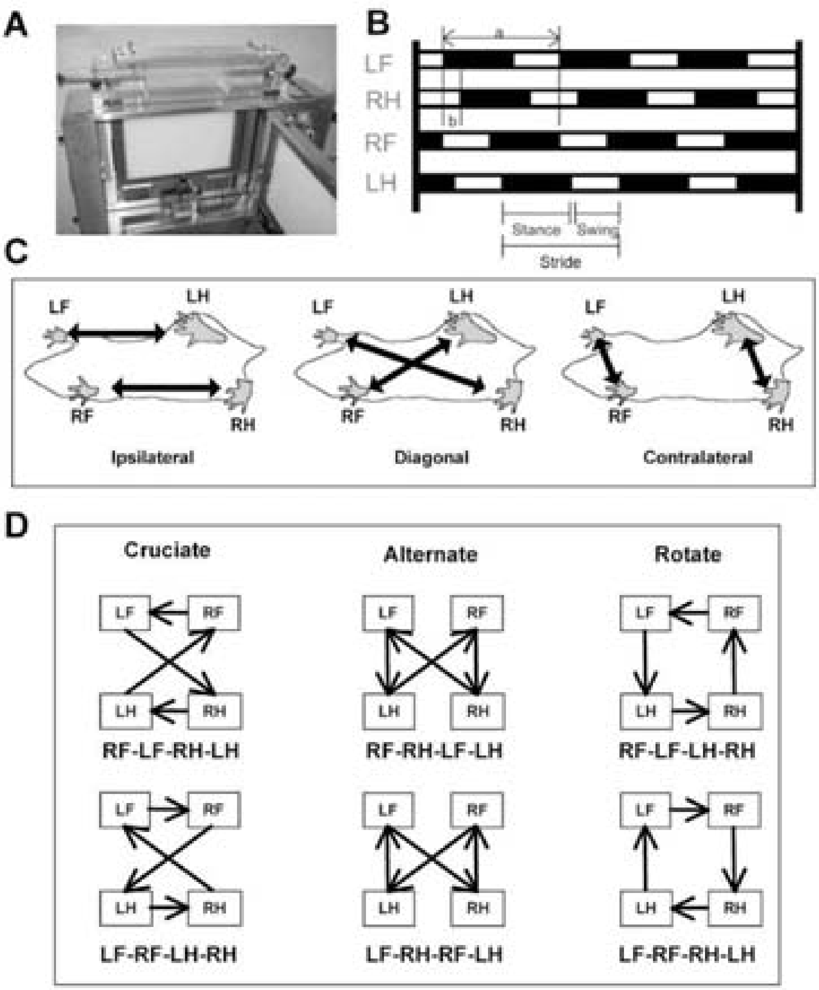

Fig. 1. Calculation of phase dispersion (PD) and interlimb relations. (A) Image of the Digigait Imaging system, with the running belt and the camera in the bottom part. (B) Footfall diagrams were constructed with stance times directly extracted from the videos. Black boxes represent the stance time and white boxes the swing time. LF: left forelimb; RH: right hindlimb; RF: right forelimb; LH: left hindlimb. Phase dispersions were calculated as the delay between the start of the stance phase in the target limb and the corresponding start of the stance phase of the reference limb (*b*), divided by the stride time of the reference limb (*a*). Therefore, phase dispersion is calculated as *b*/*a*, being LF the reference limb. (C) Schematic representation of the different types of interlimb coordination: ipsilateral, diagonal and contralateral. (D) Diagrams depicting the different regular step patterns: cruciate, alternate and rotate. The arrows indicate the sequence in which the different paws are placed on the ground.

Animals were acclimated to the belt compartment some minutes before starting the test, and training trials were done using progressively increasing speeds, with resting periods between them. Animals unable to support their weight with the hind limbs, as well as animals that even supporting their weight were not able to run at the selected speeds (10, 20 and 30 cm/s) were not included in the analysis.

2.5. *Recording and analysis of gait parameters, coordination and step patterns*

Due to limitations when working with SCI animals (such as external rotation and dragging of the limbs), gait videos were recorded with the Digigait Imaging system (Fig. 1A) but the analysis was done manually using Virtual Dub free software (GNU, General Public License). The start and ending times of the stance phase of each stride were extracted by analyzing the videos frame by frame, so eventually a footfall gait diagram was depicted (McEwen and Springer, 2006, Fig. 1B). Thus, the frame in which one paw was placed over the belt and the frame in which the same paw left the belt were considered the start and the end of the stance phase, respectively. Considering the recording speed and the number of frames between the start and the end, the stance duration for each paw and step was calculated. The stride duration was calculated as the difference between the time of start of the stance phase of one paw in one step and in the next step of the same paw. The swing duration was obtained by subtracting the stance duration from the stride duration. The quantitative analysis of gait parameters, coordination and step pattern were obtained from footfall gait diagrams using a Visual Basic macro for Microsoft Office Excel® software (Microsoft Corporation). Quantitative values for the gait parameters (stride duration, stance duration and swing duration), their coefficient of variation (%CV; calculated as mean divided by standard deviation in percentage) and the stance/swing ratio were calculated. The coordination in locomotion is assumed here as the correct temporal and spatial sequence of steps, both considering the relationships between pairs of limbs (interlimb coordination) as well as the global step pattern. The interlimb coordination was assessed by two parameters: the correct alternation between different pairs of limbs, and the phase dispersion (PD). Alternation is considered as the percentage of paw placement performed in an expected alternated sequence involving the corresponding pairs of limbs. The PD parameter reflects the time-relation for each limb pair or limb coupling (Leblond et al., 2003). It represents the delay in time between the start of a reference step in one limb and the start of the target limb step with respect to the total duration of the reference step cycle (Fig. 1B). For each pair of limbs the calculations done were the percentage of PD for each step cycle (%PD), the maximum percentage of PD (MaxPD), the coefficient of variation (%CV) and the percentage of alternation in each analyzed sequence. Fig. 1C shows the different combinations of pairs of limbs considered for calculations of alternation and interlimb coordination: the *ipsilateral*, between forelimbs and hindlimbs from each side (LF-LH and RF-RH); the *diagonal*, between crossed forelimb and hindlimb (LF-RH and RF-LH); and the *contralateral*, between either forelimbs or hindlimbs (LF-RF and RH-LH). The regular step pattern implies the fully coordinated locomotion, in which each paw is exactly placed one time every four times, and has to be placed or risen at a given time. Six different regular step patterns can be defined in normal locomotion of rats and mice (Fig. 1D). This is expressed as a regularity index (RI), the percentage of correct step sequence with respect to the total number of step cycles. Thus, the lower RI, the larger the number of missteps not following the correct pattern (Cheng et al., 1997; Hamers et al., 2006).

2.6. *Electrophysiological tests*

Motor-evoked potentials (MEPs) and somatosensory-evoked potentials (SSEPs) were used to evaluate the functional state of descending and ascending tracts of the spinal cord, respectively. The tests were done under light pentobarbital anesthesia (30 mg/kg i.p., each animal testing took ~30 min), and maintaining the body temperature of the rat by means of a thermostated heating pad. MEPs were elicited by transcranial electrical stimulation, using two monopolar needle electrodes placed subcutaneously over the skull, the anode over the sensorimotor cortex and the cathode on the hard palate (García-Alías et al., 2006). Single rectangular pulses of 25 mA and 100 μs width, were delivered at 1 or 9 Hz, the optimal pulse rate to elicit the brainstem component (bs-MEP) and the cortical component (c-MEP), respectively. Recording electrodes (monopolar needles, 28 G) were placed in the tibialis anterior muscle. The muscle responses were displayed in an oscilloscope (Sapphire 4M, Vickers) to measure the amplitude and latency of each component.

SSEPs were evoked by electrical pulses of 6 mA, 100 μs delivered at 6 Hz to the tibial nerve at the ankle, and recorded by needle electrodes placed subcutaneously on the skull (same sites as stimulation needles for MEPs). Signals were amplified, filtered (bandpass 1 Hz–5KHz), and displayed on the oscilloscope (Sapphire 4ME, Vickers). Up to 256 responses were averaged on-line; the peak latency and the peak-to-peak amplitude were measured for N15, N20 and N30 waves (Valero-Cabré et al., 2004), referenced here as N1, N2 and N3 waves. SSEPs were repeated three times with minutes between trials, and the responses with the highest amplitude were selected and used for analysis.

2.7. *Statistical analysis*

Data are shown as the mean ± SEM. Statistical comparisons between groups were made using one-way ANOVA for all data, except the BBB results that were compared using two-way ANOVA for repeated measures (GraphPad Prism software). Bonferroni post hoc tests were applied when necessary. Differences between groups were considered statistically significant if $p < 0.05$.

3. Results

3.1. *Functional evaluation*

Customary functional tests were performed in order to provide a general evaluation of the functional deficits that occur after different SCIs.

3.1.1. *Open field locomotion (BBB)*

The results of this test indicate differences in locomotion deficits according to the severity of the lesion. All the rats presented normal locomotion before the surgery (21 points in the BBB scale). The animals of each group had the lowest scores during the first week after the surgery, to later recover some points. Rats of the 100 kdyn group showed plantar stepping and coordinated gait although with some deficits regarding toe spreading and paw position (15–16 points); in the 200 kdyn group the deficits were more marked, including uncoordinated gait and only occasional plantar stepping (9–10 points). Hemisection animals showed consistent plantar stepping although the gait was not consistently coordinated (13 points). All values from injured groups were significantly different from intact preoperative values ($p < 0.001$), and at some time points also between them (see Fig. 2A).

3.1.2. *Inclined plane*

This test was performed to evaluate the general motor function of intact and injured animals. In preoperative testing, rats were able to maintain standing position until 49–50 degrees, whereas the angle values were significantly reduced at 42 dpo in all injured groups: 42 ± 1 in the 100 kdyn group, 40 ± 1.5 in the 200 kdyn group, 43 ± 0.7 in the hemisection group (Fig. 2B).

3.1.3. *Narrow beam test*

This test assesses fine coordination, since only animals able to grasp the beam are able to cross it correctly. In preoperative testing sessions, animals made a few mistakes when walking on the beam (0–1 missteps, about 10% of the total number of steps). Six weeks after SCI, animals made significantly more foot slips in all injured groups (32.3 ± 4.7% in 100 kdyn, 70.5 ± 8.3% in 200 kdyn, 40.3 ± 3.5% in hemisection group) (Fig. 2C). The increase in missteps with respect to control values was only statistically significant for the 200 kdyn group.

3.1.4. *Walking track*

Animals receiving a spinal cord contusion lost the ability to move forelimbs and hindlimbs coordinately, as evidenced by the lack of overlapping between forepaw and hindpaw prints. In some animals with moderate contusion, some dragging of the hindpaws was also visible in the footprints. The hemisection animals showed uncoordinated gait, with little alternation of the paws and also with loss of overlapping between forepaws and hindpaws (Fig. 3).

Changes in the normal posture of the injured animals were assessed by measuring the distance between forelimbs and between hindlimbs. While intact animals showed a mean distance of 2.25 ± 0.04 cm between forelimbs, rats with SCI had an increase in this distance (2.4 ± 0.24 cm in 100 kdyn group, 3.0 ± 0.16 cm in 200 kdyn group and 2.96 ± 0.41 cm in hemisection group), although the differences did not reach significance with respect to the control value. Regarding the distance between the hindlimbs, control animals presented a mean separation of 2.87 ± 0.33 cm, whereas injured animals had also slightly higher, though not significant, values at 42 dpo (2.89 ± 0.41 cm in 100 kdyn group, 3.52 ± 0.19 cm in 200 kdyn group and 3.47 ± 0.31 cm in hemisection group, Fig. 3B).

E. Redondo-Castro et al. / Journal of Neuroscience Methods 213 (2013) 165–178 169

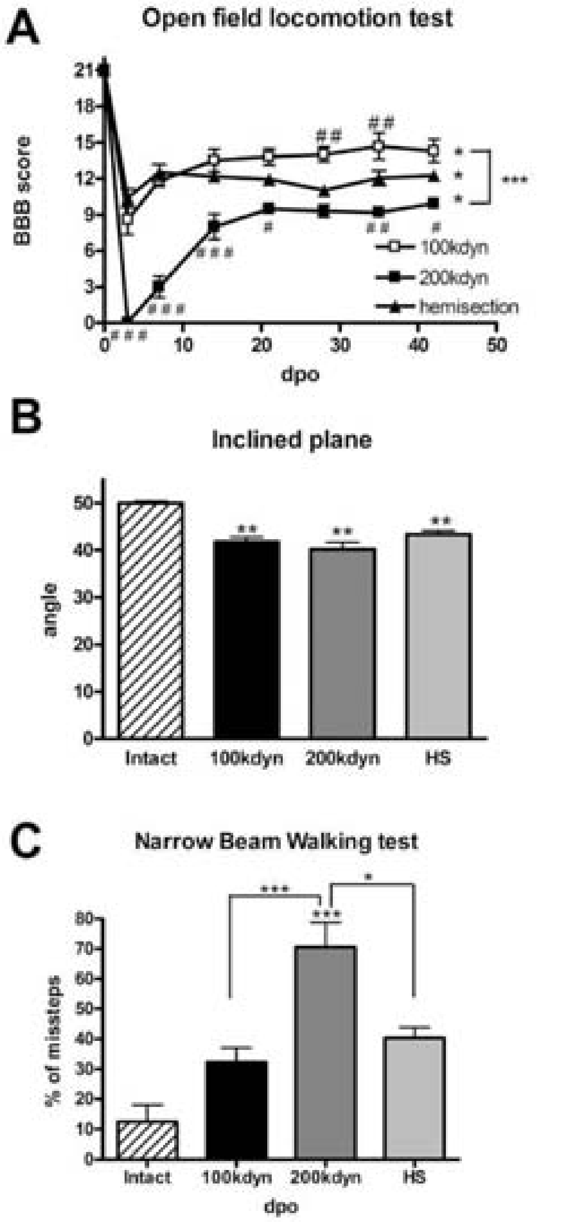

Fig. 2. Results of functional tests. (A) Open field locomotion test: all groups presented the lowest score 3 days after the surgery, and then recovered to stable values from 2 to 3 weeks. Rats with mild contusion (100 kdyn) showed the highest scores, followed by the hemisection group animals, and by the 200 kdyn group. Intact values are 21 ± 0 points, not represented in the figure for convenience. There were statistical differences between groups during the follow-up ($^{*}p<0.001$ vs. intact; $^{***}p<0.001$ 100 kdyn vs. 200 kdyn; $^{\#}p<0.01$ vs. hemisection group). dpo: days post operation. (B) Inclined plane: all injured groups showed a similar performance in this test, with slightly lower values than intact animals at 42 dpo. The differences were statistically significant compared to intact values ($^{**}p<0.01$). (C) Narrow beam walking test: all the SCI rats made a higher number of footslips than intact rats. The proportion of missteps in the 200 kdyn group was significantly higher than values of intact rats ($^{***}p<0.001$), 100 kdyn rats ($^{***}p<0.001$), and hemisection rats ($^{*}p<0.05$).

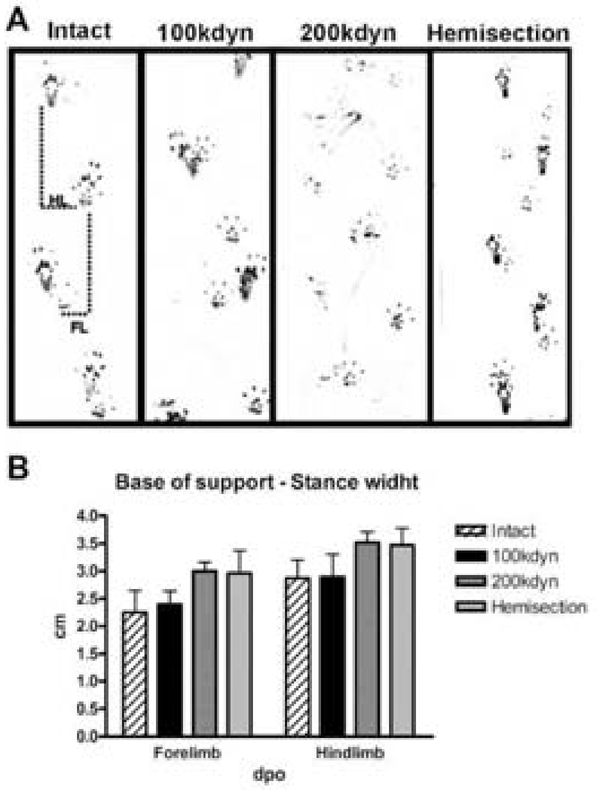

Fig. 3. Walking track test. (A) Representative images of the walking track performance in each group. Dashed lines indicate the hindlimb stance width and the forelimb stance width. Overlapping of fore and hind limbs is visible in intact animals, but is lost in injured animals (indicated by asterisks). Paw dragging in the 200 kdyn rat is indicated with black arrows. Note also the external rotation detected in 100 kdyn printing, indicated with an arrowhead. (B) Measurements of the distance between hindpaws and forepaws during the stance phase of stride. Hemisection and 200 kdyn group have increased distances between paws, although without statistical significance.

3.2. *Gait parameters and coordination in intact rats*

A group of intact animals was evaluated in order to obtain values from normal locomotion. These features were evaluated using more sophisticated techniques. Afterwards, animals receiving SCI with different severities were also evaluated, and values obtained were compared to the reference values obtained in intact animals.

3.2.1. *Validation of the technique*

Normal gait locomotion was first assessed in intact animals running at different speeds (10, 20 and 30 cm/s), and results were used to validate the technique (Clarke and Still, 1999; Mancuso et al., 2011). The time of stance of forelimbs and hindlimbs was similarly reduced as the speed increased (Fig. 4A and Table 1), but the duration of the swing was quite constant in hindlimbs and in forelimbs (Fig. 4B). The stride time diminished as the velocity increased in both forelimbs and hindlimbs steps (Fig. 4C). Consequently, the ratio between stance and swing duration showed the same trend to decrease as the speed was increased. The ratio for forelimb values was slightly lower than that of hindlimb values (Fig. 4D). The coefficient of variation, calculated for each parameter in order to assess regularity of the gait, was lower at the higher speeds than at 10 cm/s (Fig. 4E–G).

Different regular step patterns and limb coordinations were assessed in at least 9–10 steps for each animal and treadmill

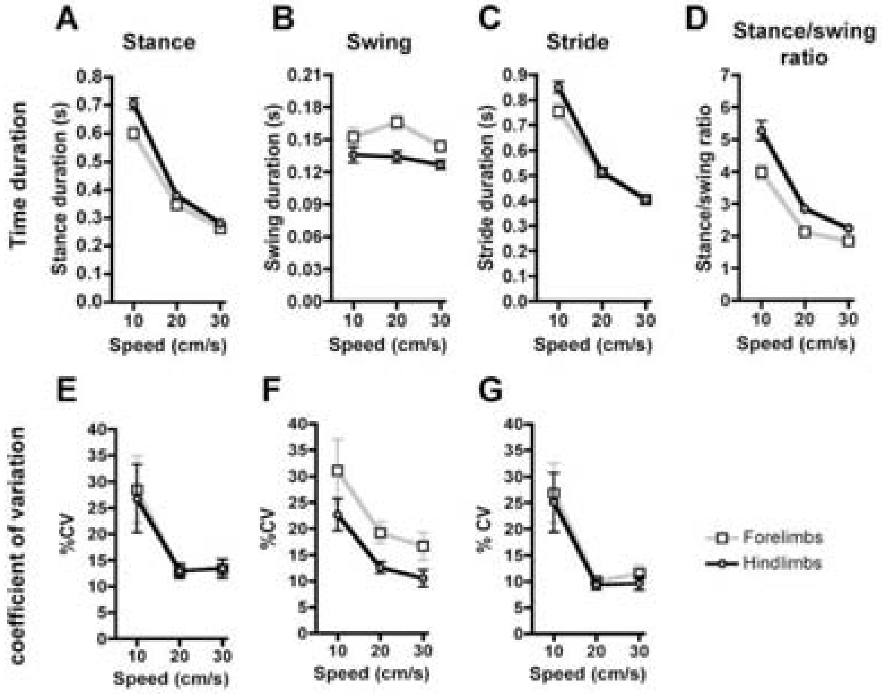

Fig. 4. Gait parameters in intact animals. Plots of the gait parameters for forelimbs and hindlimbs in control rats running at different speeds. Stance (A) and stride (C) times decrease as the speed increases. Swing time is maintained at all the speeds tested (B). The ratio between stance and swing times (D) also tends to decrease with increasing walking speed. The coefficient of variation was calculated for the stance time (E), the swing time (F) and the stride time (G). In all cases, increasing the speed reduces heterogeneity.

velocity. The only regular step pattern observed in intact rats was the alternated pattern (LF–RH–RF–LH, Fig. 1D) at 20 and 30 cm/s, while at 10 cm/s another alternated pattern (LF–LH–RF–RH, Fig. 1D) was observed in a few steps (15%). The alternated pattern LF–RH–RF–LH was therefore considered as the correct step sequence.

3.2.2. Interlimb coordination in intact animals

The interlimb alternations were also calculated for the ipsilateral (LF–LH and RF–RH), the diagonal (LF–RH and RF–LH) and the contralateral pair of limbs (LF–RF and RH–LH). Similarly to what happened with the regular step pattern, as the speed increased, the mistakes were reduced in ipsilateral, diagonal and contralateral alternations (Fig. 5A).

The phase dispersion was evaluated in intact animals running at increasing speeds, and results were expressed as a %PD, MaxPD and %CV for each speed. Ipsilateral limb pairs had an initial PD value of 60% that was maintained during the 10 steps at 20 and 30 cm/s, while the value at 10 cm/s rose to 150–200% as the animal walked (Fig. 5B). The highest MaxPD achieved was at the low speed (260%) and decreased at higher speeds (75%, Fig. 5C). The coefficient of variation followed the same tendency than the maximum PD, being more variable at 10 cm/s (Fig. 5D). Phase dispersion in the diagonal pairs of limbs displayed a similar pattern than the ipsilateral, starting with a low PD value (15%) and reaching higher values (75–150%) only at 10 cm/s (Fig. 5E). The maximum PD was 200% for the 10 cm/s speed, and about 25% for higher speeds (Fig. 5F). The CVs were around 30% for the three velocities (Fig. 5G). Contralateral combination of forelimbs increased from 50% to 125–200% at 10 cm/s, while it remained constant at higher speeds (Fig. 5H). Again, the higher maximum PD and CV was at 10 cm/s speed (180%), and higher speeds resulted in lower values (60%) (Fig. 5I and J). For the contralateral relationship of hindlimbs, PD values remained stable along the cycle of steps (around 50%) at all the speeds (Fig. 5K–M).

Table 1
Results of gait parameters in intact rats, used for validation of the technique. Values are given as mean ± SD.

Running speed	10 cm/s		20 cm/s		30 cm/s	
Parameter	Duration	%CV	Duration	%CV	Duration	%CV
Forelimbs						
Stride (s)	0.75 ± 0.09	26.85 ± 14.95	0.51 ± 0.03	10.06 ± 2.97	0.40 ± 0.02	11.48 ± 4.70
Stance (s)	0.60 ± 0.07	28.48 ± 16.9	0.34 ± 0.02	12.90 ± 4.59	0.26 ± 0.01	13.28 ± 5.72
Swing (s)	0.15 ± 0.22	16.61 ± 7.93	0.17 ± 0.02	19.21 ± 6.54	0.14 ± 0.01	16.61 ± 7.93
Stance/swing	3.98 ± 0.23		2.13 ± 0.09		1.84 ± 0.06	
Hindlimbs						
Stride (s)	0.85 ± 0.06	25.06 ± 15.03	0.51 ± 0.04	9.40 ± 2.83	0.50 ± 0.02	9.67 ± 3.99
Stance (s)	0.76 ± 0.05	26.74 ± 17.08	0.38 ± 0.02	12.97 ± 4.22	0.28 ± 0.01	13.41 ± 5.10
Swing (s)	0.13 ± 0.02	22.69 ± 8.23	0.13 ± 0.02	12.55 ± 3.37	0.13 ± 0.01	10.50 ± 4.81
Stance/swing	5.26 ± 0.29		2.85 ± 0.09		2.22 ± 0.07	

E. Redondo-Castro et al. / Journal of Neuroscience Methods 213 (2013) 165–178 171

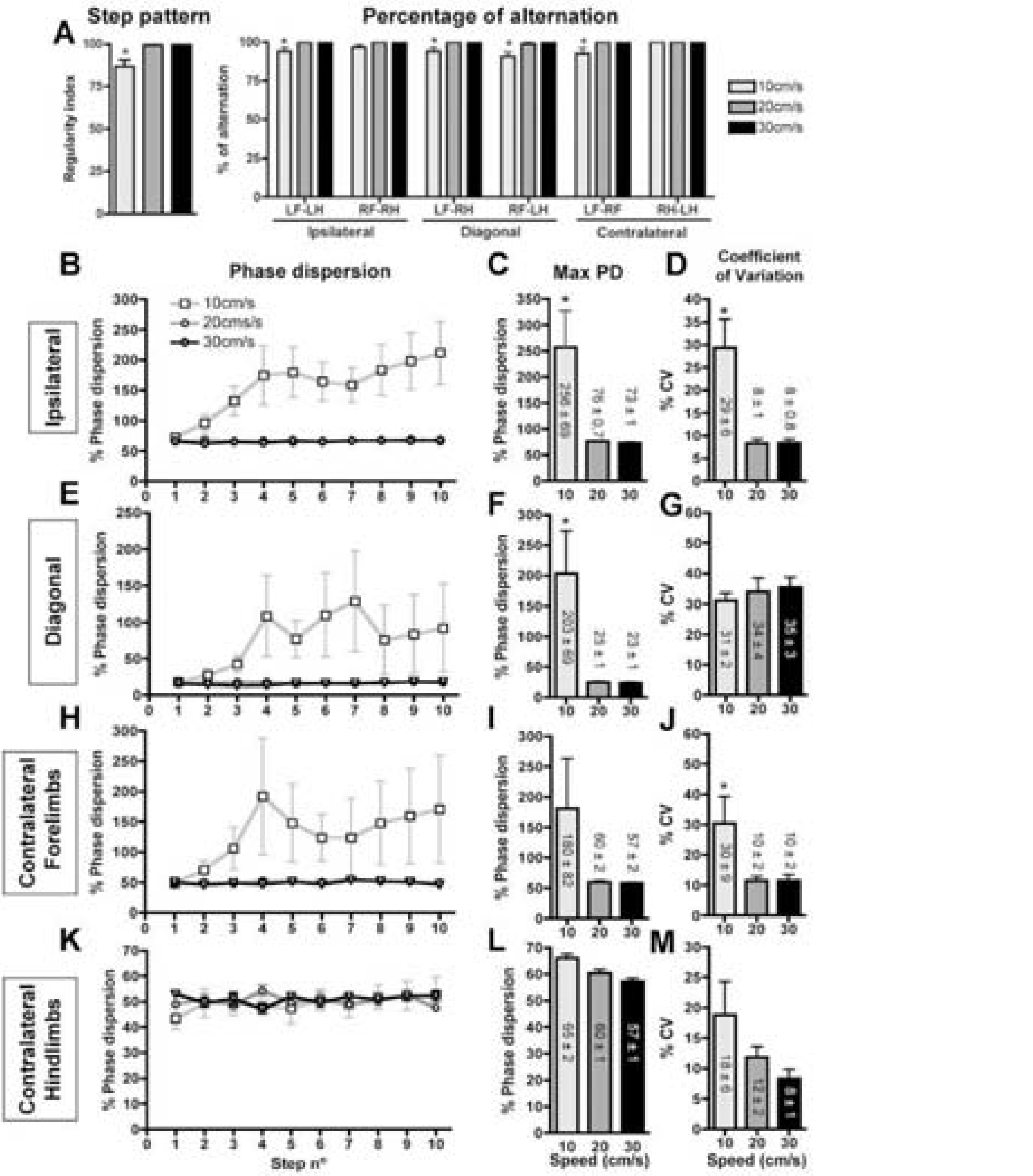

Fig. 5. Alternation and coordination in intact animals. (A) Left bar graph: regularity index of the alternated step pattern (LF–RH–RF–LH). Right bar graphs: the correct interlimb alternation was evaluated considering different combinations of limbs, and at different speeds. Animals running at 10 cm/s made some mistakes when performing the correct sequence in all combinations (ipsilateral, diagonal and contralateral). Accumulated percentual phase dispersion depicted for ipsilateral (B), diagonal (E) and contralateral (H, forelimbs; K, hindlimbs) coordinations at different speeds. Except for the hindlimbs (K), in all cases animals showed more homogeneous gait pattern and better coordination when walking at higher speeds. Maximum phase dispersions were calculated for each speed and combination (C, F, I, L), as well as the coefficient of variation (D, G, J, M). *$p < 0.05$ vs. 20 and 30 cm/s.

3.3. *Gait parameters and coordination in SCI rats*

The speed of 20 cm/s was chosen to perform gait analysis in SCI animals, since at 10 cm/s the gait is heterogeneous even in intact animals and at 30 cm/s some injured animals were not able to perform the test correctly (not weight support, short step sequences, etc.). At 20 cm/s speed it is considered that the rats follow a trot locomotion pattern.

3.3.1. *Gait parameters*

Table 2 shows the results obtained in each group of rats studied for the different parameters of the gait. The mean duration of forelimb gait parameters in 100 kdyn and hemisection animals was not significantly different from presurgical values (Fig. 6A). In the group of 200 kdyn, a significant reduction in the swing and the stride duration was found ($p < 0.05$ vs. intact). The stance/swing ratio increased after SCI, but only significantly in the 200 kdyn group ($p < 0.05$ vs. all groups, Fig. 6B). The CV of the three gait parameters analyzed was similarly increased in all injured groups with respect to intact animals, but without reaching statistical significance (Fig. 6C).

The changes in gait parameters were more evident in the hindlimbs. The time of stance showed a significant increase in both contused groups ($p < 0.05$, Fig. 6D) as well as a slight increase in the

Table 2
Results of gait parameters in spinal cord injured rats. Values are mean ± SD. Statistical significance.

Group	Intact		100 kdyn		200 kdyn		Hemisection	
Parameter	Duration	%CV	Duration	%CV	Duration	%CV	Duration	%CV
Forelimbs								
Stride (s)	0.51 ± 0.03	10.06 ± 2.97	0.50 ± 0.05	15.92 ± 6.64	0.43 ± 0.05$^{*,\#}$	14.22 ± 4.86	0.48 ± 0.08	16.77 ± 8.29
Stance (s)	0.34 ± 0.02	12.90 ± 4.59	0.36 ± 0.04	19.87 ± 7.44	0.32 ± 0.04	17.14 ± 4.49	0.34 ± 0.06	19.16 ± 7.13
Swing (s)	0.16 ± 0.02	19.22 ± 6.54	0.14 ± 0.02	25.19 ± 8.41	0.11 ± 0.02*	24.67 ± 6.07	0.14 ± 0.02	23.34 ± 8.54
Stance/swing	2.13 ± 0.29		2.56 ± 0.38		2.98 ± 0.57$^{*,\#}$		2.43 ± 0.32	
Hindlimbs								
Stride (s)	0.51 ± 0.04	12.97 ± 1.33	0.59 ± 0.04*	19.28 ± 2.09	0.55 ± 0.06	26.34 ± 3.53$^{*,\#}$	0.54 ± 0.05	20.62 ± 2.75
Stance (s)	0.38 ± 0.02	12.55 ± 1.06	0.46 ± 0.04*	18.64 ± 2.84*	0.44 ± 0.05*	20.29 ± 2.65	0.41 ± 0.05	17.79 ± 2.79
Swing (s)	0.13 ± 0.02	9.41 ± 0.89	0.13 ± 0.01	16.04 ± 2.01	0.11 ± 0.02	24.62 ± 3.59	0.12 ± 0.02	15.52 ± 1.34
Stance/swing	2.85 ± 0.3		3.57 ± 0.34*		4.18 ± 0.99$^{*,\#}$		3.51 ± 0.63*	

* $p < 0.05$ vs. intact values.
$^{\#}$ $p < 0.05$ vs. all other injured groups.

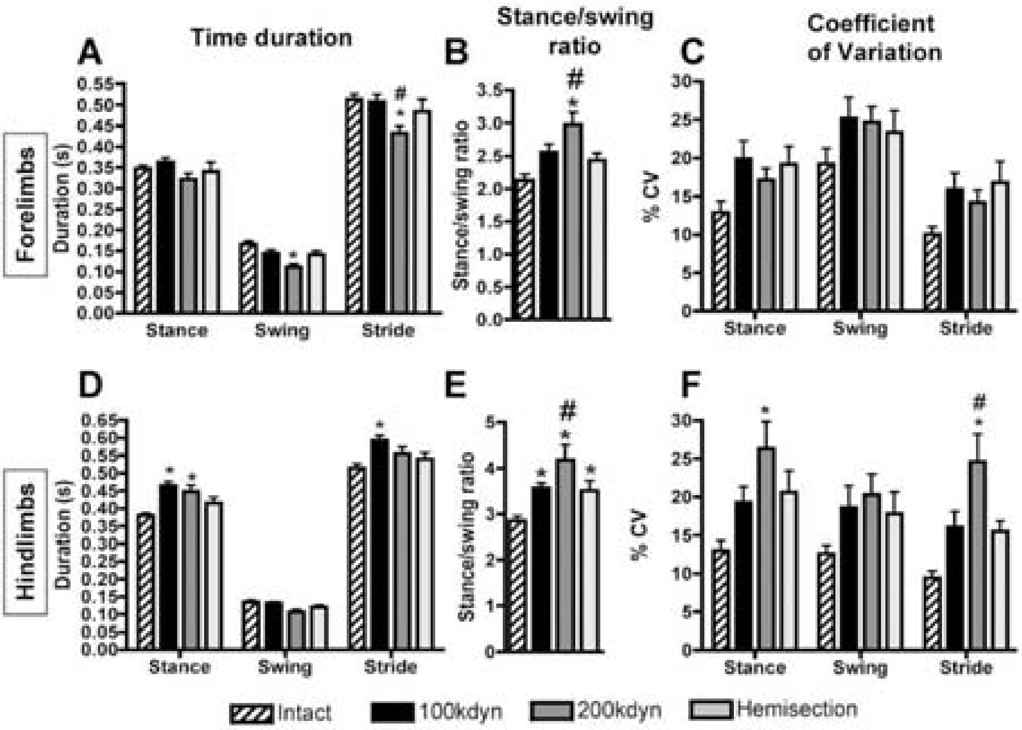

Fig. 6. Gait parameters in SCI rats. Measurements were performed from recordings obtained at 20 cm/s. The 200 kdyn group showed significant reduction in the time of swing and stride in the forelimbs (A) when compared to intact animals and to the other injured groups. A corresponding increase of the stance/swing ratio was also found (B). Despite the minor variations in the absolute values of the gait parameters, the coefficient of variation indicates an increase in the heterogeneity of gait in all SCI groups (C). Changes were more evident in the hindlimb parameters, with a significant increase in stance time in the two contused groups (D). The ratio between stance and swing times was increased in all the SCI groups (E). Consequently, the three injured groups had an increase in the coefficient of variation for all the parameters, indicating a loss of homogeneity in the gait (F). $^{*}p < 0.05$ vs. intact value; $^{\#}p < 0.05$ vs. other injured groups.

hemisection animals. Changes in stance time implied an increase of stride time that was significant in the 100 kdyn rats ($p < 0.05$, Fig. 6D), whereas the swing duration did not change in the injured groups. The stance/swing ratio was increased in all injured groups ($p < 0.05$; Fig. 6E). Similarly to what happened in the forelimbs, the CVs in injured groups were higher than intact values (Fig. 6F), but only in the 200 kdyn group reached statistical significance compared to intact animals for stance and stride duration, and to the other injured groups ($p < 0.05$).

3.3.2. Regular step patterns in SCI rats

Although different step patterns have been described in rodents, the alternated pattern is the most common (Cheng et al., 1997; Hamers et al., 2006). We confirmed that intact animals displayed an alternated pattern at 20 cm/s. After SCI the most commonly observed pattern was also the alternated one (LF–RH–RF–LH, Fig. 1D), with other sequences found in a few step cycles (less than 10%, data not shown) and some non-alternated steps following erratical sequences. Thus, only this alternated pattern was considered to calculate the RI. Fig. 7A illustrates the percentage of step sequences correctly performed, following the alternated pattern for intact and SCI animals while walking at 20 cm/s. At this speed, the RI of the four limbs was significantly affected in the three SCI groups (83 ± 5 in 100 kdyn, 23 ± 4 in 200 kdyn and 84 ± 5 in hemisection groups) compared to the 100% correctness observed in control rats.

E. Redondo-Castro et al. / Journal of Neuroscience Methods 213 (2013) 165–178 173

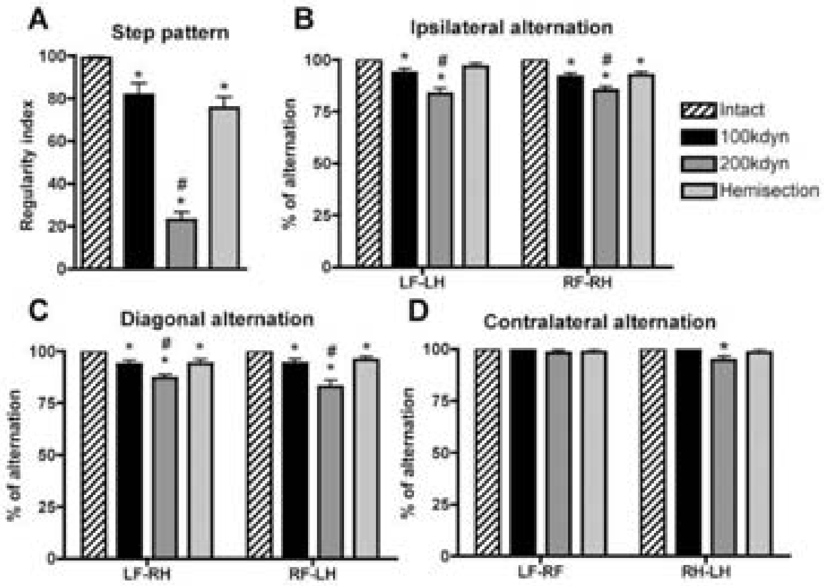

Fig. 7. Alternation in SCI rats. Regular step pattern data (A) indicates that all the SCI groups showed a reduction in the performance of correct stepping sequences, being the group of 200 kdyn the most abnormal. Ipsilateral (B) and diagonal alternations (C) offered similar results. All the injured groups presented a reduction in the percentage of correct stepping sequences, with the lowest values corresponding to the 200 kdyn group. Contralateral alternations in forelimbs and hindlimbs (D) were maintained in all groups, except in 200 kdyn group that presented a slight deficit in the hindlimbs. *$p < 0.05$ vs. intact value; #$p < 0.05$ vs. other injured groups.

3.3.3. *Interlimb coordination in SCI rats*

The ipsilateral alternation worsened significantly in both sides in the contused animals, and only in the right side for the hemisection rats (Fig. 7B). The diagonal alternation was affected in all injured groups (Fig. 7C). The contralateral alternation of the forelimbs was maintained as normal in all injured animals, whereas that of the hindlimbs was slightly decreased in the 200 kdyn group (Fig. 7D). In general, the deficits in alternations were more pronounced after the 200 kdyn contusion injury than after milder contusion and hemisection.

Interlimb time relationships were affected after SCI. Contused animals displayed an increase in the PD of ipsilateral limbs. In consecutive steps, values increased from 60 to 150% in the 100 kdyn group and to 400% in the 200 kdyn group while walking at 20 cm/s (Fig. 8A). The increase of the PD was statistically significant compared to intact values ($p < 0.05$), and also between the contused groups ($p < 0.05$, Fig. 8B). Similar differences were found for the %CV (Fig. 8C). In the hemisection rats, PD of ipsilateral limbs showed also a progressive increase more marked for the limbs ipsilateral to the lesion than the contralateral pair (Fig. 8D–F). In this case the maximum PD achieved was 145% in the contralateral side and 280% in the ipsilateral side ($p < 0.05$ vs. intact values, Fig. 8E). The CV was also higher in both sides, but only significantly in the ipsilateral side, compared to the intact value ($p < 0.05$, Fig. 8F).

Since both diagonal coordinations assessed (LF-RH and RF-LH) did not show significant differences between them, values have been pooled and only one value for diagonal coordination is expressed (Fig. 8G). Animals with a 200 kdyn contusion displayed the most marked loss of diagonal coordination, with values of PD increasing from 25% to almost 400%, whereas animals with 100 kdyn contusion and hemisection showed similar values, increasing to 100%. The maximum PD was increased in all injured groups compared to intact values, and in the 200 kdyn group was also significantly higher than in the other injured groups (Fig. 8H). As expected, the coefficients of variation were also increased in injured animals, although only the values of the 200 kdyn and the hemisection groups reached statistical significance versus intact values ($p < 0.05$, Fig. 8I).

Contralateral coordination in the forelimbs was not affected after any of the SCIs performed (Fig. 8J). The maximum PD values were very similar to the intact values in all the injured groups (Fig. 8K), whereas the coefficients of variation were higher than intact values, although without reaching statistical significance (Fig. 8L).

For the hindlimbs, contralateral coordination tended to worsen only in the hemisection group; while the intact and the contused groups showed a regular PD around 50%, in the hemisection group values rose to 70% in some steps (Fig. 8M). Consequently, the maximum PD was only slightly, non significantly higher than intact values (Fig. 8N). The CV increased in all the injured groups, but only significantly in the 200 kdyn group with respect to controls (Fig. 8O).

3.4. *Motor and sensory evoked potentials*

Electrophysiological techniques were used in order to assess the functionality of the spinal circuits as well as the traffic of information along the spinal cord. Motor evoked potentials were elicited at 1 Hz to record the brainstem component (bs-MEP), and at 9 Hz to record the cortical component (c-MEP, see Fig. 9A). The first component (with latency around 7 ms and amplitudes of 12–13 mV) was lost in all contused animals, except in one rat of the 100 kdyn group with a response of small amplitude. The bs-MEP was preserved in the contralateral side in the hemisection rats, although with a reduction in amplitude to about half of the control at 42 dpo, whereas in the ipsilateral side it was present in only two rats with very small amplitude (Fig. 9A–C).

When MEPs were elicited with a higher frequency (9 Hz), the second component was recorded with latency around 20 ms, and mean amplitude of about 2 mV in the preoperative tests. After injury, the c-MEP was absent in the 200 kdyn group and present in the rats with 100 kdyn contusion and with hemisection but with lower amplitudes than preoperative values (Fig. 9D–F).

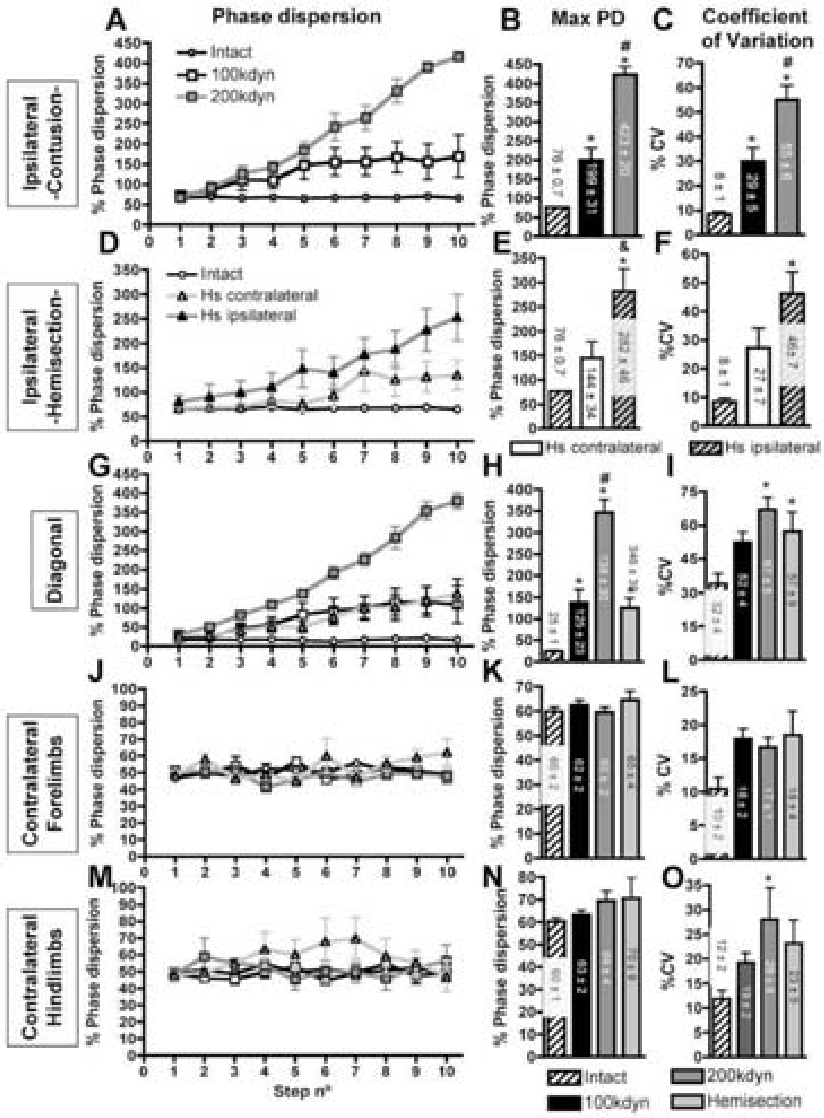

Fig. 8. Coordination in SCI rats. The accumulated phase dispersion of ipsilateral coordination in the contusion groups (A) indicated that the animals with more severe lesions had worst coordination, as indicated also by the maximum PD (B), and the coefficient of variation (C). Ipsilateral coordination in hemisection animals is worse in the injured side than in the contralateral side (D–F). Diagonal coordination was markedly affected in the 200 kdyn group. Animals with 100 kdyn contusion and hemisection showed similar impairment of diagonal coordination (G–I). Contralateral coordination appeared not to be affected in forelimbs (J) and hindlimbs (M), since PD values were maintained quite constant. Although the maximum PD was similar in all injured groups (K and N), the coefficient of variation was increased, especially for the hindlimbs (L and O). *$p < 0.05$ vs. intact values; #$p < 0.05$ vs. other injured groups; &$p < 0.05$ vs. contralateral side.

Regarding the SSEPs, only the mild contusion group and the hemisection group in the contralateral side presented partial preservation of the three components. Their amplitude was near normal in the hemisection group, but reduced in the 100 kdyn group (Fig. 9G–M).

4. Discussion

In this work we have assessed and compared the deficits in locomotion after SCIs of different severity in the rat, by means of simple methods that imply voluntary locomotion and stereotyped tasks (Basso et al., 1995; Collazos-Castro et al., 2005; De Medinaceli et al., 1982), and a more sophisticated digitized locomotion test under forced locomotion on a treadmill. The information obtained provides a comparative evaluation of the sensitivity and suitability of the different methods for performing a detailed assessment of the functional state of animals after different SCIs, as well as to improve the detection of possible changes following treatments or repair strategies (Kuerzi et al., 2010). Moreover, they offer an overview of the functional outcome after different kinds of spinal cord lesions.

4.1. Common tests for functional evaluation of locomotion

There are several tests and scoring systems to evaluate deficits of locomotion after CNS injuries. The most used are probably the 5 points Tarlov scale (Tarlov and Klinger, 1954) and the BBB open field walking test (Basso et al., 1995), which permit to detect gross deficits in locomotion, and are especially useful in discriminating animals receiving lesions of different severity. The main problems

E. Redondo-Castro et al. / Journal of Neuroscience Methods 213 (2013) 165–178 175

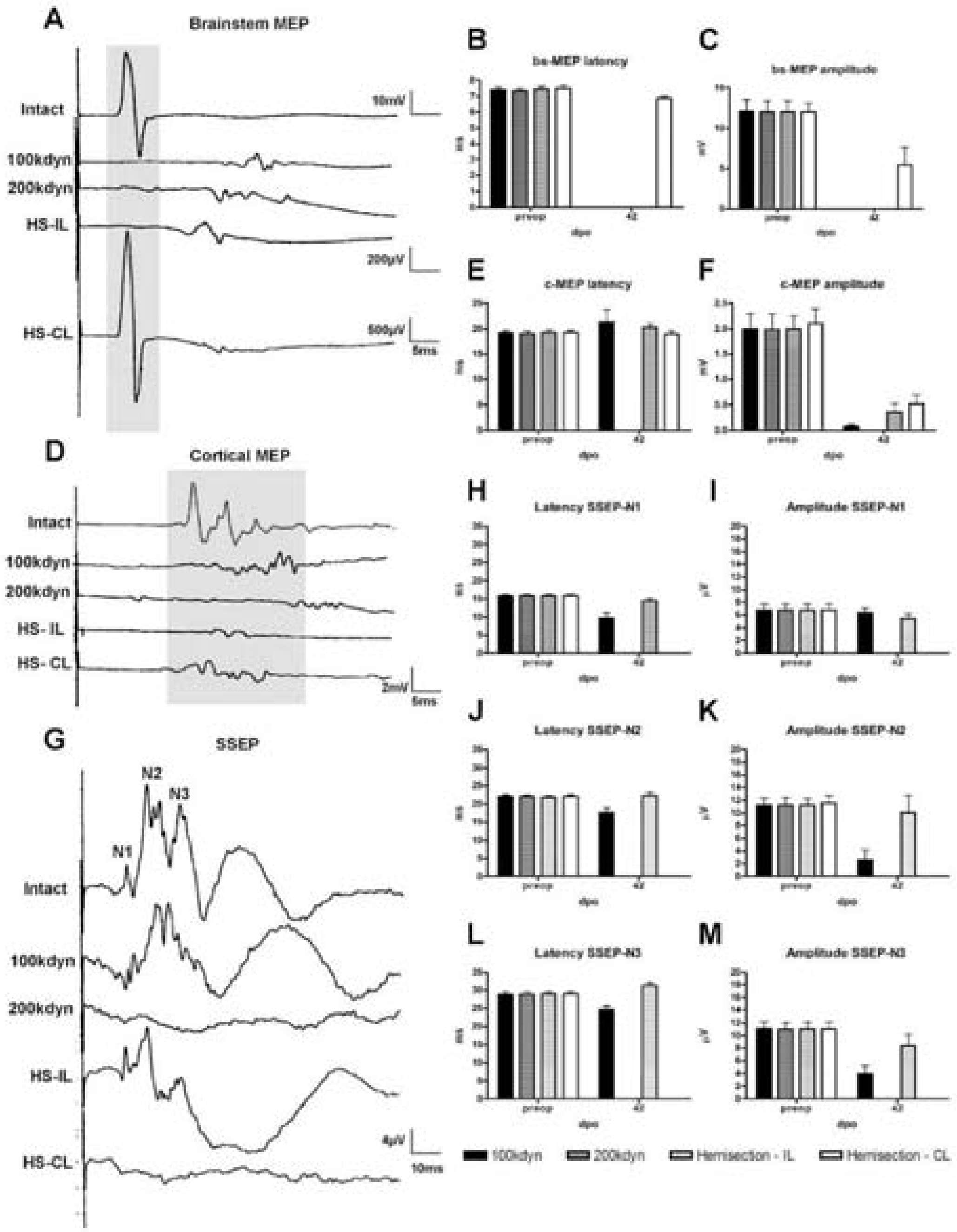

Fig. 9. Electrophysiology. (A) Brainstem motor evoked potentials (bs-MEP): representative recordings from rats of each group. Only the group with hemisection had preserved the bs-MEP in the contralateral side to the injury. (B) The latency of the first MEP component was normal in those cases (hemisection). (C) The amplitude of the preserved bs-MEPs was reduced around 50% compared to preoperative values. (D) Cortical motor evoked potentials (c-MEP): the second component of the MEPs was recordable in all injured groups except the 200 kdyn group, with longer latency than the bs-MEPs. (E) The latency of c-MEP was increased in the contusion groups, but not in hemisection rats. (F) The amplitude of the c-MEPs was very small in all 100 kdyn and hemisection rats six weeks after injury. (G) Somatosensory evoked potentials (SSEPs): representative recordings from each group. Three components (labeled N1–N3) are recorded in intact animals. After injury, only some of these components were recorded in rats of groups 100 kdyn and hemisection. (H, J and L). Latencies of the SSEP waves did not change significantly after injury. (I, K and M) The amplitudes of N1–N3 components were near normal in the ipsilateral side of the hemisection rats, reduced in the 100 kdyn rats, and absent in the 200 kdyn rats.

with such methods are the subjectivity associated with the observational nature of assessment, as well as the limited discriminative power mainly in the upper part of the scale (Basso et al., 1996). Despite additional subscorings were introduced to give an extra refinement to the final part of the BBB scale (Basso, 2004; Ferguson et al., 2004), the quantification of the coordination between forelimbs and hindlimbs still remains conflictive (Koopmans et al., 2005). Assuming this, treatments unable to reach differences in this part of the scale may have probably been discarded for further testing, because of the inability to detect small improvements in the coordination part. Nevertheless, it constitutes one of the best tests to do a fast evaluation of the functional state of an animal after SCI. In our animals with spinal cord contusion there was good relationship between the BBB score and the severity of the lesion, as originally reported (Basso et al., 1995). Hemisection animals, receiving a lesion supposed to be milder than spinal cord contusion, presented similar results to the 100 kdyn group, mainly characterized by the loss of coordinated gait. It is important to note that the BBB scale was designed to evaluate functional outcomes after thoracic contusion injuries and not for partial sections, although it is often used also for these lesions (García-Alías et al., 2011; Sharp et al., 2012). Thus, these two different injuries result in similar BBB scores.

The inclined plane test was used to assess the functional integrity of some supraspinal pathways (Zhang et al., 2009). In this test forelimbs are also assessed, as well as general balance. The narrow beam test is more focused on assessment of fine coordination, since animals have to be skilled enough to cross the beam without foot slips. In contrast, other tests, like the BBB test, can be performed even by moderately injured animals (Collazos-Castro et al., 2005). The *difficult locomotion* is partially driven by the corticospinal tract, which is not so relevant in *routine* locomotion in rodents (Drew et al., 2004; Majczyński and Sławińska, 2007; Rossignol and Frigon, 2011). Thus, changes in the narrow beam test may reveal involvement of corticospinal tracts (at least ventral and lateral fascicles), in contrast to the open field walking test that does not depend on corticospinal pathways (Basso et al., 1996).

Tests like the walking track foot print analysis are aimed to assess changes regarding gait coordination and base of support (García-Alías et al., 2011; De Medinaceli et al., 1982; Metz and Schwab, 2004). An increase in the distance between paws may indicate that the animal is adapting its support base in order to improve equilibrium and to reduce the torque suffered by joints and muscles (Ballermann et al., 2006; Kloos et al., 2005), constituting compensatory mechanisms more than recovery of the lost function (Majczyński and Sławińska, 2007). Another detectable aspect in the walking track prints is the overlapping between ipsilateral forepaw and hindpaw steps that occurs in animals with a coordinated gait. Unfortunately, this parameter is difficult to quantify with this technique, so only large deficits in coordination are easily detected. Moreover, frequent deficits such as dorsal stepping or paw dragging are rarely evaluated in this method, and they may introduce mistakes in the measurements. Without video recordings, the speed of the locomotion is missed, as well as the duration of the step or the synchrony between steps. Similarly, the possibility to obtain a regular and long gait sequence at a similar speed in each animal is unlikely. Although SCI animals present signs of improvement in the walking track test (García-Alías et al., 2010), these do not necessarily imply recovery of central connections, but most likely depend on postural adaptations and some spontaneous recovery of the ability to support weight with the hindlimbs, a feature essential for performing patterned locomotion (Kloos et al., 2005; Kuerzi et al., 2010).

4.2. Evaluation of locomotion and coordination

In the last years new methods have been developed in order to provide objective quantitative measurements related to locomotion and functional recovery after neural injuries. One of them is the CatWalk system (Hamers et al., 2001, 2006; Koopmans et al., 2005) based on recording the animal walking in a corridor above a mirror where the paw contact with the floor can be taped and analyzed. The main parameters used are the step sequence distribution, the regularity index, the print area and the maximum contact during the stance phase, the duration of the swing and stance phases, the base of support and the dragging of the tail and the abdomen. The main disadvantages of this technique are the problems with the overlapping of paws in animals with uncoordinated gaits, as well as the variable speed that each animal can take when crossing the corridor. Other new techniques, such as the Treadscan (Beare et al., 2009) and the Digigait system, allow also recording and analysis of the gait but include a programmable running belt in order to control the speed of the animal walk. By controlling the speed factor the locomotion may become forced at some point, and give a reliable indication of the animals locomotor capability (Mancuso et al., 2011). Adding controllable difficulty to the locomotion task implies a better discrimination between lesions or treatments, since only animals with better conditions are able to perform the more demanding test condition.

Previous works have used the Digigait Imaging system to evaluate the pattern of locomotion in different animal models (Amende et al., 2005; Berryman et al., 2009; Hampton et al., 2004; Kale et al., 2004), but only a few in SCI models (McEwen and Springer, 2006; Springer, 2010). Unfortunately, physical limitations of the more severely injured animals (external paw rotation, problems regarding the orientation of the body, etc.), precluded the use of Digigait Imaging system software directly, and we have added programmed simple Visual Basic® macros to manually calculate some parameters directly from the footfall diagrams.

Our initial validation in intact rats presented the expected decrease of the duration of the different gait parameters at increasing treadmill speed (Clarke and Still, 1999; Mancuso et al., 2011). Moreover, the limbs alternation tends to be perfect for all possible calculations (ipsilateral, diagonal and contralateral) at 20–30 cm/s, velocities that are around the physiological walking speed (~25 cm/s, Berryman et al., 2009). At the low speed of 10 cm/s the animals made some missteps, resulting in increasing values of phase dispersion. These mistakes were especially frequent in the forelimbs and consequently affected the ipsilateral and diagonal coordinations, in which the connectivity between forelimbs and hindlimbs is needed, as well as in the contralateral coordination in forelimbs. In contrast, at 20 and 30 cm/s the results show a continuous and homogenous coordination, since PD values remain almost constant, indicating that normal rats walk in a regular and coordinated manner, following always the correct alternation between ipsilateral and contralateral limb pairs. The diagonal PD value lower than 15–20% indicates that at these speeds the animals run with a trot alternation pattern (Grillner, 1981).

The speed of 20 cm/s was selected to analyze the rat locomotion after SCIs, because the majority of animals were able to walk for enough time to obtain a good video recording. At 30 cm/s, some injured rats presented difficulties to make enough valid consecutive steps to analyze progression of the PD and thus to detect differences between lesions. In the analysis of locomotion after SCI the first deficits were detected in the duration of the gait parameters. Animals with contusion tend to increase the time of stance and stride, indicating that they spend more time in the foot contact phase, probably in order to add stability to the gait, as the stance/swing ratio indicates. Hemisection animals displayed the same trend, although not so markedly. Another typical feature of locomotion in SCI rats is the loss of regularity, as indicated by the increase in the coefficient of variation.

The regular step pattern provides an intuitive representation of the coordination deficits after SCI. This measure is one of the most useful, since it is correlated with the BBB results, but being a more quantitative and objective approach. Significant deficits in alternation were found for forelimb–hindlimb relationships (diagonal and ipsilateral alternation), but not across the shoulder and pelvic girdles (contralateral alternation). The contralateral alternation presented only slight deficits in the moderate contusion group, but tended to be unaffected at six weeks after injury, demonstrating that connectivity between forelimbs and between hindlimbs was preserved. When the connectivity implies limbs from the anterior and the posterior trains deficits become evident, especially in the 200 kdyn group. The loss of alternation indicates that injured animals make mistakes in the stepping sequence, mainly because they add some extra steps to compensate the increase in the stride time.

Animals with a 200 kdyn contusion presented the most severe deficits, with high values of PD and CV, indicating uncoordinated gait. The animals with mild contusion showed lower degree of uncoordination and less heterogeneity in the steps. In the hemisection rats, the deficits were similar to the 100 kdyn ones, but more marked in the side ipsilateral to the lesion, affecting ipsilateral and diagonal relationships, in which connectivity between the shoulder and the girdle limbs is needed. These data indicate that the spinal cord lesions interrupted propiospinal connections between anterior and posterior central pattern generators (CPGs), but that each CPG was not affected. Therefore, the coordination between forelimbs and between hindlimbs remained unaffected, as indicated by the values of PD and CV.

It is important to note that, although digitizing systems have been previously used in the literature, the novel methodology developed in this work is comparatively simple and not time consuming. The results obtained are easy to interpret and do not need exhaustive analyses, although they provide a quantitative detailed evaluation of locomotion in SCI rats, and are well correlated with the most common observational methods. Amongst all the calculated values and parameters, the most useful and simple to explain locomotion deficits, are the maximum PD and the correct performance of the regular step patterns. Nevertheless, depending upon the experimental design, different parameters may result more sensitive for the detection of slight changes, and thus more useful for the study.

4.3. Motor and somatosensory evoked potentials

Most functional deficits after SCIs are caused by the partial or total loss of ascending and descending tracts, so electrophysiological tests are very useful to complement the functional assessment of animals (Cao et al., 2005; García-Alías et al., 2006; Redondo Castro et al., 2011; Valero-Cabré et al., 2004).

The brainstem component of MEPs was lost in all SCI rats, except in the left side of the hemisection group; this implies a direct pathway from supraspinal centers, without side crossing. Regarding the second component, it was partially preserved after SCI, except in the 200 kdyn contusion. The results of MEPs corroborate the disruption of dorsal and lateral motor pathways, although the partial preservation of ventral tracts permits the uncoordinated stepping, and in some cases even some coordinate steps, in rats with mild thoracic cord contusion. The main deficits in the 100 kdyn contusion and in the hemisection groups were the loss of coordination, and this might be due to involvement of the dorsal corticospinal tract (Majczyński and Sławińska, 2007). The higher preservation of the dorsolateral tracts would be the cause of the functional differences compared to the more severe spinal cord contusion.

In this work we have addressed the quantification of different features of locomotion after different SCIs in the rat, in order to provide objective tests that can be easily performed in the experimental laboratory. We propose a set of measurements derived from the recorded paws of the rats during forced walking on a treadmill in order to quantify the functional deficits after SCI. The main advantage of this new approach is the quantification of limb coordination features, as well as the relative simplicity and short time needed of the technique. In addition to the classical functional tests, our analysis provides a complete characterization of the deficits occurring after SCI, and allows clear discrimination between lesions of different severity.

Conflict of interest

No competing financial interests exist.

Acknowledgements

This work was supported by grants from the Fundació MaratóTV3 (grant 070210), the Ministerio de Ciencia e Innovación (grant SAF2009-12495), and funds from Red de Terapia Celular (TERCEL) of Spain. We thank the technical assistance of Monica Espejo, Jessica Jaramillo and Marta Morell.

The Visual Basic® macro for Excel programs developed in this study is available under request to the authors.

References

Amende I, Kale A, Mccue S, Glazier S, Morgan JP, Hampton TG. Gait dynamics in mouse models of Parkinson's disease and Huntington's disease. J Neuroeng Rehabil 2005;13:1–13.

Ballermann M, Tse ADY, Misiaszek JE, Fouad K. Adaptations in the walking pattern of spinal cord injured rats. J Neurotrauma 2006;23:897–907.

Basso DM, Beattie MS, Bresnahan JC. A sensitive and reliable locomotor rating scale for open field testing in rats. J Neurotrauma 1995;12:1–21.

Basso DM, Beattie MS, Bresnahan JC. Graded histological and locomotor outcomes after spinal cord contusion using the NYU weight-drop device versus transection. Exp Neurol 1996;139:244–56.

Basso DM. Behavioral testing after spinal cord injury: congruities, complexities, and controversies. J Neurotrauma 2004;21:395–404.

Beare JE, Morehouse JR, Devries WH, Enzmann GU, Burke DA, Magnuson DSK, et al. Gait analysis in normal and spinal contused mice using the TreadScan system. J Neurotrauma 2009;26:2045–56.

Berryman ER, Harris RL, Moalli M, Bagi CM. Digigait quantitation of gait dynamics in rat rheumatoid arthritis model. J Musculoskelet Neuronal Interact 2009;9:89–98.

Cao Q, Zhang YP, Iannotti C, DeVries WH, Xu X-M, Shields CB, et al. Functional and electrophysiological changes after graded traumatic spinal cord injury in adult rat. Exp Neurol 2005;191(Suppl.):S3–16.

Cheng H, Almström S, Giménez-Llort L, Chang R, Ove Ogren S, Hoffer B, et al. Gait analysis of adult paraplegic rats after spinal cord repair. Exp Neurol 1997;148:544–57.

Clarke K, Still J. Gait analysis in the mouse. Physiol Behav 1999;66:723–9.

Collazos-Castro JE, Soto VM, Gutiérrez-Dávila M, Nieto-Sampedro M. Motoneuron loss associated with chronic locomotion impairments after spinal cord contusion in the rat. J Neurotrauma 2005;22:544–58.

Curt A, Van Hedel HJ, Klaus D, Dietz V. Recovery from a spinal cord injury: significance of compensation, neural plasticity, and repair. J Neurotrauma 2008;25:677–85.

Drew T, Prentice S, Schepens B. Cortical and brainstem control of locomotion. Prog Brain Res 2004;143:251–61.

Ferguson AR, Hook M, Garcia G, Bresnahan JC, Beattie MS, Grau JW. A simple post hoc transformation that improves the metric properties of the BBB scale for rats with moderate to severe spinal cord injury. J Neurotrauma 2004;21:1601–13.

García-Alías G, Petrosyan HA, Schnell L, Horner PJ, Bowers WJ, Mendell LM, et al. Chondroitinase ABC combined with neurotrophin NT-3 secretion and NR2D expression promotes axonal plasticity and functional recovery in rats with lateral hemisection of the spinal cord. J Neurosci 2011;31:17788–99.

García-Alías G, Torres-Espín A, Vallejo C, Navarro X. Functional involvement of the lumbar spinal cord after contusion to T8 spinal segment of the rat. Restor Neurol Neurosci 2010;28:781–92.

García-Alías G, Valero-Cabré A, López-Vales R, Forés J, Verdú E, Navarro X. Differential motor and electrophysiological outcome in rats with mid-thoracic or high lumbar incomplete spinal cord injuries. Brain Res 2006;1108:195–204.

Grillner S. Control of locomotion in bipeds, tetrapods, and fish. In: Handbook of physiology. The nervous system. Baltimore: Waverly Press; 1981.

Gulino R, Dimartino M, Casabona A, Lombardo SA, Perciavalle V. Synaptic plasticity modulates the spontaneous recovery of locomotion after spinal cord hemisection. Neurosci Res 2007;57:148–56.

Hamers FP, Lankhorst a J, van Laar TJ, Veldhuis WB, Gispen WH. Automated quantitative gait analysis during overground locomotion in the rat: its application to spinal cord contusion and transection injuries. J Neurotrauma 2001;18:187–201.

Hamers FP, Koopmans GC, Joosten EA. CatWalk-assisted gait analysis in the assessment of spinal cord injury. J Neurotrauma 2006;23:537–48.

Hampton TG, Stasko MR, Kale A, Amende I, Costa ACS. Gait dynamics in trisomic mice: quantitative neurological traits of Down syndrome. Physiol Behav 2004;82:381–9.

Kale A, Amende I, Meyer GP, Crabbe JC, Hampton TG. Ethanol's effects on gait dynamics in mice investigated by ventral plane videography. Alcohol Clin Exp Res 2004;28:1839–48.

Kloos AD, Fisher LC, Detloff MR, Hassenzahl DL, Basso DM. Stepwise motor and all-or-none sensory recovery is associated with nonlinear sparing after incremental spinal cord injury in rats. Exp Neurol 2005;191:251–65.

Koopmans GC, Deumens R, Honig WMM, Hamers FPT, Steinbusch HWM, Joosten EA. The assessment of locomotor function in spinal cord injured rats: the importance of objective analysis of coordination. J Neurotrauma 2005;22:214–25.

Kuerzi J, Brown EH, Shum-Siu A, Siu A, Burke D, Morehouse J, et al. Task-specificity vs. ceiling effect: step-training in shallow water after spinal cord injury. Exp Neurol 2010;224:178–87.

Leblond H, L'Espérance M, Orsal D, Rossignol S. Treadmill locomotion in the intact and spinal mouse. J Neurosci 2003;23:11411–9.

Majczyński H, Sławińska U. Locomotor recovery after thoracic spinal cord lesions in cats, rats and humans. Acta Neurobiol Exp 2007;67:235–57.

Mancuso R, Oliván S, Osta R, Navarro X. Evolution of gait abnormalities in SOD1(G93A) transgenic mice. Brain Res 2011:1–9.

McEwen ML, Springer JE. Quantification of locomotor recovery following spinal cord contusion in adult rats. J Neurotrauma 2006;23:1632–53.

De Medinaceli L, Freed WJ, Wyatt RJ. An index of the functional condition of rat sciatic nerve based on measurements made from walking tracks. Exp Neurol 1982;77:634–43.

Metz GA, Schwab ME. Behavioral characterization in a comprehensive mouse test battery reveals motor and sensory impairments in growth-associated protein-43 null mutant mice. Neuroscience 2004;129:563–74.

Redondo Castro E, Udina E, Verdú E, Navarro X. Longitudinal study of wind-up responses after graded spinal cord injuries in the adult rat. Restor Neurol Neurosci 2011;29:115–26.

Rossignol S, Frigon A. Recovery of locomotion after spinal cord injury: some facts and mechanisms. Annu Rev Neurosci 2011;34:413–40.

Sharp KG, Dickson AR, Marchenko SA, Yee KM, Emery PN, Laidmåe I, et al. Salmon fibrin treatment of spinal cord injury promotes functional recovery and density of serotonergic innervation. Exp Neurol 2012;235:345–56.

Springer JE. The functional and neuroprotective actions in the treatment of acute spinal cord injury. J Neurotrauma 2010;27:139–49.

Tarlov IM, Klinger H. Spinal cord compression studies. II. Time limits for recovery after acute compression in dogs. AMA Arch Neurol Psychiatry 1954;71:271–90.

Valero-Cabré A, Forés J, Navarro X. Reorganization of reflex responses mediated by different afferent sensory fibers after spinal cord transection. J Neurophysiol 2004;91:2838–48.

Vincelette J, Xu Y, Zhang L-N, Schaefer CJ, Vergona R, Sullivan ME, et al. Gait analysis in a murine model of collagen-induced arthritis. Arthritis Res Ther 2007;9:R123.

Zhang J, Zhang A, Sun Y, Cao X, Zhang N. Treatment with immunosuppressants FTY720 and tacrolimus promotes functional recovery after spinal cord injury in rats. Tohoku J Exp Med 2009;219:295–302.

3

Study of plastic and functional changes occurring at caudal segments of the spinal cord injury

Specific objectives

Spinal cord injury effects are not limited to the injury site itself but expand caudal and rostrally to other regions of the nervous system. Moreover, not only the damaged elements play a role in the appearance of functional, motor and sensory deficits, but the apparently preserved elements can also be involved. This fact is mainly based in the limited regenerative possibilities of the spinal cord and in the plasticity of the spinal circuits and cells.

Due to the catastrophic nature of the SCI, little can be done to restore the injury site, and most therapeutical attempts are focused to reduce the extension of tissue damage in the secondary injury phase, although with limited success until now. Contrarily, segments away from the injury site can be remodeled and readapted to the new situation, and offer challenging opportunities for the development of new strategies. In order to have an integrated view of the plasticity in remote regions from the lesion, we have investigated the changes affecting several elements along the nociceptive spinal circuit, which may play a relevant role in the development of neuropathic pain and hyperreflexia. Moreover, it is important to take into account the preservation of peripheral nerve functionality. The specific objectives for this chapter are:

1. Study of the changes in the central projections of sensory afferences to the dorsal horn and in the local inhibitory tone.

2. Assessment of the glial activation in the spinal cord after chronic SCI.

3. Evaluation of the descending inhibitory pathways and the spinal inhibitory synapses.

4. Functional evaluation of plastic changes in the spinal circuits, by means of electrophysiological techniques.

5. Study of the sensory dysfunctions, particularly of neuropathic pain, occurring as a consequence of the plastic changes in the spinal cord caudal to a SCI.

6. Assessment of axonal preservation in the sciatic nerve after different spinal cord injuries.

To achieve all these objectives, we used experimental models of SCI of varying severity to evaluate the relative importance of plastic changes in each type of lesion in relation with the type of injury. The obtained results are organized in two publications.

Publication

Plastic changes in lumbar segments after thoracic spinal cord injuries in adult rats: an integrative view of nociceptive dysfunctions

E.Redondo Castro, G. García-Alías, X.Navarro

Submitted to Journal of Restorative Neurology and Neuroscience

Plastic changes in lumbar segments after thoracic spinal cord injuries in adult rats: an integrative view of spinal nociceptive dysfunctions.

Elena Redondo Castro[1], Guillermo García-Alías[2], Xavier Navarro[1].

[1] Group of Neuroplasticity and Regeneration, Institute of Neurosciences and Department of Cell Biology, Physiology and Immunology, Universitat Autònoma de Barcelona, and Centro de Investigación Biomédica en Red sobre Enfermedades Neurodegenerativas (CIBERNED), Bellaterra, Spain.

[2] Department of Integrative Biology and Physiology. University of California Los Angeles. Los Angeles, CA 90095-1606, US.

Corresponding author: Dr. Xavier Navarro, Unitat de Fisiologia Mèdica, Facultat de Medicina, Universitat Autònoma de Barcelona, E-08193 Bellaterra, Spain. E-mail: xavier.navarro@uab.cat

Key words: neuropathic pain, spinal cord injury, disinhibition, hyperreflexia, plasticity.

ABSTRACT:

Purpose: Spinal cord injuries (SCI) cause motor, sensory and autonomic dysfunctions below the level of lesion, and one of the most disabling consequences is neuropathic pain. Since segments away from the epicenter lesion are also affected, we investigated plastic changes occurring in lumbar segments, to assess their contribution to pain states after SCI. **Methods**: Different thoracic SCIs were performed in adult rats. Several elements of the spinal nociceptive circuit were assessed, mainly by immunohistochemistry. **Results**: We detected alterations in different markers placed along all the spinal nociceptive circuitry. The increase detected in the GAD65/67 enzyme and in gephyrin may indicate a boost in spinal inhibition. Contrarily, other elements were indicative of hyperexcitability, such as gliosis, the major presence of sensory afferences, and the loss of serotoninergic fibers. Not all changes kept direct relationship to the severity of the injury. **Conclusion**: The presence of neuropathic pain despite the increase in inhibitory tone confirmed the unbalance between excitation and inhibition mechanisms, in this case leading to a general disinhibition. Since widespread dysfunctions in apparently intact caudal segments after a central injury are relevant to the appearance of pain, they emerge as new targets for therapies aimed to modulate spinal function.

1. INTRODUCTION

Spinal cord injuries (SCIs) cause deficits of motor, sensory and autonomic functions below the lesion level, that are also accompanied by the development of positive signs due to abnormal signal processing in the remaining circuitry. These dysfunctions are usually permanent, and different mechanisms are involved in their appearance and maintenance: abnormally persistent gliosis and inflammation, central and peripheral sensitization, as well as a wide range of molecular events that induce functional alterations in the spinal cord after injury (for reviews see Costigan and Woolf, 2000; Yezierski, 2005; Hulsebosch, 2008, 2009)). They provoke a maladaptive response of the spinal system, leading to the appearance of hyperreflexia and spasticity, as well as neuropathic pain. Among these symptoms, the most devastating is neuropathic pain, that severely affects the quality of life of the patients (Hulsebosch et al., 2009; Soler et al., 2007; Yezierski, 2005). Moreover, most pharmacological treatments are ineffective for neuropathic pain, hardening even more the daily life of those who suffer from it (Finnerup et al., 2007; Hulsebosch, 2002).

.

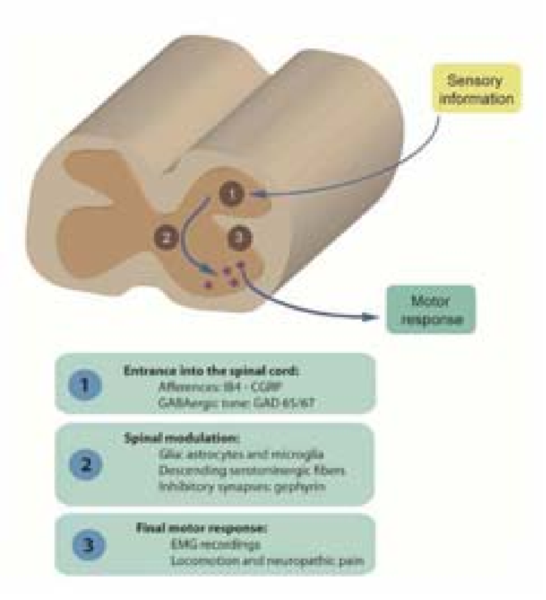

Figure 1: *Schematic view of the nociceptive circuitry in the lumbar spinal cord. Sensory afferences (IB4 and CGRP labeled fibers) enter to the spinal cord by the dorsal horn (1), where they connect with second order neurons. These synaptic connections are subjected to inhibitory modulation by the interneurons of the GABAergic system. Once in the spinal cord (2), glial cells and monoaminergic descending fibers provide an extra modulation to the nociceptive information. On the efferent side, gephyrin modulates the clusterization and functionality of inhibitory synapses on motoneurons (3). The nociceptive response travels to the periphery in form of motor reflex response, that can be recorded by electromyography.*

Alterations in the pain pathways after a SCI are numerous, and may act simultaneously at different points of the pain circuitry. Since the lesion is devastating in the epicenter, little can be done to repair the injured area, but in the last years, many researchers are focusing their efforts in areas far away from the lesion site. This is the case of the lumbar segments, which although not being affected by the primary lesion, present important changes in their functions after a thoracic cord injury (García-Alías et al., 2010; Detloff et al., 2008; Carlton et al., 2009; Lee et al., 2005). Therefore, it is important to know how segments caudal to the injury modify the sensory and motor information which travels along them, and how these adaptations can influence the pain circuitry and the neuropathic pain symptoms, such as hyperalgesia (i.e. exaggerated response to noxious stimuli) and allodynia (i.e. painful response to innocuous stimuli).

The dorsal horn is an important component of the sensory pathways since it receives the input of nociceptive fibers, which are susceptible of changes after an injury. Moreover, it is also the first site of modulation and integration of pain signals in the spinal cord (Ondarza, et al., 2003; Takazaa and MacDermott, 2010). This modulation is mainly done by inhibitory interneurons secreting GABA, as well as by descending pathways from supraspinal centers releasing noradrenaline and serotonin (Vanegas and Schaible, 2004). The GABAergic interneurons mediate presynaptic inhibition of primary afferents and postsynaptic inhibition of spinal second order sensory neurons. The main aim of this inhibition is to suppress the response of dorsal horn neurons to low threshold mechanical stimuli (Mackie, 2003), but this system is usually altered after central injuries (Hossaini et al., 2010; Tillakaratne et al., 2000). Glial cells play an essential role in maintaining the spinal homeostasis as well as modulating synaptic function. After an SCI, astroglia and microglia become reactive and acquire pronociceptive and proinflammatory properties that contribute to the maintenance of hyperexcitability and central sensitization in the spinal cord (Gwak and Hulsebosch, 2009; Inoue and Tsuda, 2009; Watkins et al., 2001). These phenomena greatly influence the final response of the spinal system in front of the nociceptive stimulus. The outcome response is conveyed by the ventral horn, where motoneurons also suffer changes while immersed in a hyperexcitable environment, becoming more excitable (Sadlaoud et al., 2010; Rekling et al., 2000; Floyd et al., 1998), and therefore contributing to hyperreflexia. In addition, descending inhibitory pathways are disrupted after a SCI injury, implying an additional loss of central control of motoneuron activity.

Taking together all these alterations, it is important to have an integrated view of all these elements, and also to take in consideration the plasticity of the spinal cord circuits. For this reason, in this work we have chosen some key elements of the nociceptive spinal system and have evaluated them in SCI models of varying severities (mild contusion, severe contusion and complete section). The main advantage of this experimental design is the opportunity to study alterations of several elements in the same animal and at the same time after a SCI.

We firstly assessed the functional deficits as well as the appearance of neuropathic pain after SCI. Three months after injury we performed an immunohistochemical study of some potential contributors to the development of neuropathic pain, at different sites of the nociceptive circuitry (Fig. 1). We studied the distribution and density of afferent fibers arriving to the dorsal horn, as well as the general GABAergic tone. Glial reactivity was measured as a potential contributor to spinal hyperexcitability, and changes in the descending serotoninergic fibers were also measured. The preservation of inhibitory contacts in motoneurons was assessed by the study of gephyrin, a scaffold protein present in inhibitory synapses and essential for their correct function. Finally, the final motor response was studied by electromyographic recordings of wind-up responses and withdrawal reflexes, in order to correlate the functional findings with the histological results. Our data indicate that although there are several changes affecting the nociceptive spinal pathway, the degree and direction of these changes do not always directly correlate with the severity of the injury. Our results highlight the disbalance between excitatory and inhibitory systems, and also the presence of important plastic changes occurring in the spinal cord during the first months after injury.

2. EXPERIMENTAL PROCEDURES

2.1. Laboratory animals

Adult female Sprague Dawley rats (8 weeks old; 250-300 grams) were housed with free access to food and water at a room temperature of 22±2ºC under a 12:12 light-dark cycles. All experimental procedures were approved by the Ethics Committee of our institution, and followed the European Communities Council Directive 86/609/EEC.

2.2. Surgical procedure

Operations were performed under pentobarbital anesthesia (50 mg/kg i.p., Sigma), and after subcutaneous injection of buprenorphine (0.05 mg/kg, Buprex, Schering-Plough) near the incision site. After dorsal laminectomy of the T8-T9 vertebra, in two groups of rats the spinal cord was contused at T8 level using the Infinite Horizon impactor device (Precision Scientific Instruments; Lexington, UK), applying a force of 100 kilodynes (kdyn; group 100kdyn, n=8) or 200 kdyn (group 200kdyn, n=8). Data from displacement and force applied was collected for each contusion. In another group of animals the spinal cord was completely transected (complete section group, n=8), by means of a sharp scalpel, at T8 vertebral level. To ensure that the injury transected the whole spinal cord both stumps were gently lifted away, and repositioned back into the vertebral channel. After the injury, the wound was sutured with 5/0 silk thread at the muscular plane and the skin closed with small surgical clips and disinfected with povidone iodine solution. Animals were kept in a warm environment until full recovery from anesthesia. Bladders were expressed twice a day until reflex voiding of the bladder was re-established. Amoxicillin was given in the drinking water for 1 week to prevent postoperative infections.

2.3. Functional evaluation: locomotion

Locomotor hindlimb function and recovery was assessed using the Basso, Beattie and Bresnahan (BBB) rating scale (Basso et al., 1995) . Briefly, the BBB testing scale consists of an ordinal scale from 0 points (no discernable hind limb movement) to 21 points (consistent, coordinated gait with parallel paw placement of the hindlimb and consistent trunk stability). For measuring locomotor recovery, one animal at a time was allowed to move freely inside a circular plastic tray (90 cm diameter x 24 cm wall height) for 5 minutes, and two examiners observed the hindlimbs movements of the rat. The final score of each animal was the mean value of both examiners. Locomotion testing was performed weekly until 90 days postoperation (dpo).

2.4. Neuropathic pain: mechanical and thermal algesimetry

Mechanical nociceptive thresholds of the hindpaws were determined using an electronic von Frey unit (Bioseb, Chaville, France). Rats were placed into a plastic box with an elevated metallic fine-grid surface, and acclimated to the test chamber for 20 minutes. From the bottom of the box, a metal tip attached to the sensor was applied directly to the glabrous surface of both hindpaws. The force applied (in grams) until the withdrawal of the paw was measured, and the value of the test was the mean of at least three trials separated by 5 min resting periods (Casals-Díaz et al., 2009). The maximal force was limited to 35 grams to avoid skin damage. Tests were performed before the surgery (preoperative values) and at 14, 28, 42, 60, 75 and 90 days if the animals had a BBB score higher than 8, indicating the ability to support their weight with the hindlimbs.

Thermal nociceptive sensitivity was evaluated using a thermal plantar algesimeter (Ugo Basile, Comerio, Italy). Animals were acclimated in a plexiglas testing chamber for 20 minutes. The light of a projection lamp (150W) was focused directly onto the plantar surface of the right and left hindpaws. The time to withdrawal of the heated paw (withdrawal latency) was measured through a time-meter coupled with infrared detectors directed to the plantar surface. The maximal time of stimulation was limited to 20 seconds to avoid skin damage. The value for each test was the mean of three trials separated by 5 min resting periods (Hargreaves et al., 1988). Tests were performed before the surgery (preoperative values) and at the same days as the mechanical algesimetry test, in rats with a BBB higher than 8.

The Randall-Selitto test (Digital Paw Pressure Meter, IITC Life Science, Woodland Hills, CA) was performed in all animals in order to have algesimetric data also from complete section animals (and therefore with BBB score lower than 8). Before the test, each animal received 5 min of handling to get used to manipulation; then it was placed under a soft cotton cloth and carefully immobilized. The test consisted in the application of an increasing mechanical force by the tip of the device placed onto the medial portion of the plantar or the dorsal surface of both fore and hind paws until a withdrawal response resulted (Santos-Nogueira et al., 2011). The maximum force applied was limited to 250 g to avoid skin damage. This test was performed at 14, 42 and 90 dpo.

2.5. Retrograde labeling

At the end of the follow up, four animals from each experimental group and four intact animals were anesthetized with pentobarbital (40 mg/kg). The right hindlimb was gently shaved and disinfected. A small incision was done in the skin above the tibialis anterior muscle, and 5µl of 0.5% cholera toxin subunit B (CTB, List Biological Laboratories) were injected, using a Hamilton syringe coupled with a 30G needle, in the proximal third of the muscle, close to the entrance of the peroneal nerve branch. The injected volume was distributed in three injection sites to avoid muscle damage, and after every injection the needle was left in place for 20 seconds and then slowly removed to avoid leaking out of the tissue. The skin was closed and disinfected, and animals were rehydrated with saline solution. Five days later, animals were perfused (see below).

2.6. Immunohistochemistry

Perfusion and tissue harvesting: Transcardiac perfusion with 4% paraformaldehyde in phosphate-buffered saline was carried out in anesthetized rats at 90 days after surgery. A T7-T10 spinal cord segment around the lesion epicenter was removed, post-fixed overnight and cryoprotected in 30% sucrose. The thoracic spinal cord segments were serially cut (30 µm thickness) in the transverse plane in a cryostat. Lumbar segments L1-L6 were also removed and processed. Four animals from each SCI group and four intact animals were used for CTB retrotracing, and their lumbar segments were cut in the sagital plane. The other four rats of each group and four more intact animals were used for other immunohistochemistries, and their lumbar segments were cut transversally (20 µm thickness). Thoracic and lumbar sections were collected onto gelatin-coated glass slides and immunostained with different antibodies.

Immunohistochemistry procedures: all the compared cord sections were processed simultaneously, in order to apply the same conditions. The sections were first rinsed in phosphate buffer (PB) and blocked with PB saline supplemented with normal donkey serum (10%) and triton (0.3%; PBST+NDS). After 30 minutes of blocking at room temperature, sections were rinsed and incubated with primary antibodies overnight at 4°C. After washes, secondary antibodies were added for 2h at room temperature (in the dark). All the antibodies were diluted in PBST+1% NDS. Later on, sections were rinsed several times with PBS, and a final rinse with PB before dehydrating the samples in graded ethanol solutions (50%, 70%, 96%, 100%, 5 minutes each). Sections were mounted with Cytoseal Mounting Medium (Aname) and kept at room temperature.

Antibodies: Primary antibodies used, dilutions and manufacturers are the following: Goat polyclonal anti-cholera toxin subunit B (CTB), 1:5000, List Biological Laboratories. Goat polyclonal anti-choline acetyl transferase (ChAT), 1:50, Millipore. Rabbit polyclonal anti-glutamic acid decarboxylase (GAD), 1:1000, Abcam. Rabbit polyclonal anti-gephyrin, 1:300, Abcam. Mouse monoclonal anti-glial fibrillary acidic protein (GFAP), 1:1000, Sigma-Aldrich. Goat polyclonal anti-isolectin B4 (IB4), 1:1000, Vector. Rabbit policlonal anti-ionised calcium binding adaptor molecule 1 (Iba1), 1:1000, Wako. Goat polyclonal anti-calcitonin gene related peptide (CGRP), 1:500, Abcam. Rabbit polyclonal anti-serotonin, 1:5000, Sigma-Aldrich. Cy3 anti-mouse/rabbit secondary antibody (made in donkey, 1:200, Jackson Immunoresearch, UK) was used for GFAP and Iba1 single immunohistochemistry, whereas for double immunodetections Alexa Fluor 488 and 594 were used (made in donkey, 1:200, Invitrogen). Specificity and dilutions were tested for every primary and secondary antibody when purchased. For evaluating antibody specificity, tissue samples (control and operated) were processed as described above but the primary antibody was not added

Images and measurements: Images were taken with the same sensitivity for each marker analyzed, with the aid of a digital camera (Olympus DP50) attached to the microscope (Olympus BX51). The images were transformed to a gray scale and analyzed using ImageJ software. Immunoreactivity was assessed by calculating the integrated density (mean grey value multiplied by labeled area), after defining a threshold for background correction. In some cases, the parameter used was the integrated density that includes the extension and the intensity of labeling. In other measurements, the labeled area and the intensity of labeling were analyzed separately.

GFAP permits a clear visualization of the glial scar that limits the cavity, so this staining was used in thoracic sections to detect the cystic cavity, and to measure the preserved tissue. For glial immunoreactivity (GFAP for astrocytes and Iba1 for microglia labeling) measurements were done using ROIs (regions of interest) placed on the dorsal horn, and comprising the medial part of laminae I to IV. In ventral horn measurements, the ROI was placed on lamina IX, including the area occupied by the motoneurons. Images were taken at 20x magnification, and the integrated density was measured. At least five sections from L4-L5 segments were used. Quantification of GAD, IB4 and CGRP immunoreactivities were done using ROIs in the dorsal horn, comprising laminae I to IV. Measurements of both the labeled area and the intensity of labeling were made in images taken at 10X magnification from at least five sections of L4-L5 segments. Gephyrin measurements were done in motoneurons labeled by ChAT. A minimum of twenty neurons (with a minimum diameter of 40 µm) were selected in each animal, and gephyrin immunoreactivity (integrated density) was measured in images taken at 40X from each selected neuron. The mean of the twenty measurements was used as the mean value for each animal, and then used to calculate the mean of each group. Integrated density measured in intact animals was considered as 100%, and values from injured groups were referred to it. All the selected neurons were similar in size, so no area correction was necessary.

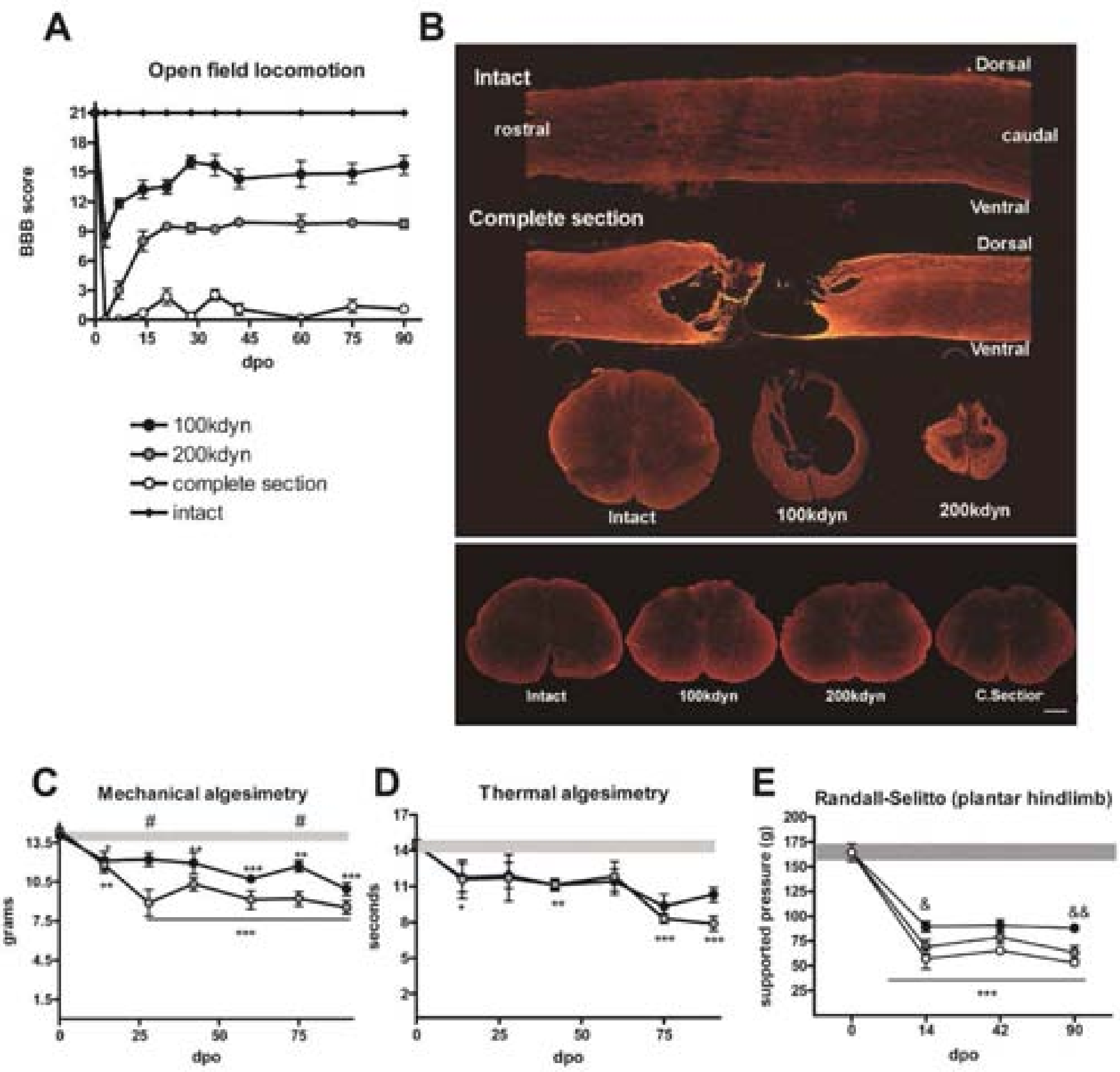

Figure 2: *Functional and histological effects of the spinal cord injuries.* ***A)*** *Open field locomotion test, using the BBB scale: Normal locomotion is scored as 21 points. Animals with mild contusion present coordinated locomotion with mild deficits, whereas animals with severe contusion barely stand their own weight with the hindlimbs. Animals with complete section present hindlimb paralysis, with only slight movements in some joints.* ***B)*** *Representative images of the spinal cord of the different groups, in sagital (intact and complete section) and transversal views (intact, 100kdyn and 200kdyn). These images confirm the graded severity of the injury. Scale bar: 500µm.* ***C-D)*** *Mechanical and thermal algesimetry tests indicate that contused animals presented a reduction in nociceptive thresholds maintained during three months postinjury.* ***E)*** *Randall-Selitto test measurements indicated that partial and complete injuries produced a significant reduction in mechanical nociceptive thresholds at all time points. In all algesimetry tests (C, D, E) values were significantly reduced compared to preoperative values (indicated as dashed lines) (*, $p<0.05$; **, $p<0.01$; ***, $p<0.001$ vs. preoperative values), and only some differences were detected when comparing injured groups, indicating an all-or-none response (# $p<0.05$ 100kdyn vs. 200kdyn group; & $p<0.05$, && $p<0.01$ 100kdyn vs. complete section).*

Serotonin immunohistochemistry was performed on sagital sections of 20 µm thickness. In order to detect only the motoneuron pool innervating the tibialis anterior muscle, CTB was also immunodetected. Images from each animal were taken at 20X, and a line was drawn perpendicular to the main direction of the fibers. Using the plot profile tool of ImageJ software, all the fibers crossing this line above a determined threshold were seen as peaks, and counted. This procedure was done in at least five different sections to obtain a mean value for each animal.

2.7. Electrophysiological tests

Animals were anaesthetized with pentobarbital (30 mg/kg, i.p.) and placed prone over a warmed flat coil controlled by a hot water circulating pump to maintain body temperature. Electrophysiological tests were performed preoperatively and at the end of the follow-up period.

Peripheral nerve conduction tests: Single electrical pulses (100 µs duration at supramaximal intensity) were delivered by monopolar needles inserted percutaneously at the sciatic notch. The compound muscle action potentials (CMAP) were recorded from tibialis anterior and from plantar interosseus muscles, by means of an active electrode inserted on the belly of the muscle and the reference electrode at the fourth toe (Valero-Cabré and Navarro, 2001; Valero-Cabré, et al., 2004). Signals were amplified, filtered (bandpass 1 Hz – 5 KHz), displayed on an electromyograph (Sapphyre 4ME, Vickers) and analyzed. The direct muscle response (M wave) and the monosynaptic reflex response (H wave) with the highest amplitude were selected and their amplitude and latency measured. The degree of hyperreflexia was calculated as the ratio between the maximal amplitude of the H wave and that of the M wave (Valero-Cabré and Navarro, 2001). Values from both hindlimbs were averaged for of each rat.

Wind-up responses and withdrawal reflexes: Wind-up evoked responses were recorded from the right tibialis anterior muscle using a modified protocol (Solano et al., 2003; Redondo-Castro et al., 2011). Trains of repetitive electrical stimulation (16 pulses at 1 Hz, 1 ms width and 20 mA, intensity corresponding to 70-80% of the threshold required to elicit a withdrawal reflex in intact animals using the same preparation) were applied by means of monopolar needle electrodes, the cathode inserted near the medial plantar nerve in the right paw and the anode between fourth and fifth toes. Electrical stimuli were supplied by a Grass S44 stimulator using an isolation unit (PSIU6; Grass Instruments). For recording, the active needle electrode was placed in the tibialis anterior muscle, the reference electrode at the ankle, and a ground electrode at the base of the tail. Responses were amplified 100 times with a Grass P511 amplifier, fed into a PowerLab/16SP system and recorded with Chart software (ADInstruments Ltd.). In each session, electromyographic wind-up responses were recorded and analyzed to measure the area under the curve (AUC) of each response, using Chart software and the RMS and Noise extension that determines the power content of a signal. Data of wind-up recordings are expressed in two different ways. The mean total activity is the mean increment achieved from the 2nd to the 16th stimuli when rectified for the first response; this representation is useful to see the general amplification. The second is the measure of the AUC of the first stimuli, as an indicator of the central excitability of the spinal cord before the train of repetitive stimuli (Redondo-Castro et al., 2011).

Withdrawal reflexes were measured by delivering single electrical stimuli of 50 mA and 1 ms, using the same setting used in wind-up recordings. Measurements of the AUC of the C-fiber mediated response during the first second of the response were made to assess the intensity of the withdrawal reflex response (Valero-Cabré et al., 2004).

2.8. Statistical analysis

Data are shown as the mean ± SEM. Statistical comparisons between groups were made using two way ANOVA for repeated measures with Bonferroni *post hoc* tests (GraphPad Prism software). Differences between groups were considered statistically significant if $p<0.05$.

3. RESULTS

3.1. Locomotion

To secure reproducibility of the contusion lesions, the force applied and the displacement suffered by the spinal cord were measured (Cao et al., 2005). The mean force applied was 104±1 kdyn in the 100kdyn group and 204±2 kdyn in the 200kdyn group. The displacements received were 836±33 µm and 1496±44 µm, respectively, which were significantly different between them ($p<0.001$). Complete section injuries were confirmed histologically by longitudinal sections of the spinal cord, and contusion injuries by transversal sections with GFAP labeling (Fig. 2B). Integrity of lumbar segments of the spinal cord was assessed in the same way (Fig. 2B, bottom panel).

The locomotor test results indicate different functional deficits depending on the severity of the lesion (Fig. 2A). Intact animals presented normal locomotion (21 points in the BBB scale); rats of the 100kdyn group showed plantar stepping and coordinated gait, but some deficits regarding toe clearance and rotation of the hindpaw position (15-16 points); rats of the 200kdyn group presented more marked deficits, such as uncoordinated gait and only occasional plantar stepping (9-10 points). Animals with complete transection displayed nearly complete paralysis, reaching only 1-2 points during the follow-up (slight movement of some joints). There were significant differences between all groups ($p<0.001$) at all time points after injury.

3.2. Neuropathic pain

Regarding pain responses, all contused animals manifested hyperalgesia in response to mechanical and thermal stimuli during the three months of follow-up (Fig. 2C-D). Mechanical thresholds were around 14 grams in intact animals, and fell progressively to 8-9 grams in contused animals. These values were significantly lower than preoperative values, but no differences were detected between groups. The thermal withdrawal threshold averaged around 14 seconds in intact animals, while it was reduced in contused animals to 11 seconds in the 100kdyn group and 8.5 seconds in the 200kdyn group. Differences were detected between SCI groups and preoperative values, but again not between injured groups. Animals with complete transection were not tested with these algesimetry tests because of their inability to support weight with the hindlimbs, but could be tested with the Randall-Selitto test. This test indicated persistent pressure hyperalgesia in the hindlimbs during the three months follow up in the three SCI groups. Preoperative pressure threshold averaged about 165 grams, and decreased to 88 grams in the 100kdyn group, 64 grams in the 200kdyn group, and 53 grams in the complete section group (Fig. 2E). The decrease of thresholds was statistically significant ($p<0.001$) in all groups compared to preoperative values, and differences were also found between the 100kdyn group and the complete section group ($p<0.05$ at 14 dpo, and $p<0.01$ at 90 dpo). Only in this algesimetry test we could detect a trend to present more hyperalgesia in more severe lesions.

3.3. GABAergic tone: GABA synthesizing enzyme

The expression of the GAD65/67 enzyme in the superficial dorsal horn laminae (Fig. 3A) was increased in all the injured groups compared to intact animals ($p<0.05$), for measurements of the labeled area (Fig. 3B) and of the intensity of labeling (Fig. 3F). These increases were similar in all the injured groups (45-50% higher than intact animals, $p<0.05$), although it was slightly higher in the complete section rats (60%).

3.4. Peptidergic and non-peptidergic nociceptive afferences

Images taken from laminae I to IV of the dorsal horn indicated that the nociceptive afferents were boosted three months after injury (Fig. 3A). Labeling of IB4 was found in lamina II of the dorsal horn, with a significantly increased immunolabeled area in the SCI groups ($p<0.05$, 570% in 100kdyn group, 670% in 200kdyn group and 520% in complete section group; see Fig. 3C). Regarding the intensity, no changes were detected.

CGRP positive afferents presented a dense projection pattern in laminae I and II (Fig. 3A). Although the labeled area was not significantly changed, the intensity of immunolabeling was significantly increased in all SCI groups ($p<0.01$) compared to intact rats (Fig. 3H). Some CGRP positive fibers arrived to deeper laminae III-V. The number of such fibers was higher as the severity of the lesion increased (mean number, intact: 1.2; 100kdyn: 3.2; 200kdyn: 6.6; complete section: 5.6) although their length tended to decrease (mean of 265 μm in intact animals, 250μm in 100kdyn group, 200μm in 200kdyn group and 175μm in complete section group. In all groups, the thickness of the laminae from where the projections arose was unchanged. In addition, numerous short CGRP positive profiles were observed arising from the inner part of the superficial dorsal laminae.

3.5. Glial reactivity: microglia and astroglia

Glial cell reactivity was assessed in dorsal and ventral horns of L4 and L5 spinal segments (Fig. 4A, 4C), and expressed as the mean integrated density of immunolabeling of GFAP (astrocytes) and Iba1 (microglia), and normalized versus the control value.

Microglial cells displayed a resting morphology in samples from intact animals, in contrast with a characteristic reactive morphology in all injured groups three months after the lesion. The increase in immunoreactivity for Iba1 was statistically significant in all groups compared to intact animals, and tended to be higher with the severity of the injury (Fig. 4B), although in the ventral horn measurements from the complete section group displayed lower values of integrated density than the contused groups.

The immunoreactivity for astroglia was also increased in dorsal and ventral horns of all the injured rats. The astrogliosis was higher with increasing severity of the injury (Fig. 4D), with significant differences for the 200kdyn contusion and the complete section group with respect to intact controls.

3.6. Serotoninergic fibers

In intact animals serotoninergic fibers traveling along the spinal cord were particularly visible in the ventral horns and near the lumbar motoneuronal pools (Fig. 5D). In injured animals, the number of descending serotoninergic fibers was clearly reduced when compared to the controls (Fig. 5A, 5C), showing a progressive decrease as the severity of the lesion increased. Intact animals presented a mean of 15 long fibers per cord section, whereas this number was reduced to around 12 in the 100kdyn group, 4 in the 200kdyn group and 0 in the complete section group. A qualitative study of the images revealed that animals with 100kdyn contusion displayed more serotoninergic fibers and more contacts on motoneurons than 200kdyn animals, whereas animals with complete section showed complete absence of fibers and contacts (Fig.5B).

3.7. Inhibitory synapses on motoneurons

Measurements performed on the surface of spinal cord motoneurons (Fig. 6C) indicated an increase in gephyrin immunoreactivity (Fig. 6A,B) in all the injured groups, although without reaching statistical significance. The increase was more important in the mild contusion group (163% of intact value), followed by the severe contusion group (144%) and the complete section group (129%). It is important to note that only large motoneurons were measured (minimum of 40 μm in diameter), and most of them presented colabeling for ChAT and gephyrin (Fig. 6A). Smaller ChAT positive neurons did not show gephyrin immunoreactivity on their surface.

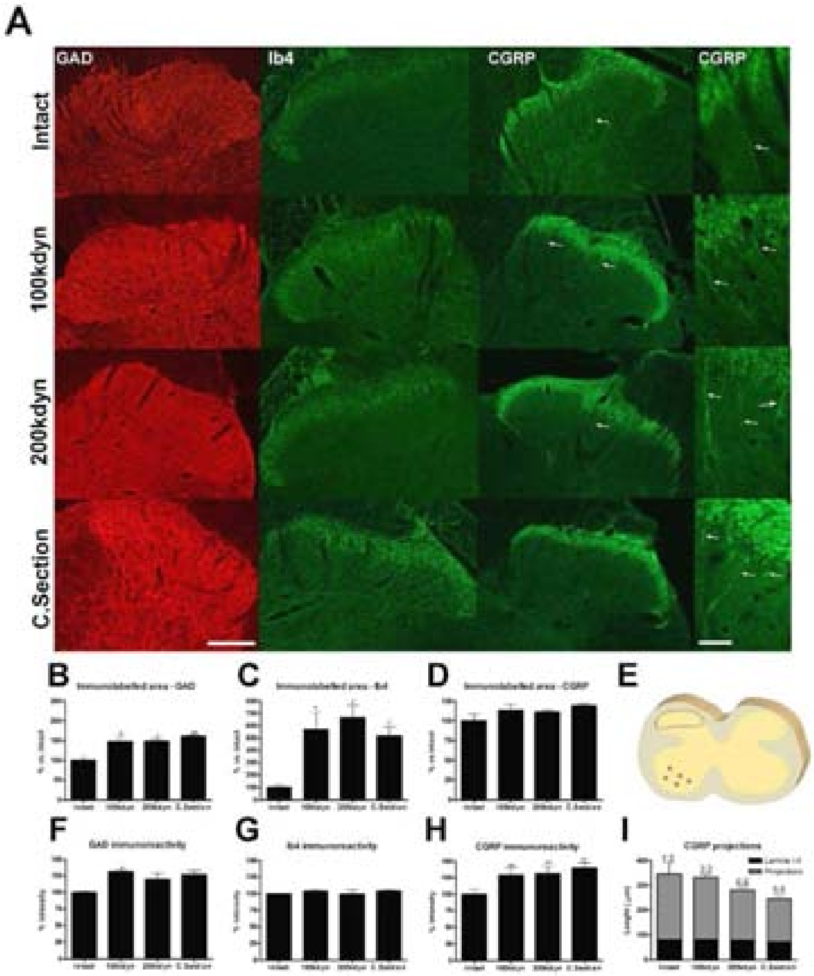

***Figure 3: :** Changes in inhibitory interneurons and afferent projections in the dorsal horn. **A)** Representative images from the dorsal horn at L4-L5 segments (schema in **E**), labeled against GAD, IB4 and CGRP. Scale bar: 200 μm; 50 μm in the right column. GAD immunohistochemistry revealed an increase in the area **(B)** and the intensity **(F)** of labeling in all injury groups. Labeling for IB4 positive afferences displayed an increase in the area **(C)** but not in the intensity **(G)**. Immunolabeling for CGRP afferences showed an increase of both the area **(D)** and the intensity **(H)**. CGRP projections increased in number and length to deep laminae (**I**, indicated by white arrows in the right panels of **A**). Statistical significance: * p<0.05; ** p<0.01; *** p<0.001 vs. intact animals; #, p<0.05 vs. complete section group.*

3.6. Inhibitory synapses on motoneurons

Measurements performed on the surface of spinal cord motoneurons indicated an increase in gephyrin immunoreactivity (Fig. 6A,B) in all the injured groups, although without reaching statistical significance. The increase was more important in the mild contusion group (163% of intact value), followed by the severe contusion group (144%) and the complete section group (129%). It is important to note that only large motoneurons were measured (minimum of 40 μm in diameter), and most of them presented colabeling for ChAT and gephyrin (Fig. 6A). Smaller ChAT positive neurons did not show gephyrin immunoreactivity on their surface.

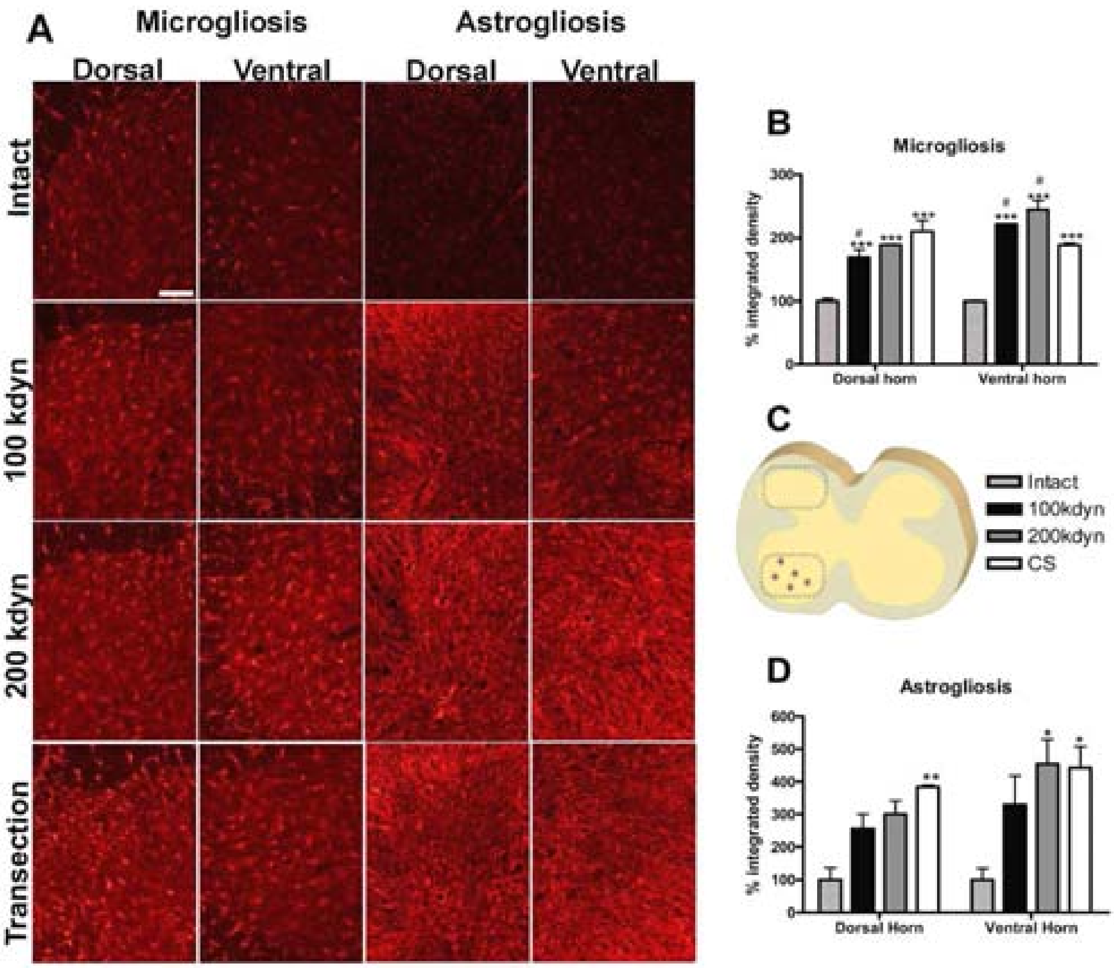

Figure 4: Chronic gliosis in the spinal cord. Representative images taken from the dorsal and the ventral horn of the spinal cord at L4-L5 level ***(C)****, immunolabeled for GFAP and Iba1* ***(A)****. Quantification of Iba1 integrated density indicated an increase in microglial reactivity in all SCI groups compared to intact animals in both dorsal and ventral horns. Dorsal horn values of microgliosis increase with the severity of the injury. In ventral horns, microgliosis was lower after complete section than after contusion injuries* ***(B)****. GFAP quantification showed also an increase in astrogliosis in all injured groups* ***(D)****, and both dorsal and ventral horns showed higher immunoreactivity with the severity of the injury. Statistical significance: * $p<0.05$; ** $p<0.01$ versus intact animals; # $p<0.05$ vs. complete section group.*

3.7. Electrophysiology: spinal reflexes and wind-up responses

CMAPs recorded in the tibialis anterior muscle had a mean amplitude around 52 mV in preoperative tests (Fig. 7A). Three months after injury, all groups presented a slight reduction in the amplitude, although it was significant only in the complete section group (40 mV, $p<0.05$). No significant changes were detected in the amplitude of CMAPs of the plantar muscles (average 8.60 mV). Latencies were not significantly changed in any of the muscles considered.

The monosynaptic spinal reflex showed significant facilitation, measured as the H/M ratio, from a value around 0.05 at baseline to higher values of 0.28 in the 100 and 200 kdyn groups (Fig. 7B). The complete transection group had a lower degree of hyperreflexia, with a mean H/M ratio of 0.15 ($p<0.001$ versus the contused groups). Withdrawal reflex responses mediated by stimulation of C fibers (Fig. 7G) showed mean values of 800 µV·s in the 100kdyn group, 525 µV·s in the 200kdyn group and 240 µV·s in the complete section group, the later being similar to the control values (Fig. 7E). Thus, both mono- and polysynaptic spinal reflexes showed more marked facilitation after contusion injury than after complete transection of the spinal cord at the thoracic level.

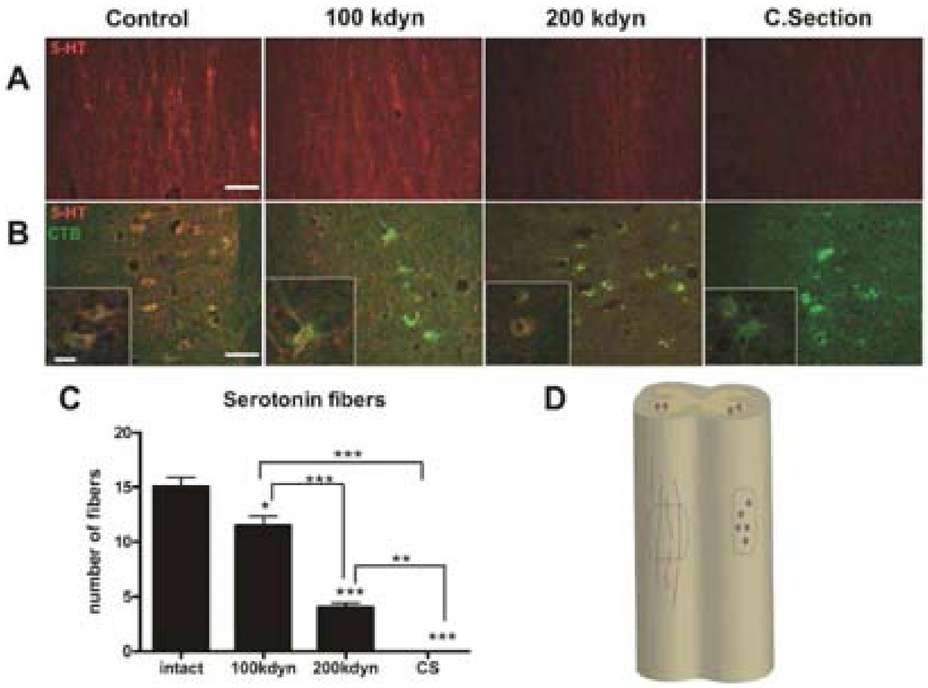

Figure 5: *Serotonin fibers and motoneurons* ***(D)****. Descending serotoninergic fibers were visible along the entire lumbar segment in control samples* ***(A)****. The number of fibers diminished as the lesion severity increased, being completely absent in the complete section group* ***(C)****. Serotoninergic fibers made contacts on motoneurons of the pool innervating the tibialis anterior muscle, retrolabeled with CTB* ***(B)****, and the number of contacts were progressively reduced as the injury severity increased (details at higher magnification in the insets of* ***B****). Statistical significance: * p<0.05; ** p<0.01; *** p<0.001 injured group vs. intact animals. Lines indicate differences between injured groups. Scale bar: 200 µm in A and B, 30 µm in insets in B.*

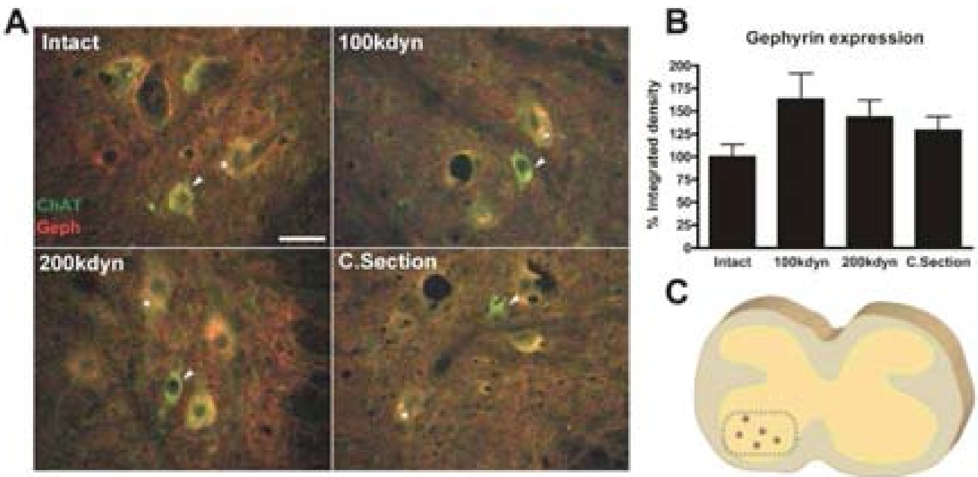

Figure 6: Gephyrin labeled synapses on motoneurons of lumbar segments L4-L5 **(C)**. Motoneurons labeled with ChAT displayed a diffuse pattern of gephyrin expression **(A)**. Colabeling for both markers was present in most motoneurons except in the small ones. Quantification of the gephyrin immunolabeling in motoneurons revealed a tendency to increase in injured spinal cords **(B)**. Scale bar: 50 µm.

Wind-up recordings (Fig. 7F) indicate marked facilitation after SCI. Wind-up measured as the total activity in the 16 stimuli (expressed as the AUC, Fig. 7C) gave preoperative values around 5500 µVs in all groups, whereas it increased at the end of the follow up to 9470 µVs in the 100kdyn group, 6950 µVs in the 200kdyn group and 7940 µVs in the complete section group. Due to the intrinsic variability of the technique (Svendsen, 1999; Redondo-Castro et al., 2011), these increases were not significantly different from preoperative values. When measuring only the first response (Fig. 7D), baseline values of about 150 µVs increased to 490 µVs in the 100kdyn group, 330µVs in the 200kdyn group, and 200µVs in the complete section group.

4. DISCUSSION

In this study we made a detailed study of some of the key components of the spinal reflex circuitry and central control pathways at segments caudal to a SCI, with the aim of providing an integrative view of the alterations in the spinal nociceptive pathway and its relationship with the severity of the injury and with the measurement of neuropathic pain. Moreover, it may bring information on the relative contributions of each element and, thus, help to find potential targets for therapies aimed to ameliorate neuropathic pain and hyperreflexia, frequent and disabling secondary complications of SCIs. Three months after a SCI in the rat is considered a chronic stage, when the primary consequences of the injury are already resolved (such as circulatory and inflammatory events, excitotoxicity, etc), and the plastic changes in spinal neural circuits have already occurred. In fact, chronic time points are usually the starting point of most therapies, when the situation has become stable and the final consequences are already established.

SCI causes a wide range of functional consequences, one of the most evident being the locomotion deficits, which appear in a severity dependent manner. Another consequence of SCI is the appearance of chronic neuropathic pain, which was also evidenced in all the experimental groups included in this study. In this work only groups with partial SCI by contusion were subjected to the common mechanical and thermal algesimetry tests, due to the limitations of these methods since animals need to be able to support their weight on the hindlimbs. Nevertheless, the Randall-Selitto test is useful for detecting neuropathic pain also in animals with complete spinal cord section (Santos-Nogueira et al., 2011; Lee et al., 2005). The decrease of nociceptive thresholds was maintained during the three months postinjury, without significant differences between the groups, except for a gradation observed in the Randall-Selitto test results. Even if controversial, this lack of correlation between the degree of hyperalgesia detected and the severity of the SCI was already observed in previous studies (Redondo-Castro et al., 2011; Zhang et al., 2008), and may respond to an all-or-none mechanism. Other positive phenomena commonly seen in human SCI patients and that have been also demonstrated in SCI rats are caused by hyperexcitability of the spinal circuitry caudal to the lesion, manifested as hyperreflexia and exaggerated wind-up responses (Valero-Cabré et al., 2004; Redondo-Castro et al., 2011). These positive symptoms can be related to neuropathic pain, since they act as amplifiers of the nociceptive signaling, acting on the final motor response or on the integration of the input.

4.1. Increase in afferent projections and in GABAergic tone after SCI

Once confirmed the appearance and long-term maintenance of signs of neuropathic pain in the SCI rats, we studied changes in the central projections of nociceptive afferents (CGRP and IB4 labeled fibers) and the expression of GAD, the main enzyme that synthesizes GABA and thus a general marker for GABAergic interneurons in the dorsal horn. Dorsal horns presented an increase in GAD expression after the injury, as well as an increase in the projections of peptidergic and non-peptidergic afferences.

The transduction of noxious stimuli is done through primary sensory neurons with small cell bodies and unmyelinated or thinly myelinated axons. Two types of C-fiber afferents can be distinguished by their sensitivity to trophic factors and the presence of neuropeptides. The *non-peptidergic* neurons, detected by their binding to IB4, are dependent on the GDNF (glial derived neurotrophic factor) family of growth factors, and their projections end in the inner lamina II of the spinal cord. The *peptidergic* neurons, detected by CGRP and substance P labeling, are dependent on NGF (nerve growth factor), and mainly project to lamina I and outer lamina II (Snider and McMahon, 1998; Vulchanova et al., 2001).

We found a general increase of nociceptive afferents density in the dorsal horn at lumbar levels following thoracic SCI. The increase in density and size of the projection area of nociceptive fibers caudal to SCI has been attributed to sprouting of these fibers, since they usually colocalize with Gap-43, a marker of growth cones (Ondarza et al., 2003). These changes may imply an increase in the afferent input, as a first amplification in the pain pathway and in spinal motor and autonomic reflexes (Zinck and Downie, 2008), or alternatively represent a compensatory response for the loss of descending information in order to increase the sensory feedback, essential for recovery (Tillakaratne et al., 2000; Little et al., 1999; Rossignol and Frigon, 2011). Touch sensitive fibers normally terminate deeper in the dorsal horn than nociceptive fibers (Takazawa and MacDermott, 2010).

Our results also show an increase in the number of CGRP fibers reaching deep laminae, which may indicate a shift in the nociceptive input to second order spinal neurons, as has been reported in other models of pain (Keller et al., 2007). This could explain, at least in part, the appearance of allodynia below the injury site. Moreover, the increase in the intensity of IB4 labeled fibers may be also related to the hyperalgesic manifestations, since IB4 fibers are known to mediate thermal and mechanical nociception (Vulchanova et al., 2001).

GABAergic interneurons contribute to attenuate pain signal modulation in the spinal cord in normal conditions, but in pathological situations changes in the GABAergic system can contribute to abnormal nociceptive responses (Gwak et al., 2006). An increase in GABA synthesis was already described after peripheral and central injuries accompanied by neuropathic pain (Satoh and Omote, 1996; Kontinen et al., 2001; Diaz-Ruiz et al., 2007), suggesting a change in the activity or function of the GABAergic system. Different causes may be underlying this change; the first is a shift in function, from inhibition to excitation, similar to what happens during development, when GABA acts as a excitatory transmitter, depending on the functional state of chloride transporters like NKCC1 and KCC2 (Sadlaoud et al., 2010; Boulenguez et al., 2010; Lu et al., 2008; Edgerton and Roy, 2010). This would be translated into a lack of inhibitory influences at the entrance of the spinal pain circuit, since GABA function is tightly correlated with the degree of neuropathic manifestations (Gwak et al., 2006). One important point to note is the existence of two isoforms of the GAD enzyme: GAD65 isoform generates GABA to act as an inhibitory neurotransmitter, and GAD67 for nonsynaptic purposes (Erlander and Tobin, 1991). Despite the immunohistochemical analysis did not allow to differentiate between the expression of these two isoforms (both highly expressed in superficial laminae of the dorsal horn), the presence of signs of neuropathic pain during three months after SCI makes more likely that the increase detected is mainly due to an increase of GAD67, that produces GABA for nonsynaptic issues. On another hand, after a SCI GABA may not be used solely as an inhibitor but as a modulator of plastic changes aimed to compensate functional deficits and gain locomotion skills at the spinal level (Tillakaratne et al. 2000).

In summary, we found that caudal to the thoracic SCI there is an increase in projections of nociceptive afferents combined with an alteration of the inhibitory GABaergic system, thus constituting the first abnormal processing point in the spinal pain circuit. Interestingly, these changes do not show a clear relation with the severity of the injury.

4.2. Chronic gliosis is related to neuropathic pain and hyperreflexia

Abnormally persistent glial reactivity is one of the most accepted causes of central hyperexcitability and of the development of neuropathic pain after SCI (Hulsebosch, 2008; Hains and Waxman, 2006; Watkins et al., 2001; Vallejo et al., 2010; Scholz and Woolf, 2007). We found an important degree of gliosis in the lumbar dorsal horns of all injured rats, for both astrocytes and microglia, in relation with the severity of the injury. Glial cell reactivity may contribute to the chronification of neuropathic pain, by maintaining sensitization of secondary neurons in the dorsal horn (Ji and Suter, 2007; Keller et al., 2007), thus representing a second point of amplification of the nociceptive information in the spinal cord.

The ventral horns presented a similar degree of gliosis three months after SCI. The complete section group had a slightly reduced microgliosis compared to the contused groups, because a cord transection promotes a lower inflammatory component or because the replacement of microglia by astroglia has already started (Vallejo et al., 2010). In the ventral horn, the implications of gliosis are mainly related to the efferent reflex responses, which would be enhanced by central hyperexcitability induced by reactive glia. It has been also proposed that reactive microglia may be able to promote the growth of new synaptic buttons, contributing to hyperreflexia (Little et al., 1999). Both reactive astrocytes and microglia contribute to the general state of hyperexcitability in the spinal cord, and therefore promote the amplification of the information traveling along the nociceptive system.

4.3. Serotonin descending pathways are reduced after SCI

In the experimental groups, as expected, there was a progressive loss of serotoninergic descending fibers and, therefore, of the number of contacts on spinal lumbar motoneurons as the severity of the lesion increased. Serotonin projections arise from ventral medullary raphe, raphe pallidus and raphe obscurus nuclei, and project to all laminae in the spinal cord. They give a tonic inhibition that constitutes an important modulation to spinal pain systems, attenuating nociceptive responses in dorsal horn neurons (Hains, 2003). Nevertheless, it has been described that serotoninergic projections may also have a pronociceptive or facilitatory role in some models of persistent pain (Vanegas and Schaible, 2004, Millan, 2002). Such dual actions depend on different receptors as well as on different concentrations of released serotonin, and on the balance between facilitatory and inhibitory elements in the spinal cord. Serotonin receptors suffer an important regulation after injury, that could eventually make motoneurons hyperexcitable, together with the appearance of persistent inward currents that promote long depolarizations in motoneurons (Murray et al., 2010; Heckmann et al., 2005; Lee et al., 2005). The observed loss in the number of serotoninergic fibers arriving to the lumbar segments from rostral centers can be translated into a direct loss of inhibition in the dorsal horn. This progressive loss correlates with the results of algesimetry and reflex tests, which indicate that the more severe the lesion, the more marked the abnormalities.

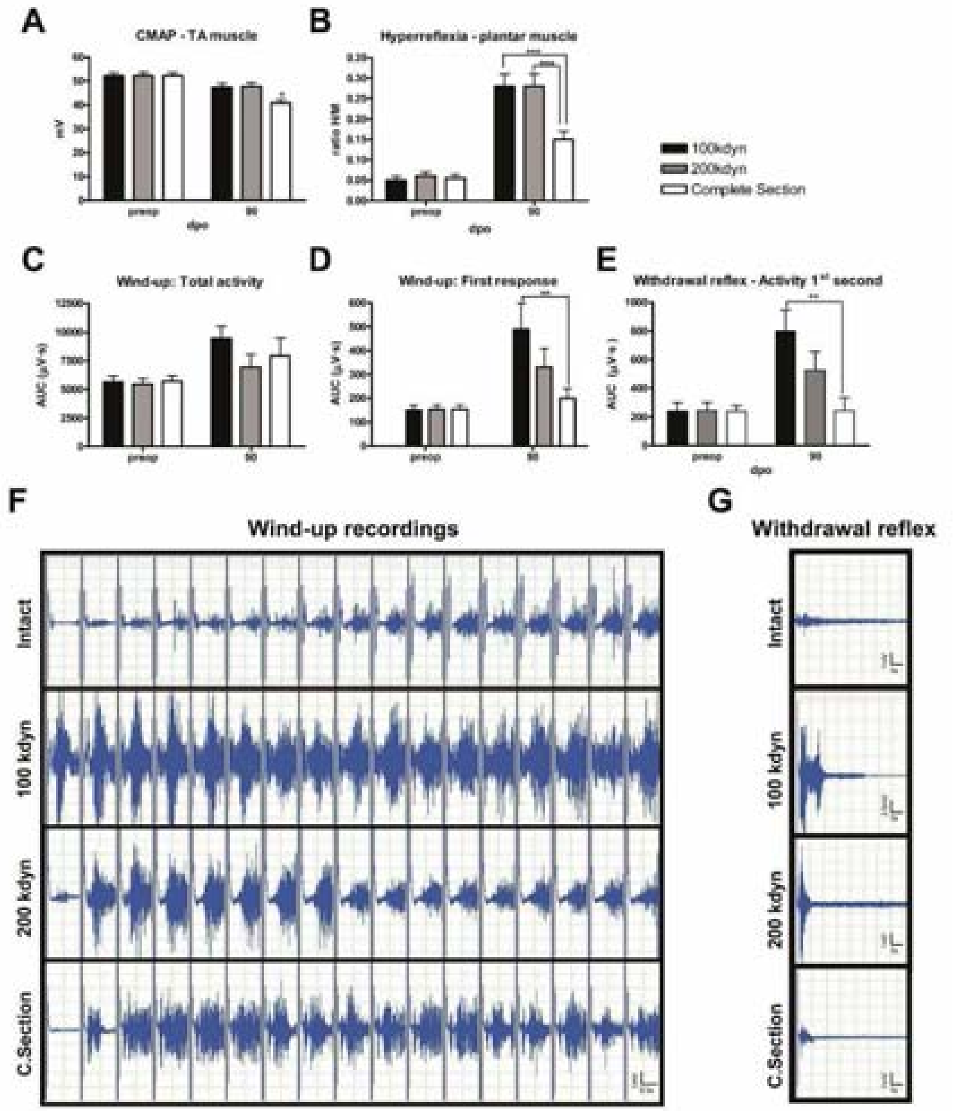

Figure 7:** Electromyographic responses. **(A)** Compound muscle action potentials recorded from the tibialis anterior muscle showed only a small reduction in amplitude in the complete section group (* p<0.05 vs preoperative value). **(B)** Hyperreflexia, expressed as the ratio between the H wave and the M wave, was evident in all injured groups, especially after spinal cord contusion. Complete section animals had a significantly lower increase of the H/M ratio than contused animals (p<0.001). **(C)** Wind-up quantification, measuring the total activity as the area under the curve (AUC) of the 16 responses, showed increased facilitation in all groups after SCI. **(D)** Quantification of the first response of the wind-up test as a measure of basal excitability. All injured groups presented a clear increase, being the mild injury group the one with the highest excitability, followed by the severe contusion group and the complete section group (** p<0.01 100kdyn vs. complete section). **(E)** Withdrawal reflexes responses. Three months after injury, contused groups displayed hyperreflexia compared to preoperative values. The complete section group had a mean value similar to the control, and lower than the 100kdyn contusion (** p<0.01). **(F)** Representative recordings of wind-up, with the train of 16 responses. **(G)** Representative recordings of withdrawal reflexes. Note the changes in the scale in each recording.*

Motoneurons are the last modulatory site of the spinal circuitry, which elaborate the output of reflex responses initiated by noxious stimuli in the periphery. In addition to the loss of descending modulatory inputs, we found also changes in the inhibitory synapses detected on the motoneuron surface, as indicated by the gephyrin immunohistochemistry results. Postsynaptic receptors at inhibitory synapses (mainly glycine and GABA-A receptors) are aggregated in clusters whose formation and anchorage to the cytoskeleton is regulated by gephyrin (Jacob et al., 2005; Fritschy et al., 2008; van Zundert et al., 2005; Alvarez et al., 1997). Gephyrin also has roles regarding synapse formation, receptor mobilization and plasticity (Fritschy et al., 2008; Calamai et al., 2009). Since inhibitory synaptic transmission relies essentially on glycine (Sadlaoud et al., 2010), gephyrin labeling can be used as a good marker to monitor changes in glycinergic inhibitory synapses in the ventral horns (Jacob et al., 2005). It is especially found in α-motoneurons, although interneurons and γ-motoneurons are also known to display some gephyrin clusters (Destombes et al., 1992).

An increase in gephyrin may be related to an increased glycinergic transmission to the motoneurons, and therefore a reduction in their excitability. In our work we have detected a trend to increase the presence of gephyrin after SCIs, especially in the mild lesions, but it does not seem effective enough since the reflex motor responses assessed by electrophysiological tests were markedly facilitated. Thus, this increase in inhibitory signaling can be interpreted as a compensatory strategy to counteract the hyperexcitability present in the system, with a disbalance between excitatory and inhibitory inputs to motoneurons following SCI. Nevertheless, the eficacy of this increase in inhibitory signalling can be unsuccessful if the chloride homeostasis is also altered, as has been described after SCI (Boulenguez et al., 2010; Lu et al., 2008; Hasbargen et al., 2010).

4.5. Hyperreflexia and plasticity of reflex circuits

We assessed the functional state of the spinal reflex circuits by means of in vivo electrophysiological tests. The polysynaptic withdrawal reflexes have been widely used to study nociceptive responsiveness in animals and provide quantitative data about physiological changes in lumbar segments after neural lesions (Cervero, 2009; Lee et al., 2005; Valero-Cabré and Navarro, 2001, 2002; Valero-Cabré et al., 2004). Measurements of the H/M ratio, used to evaluate spinal excitability, indicate marked hyperreflexia in the contused groups, and only a slight increase in the group with complete section. Withdrawal reflex results showed a similar trend of hyperreflexia (Yoon et al., 2004). After a central injury, the supraspinal control is partially or completely lost, and this has a facilitatory effect on spinal reflexes below the lesion site (Valero-Cabré et al., 2004; Gozariu et al., 1997). Inflammatory processes and dysfunctions of the inhibitory systems are known to contribute to hyperreflexia and therefore to spasticity (Mackie, 2003). Hyperreflexia has been also proposed as a mechanism to compensate the loss of descending information (Lee et al., 2005). Thus, mild lesions imply a limited loss of tissue, but the spared tissue presents hyperexcitability and enhanced plasticity, which will eventually lead to better recovery, but also to a higher degree of hyperreflexia or neuropathic pain, since sensory information can also be amplified.

Wind-up is a phenomenon of temporal summation that has been widely used as expression of the sensitization of spinal neurons, and consequently related to chronic pain states (Herrero et al., 2000; Redondo-Castro et al., 2011; Cervero, 2009). Despite sensory and motor wind-up can be modulated partially independently (Cervero, 2009; Herrero et al., 2000), both phenomena indicate the presence of spinal amplificatory mechanisms that can lead to pain and hyperreflexia, respectively. We have assessed wind-up by means of electromyography, using a preparation that allows a physiological condition to study the full reflex responses (Gozariu et al., 1997; Redondo-Castro et al., 2011). In our study, wind-up increased after SCIs, indicating central excitability and amplification of the nociceptive signaling. When only the first response is measured, a graded increase appears with the severity of the SCI.

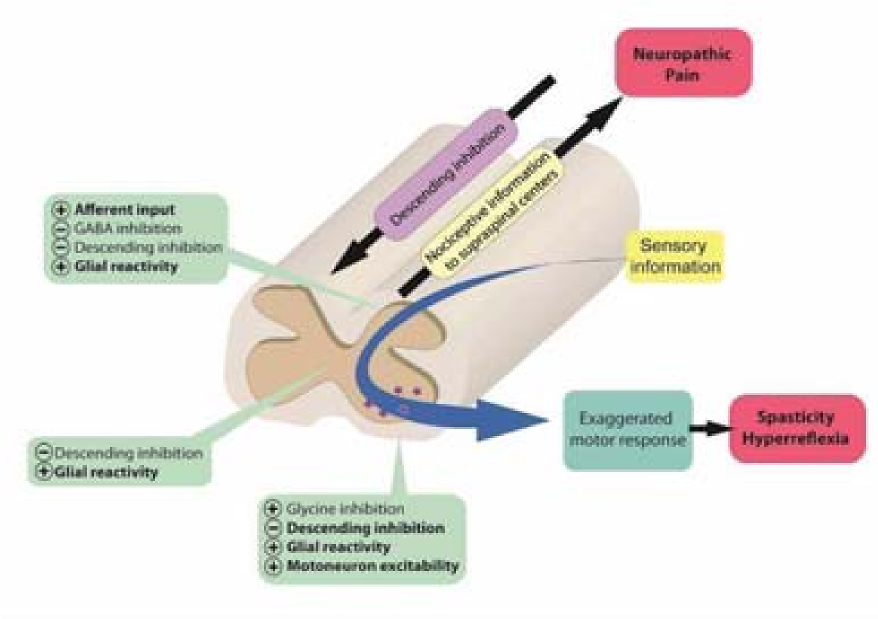

Figure 8: *Schematic representation of the abnormalities found in the spinal nociceptive system. Boxes indicate the main points of modulation and integration of the sensory information in the spinal cord. The loss of efficacy of inhibitory systems in front of the central hyperexcitability of the spinal cord promotes amplification of the responses, contributing to neuropathic pain and hyperreflexia.*

5. CONCLUSIONS

Our results indicate that after SCI there is an increase of afferent input, glial reactivity and loss of serotoninergic descending pathways at segments far caudal to the injury, which contribute to the development of pain and hyperreflexia. Compensatory mechanisms to inhibit the abnormal influx of nociceptive information in the spinal cord, such as an increase in GABA synthesis and of glycinergic inhibitory synapses on the motoneurons also occur, but they seem not enough to counteract the state of hyperexcitability. We cannot discard some other mechanisms, such as increases in persistent inward currents, changes in receptor function and plasticity regarding inhibition effectiveness in the spinal cord, as well as supraspinal changes. The unbalance between excitation and inhibition induces a predominant disinhibition in the spinal cord that has functional consequences, like the appearance of neuropathic pain and hyperreflexia (Fig. 8). Moreover, this works highlights the spread localization of the changes occurring after an SCI, not limited to the area of injury, neither to a single mechanism. It is also important to note that not all the changes are directly related to the severity of the injury, but some of them occur as all-or-none responses, with a similar degree in all the lesions studied. The results of this study indicate that the most relevant changes are due to plasticity and differential modulation of the preserved systems, and not to the loss of their function. For this reason, they open a window for new strategies designed to modulate the plastic changes developing at caudal segments after SCI.

Acknowledgements

This work was supported by grants from the Fundació MaratóTV3 (grant 070210), the Ministerio de Ciencia y Innovación (grant SAF2009-12495), and funds from Red de Terapia Celular (TERCEL) of Spain. We thank the technical assistance of Monica Espejo, Jessica Jaramillo and Marta Morell.

REFERENCES:

Alvarez FJ, Dewey DE, Harrington D, Fyffe RE (1997) Cell-type specific organization of glycine receptor clusters in the mammalian spinal cord. Journal of Comparative Neurology 379:150–70

Basso DM, Beattie MS, Bresnahan JC (1995) A sensitive and reliable locomotor rating scale for open field testing in rats. Journal of Neurotrauma 12:1–21

Boulenguez P, Liabeuf S, Bos R, Bras H, Jean-Xavier C, Brocard C, Stil A, Darbon P, Cattaert D, Delpire E, Marsala M, Vinay L (2010) Down-regulation of the potassium-chloride cotransporter KCC2 contributes to spasticity after spinal cord injury. Nature Medicine 16:302–7

Calamai M, Specht CG, Heller J, Alcor D, Machado P, Vannier C, Triller A (2009) Gephyrin oligomerization controls GlyR mobility and synaptic clustering. Journal of Neuroscience 29:7639–48

Cao Q, Zhang YP, Iannotti C, DeVries WH, Xu X-M, Shields CB, Whittemore SR (2005) Functional and electrophysiological changes after graded traumatic spinal cord injury in adult rat. Experimental Neurology 191 Suppl:S3–S16

Carlton SM, Du J, Tan HY, Nesic O, Hargett GL, Bopp AC, Yamani A, Lin Q, Willis WD, Hulsebosch CE (2009) Peripheral and central sensitization in remote spinal cord regions contribute to central neuropathic pain after spinal cord injury. Pain 147:265–76

Casals-Díaz L, Vivó M, Navarro X (2009) Nociceptive responses and spinal plastic changes of afferent C-fibers in three neuropathic pain models induced by sciatic nerve injury in the rat. Experimental Neurology 217:84–95

Cervero F (2009) Spinal cord hyperexcitability and its role in pain and hyperalgesia. Experimental Brain Research 196:129–37

Costigan M, Woolf C. (2000) Pain: Molecular mechanisms*1. Journal of Pain 1:35–44

Destombes J, Horcholle-Bossavit G, Thiesson D (1992) Distribution of glycinergic terminals on lumbar motoneurons of the adult cat: an ultrastructural study. Brain Research 599:353–360

Detloff MR, Fisher LC, McGaughy V, Longbrake EE, Popovich PG, Basso DM (2008) Remote activation of microglia and pro-inflammatory cytokines predict the onset and severity of below-level neuropathic pain after spinal cord injury in rats. Experimental Neurology 212:337–47

Diaz-Ruiz A, Salgado-Ceballos H, Montes S, Maldonado V, Tristan L, Alcaraz-Zubeldia M, Ríos C (2007) Acute alterations of glutamate, glutamine, GABA, and other amino acids after spinal cord contusion in rats. Neurochemical Research 32:57–63

Edgerton VR, Roy RR (2010) Spasticity: a switch from inhibition to excitation. Nature Medicine 16:270–1

Erlander MG, Tobin AJ (1991) The structural and functional heterogeneity of glutamic acid decarboxylase: a review. Neurochemical Research 16:215–226

Finnerup NB, Sindrup SH, Jensen TS (2007) Chronic neuropathic pain: mechanisms, drug targets and measurement. Fundamental Clinical Pharmacology 21:129–36

Floyd J, Parmer R, Reier PJ (1998) Motoneurons after midthoracic spinal cord injury in the rat. Spasticity. Animals 15

Fritschy J-M, Harvey RJ, Schwarz G (2008) Gephyrin: where do we stand, where do we go? Trends in Neurosciences 31:257–64

García-Alías G, Torres-Espín A, Vallejo C, Navarro X (2010) Functional involvement of the lumbar spinal cord after contusion to T8 spinal segment of the rat. Restorative Neurology and Neuroscience 28:781–92

Gozariu M, Bragard D, Willer JC, Le Bars D (1997) Temporal summation of C-fiber afferent inputs: competition between facilitatory and inhibitory effects on C-fiber reflex in the rat. Journal of Neurophysiology 78:3165–79

Gwak YS, Hulsebosch CE (2009) Remote astrocytic and microglial activation modulates neuronal hyperexcitability and below-level neuropathic pain after spinal injury in rat. Neuroscience 161:895–903

Gwak YS, Tan HY, Nam TS, Paik KS, Hulsebosch CE, Leem JW (2006) Activation of spinal GABA receptors attenuates chronic central neuropathic pain after spinal cord injury. Journal of Neurotrauma 23:1111–24

Hains B (2003) Serotonergic neural precursor cell grafts attenuate bilateral hyperexcitability of dorsal horn neurons after spinal hemisection in rat. Neuroscience 116:1097–1110

Hains BC, Waxman SG (2006) Activated microglia contribute to the maintenance of chronic pain after spinal cord injury. Journal of Neuroscience 26:4308–17

Hargreaves K, Dubner R, Brown F, Flores C, Joris J (1988) A new and sensitive method for measuring thermal nociception in cutaneous hyperalgesia. Pain 32:77–88

Heckmann CJ, Gorassini M a, Bennett DJ (2005) Persistent inward currents in motoneuron dendrites: implications for motor output. Muscle Nerve 31:135–56

Herrero JF, Laird JM, López-García J a (2000) Wind-up of spinal cord neurones and pain sensation: much ado about something? Progress in Neurobiology 61:169–203

Hossaini M, Duraku LS, Saraç C, Jongen JLM, Holstege JC (2010) Differential distribution of activated spinal neurons containing glycine and/or GABA and expressing c-fos in acute and chronic pain models. Pain 151:356–365

Hulsebosch CE (2002) Recent advances in pathophysiology and treatment of spinal cord injury. Advances in Physiology Edcucation 26:238–255

Hulsebosch CE (2008) Gliopathy ensures persistent inflammation and chronic pain after spinal cord injury. Experimental Neurology 214:6–9

Hulsebosch CE, Hains BC, Crown ED, Carlton SM (2009) Mechanisms of chronic central neuropathic pain after spinal cord injury. Brain Research Reviews 60:202–13

Inoue K, Tsuda M (2009) Microglia and neuropathic pain. Glia 57:1469–79

Jacob TC, Bogdanov YD, Magnus C, Saliba RS, Kittler JT, Haydon PG, Moss SJ (2005) Gephyrin regulates the cell surface dynamics of synaptic GABAA receptors. Journal of Neuroscience 25:10469–78

Ji R-R, Suter MR (2007) p38 MAPK, microglial signaling, and neuropathic pain. Molecular Pain 3:33

Keller a F, Beggs S, Salter MW, Koninck Y De (2007) Transformation of the output of spinal lamina I neurons after nerve injury and microglia stimulation underlying neuropathic pain. Molecular Pain 3:27

Kontinen VK, Stanfa LC, Basu A, Dickenson AH (2001) Electrophysiologic evidence for increased endogenous gabaergic but not glycinergic inhibitory tone in the rat spinal nerve ligation model of neuropathy. Anesthesiology 94:333–9

Lee JK, Emch GS, Johnson CS, Wrathall JR (2005) Effect of spinal cord injury severity on alterations of the H-reflex. Experimental Neurology 196:430–40

Little JW, Ditunno JI, Stiens SA, Harris RM (1999) Incomplete spinal cord injury: neuronal mechanisms of motor recovery and hyperreflexia. Arch Phys Med Rehabil 80:587-99

Lu Y, Zheng J, Xiong L, Zimmermann M, Yang J (2008) Spinal cord injury-induced attenuation of GABAergic inhibition in spinal dorsal horn circuits is associated with down-regulation of the chloride transporter KCC2 in rat. Journal of Physiology 586:5701–15

Mackie M (2003) Distribution and colocalisation of glutamate decarboxylase isoforms in the rat spinal cord. Neuroscience 119:461–472

Millan MJ (2002) Descending control of pain. Progress in Neurobiology 66:355–474

Murray KC, Nakae A, Stephens MJ, Rank M, D'Amico J, Harvey PJ, Li X, Harris RLW, Ballou EW, Anelli R, Heckman CJ, Mashimo T, Vavrek R, Sanelli L, Gorassini MA, Bennett DJ, Fouad K (2010) Recovery of motoneuron and locomotor function after spinal cord injury depends on constitutive activity in 5-HT2C receptors. Nature Medicine 16:694–700

Ondarza AB, Ye Z, Hulsebosch CE (2003) Direct evidence of primary afferent sprouting in distant segments following spinal cord injury in the rat: colocalization of GAP-43 and CGRP. Spinal Cord 184:373–380

Redondo Castro E, Udina E, Verdú E, Navarro X (2011) Longitudinal study of wind-up responses after graded spinal cord injuries in the adult rat. Restorative Neurology and Neuroscience 29:115–26

Rekling JC, Funk GD, Bayliss D, Dong XW, Feldman JL (2000) Synaptic control of motoneuronal excitability. Physiological Reviews 80:767–852

Rossignol S, Frigon A (2011) Recovery of locomotion after spinal cord injury: some facts and mechanisms. Annual Review of Neuroscience 34:413–40

Sadlaoud K, Tazerart S, Brocard C, Jean-Xavier C, Portalier P, Brocard F, Vinay L, Bras H (2010) Differential plasticity of the GABAergic and glycinergic synaptic transmission to rat lumbar motoneurons after spinal cord injury. Journal of Neuroscience 30:3358–69

Santos-Nogueira E, Redondo Castro E, Mancuso R, Navarro X (2011) Randall-Selitto test: A new approach for the detection of neuropathic pain after spinal cord injury. Journal of Neurotrauma 8:1–8

Satoh O, Omote K (1996) Roles of monoaminergic, glycinergic and GABAergic inhibitory systems in the spinal cord in rats with peripheral mononeuropathy. Brain Research 728:27–36

Scholz J, Woolf CJ (2007) The neuropathic pain triad: neurons, immune cells and glia. Nature Neuroscience 10:1361–8

Snider WD, McMahon SB (1998) Tackling pain at the source: new ideas about nociceptors. Neuron 20:629–32

Solano R, Mazario J, Orellana JM, Herrero JF (2003) Male Wistar rats show uniform wind-up responses in carrageenan-induced inflammation but not in the normal situation. Laboratory Animals 37:207–14

Soler MD, Sauri-Ruiz J, Curcoll-Gallemi ML, Benito-Penalva J, Opisso-Salleras E, Chamarro-Lusar A, Vidal-Samso J (2007) Characteristics of chronic neuropathic pain and their relationship with psychological well-being in spinal cord injury patients. Rev Neurol 44:3–9

Svendsen F (1999) Some problems with wind-up and its calculation. Pain 83:109–114

Takazawa T, MacDermott AB (2010) Synaptic pathways and inhibitory gates in the spinal cord dorsal horn. Annals New York Academy of Sciences 1198:153–158

Tillakaratne NJ, Mouria M, Ziv NB, Roy RR, Edgerton VR, Tobin a J (2000) Increased expression of glutamate decarboxylase (GAD(67)) in feline lumbar spinal cord after complete thoracic spinal cord transection. Journal of Neuroscience Research 60:219–30

Valero-Cabré A, Forés J, Navarro X (2004) Reorganization of reflex responses mediated by different afferent sensory fibers after spinal cord transection. Journal of Neurophysiology 91:2838–48

Valero-Cabré A, Navarro X (2001) H reflex restitution and facilitation after different types of peripheral nerve injury and repair. Brain Research 919:302–12

Valero-Cabré A, Navarro X (2002) Changes in crossed spinal reflexes after peripheral nerve injury and repair. Journal of neurophysiology 87:1763–71

Vallejo R, Tilley DM, Vogel L, Benyamin R (2010) The role of glia and the immune system in the development and maintenance of neuropathic pain. Pain Practice 10:167–84

Vanegas H, Schaible H-G (2004) Descending control of persistent pain: inhibitory or facilitatory? Brain research. Brain Research Reviews 46:295–309

Vulchanova L, Olson TH, Stone LS, Riedl MS, Elde R, Honda CN (2001) Cytotoxic targeting of isolectin IB4-binding sensory neurons. Neuroscience 108:143–55

Watkins LR, Milligan ED, Maier SF (2001) Glial activation: a driving force for pathological pain. Trends in Neurosciences 24:450–5

Yezierski RP (2005) Spinal cord injury: a model of central neuropathic pain. Neuro-Signals 14:182–93

Yoon YW, Dong H, Arends JJ, Jacquin MF (2004) Mechanical and cold allodynia in a rat spinal cord contusion model. Somatosensory Motor Research 21:25–31

Zhang YP, Burke D a, Shields LBE, Chekmenev SY, Dincman T, Zhang Y, Zheng Y, Smith RR, Benton RL, DeVries WH, Hu X, Magnuson DSK, Whittemore SR, Shields CB (2008) Spinal cord contusion based on precise vertebral stabilization and tissue displacement measured by combined assessment to discriminate small functional differences. Journal of Neurotrauma 25:1227–40

Zinck NDT, Downie JW (2008) IB4 afferent sprouting contributes to bladder dysfunction in spinal rats. Experimental Neurology 213:293–302

Zundert B van, Castro P, Aguayo LG (2005) Glycinergic and GABAergic synaptic transmission are differentially affected by gephyrin in spinal neurons. Brain Research 1050:40–7

Publication

Peripheral nerve alterations after thoracic spinal cord injuries in the adult rat

E.Redondo Castro, X.Navarro

Submitted to Spinal Cord

Peripheral nerve alterations after thoracic spinal cord injury in the adult rat

Elena Redondo Castro, Xavier Navarro.

Group of Neuroplasticity and Regeneration, Institute of Neurosciences and Department of Cell Biology, Physiology and Immunology, Universitat Autònoma de Barcelona, and Centro de Investigación Biomédica en Red sobre Enfermedades Neurodegenerativas (CIBERNED), Bellaterra, Spain.

Corresponding author: Dr. Xavier Navarro, Unitat de Fisiologia Mèdica, Facultat de Medicina, Universitat Autònoma de Barcelona, E-08193 Bellaterra, Spain. E-mail: xavier.navarro@uab.cat

ABSTRACT

Objective: To assess if spinal cord injury (SCI) can produce alterations in axons of peripheral nerves emerging caudal to the injury. **Methods**: Mild/severe contusion or complete transection was performed at T8 in adult rats. The function and morphology of the sciatic nerve were assessed three months after the lesion. **Results**: There was a decrease in the amplitudes of muscle responses in nerve conduction tests. The number of myelinated fibers was maintained, but some of them presented structural abnormalities. **Conclusion**: Spinal cord injuries cause alterations in peripheral axons not affected by the injury. Preservation of the peripheral components is essential for potential regenerative and rehabilitation therapies. Thus, especial care has to be taken to avoid secondary complications, due to compressions or immobility, in SCI humans.

Abbreviations: CMAP: compound muscle action potential; kdyn: kilodynes; NP: neuropathic pain; SCI: spinal cord injury; TA: tibialis anterior.

Key words: spinal cord injury, axonal count, myelinated nerve fibers, peripheral nerve, sciatic nerve.

INTRODUCTION

Spinal cord injuries (SCIs) cause disruption of ascending and descending pathways leading to paralysis and loss of sensitivity below the lesion site, as well as to positive symptoms such as spasticity and neuropathic pain. It is generally assumed that SCIs do not affect the peripheral systems, but the consequences of a SCI can expand to remote regions, cranially and caudally, and lead to secondary plastic changes involving supraspinal circuits and also the peripheral nervous system [1-3]. The motoneuron pools distal to the lesion may suffer atrophy and degeneration [4,5]. The SCI may also affect the central axons of primary sensory neurons conveyed in the dorsal column tracts. Central axotomy and retrograde degeneration may affect the neuron soma in the dorsal root ganglia and lead to degeneration of the peripheral axon branch [4]. Indeed, changes in peripheral excitability and function have already been described in human SCI patients [2,3,6,7], mainly using electrophysiological techniques.

Maintenance of peripheral nerve functions is essential in SCI rehabilitation, regenerative therapies, surgical bridges and neuroprosthetic stimulation strategies [1,3,6-8]. In this work we have performed histological and electrophysiological analyses of the peripheral nerve following SCIs of different severities in adult rats, in order to assess if there were secondary peripheral alterations, and if the severity of the injury was correlated with these alterations.

MATERIALS AND METHODS

Adult female Sprague Dawley rats (8 weeks old; 250-300 grams) were housed with free access to food and water at a room temperature of 22±2°C under a 12:12h light-dark cycles. All experimental procedures were approved by the Ethics Committee of our institution, and followed the European Communities Council Directive 86/609/EEC. All applicable institutional and governmental regulations concerning the ethical use of animals were followed during the course of this research. Researchers participating in this work were blinded to the severity of the injury received by animals.

Surgical procedure: Operations were performed under pentobarbital anesthesia (50 mg/kg i.p., Sigma), and after subcutaneous injection of buprenorphine (0.05mg/kg, Buprex, Schering-Plough) near the incision site. After dorsal laminectomy of the T8-T9 vertebra, the spinal cord was contused at T8 level using the Infinite Horizon impactor device (Precision Scientific Instruments; Lexington, UK), applying a force of 100 kilodynes (kdyn; group 100kdyn, n=5) or 200 kdyn (group 200kdyn, n=5); displacement and force applied was collected for each contusion. In another group of animals the spinal cord was completely transected (complete section group, n=5), by means of a sharp scalpel, at T8 vertebral level. To ensure that the injury transected the whole spinal cord both stumps were gently lifted away, and repositioned back into the vertebral channel. In all the surgeries, the wound was sutured with 5/0 silk thread at the muscular plane and the skin closed with small surgical clips and disinfected with povidone iodine. Animals were kept in a warm environment until full recovery from anesthesia. Bladders were expressed twice a day until reflex voiding of the bladder was re-established. Amoxicillin was given in the drinking water for 1 week to prevent postoperative infections.

Evaluation of locomotion: Locomotor hindlimb function and recovery was assessed using the Basso, Beattie and Bresnahan (BBB) rating scale in open-field walking [9]. Briefly, the BBB testing scale consists of an ordinal scale from 0 points (no discernable hind limb movement) to 21 points (consistent, coordinated gait with parallel paw placement of the hindlimb and consistent trunk stability). For measuring locomotor recovery, one animal at a time was allowed to move freely inside a circular plastic tray (90 cm diameter x 24 cm wall height) for 5 minutes, and two examiners observed the hindlimbs movements of the rat. The final score of each animal was the mean value of both examiners. Locomotion testing was performed weekly until 90 days postoperation (dpo).

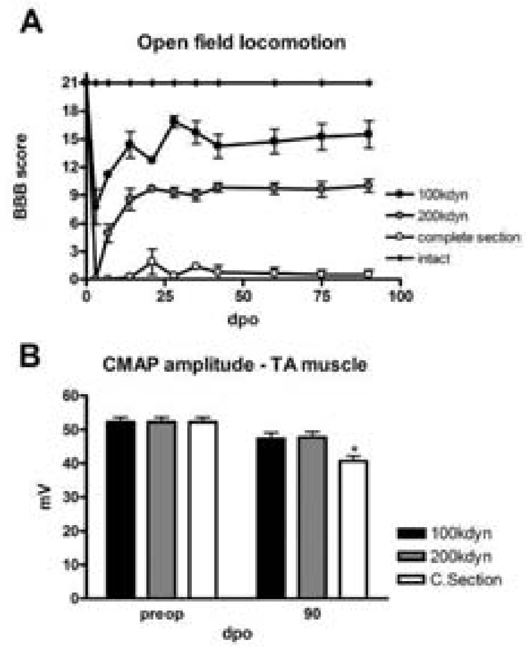

Figure 1: A) *Locomotor evaluation (BBB score) indicate graded functional deficits related to the severity of the injury. Groups displayed results significantly different between them at all time points (p<0.05). B) Amplitude of the CMAP recorded in the tibialis anterior muscle (TA) 90 days after SCI. There was a reduction in amplitude after SCI compared with prelesional values, that was only significant in the complete section group (* p<0.05 vs. prelesional value).*

Peripheral nerve conduction tests: Electrophysiological tests were performed preoperatively and after three months of follow-up. Animals were anaesthetized with pentobarbital (30 mg/kg, i.p.) and placed prone over a warmed flat coil controlled by a hot water circulating pump to maintain body temperature. Single electrical pulses (100 µs duration at supramaximal intensity) were delivered by monopolar needles (27G) inserted percutaneously at the sciatic notch. The compound muscle action potentials (CMAP) were recorded from the anterior tibialis and from the plantar interosseus muscles by means of an active electrode inserted on the belly of the muscle and the reference electrode at the fourth toe [10,11]. CMAPs were amplified, filtered (bandpass 1 Hz – 5 KHz), displayed on an electromyograph (Sapphyre 4ME, Vickers) and measured. The responses with the highest amplitude were selected and used for analysis. Values from both hindlimbs of each animal were averaged.

Histological processing and axonal counting: At 90 dpo the animals were perfused with 4% paraformaldehyde in 0.1M phosphate buffer. The sciatic nerve was harvested proximal to its trifurcation (distal part of the thigh), and fixed with Webster's fixative (3% paraformaldehyde and 3% glutaraldehyde in 0.1M phosphate buffer) overnight. The nerve segments were postfixed with 2% osmium tetroxide in 0.1M phosphate buffer for two hours. Samples were dehydrated using increasing graded solutions of ethanol, incubated in propylene oxide for one hour and then in a mixture of 50% propylene oxide and 50% Epon for 90 minutes, followed by incubation in 100% Epon overnight. Transverse sections 0.5 µm thick were taken in an ultramicrotome, collected into glass slides, and stained with toluidine blue. Images were acquired at 100X under light microscopy, and counts of the myelinated fibers were performed using NIH Image J software. The density of myelinated fibers was obtained from counts in fields chosen by systematic sampling representing at least 50% of the total area of the nerve. The total number of myelinated fibers was calculated by multiplying the myelinated fiber density per the cross-sectional area of the nerve [12,13].

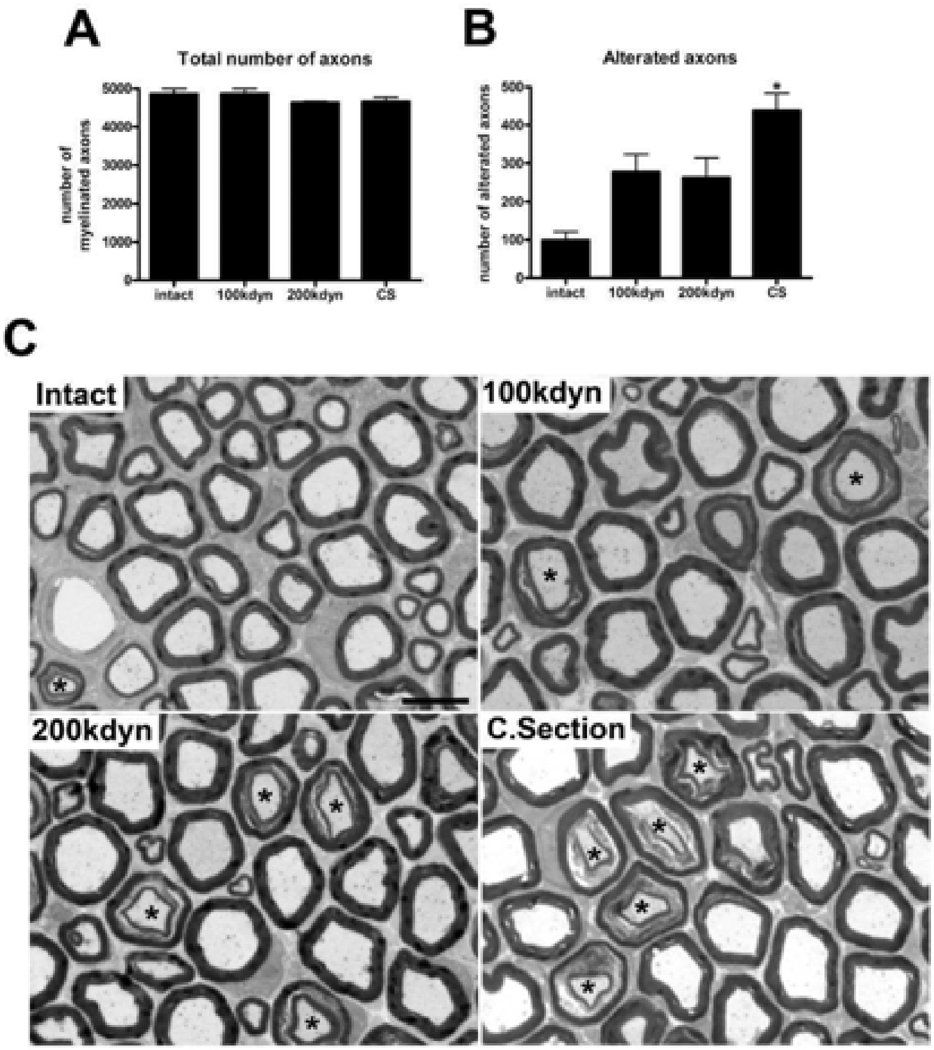

***Figure 2:** **A)** The total number of myelinated axons in the sciatic nerve was not significantly changed after SCI. **B)** Number of altered fibers in different spinal cord injuries revealed an increase with the severity of the injury. Animals with complete section had the highest number of altered axons (* $p<0.05$ vs. intact rats). **C)** Representative micrographs of transversal sections of the sciatic nerve. Abnormalities of myelinated fibers (indicated by asterisks *) are more numerous in rats after SCI. Scale bar: 10 µm.*

RESULTS

Locomotion

After the SCI, the rats showed a reduction in the BBB score in relation with the severity of the lesion (Fig. 1A). Animals receiving 100kdyn contusion reached a plateau at 15-16 points, indicating plantar stepping and coordinated gait, although with some deficits regarding toe clearance and rotation of the hindpaw position; rats of the 200kdyn contusion group presented more marked deficits, such as uncoordinated gait and only occasional plantar stepping (score about 9-10 points). Animals with complete transection displayed nearly complete paralysis, so they reached scores of 1-2 points during the follow-up (only slight movement of some joints). There were significant differences between the three groups ($p<0.001$) at all time points after injury.

Electrophysiology

CMAPs of the anterior tibialis muscle showed a progressive reduction as the severity of the injury increased (Fig. 1B). Intact animals had a mean amplitude of 52.3±1.4 mV, whereas animals with mild and severe contusions presented slightly reduced values (100 kdyn: 47.4±1.8 mV; 200 kdyn: 47.8±1.6 mV), and complete section animals showed a significant reduction (40.8±1.5 mV, $p<0.05$ vs. presurgical values). The latency presented a non significant reduction in all injured groups (intact latency: ~1.45ms; injured animals ~1.30ms). Latencies and amplitudes of the plantar muscles CMAPs displayed similar results, with a small reduction in amplitude and no changes in latencies.

Histology

Axonal counts were done to assess if the reduction of CMAP amplitude was due to axonal loss. Measurements were performed in the tibial nerve, the main fascicle of the sciatic nerve. Injured rats had a total number of myelinated fibers similar to intact nerves (Fig.2A; intact: 4851±143; 100kdyn: 4864±129; 200kdyn: 4629±29; section: 4650±120), but they had an increased number of fibers with abnormal appearance (Fig. 2B; intact: 99±21; 100 kdyn: 277±46; 200 kdyn: 262±51; section 438±45). The abnormalities observed were mainly detachment of the myelin sheath and axonal atrophy, but no clear signs of degeneration were found in any of the rats (Fig.2C). Some of these altered figures correspond to Schmidt–Lanterman incisures. The abnormal fibers did not display a fascicular organization within the section, although in SCI groups there were more frequent at the periphery of the nerve section. The sural and peroneal fascicles on the sciatic nerve did not display so noticeable abnormalities.

DISCUSSION

The effects of a SCI are not restricted to the spinal cord itself but can expand to remote areas of the spinal cord as well as to the peripheral nervous system [1,3]. Our results indicate that thoracic SCI causes clear functional deficits, especially visible in locomotion. These deficits keep a direct relationship with the severity of the injury received [14–16]. On the other hand, SCI did not cause axonal degeneration in the sciatic nerve, although it induced some axonal alterations, despite the lesion did not primarily affect its contributing neurons. Electrophysiological tests showed also a mild functional decline of the CMAP amplitude in muscles of the hindlimb.

Three months after a thoracic SCI there was not significant loss of myelinated axons in the sciatic nerve compared to intact nerves. However, the number of abnormalities observed in myelinated fibers increased, particularly in the rats with complete cord section. We cannot ensure that these alterations would eventually lead to degeneration, as there were not typical features of axonal degeneration (disorganized myelin forming bundles, presence of myelin bodies in the axoplasm, swelling, hyperplasia, axonal atrophy, etc). Indeed, the observed alterations may correspond to Schmidt-Lanterman incisures, placed near the nodes of Ranvier, where the myelin sheath is partially reorganized. The increased presence of this cisures in the injured animals may be considered as a sign of nerve fiber dysfunction. In fact, an increase of these structures was described at the onset of Wallerian degeneration [17,18], and in nerve compression injuries [19].

The loss of function of the hindlimbs after the SCI causes muscle atrophy, but immobilization and muscle atrophy by disuse seem to have small effects on preservation of CMAP amplitudes and histological outcomes [2,20], as our results indicate. Contrarily, axonal degeneration has been reported in humans after SCI. This leads to the assumption that the loss detected in humans may be secondary not only to disuse, but also to compression in paralyzed limbs. Other causes may include edema caused by inactivity and reduced blood flow following SCI [1,2]. Since locomotion is more easily recovered in rodents than in humans after SCI, the secondary complications associated to disuse and immobility would be less important in quadrupedal animals. Special attention must be given to avoid such secondary complications of SCI in humans (disuse, immobility, atrophy, nerve compressions) that may eventually lead to peripheral nerve damage and loss of functionality. This should be taken into consideration when designing rehabilitation or regenerative therapies, providing especial care to maintain peripheral neuromuscular function [1,6,7].

Acknowledgments
This work was supported by grants from the Fundació MaratóTV3 (grant 070210), the Ministerio de Ciencia y Innovación (grant SAF2009-12495), and funds from Red de Terapia Celular (TERCEL) of Spain. We thank the technical assistance of Monica Espejo and Marta Morell, the surgical help of Abel Torres-Espín, and the histological work of Jessica Jaramillo.

References

1. Riley DA, Burns AS, Carrion-Jones M, Dillingham TR. Electrophysiological dysfunction in the peripheral nervous system following spinal cord injury. *PMR* 2011;3(5):419–25; quiz 425.
2. Van De Meent H, Hosman AJ, Hendriks J, et al. Severe degeneration of peripheral motor axons after spinal cord injury: a European multicenter study in 345 patients. *Neurorehabil Neural Repair* 2010;24(7):657–65.
3. Lin CS-Y, Macefield VG, Elam M, et al. Axonal changes in spinal cord injured patients distal to the site of injury. *Brain* 2007;130(Pt 4):985–94.
4. Kitzman P. Alteration in axial motoneuronal morphology in the spinal cord injured spastic rat. *Exp Neurol* 2005;192(1):100–8.
5. García-Alías G, Torres-Espín A, Vallejo C, Navarro X. Functional involvement of the lumbar spinal cord after contusion to T8 spinal segment of the rat. *Restor Neurol Neurosci* 2010;28(6):781–92.
6. Berman SA, Young RR, Sarkarati M, Sherfner J. Injury zone denervation in traumatic quadriplegia in humans. *Muscle Nerve* 1996;19(6):701–6.
7. Nogajski J., Engel S, Kiernan MC. Focal and generalized peripheral nerve dysfunction in spinal cord-injured patients. *J Clin Neurophysiol* 2006;23(3):273–9.
8. Mackinnon SE, Yee A, Ray WZ. Nerve transfers for the restoration of hand function after spinal cord injury. *J Neurosurg* 2012;117(1):176–85.
9. Basso DM, Beattie MS, Bresnahan JC. A sensitive and reliable locomotor rating scale for open field testing in rats. *J Neurotrauma* 1995;12(1):1–21.
10. Valero-Cabré A, Navarro X. H reflex restitution and facilitation after different types of peripheral nerve injury and repair. *Brain Res* 2001;919(2):302–12.
11. Valero-Cabré A, Forés J, Navarro X. Reorganization of reflex responses mediated by different afferent sensory fibers after spinal cord transection. *J Neurophysiol* 2004;91(6):2838–48.
12. Bruna J, Alé A, Velasco R, et al. Evaluation of pre-existing neuropathy and bortezomib retreatment as risk factors to develop severe neuropathy in a mouse model. *J Periph Nerv Syst* 2011;16(3):199–212.
13. Gómez N, Cuadras J, Buti M, Navarro X. Histologic assessment of sciatic nerve regeneration following resection and graft or tube repair in the mouse. *Restor Neurol Neurosci* 1996;10(4):187–96.
14. Redondo-Castro E, Udina E, Verdú E, Navarro X. Longitudinal study of wind-up responses after graded spinal cord injuries in the adult rat. *Restor Neurol Neurosci* 2011;29(2):115–26.
15. Scheff SW, Rabchevsky AG, Fugaccia I, et al. Experimental modeling of spinal cord injury: characterization of a force-defined injury device. *J Neurotrauma* 2003;20(2):179–93.
16. Cao Q, Zhang YP, Iannotti C, et al. Functional and electrophysiological changes after graded traumatic spinal cord injury in adult rat. *Expl Neurol* 2005;191 Suppl :S3–S16.
17. Webster H. The relationship between Schmidt-Lanterman incisures and myelin segmentation during Wallerian degeneration. *Ann N Y Acad Sci* 1965;31(122):29–38.
18. Hall SM, Williams PL. Studies on the "incisures" of Schmidt and Lanterman. *J Cell Sci* 1970;6(3):767–91.
19. Hunter DA, Moradzadeh A, Whitlock EL, et al. Binary imaging analysis for comprehensive quantitative histomorphometry of peripheral nerve. *J Neurosci Methods* 2007;166(1):116–24.
20. Urso ML, Clarkson PM, Price TB. Immobilization effects in young and older adults. *Eur J Appl Phys* 2006;96(5):564–71.

4

Study of pharmacological treatments for neuropathic pain responses based on modulation of glial activity

Specific objectives:

Some decades ago pain was firstly described as a neuronal phenomenon. More recently glial cells have achieved a leading role as contributors to the appearance of NP. Whilst microglia is especially related to the initiation of pain, astroglia is supposed to act later in the maintainenance of chronic pain. These two glial cells are already known to play a beneficial role after a neural injury, but the chronicity of some of their effects may become detrimental after a spinal cord injury, and eventually contribute to pain, hyperreflexia and spasticity, among other positive signs of dysfunction. Fortunately, understanding the roles of both populations after a spinal cord injury gives us a good opportunity to use them and modulate their action in the right direction.

The specific objectives for this chapter are the following:

1. Study the effect of glibenclamide as a trigger of microglial activation, administered acutely after the spinal cord contusion, in order to promote the initial action of microglial cells.

2. Study the anti-inflammatory effect of administration of ibuprofen in order to control the pathological chronic inflammatory response after the SCI.

3. Combine both drugs in order to obtain synergic addition of the effects produced when they are administered independently.

4. Assess the *in vitro* effects of each drug on glial cell cultures.

Publication

Phagocitic microglial phenotype induced by glibenclamide improves functional recovery but worsens hyperalgesia after spinal cord injury in adult rats

E.Redondo Castro, J. Hernández, N.Mahy, X.Navarro

Submitted to Experimental Neurology

Phagocytic microglial phenotype induced by glibenclamide improves functional recovery but worsens hyperalgesia after spinal cord injury in adult rats

Elena Redondo-Castro[1], Joaquim Hernández[1], Nicole Mahy[2], Xavier Navarro[1].

[1] Group of Neuroplasticity and Regeneration, Institute of Neurosciences and Department of Cell Biology, Physiology and Immunology, Universitat Autònoma de Barcelona, and Centro de Investigación Biomédica en Red sobre Enfermedades Neurodegenerativas (CIBERNED), Bellaterra, Spain.
[2] Departament de Ciències Fisiològiques I, Facultat de Medicina, Institut d'Investigacions Biomèdiques August Pi i Sunyer (IDIBAPS), Universitat de Barcelona and Centro de Investigación Biomédica en Red sobre Enfermedades Neurodegenerativas (CIBERNED), Barcelona, Spain.

Corresponding author: Xavier Navarro, Unitat de Fisiologia Mèdica, Edif. M, Universitat Autònoma de Barcelona, E-08193 Bellaterra, Spain.
Tel: +34-935811966, Fax: +34-935812986, E-mail: xavier.navarro@uab.cat

Running title: GB promotes functional recovery after SCI
Keywords: microglia, glibenclamide, contusion, neuropathic pain, functional recovery.

ABSTRACT

Microglia plays a crucial role in the development and establishment of chronic neuropathic pain after spinal cord injuries. Since neuropathic pain is refractory to many treatments and some drugs only present partial efficacy, it is essential to study new targets and mechanisms to ameliorate pain signs. For this reason we have used glibenclamide (GB), a blocker of K_{ATP} channels that are over expressed in microglia under activation conditions. Using GB we expected to trigger the early scavenger activity of microglia in order to promote a better removal of dead cells and myelin debris and support the microglia neuroprotective phenotype. Our results indicate that a single dose of GB (1μg) injected after spinal cord injury is sufficient to promote long lasting functional improvements in locomotion and coordination. Nevertheless, these improvements are accompanied by enhanced mechanical hyperalgesia. Combining in vivo and in vitro methodologies, we assess the role of GB in promoting different microglial phenotypes that may be used for the treatment of neuropathic pain.

INTRODUCTION

Amongst symptoms, such as motor paralysis, loss of sensibility and autonomic dysfunctions below the lesion site, neuropathic pain is one of the most disabling consequences of spinal cord injuries, considerably affecting the quality of life of the patients. Neuropathic pain is refractory to most existing treatments, and for this reason many studies are focused on discovering new treatments or therapies for ameliorating the painful symptoms. Presently, the most used drug treatments are tricyclic antidepressants, GABA modulators (gabapentin and pregabalin), serotonin and norepinephrine reuptake inhibitors, and different blockers of voltage dependent sodium channels. Nevertheless, despite they target different mechanisms to reduce activity in the nociceptive system, the efficacy and effectiveness of these treatments are usually difficult to predict and most clinical trials have reported negative effects (Finnerup et al., 2007; Baastrup and Finnerup, 2008).

In the last years, dysfunctions of glial cells, particularly of microglia, have emerged as important contributors in the appearance and maintenance of neuropathic pain (Watkins et al., 2001; Tsuda et al., 2005; Hains and Waxman, 2006; Hulsebosch, 2008; Milligan and Watkins, 2009; Inoue and Tsuda, 2009; Vallejo et al., 2010; Gwak et al., 2012). Glial cells do not limit their effects to the lesion site, but show also reactive characteristics in remote regions, such as supraspinal centers (Zhao et al., 2007), rostral spinal cord regions (Carlton et al., 2009) and especially caudal regions (Detloff et al., 2008; Gwak and Hulsebosch, 2009; García-Alías et al., 2010), where they contribute to the development of spinal hyperexcitability as well as to below-level neuropathic pain. Some recent approaches are, thus, focused to the modulation of glial reactivity after spinal cord injuries. The most commonly used drugs are minocycline, propentofylline and pentoxyfilline. Minocycline is a tetracycline derived compound that inhibits or delays microglia activation and proliferation, and also attenuates the expression of proinflammatory cytokines (Ledeboer et al., 2005; Hains and Waxman, 2006; Nie et al., 2010; Chang and Waxman, 2010). Propentofylline has neuroprotective properties by limiting astrocytic and microglial activation in pathological conditions, and it is thought to act as a selective phosphodiesterase inhibitor modulating the secretion of cytokines that trigger nociceptive transmission (Sweitzer et al., 2001; Gwak and Hulsebosch, 2009). Pentoxifylline is also a global inhibitor of astroglial and microglial proliferation and activity, inhibiting extracellular adenosine transporters and phosphodiesterases, that has provided good results reducing neuropathic pain manifestations (Scholz and Woolf, 2007).

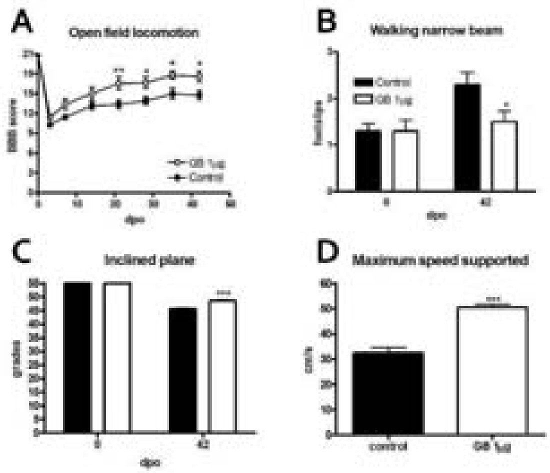

Figure 1. Functional results: animals treated with GB showed a better performance in the open field locomotion test (A), the walking narrow beam (B), the inclined plane (C) and the maximum speed supported in a treadmill (D). For the four tests, differences between groups were statistically significant (* $p<0.05$; ** $p<0.01$; *** $p<0.001$).

Quiescent microglia lacks an outward K^+ current that appears when activated, in response to increase in intracellular ADP and hypoxic conditions, leading to K^+ efflux. These K^+ channels associated with glucokinase expression act as energy sensors of the ATP production, and therefore couple the metabolic state of the cell with its electrical activity (Ramonet et al., 2004; Ostroumov et al., 2007; Sun and Hu, 2010; Ortega et al., 2012b). Glibenclamide (Glyburide, GB) is a powerful blocker of the K_{ATP} channels (Simard et al., 2008; Ortega et al., 2012b), widely used to treat type 2 diabetes mellitus, and has also diverse actions suppressing neutrophil migration and chemotaxis in acute inflammatory conditions (Da Silva-Santos et al., 2002; Pompermayer et al., 2007), and antioxidant or anti-inflammatory properties (Virgili et al., 2011; Abdallah et al., 2011). In the nervous system the functional role of K_{ATP} channels is controversial, since both beneficial and detrimental effects have been attributed to its activation. Whilst opening of K_{ATP} channels is beneficial in the induced experimental autoinmune encephalomyelitis mouse model of multiple sclerosis (Virgili et al., 2011) and in some ischemic reperfusion injuries (Zarch et al., 2009; Sun and Hu, 2010), their blockade by GB has also provided positive effects in ischemic models (Simard et al., 2006, 2009; Ortega et al., 2012a) and in spinal cord injury models (Simard et al., 2007; Popovich et al., 2012).

The main hypothesis of this work was based on the use of GB as a trigger of microglial activation. An early activation causes the expression of a neuroprotective phenotype (de Yebra et al., 2006; Ortega et al., 2012b), with the secretion of anti-inflammatory cytokines and glutamate transporters to reduce excitotoxic damage. Moreover, the enhancement of the scavenger and phagocytic properties of microglia could eventually lead to an earlier resolution of the initial traumatic events, and therefore improve the functional outcome at long term (Ortega et al., 2012b). In this work we have injected GB into the injured spinal cord and have followed up the animals until 6 weeks, in order to assess functional improvement as well as changes in neuropathic pain signs.

METHODS AND MATERIALS

Laboratory animals

Adult female Sprague Dawley rats (8 weeks old; 250-300 g) were housed with free access to food and water at room temperature of 22±2ºC under a 12:12 h light-dark cycles. All experimental procedures were approved by the Ethic Committee of our institution, and followed the European Communities Council Directive 86/609/EEC. Researchers involved in experimental tests were blinded to the treatment received by each animal.

Surgical procedure

Operations were performed under ketamine/xylacine anesthesia (90/10 mg/kg i.p.), and after subcutaneous injection of buprenorphine (0.05 mg/kg) at the incision site. After dorsal laminectomy of T8-T9, the spinal cord was contused at T8 vertebral level using the Infinite Horizon impactor device (Precision Scientific Instruments; Lexington, UK), applying a force of 100 kilodynes. Data from displacement and force applied was collected for each contusion. After the contusion, two injections were performed at 1 mm rostral and caudal from the epicenter, using a microsyringe coupled to an infusion pump (KDS310; KD Scientific Inc.). In each injection, 1µl was introduced in the spinal cord using a glass capillary (customtips, type IV, Eppendorf), that was maintained in site for 5 minutes after injection to avoid liquid leaking. Experimental groups were GB (glibenclamide, 0.5µg/µl in each injection, 1µg total, n=9 rats) and control (saline solution, 1µl/injection, n=9 rats). Glibenclamide (Sigma-Aldrich, St Louis, MO) was prepared in dimethyl sulfoxide and diluted in 0.01 mol/L PBS to final concentration (dimethyl sulfoxide final concentration <0.5%). The wound was sutured with 5/0 silk thread in the muscular plane and small surgical clips in the skin, and disinfected with povidone iodine solution. Animals were rehydrated with saline solution supplemented with glucose (in order to avoid possible hypoglycemia caused by glibenclamide) and kept in a warm environment until full recovery from anesthesia. Bladders were expressed twice a day until reflex voiding of the bladder was re-established. Amoxicillin was given in the drinking water for 1 week to prevent postoperative infections.

Functional evaluation

Assessment of locomotion: Locomotor hindlimb function was assessed using the Basso, Beattie and Bresnahan (BBB) rating scale (Basso et al., 1995) during open field walking. The BBB scale ranges from 0 points (no discernable hindlimb movement) to 21 points (consistent, coordinated gait with parallel paw placement of the hindlimbs and consistent trunk stability). For measuring locomotor recovery, one animal at a time was allowed to move inside a circular plastic tray for 5 minutes, and two examiners observed the hindlimbs movements of the rat. The final score of each animal was the mean value of both examiners. Locomotor test was performed weekly until 42 days postoperation (dpo).

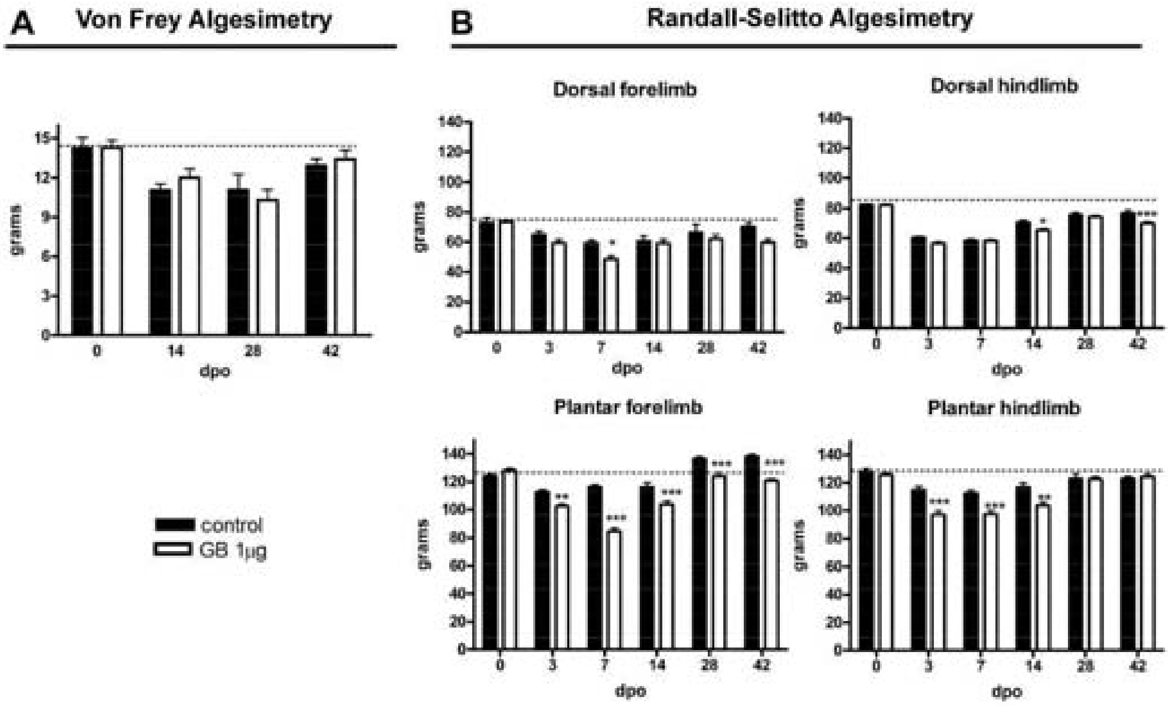

Figure 2. Neuropathic pain: Mechanical algesimetry tests (A) indicated that GB caused a slight reduction of nociceptive thresholds in the plantar surface of the hindpaws, although without reaching statistical significance. Randall-Selitto test (B) revealed the same tendency in forepaws and hindpaws, and in dorsal and plantar surfaces. In this test, differences reached statistical significance at some testing days (* $p<0.05$; ** $p<0.01$; *** $p<0.001$). Dotted lines indicate the mean values in intact rats.

Beam test for fine coordination: The rats walked inside a dark tunnel along an elevated beam (beam dimensions: 2.5 cm width, 2 cm height, 2 mm elevated from the ground to place a paper sheet to print the inked paws). Hindpaw plantar surfaces were inked, and animals had to walk along the beam so only the missteps were recorded by ink in the paper sheet placed under the beam. Three consecutive runs were performed, and the left and right missteps done in the first 30 cm were counted in each run. The mean of these values was considered as the result for each rat in the testing day.

Inclined plane test: This test measures the ability to maintain body position on an inclined plane for at least five seconds. The rats were placed on the plane and its inclination was progressively increased, until recording the maximum angle supported, that was recorded as the outcome measure. Three trials were done to obtain the average value for each animal and day.

Gait treadmill assessment: Animals were acclimated to the belt compartment of a Digigait Imaging system (Mouse Specifics Inc., Boston, MA) before starting the test, and trials were done using increasing speeds of the running belt, with resting periods between them. The maximum speed at which the rat maintained walking was calculated.

Neuropathic pain tests: mechanical algesimetry

Mechanical nociceptive thresholds of the hindpaws were determined using an electronic von Frey unit (Bioseb, Chaville, France). Rats were placed into a plastic box with an elevated metallic fine-grid surface, and acclimated to the test chamber for 20 minutes. From the bottom of the box, a metal tip attached to the sensor was applied directly to the glabrous surface of both hindpaws (Casals-Díaz et al., 2009). The force applied (in grams) until the withdrawal of the paw was measured, being the value for the test the mean of at least three trials separated by 5 min resting periods. The maximal force was limited to 35 grams to avoid skin damage. Tests were performed before the surgery (preoperative values) and at 14, 28, and 42 days after injury.

Pressure algesimetry: Randall Selitto test was performed by means of a digital paw pressure meter device (IITC 2500, IITC Life Science, Woodland Hills, CA) in all animals before the surgery and at 3, 7, 14, 28 and 42 dpo. With the animal carefully immobilized, an increasing mechanical force was applied with the tip of the device on the mid of the plantar or the dorsal surfaces of both forepaws and hindpaws until a withdrawal response resulted. The maximum force applied was limited to 250g to avoid skin damage (Santos-Nogueira et al., 2011).

Electrophysiological tests

Animals were anaesthetized with pentobarbital (30 mg/kg, i.p) and placed prone over a warmed flat coil controlled by a hot water circulating pump to maintain body temperature. Electrophysiological tests were performed preoperatively and at the end of the follow-up period.

Peripheral nerve conduction test: Single electrical pulses (100 µs at supramaximal intensity) were delivered by monopolar needles inserted percutaneously at the sciatic notch. Compound muscle action potentials (CMAPs) were recorded from the tibialis anterior (TA) muscle and the third plantar interosseus (PL) muscle, by means of an active electrode inserted on the belly of the corresponding muscle and the reference electrode at the fourth toe (Valero-Cabré et al., 2004), amplified and displayed in an

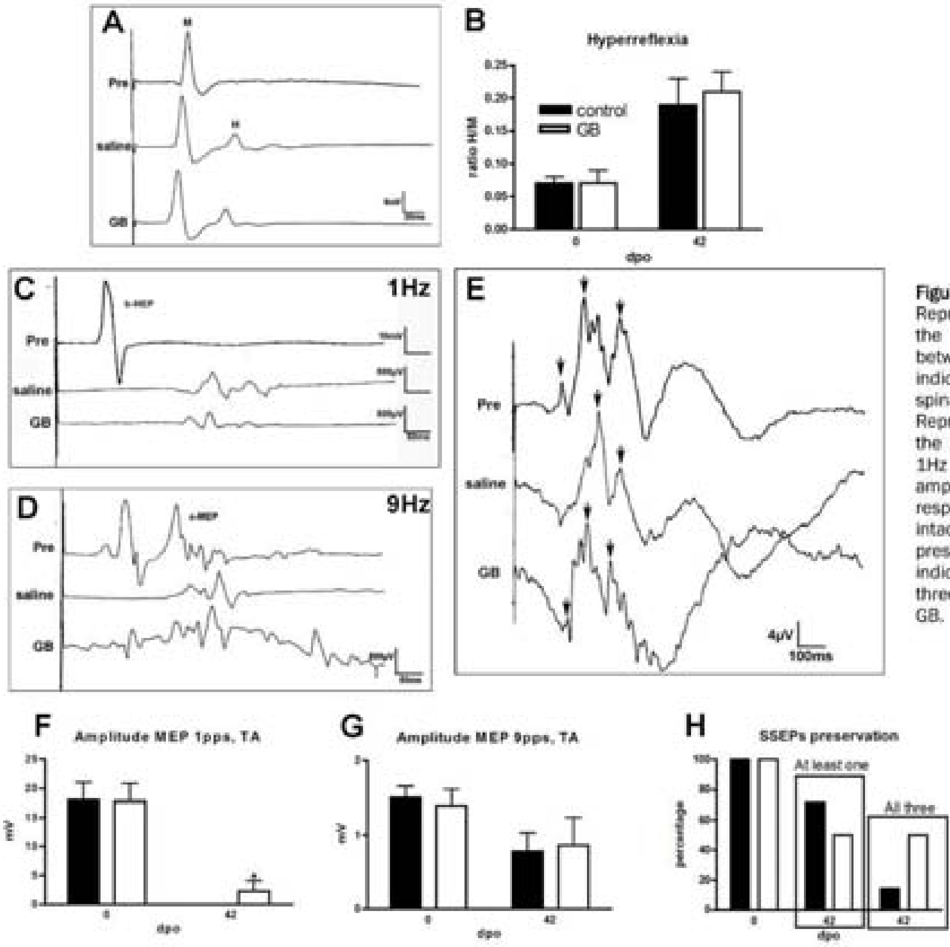

Figure 3. Electrophysiology results: Representative recordings of CMAPs of the plantar muscle (A). The ratio between H and M waves amplitudes indicates marked hyperreflexia after spinal cord contusion (B). Representative recordings of MEPs in the tibialis anterior muscle, elicited at 1Hz (C) or 9Hz (D). Their mean amplitudes are represented in F and G, respectively. Recordings of SSEPs in intact and injured rats (E). Percentage of preservation of SSEP components (H), indicating better preservation of the three components in rats treated with GB.

electromyograph (Sapphyre 4M, Vickers). The latency and amplitude of the direct muscle response (M wave) and the monosynaptic reflex response (H wave) were calculated. Values of both hindlimbs of each animal were averaged.

Motor evoked potentials (MEPs) were elicited by transcranial electrical stimulation, using two monopolar needle electrodes placed subcutaneously over the skull, the anode over the sensorimotor cortex and the cathode at the hard palate, and recorded from the TA muscle (García-Alías et al., 2006). Single pulses of 25 mA and 100 µs duration were delivered at 1 or 9 Hz, the adequate pulse rates for eliciting the brainstem component (bs-MEP) and the cortical component (c-MEP), respectively. The muscle responses were displayed in the oscilloscope to measure the amplitude and latency of each component.

Somatosensory evoked potentials (SSEPs) were evoked by electrical stimuli of 6 mA and 100 µs delivered at 6 Hz to the tibial nerve at the ankle, and recorded by needle electrodes placed subcutaneously on the skull (same sites as stimulation needles for MEPs). Up to 256 responses were averaged on-line; the peak latency and the peak-to-peak amplitude were measured for N15, N20 and N30 waves (Valero-Cabré et al., 2004), referenced here as N1, N2 and N3 components. SSEPs were repeated three times with minutes between trials, and the responses with the highest amplitude were selected and used for analysis.

Immunohistochemistry and histology

Anesthetized rats were perfused with 4% paraformaldehyde in phosphate-buffered saline at 42 days after injury. A T7-T10 spinal cord segment around the lesion epicenter was removed, post-fixed overnight and cryoprotected in 30% sucrose. The samples were embedded in TissueTek and serially cut (30 µm thickness) in the transverse plane with a cryostat. Sections were collected onto gelatin-coated glass slides and immunostained with primary antibody against glial fibrillary acidic protein (GFAP; 1:1000, Sigma-Aldrich) to visualize the cavity formed around the lesion. Neuronal survival in ventral horns was measured in sections labeled against NeuN (Neuronal Nuclei, 1:200, Millipore), and the preservation of myelinated axons in dorsal funiculus determined by immunostaining of myelin basic protein (MBP, 1:50, Ultraclone) and neurofilament (NF, 1:1000, Millipore).

Lumbar segments L1-L6 were also removed and embedded for sectioning at 20 µm thickness, and processed for immunohistochemical detection of markers of astrocytes (GFAP) and microglia (Iba1, 1:1000, Wako). Glial labeling measurements were done in L4-L5 segments using a ROI (region of interest) placed in the dorsal horn, comprising laminae I to IV, and a ROI in the ventral horn,

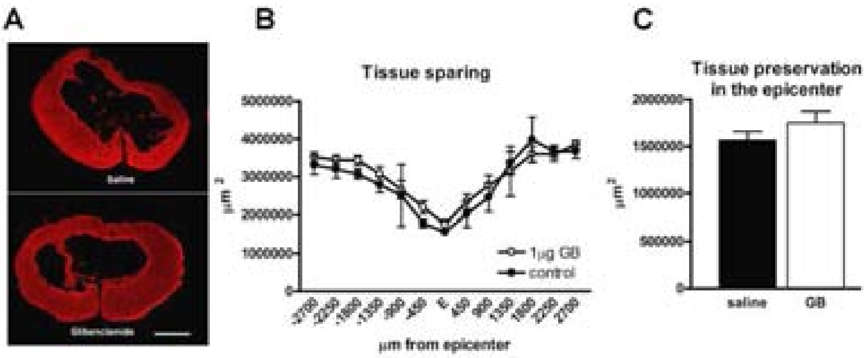

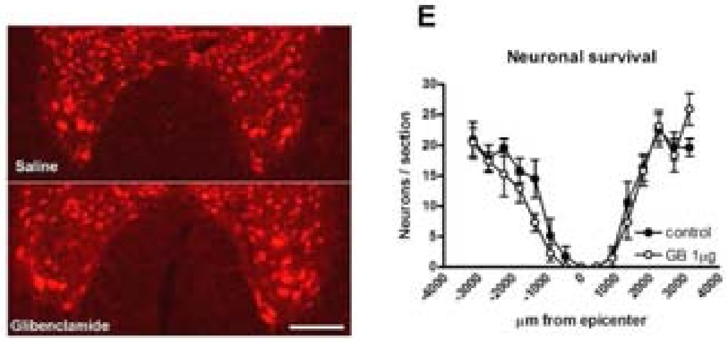

Figure 4. Tissue sparing and neuronal survival at the lesion epicenter. Representative micrographs of spinal cord transverse sections at the lesion epicenter immunolabeled against GFAP (A). Tissue spared measurements were performed caudal and rostral (B) and at the injury epicenter (C) levels. Surviving neurons were labeled for NeuN and counted in ventral horns surrounding the injury site (D, representative images taken 2mm caudal to the epicenter). Number of surviving neurons are plotted in graph E. Scale bar: 500µ in A and 200µm in D.

placed around lamina IX including the area occupied by motoneurons. Cy3 conjugated secondary antibody (1:200; Jackson Immunoresearch) was used for single labeling, and Alexa Fluor secondary antibodies for double immunohistochemistry. At least five sections per animal were used to perform the measurements.

Luxol fast blue staining was used to visualize myelin in samples from the lesion site. Sections of 30 µm of thickness and separated from the next 450 µm were used to measure the total myelinated area as well as the myelination of the dorsal funiculus.

An additional batch of animals were contused and sacrificed at 1 and 3 dpo (n=3 per time and treatment) to evaluate early microglial reactivity. Samples harvested at these early time points were cut longitudinally (30 µm thickness) and a ROI was placed in the epicenter, and rostral and caudal to it. At least five ROIs of each area were measured in different sections of the same animal. Measurements of the integrated density were performed for ED1 (1:200, Serotec) and Iba1 labelings.

Microglial cell culture

Glial cell cultures were prepared from 1 day-old Sprague Dawley rats as previously described (Servitja et al., 2000). Rats were decapitated and cortices immediately dissected out. After meninges and blood vessels were removed, the tissue was minced and incubated for 10 min at 37°C in Ca^{2+}-free Krebs-Ringer buffer containing 0.0025% trypsin. Cells were then mechanically triturated through a glass pipette and filtered through a 40-µm nylon mesh in the presence of 0.52 mg/ml soybean trypsin inhibitor and 170 IU/ml DNAse. After centrifugation (500g), the cells were stained with Trypan Blue exclusion dye, counted in a Neubauer chamber, and then resuspended (300,000 cells/ml) in 90% DMEM, 10% FBS, 20 U/ml penicillin, and 20 mg /ml streptomycin. Cells were plated and incubated at 37°C in a humidified atmosphere of 5% CO_2 and 95% air; medium was replaced every 5-7 days. After 9-11 days in vitro, microglial cells were obtained by shaking the flasks during 3-4 hours at 300 rpm. Floating cells were pelleted and subcultured at 100,000 cells/ml on mixed glial-conditioned medium.

LPS (10 ng/ml) or a spinal cord lesion extract (100 µg protein/ml) were added after 24h in order to activate microglial cells. Glibenclamide (15 nM) was added 24h after activation. Lesion extracts were obtained from injured spinal cords harvested 7 days after a 100kdyn spinal cord contusion. Fresh tissue was obtained from the lesion site (around 1 cm) and frozen with liquid nitrogen. Samples were rinsed with liquid nitrogen a few times while being mechanically disgregated. Then the frozen particles were resuspended in DMEM supplemented with a diluted cocktail of inhibitors of proteases and disgregated again. Finally samples were sonicated for 5 minutes and centrifuged (15000 rcf, 5 minutes). Quantification of the protein content was done by the BCA method.

Pictures of the cultures were taken in phase contrast to evaluate morphological changes of microglia. Cells were then fixed with 4% paraformaldehyde and immunolabeled to detect Iba1 and ED1 proteins, used as markers of microglia and phagocytic activity, respectively.

Statistical analysis

Data are shown as the mean ± SEM. Statistical comparisons between groups were made using two way ANOVA for repeated measures with Bonferroni *post hoc* tests, or t-test analyses (GraphPad Prism software). Differences between groups were considered statistically significant if $p<0.05$.

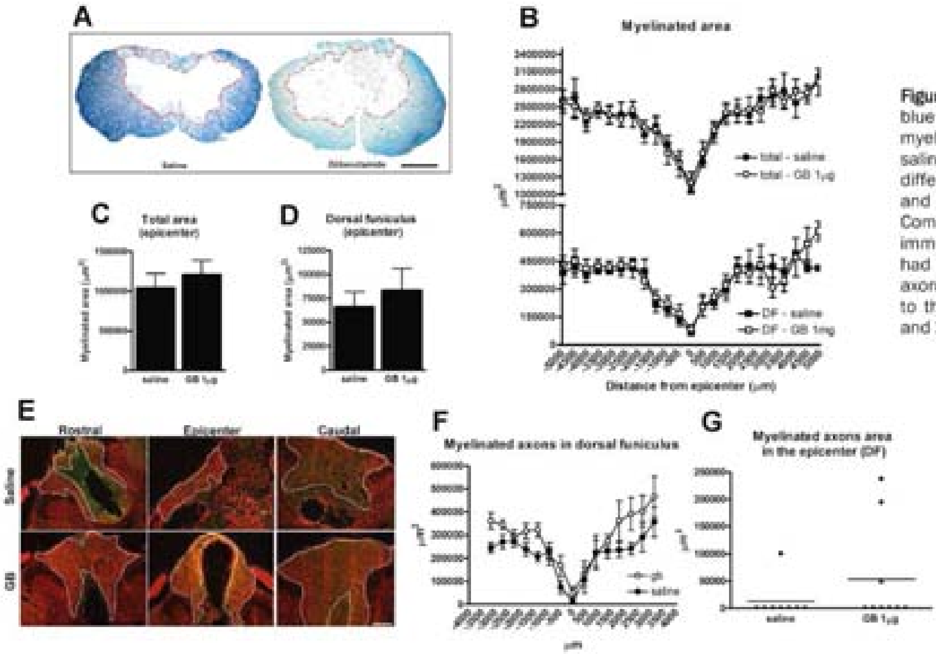

Figure 5. Myelin measurements: Luxol fast blue staining (A) showed similar profile of myelin preservation in groups injected with saline and with GB (B), although slight differences were found at the epicenter (C) and in the dorsal funiculus (D). Combination of neurofilament and MBP immunolabeling (E) revealed that group GB had higher preservation of myelinated axons from 1mm rostral and 1mm caudal to the epicenter (F). Scale bar: 500µ in A and 200µm in E.

RESULTS

Functional results

Voluntary locomotion: Injured rats showed a severe functional deficit during the first days after the injury, with BBB values around 10-11. At the end of the follow-up animals injected with saline injection reached 14 points (consistent coordination and rotated position of the paws), whereas animals treated with glibenclamide had a mean score around 17 points (consistent coordination, parallel position of the paws and toe clearance, Fig. 1A). The differences were statistically significant from day 21 ($p<0.05$).

Beam test: Intact rats displayed very few mistakes when crossing the elevated beam (average 1.3 mistakes in a total of 8-9 steps). After injury, control rats made more footslips than GB rats (2.3 ± 1.0 vs. 1.5 ± 0.9; $p<0.05$) (Fig. 1B).

Inclined plane: In preoperative testing sessions, animals stood in the inclined plane until 55°. After injury, control animals had reduced values (45.54±1.20°), whereas GB animals supported higher angles (48.67 ± 0.77°; $p<0.001$) (Fig. 1C).

Maximum treadmill speed: While intact rats were able to run at speeds up to 80 cm/s (ranging from 75 to 100 cm/s), injured animals maintained running to a mean of 32.5 ± 6.65 cm/s. GB rats showed a lower reduction, being able to run at a mean maximum speed of 50.60 ± 3.62 cm/s, significantly higher than in control injured rats ($p<0.001$) (Fig. 1D).

Neuropathic pain results

Mechanical algesimetry: Preoperative testing gave a mean mechanical threshold value of 14.30 grams (Fig. 2A). The withdrawal threshold was reduced in all the injured animals to 11-12 grams, and only at the end of the follow up the values increased slightly (around 13 g). No significant differences were detected between the two injured groups.

Randall-Selitto test: After spinal cord contusion, the pressure withdrawal threshold lowered by about 20% in dorsal skin and by 10% in plantar skin of both fore and hind paws during the first two weeks, and returned to normal values at later time points (28 and 42 dpo tested). In the GB group the thresholds followed the same tendency but were significantly lower than in control injured rats, more markedly during the first week after the lesion (Fig. 2B). GB treated animals still displayed lower values than control animals at the end of the follow up ($p<0.01$).

Electrophysiology results

Peripheral nerve conduction: The amplitude and the latency of the direct M wave did not change significantly after the spinal cord injury, despite a slight not significant reduction in the TA muscle at 42 dpo (preoperative values: ~56 mV; control group: ~50 mV; GB group ~ 53 mV), thus indicating preservation of the normal peripheral nerve function. Hyperreflexia was measured as the ratio between the M wave amplitude and the H wave amplitude in the plantar muscles (ratio H/M, Fig. 3A-B). Intact animals had a ratio around 0.07, and this value increased in both groups after the injury (0.19 ± 0.04 in control group and 0.21 ± 0.03 in GB group), without significant differences between them.

Central pathways conduction: MEPs were elicited at 1Hz (Fig. 3C) and at 9Hz (Fig. 3D), in order to elicit the brainstem and the cortical components, respectively. The brainstem component averaged around 18mV in amplitude in preoperative tests. It was completely abolished in saline injected animals during the follow up after injury, whereas 2 out of 10 GB treated rats showed partial preservation, with amplitudes about 2 mV ($p<0.05$, Fig. 3F). The cortical component had a mean amplitude around 1.5 mV in preoperative recordings, and fell to 0.78 mV in the control group and 0.86 in the GB group (Fig. 3G). For both MEP components the differences between the two injured groups were statistically significant.

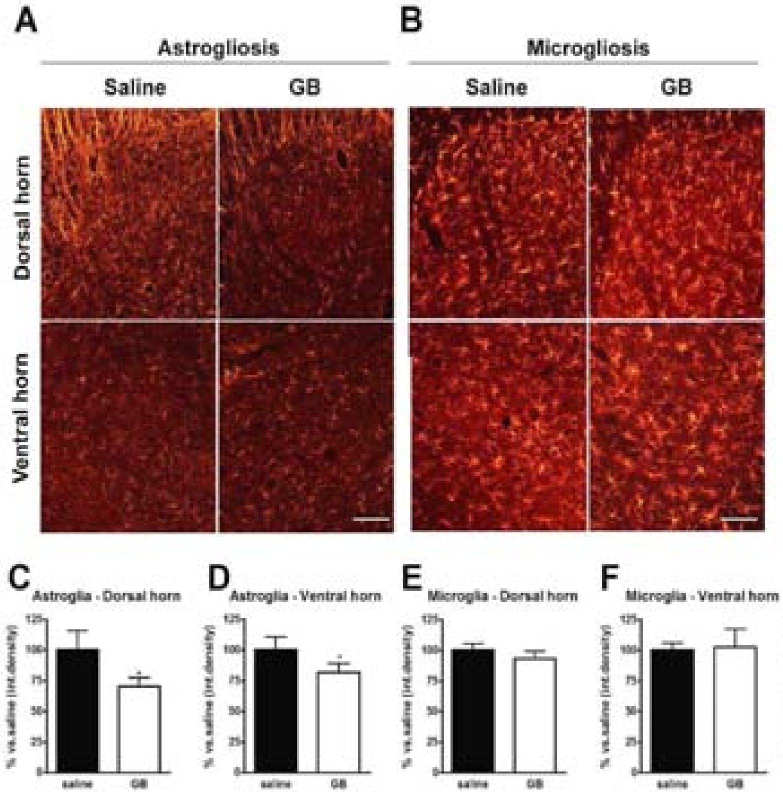

Figure 6. Glial reactivity after spinal cord contusion: Astroglia labeled for GFAP in dorsal and ventral horns (A). Measurements of GFAP integrated density revealed a significant decrease in GB treated animals, in both dorsal (C) and ventral horns (D) compared with the saline injected group. Microglial cells labeled for Iba1 (B) displayed similar levels of immunoreactivity in

Three distinguishable components can be identified in SSEP recordings from uninjured animals, based on the peak latencies. SSEPs were partially or completely abolished after the injury (Fig. 3E), but reappeared during the follow up with smaller amplitude. There were more rats (50%) of the group GB rats showing the three SSEP components at 42 dpo, than in the control group (10%) (Fig 3H).

Histology at the lesion site

Thoracic cord sections were immunostained against GFAP (Fig. 4A) in order to determine the lesion extent. Although without reaching statistical significance, the GB group had slightly more cord tissue spared than the control group (areas in the epicenter: 1.75 ± 0.12 mm^2 in GB group, 1.56 ± 0.09 mm^2 in saline group, Fig. 4B, C).

The number of surviving neurons was counted in the ventral portion of the damaged spinal cord by NeuN immunostaining (Fig. 4D), since the dorsal part was markedly destroyed by the impact. No significant differences were detected between the two groups (Fig. 4E), with the highest loss of neurons found at the epicenter of the lesion in both groups.

Measurements of the area occupied by myelin, stained with LFB, indicated that demyelination was almost complete at the epicenter (Fig.5A), and reached normal levels at 2 mm rostrally and caudally. There were no significant differences between control and GB groups (Fig. 5B), despite a slightly higher myelin area at the epicenter in the GB group (saline: 1.04 ± 0.18 mm^2; GB: 1.21 ± 0.18 mm^2, Fig. 5C). Myelin preservation in the dorsal funiculus was also similar in both groups (saline: 0.06 ± 0.015 mm^2; GB: 0.08 ± 0.022 mm^2, Fig.5D), but again there was a tendency to present more myelination in the GB group, although without reaching statistical significance.

The area occupied by myelinated axons was also quantified in the dorsal funiculus of sections around the injury site (Fig. 5E). The area was considered as occupied by functional axons only if a dense and ordered pattern of neurofilament dots surrounded by MBP layers was detected. There was a severe loss of myelinated axons at the epicenter area (Fig. 5F); in fact, only 1 saline rat and 3 GB rats had preserved measurable tissue in the epicenter (Fig. 5G).

Histology at lumbar segments

GB administration significantly reduced the astrogliosis in the dorsal horn (about 30%) and in the ventral horn (about 20%) of the lumbar cord compared with vehicle administration (Fig. 6A, C, D). In contrast, measurements of microglial reactivity indicated that there were no significant changes in dorsal and ventral horns (Fig. 6B, E, F) between GB and control groups at six weeks postinjury.

Histology at early time

In order to confirm the early effect of GB injection on microglial cells, microgliosis and phagocytosis were assessed in samples harvested at early times after the contusion. Samples at 3 days, but not yet at 1 day, showed a large increase of microglial and macrophagic cells detected in the epicenter. Caudal and rostral regions also displayed reactive microglial cells and macrophages to a minor extent. The cell morphology was rounded in the epicenter, whereas in the surrounding regions microglia were not so rounded with thick prolongations.

Microgliosis was measured as the Iba1 integrated density in the epicenter, rostral and caudal regions (Fig. 7A). Both groups presented similar results for microgliosis, although GB treated animals had slightly, but not significant, lower reactivity (Fig. 7B).

Phagocytosis was assessed by ED1 labeling integrated density (Fig. 7C). At 1 dpo, most of the ED1+ cells were accumulated in the epicenter, with only a few cells detected in the surrounding regions. At 3 dpo, there was a large increase especially in the epicenter area. The integrated density of ED1 was higher in saline injected rats than in GB injected rats in the epicenter, at 3 dpo ($p<0.001$, Fig. 7D).

Microglial reactivity in culture

Microglial cultures were performed in order to confirm the phenotypic changes shown by microglia when activated and when exposed to GB. LPS was used as a well-known activator, and lysate from injured spinal cord as a novel activation method. Resting microglial cells displayed a small and round morphology, with some short and thick prolongations. After addition of LPS to the culture medium, microglia became more flattened and rounded, indicating activation, although some cells maintained an intermediate morphology (round with some processes). The addition of GB after 24h of LPS did not provoke a significant change in morphology but a lower proportion of cells emitted prolongations, suggesting stronger activation. The addition of lysates from injured spinal cords produced a different pattern of activation, with less flattened morphologies but numerous and thicker prolongations as well as a clear increase in the amount of refringent vacuoles. After adding GB vacuolization was more evident, with cells presenting shorter and thicker prolongations (Fig. 8).

In control cultures, ED1, a lysosomal glicoprotein, was widely distributed in the soma, although some surface expression could be detected. Activation with LPS promoted a concentration of the labeling around the nucleus, with light labeling seen in the processes. Similarly, the activation with the spinal cord extract induced an increase of ED1 spread within the cells, indicating an increase of microglia phagocytic activity. The addition of GB to the activated cells accentuated the increase in ED1 expression, especially in the culture activated with the extract (Fig. 8).

DISCUSSION

Initial features occurring after a contusive trauma to the spinal cord include breakdown of the blood brain barrier, rupture of capillaries and necrotic loss of tissue together with the later formation of a cystic cavity limiting the cell death area. Another typical feature of spinal cord injuries is the important inflammatory and gliotic response after the trauma. It is considered that microglia is the first glial population acting in the lesion site. Once activated, microglia releases excitatory amino acids, cytokines and several inflammatory mediators implicated in the induction of secondary cell death and central sensitization of spinal neurons. Moreover, ATP, substance P and glutamate are released in high amounts after the injury, also contributing to central sensitization and participating in microglial activation. Thus, central sensitization further activates microglia, establishing a feedforward cycle of activation and sensitization (Hains and Waxman, 2006). However, microglia do not constitute a unique cell population, but rather, show a range of phenotypes in a dynamic equilibrium with the lesion microenvironment and the evolution of the lesion process (de Yebra et al., 2006). Thus, microglial cells have also important beneficial properties; apart from their essential function as scavengers of myelin and cell debris, they can also exert neuroprotective functions, increasing axonal sprouting, promoting synaptogenesis and neurogenesis, and modulating neuronal activity (Popovich et al., 1997; Cullheim and Thams, 2007; Tanga et al., 2004; Ortega et al., 2012b). Secondary to microglial activation, astrocytes become also reactive and proliferate, limiting the lesion

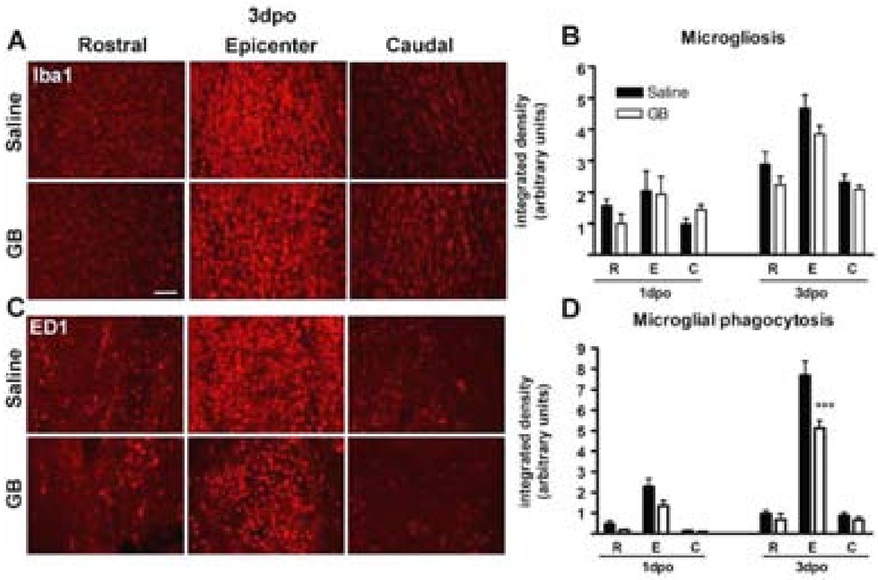

Figure 7. Early time microgliosis: Microglia in rostral regions, epicenter and caudal regions, at 3dpo (A). Results indicate increased reactivity in the injury epicenter. No clear differences were observed when comparing the two groups (B) at 1 and 3dpo. Phagocytic marker ED1 (C) had higher expression in control injured animals than in the GB group. ***, $p<0.001$ vs. saline group. Scale bar: 200μm.

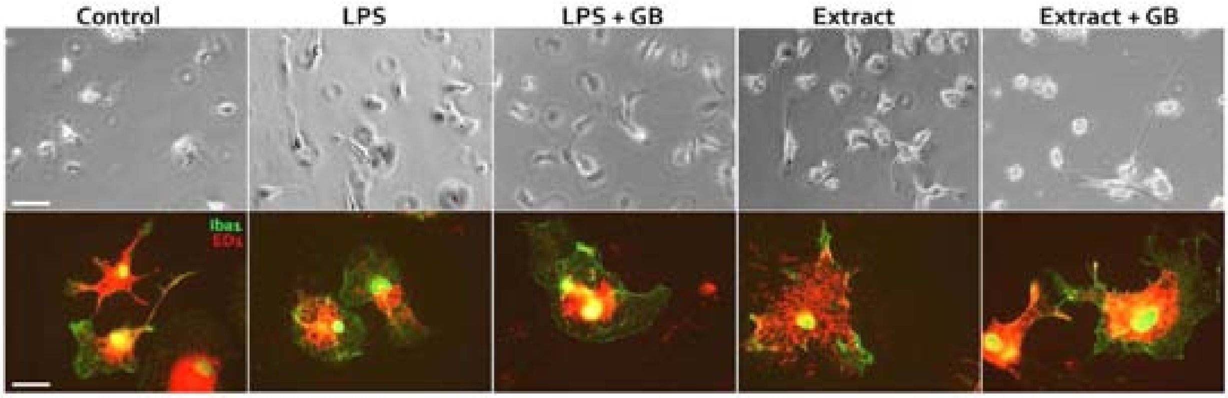

Figure 8. Microglial cell cultures: Representative images of microglial cultures under contrast phase microscopy (scale bar: 200 µm). Note the change in cell morphology after addition of LPS (rounded cells) and of cord injured extract (activated morphology, thick processes and numerous refringent vesicles). Immunofluorescence images highlight differences in the amount and distribution of ED1 protein (in red), indicative of phagocytic phenotype, in microglia (identified by Iba1 labeling in green). Scale bar: 20µm.

area by contributing to the glial scar formation and replacing microglia to sustain synaptic changes promoted by previously activated microglia (Tanga et al., 2004; de Yebra et al., 2006). Despite these beneficial effects, the two glial populations can stay pathologically activated after spinal cord injuries, contributing to perpetuate phenomena such as inhibition of axonal growth, central sensitization and hyperexcitability. For these reasons, modulation of glial actions has become a promising tool to improve the outcome of spinal cord injuries. In this context, our hypothesis was that GB, administered in situ just after the cord contusion, may enhance the initial beneficial effect of microglia after the lesion, and therefore, secondary detrimental events would be reduced, and the chronic deficits may be less severe.

GB binds the sulfonylurea receptor subunits (especially the SUR1 isoform) present in the K^{+}_{ATP} sensitive channel. GB is active at very low doses (EC_{50}=48nM at pH7.4), and its activity increases at slightly acidic pH. Due to its chemical structure, it has limited diffusion and tends to accumulate in acidic tissues, leaving intact tissues unaffected. These two features make GB an interesting drug, since it needs a low dose to be active, and its effect may be limited to the acidified injured tissue in the spinal cord therefore increasing bioavailability (Simard et al., 2008, 2007; Ortega et al., 2012b). GB is a FDA approved drug, currently used for the treatment of diabetes. Nevertheless, according to clinicaltrials.gov, there are a few clinical trials designed to test GB effectiveness in stroke (NCT:01268683, NCT:01132703, NCT: 00700856) and traumatic brain injury (NCT:01132703, NCT:014541542), but none on spinal cord injury.

Our results indicate that a single intraspinal injection of GB is able to induce marked changes in the lesion environment, and improve functional recovery. At the injury site, GB promoted slight sparing of tissue and increase of preserved myelinated axons, although without increasing the number of surviving neurons. In remote regions from the injury site, such as the lumbar segments, there were relevant changes in the glial response promoted by GB injection. At 42 days, microglia appeared with an activated morphology, showing similar immunoreactivity in both saline and GB injected groups. Contrarily, astroglia immunoreactivity was significantly reduced in animals treated with GB. Different explanations may be given for this astroglial effect: the first is that astroglia may be also a GB target (astrocytes also display SUR receptors, but not glucokinase; Ramonet et al., 2004), but further experiments have to be done to address this issue. The second may be related to the replacement of microglia by astroglia in the tissue. It has been reported that GB anticipates the peak of phagocytic activity of microglia in some injury models (Ortega et al., 2012b). Finally, a transient replacement of astrocytes by microglia to facilitate neuroprotection cannot be discarded. This effect has already been observed in the hippocampus after the astroglia removal produced by alpha-aminoadipate microinjection (Rodriguez et al., 2004). Thus, if microglia were more effective in the initial scavenging and phagocytosis, an earlier resolution or reduction of the neuroinflammatory reaction would result in a reduction of chronic astrogliosis. To confirm this point, we analyzed spinal cord tissue harvested at 1 and 3 days after contusion. Microglial reactivity was diminished in GB treated animals especially at 3dpo, and was accompanied by a reduction of the ED1 marker, probably due to a reduction in the infiltration of macrophages. The reduced infiltration in the lesion site must be accompanied with a boost of phagocytic actions of microglia as a result of GB treatments (Ortega et al., 2012b), and result, as a consequence, in a reduction in the inflammatory area.

The *in vitro* model developed by adding an injured spinal cord extract to microglial cultures attempted to mimic the signaling cues present in the *in vivo* cord injury environment. Indeed, LPS and the lesion extract produced different morphological changes indicating different activation profiles. Microglial cells treated with the lysate presented a phagocytic phenotype, with numerous refringent vacuoles and intense ED1 labeling. ED1 is a glycoprotein present in lysosomal membranes and also in the cell surface, in microglia, monocytes and macrophages, related with the expression of a phagocytic phenotype (Damoiseaux et al., 1994; Sanagi et al., 2010). The addition of GB to the culture increased accumulation of vacuoles in microglial cells and also the expression of ED1, confirming the hypothesis that GB enhances microglial activation, but without increasing inflammation in the injury site.

The beneficial effects of GB intraspinal injection were observed in improvements of voluntary locomotion (BBB open field test), as well as in functional tests that require extra skills to the animals, such as inclined plane, walking narrow beam or running at increasing speeds on a treadmill. We hypothesize that GB may exert some effect on the spinal circuitry, the central pattern generators or their connections to higher centers. In fact, activated microglia is known to promote the formation of new synapses as well as remodeling of existing circuits and neurogenesis (Tanga et al., 2004; Cullheim and Thams, 2007; Ortega et al., 2012a). Therefore, by inducing earlier and higher microglial activation GB might promote an increase in synapse strength and enhance spinal excitability (Ostroumov et al., 2007), which would lead to an increase in the volume of information traveling to caudal lumbar segments, resulting in functional improvement after the thoracic spinal cord injury. On the other hand, such increase in the activity of spinal circuits could also lead to increased hyperalgesia in the treated animals, as reflected in the algesimetry tests, since nociceptive information would also be amplified.

In summary, the intraspinal injection of GB resulted in long lasting improvement in motor functional tests, probably coupled to functional preservation of axons along the spinal cord. Unfortunately, animals treated with GB presented more marked hyperalgesia than control injured animals, which might be related to increased excitability in spinal circuits. Therefore, despite the efficacy of GB in terms of functional recovery of locomotion, a better modulation of microglia phenotypes needs to be found in order to avoid the sensory detrimental effects.

Acknowledgements
This work was supported by grants from the Fundació MaratóTV3 (grant 070210), the Ministerio de Ciencia e Innovación (grant SAF2009-12495), the MICINN (grant IPT -010000-2010-35) and the Generalitat de Catalunya (2009SGR1380), and funds from Red de Terapia Celular (TERCEL) of Spain. We thank the technical assistance of Monica Espejo, Jessica Jaramillo and Marta Morell, the help in culture work of Cristina Gutiérrez, the surgical help of Abel Torres-Espín, and the contributions of Dr. Rita Vaz.

Author Disclosure Statement
No competing financial interests exist.

REFERENCES
Abdallah DM, Nassar NN, Abd-El-Salam RM. 2011. Glibenclamide ameliorates ischemia-reperfusion injury via modulating oxidative stress and inflammatory mediators in the rat hippocampus. Brain Res 1385:257–62.
Baastrup C, Finnerup N. 2008. Pharmacological management of neuropathic pain following spinal cord injury. CNS Drugs 22:455–475.
Basso DM, Beattie MS, Bresnahan JC. 1995. A sensitive and reliable locomotor rating scale for open field testing in rats. J Neurotrauma 12:1–21.
Carlton SM, Du J, Tan HY, Nesic O, Hargett GL, Bopp AC, Yamani A, Lin Q, Willis WD, Hulsebosch CE. 2009. Peripheral and central sensitization in remote spinal cord regions contribute to central neuropathic pain after spinal cord injury. Pain 147:265–76.
Casals-Díaz L, Vivó M, Navarro X. 2009. Nociceptive responses and spinal plastic changes of afferent C-fibers in three neuropathic pain models induced by sciatic nerve injury in the rat. Exp Neurol 217:84–95.
Chang Y-W, Waxman SG. 2010. Minocycline attenuates mechanical allodynia and central sensitization following peripheral second-degree burn injury. J Pain 11:1146–54.
Cullheim S, Thams S. 2007. The microglial networks of the brain and their role in neuronal network plasticity after lesion. Brain Res Rev 55:89–96.
Damoiseaux JG, Döpp EA, Calame W, Chao D, MacPherson GG, Dijkstra CD. 1994. Rat macrophage lysosomal membrane antigen recognized by monoclonal antibody ED1. Immunology 83:140–7.
Detloff MR, Fisher LC, McGaughy V, Longbrake EE, Popovich PG, Basso DM. 2008. Remote activation of microglia and pro-inflammatory cytokines predict the onset and severity of below-level neuropathic pain after spinal cord injury in rats. Exp Neurol 212:337–47.
De Yebra L, Malpesa Y, Ursu G, Pugliese M, Lievens J, Kerkerian-Legoff L, Mahy N. 2006. Dissociation between hippocampal neuronal loss, astroglial and microglial reactivity after pharmacologically induced reverse glutamate transport. Neurochem Int 49:691–697.
Finnerup NB, Sindrup SH, Jensen TS. 2007. Chronic neuropathic pain: mechanisms, drug targets and measurement. Fundam Clin Pharmacol 21:129–36.
García-Alías G, Torres-Espín A, Vallejo C, Navarro X. 2010. Functional involvement of the lumbar spinal cord after contusion to T8 spinal segment of the rat. Restor Neurol Neurosci 28:781–92.
García-Alías G, Valero-Cabré A, López-Vales R, Forés J, Verdú E, Navarro X. 2006. Differential motor and electrophysiological outcome in rats with mid-thoracic or high lumbar incomplete spinal cord injuries. Brain Res 1108:195–204.
Gwak YS, Hulsebosch CE. 2009. Remote astrocytic and microglial activation modulates neuronal hyperexcitability and below-level neuropathic pain after spinal injury in rat. Neuroscience 161:895–903.
Gwak YS, Kang J, Unabia GC, Hulsebosch CE. 2012. Spatial and temporal activation of spinal glial cells: Role of gliopathy in central neuropathic pain following spinal cord injury in rats. Exp Neurol 234:362–72.
Hains BC, Waxman SG. 2006. Activated microglia contribute to the maintenance of chronic pain after spinal cord injury. J Neurosci 26:4308–17.
Hulsebosch CE. 2008. Gliopathy ensures persistent inflammation and chronic pain after spinal cord injury. Exp Neurol 214:6–9.
Inoue K, Tsuda M. 2009. Microglia and neuropathic pain. Glia 57:1469–79.
Ledeboer A, Sloane EM, Milligan ED, Frank MG, Mahony JH, Maier SF, Watkins LR. 2005. Minocycline attenuates mechanical allodynia and proinflammatory cytokine expression in rat models of pain facilitation. Pain 115:71–83.
Milligan ED, Watkins LR. 2009. Pathological and protective roles of glia in chronic pain. Nat Rev Neurosci 10:23–36.
Nie H, Zhang H, Weng HR. 2010. Minocycline prevents impaired glial glutamate uptake in the spinal sensory synapses of neuropathic rats. Neuroscience 170:901–12.
Ortega FJ, Jolkkonen J, Mahy N, Rodriguez M. 2012a. Glibenclamide enhances neurogenesis and improves long-term functional recovery after transient focal cerebral ischemia. J Cereb Blood Flow Metab. doi: 10.1038/jcbfm.2012.166. [Epub ahead of print].
Ortega FJ, Gimeno-Bayon J, Espinosa-Parrilla JF, Carrasco JL, Batlle M, Pugliese M, Mahy N, Rodríguez MJ. 2012b. ATP-dependent potassium channel blockade strengthens microglial neuroprotection after hypoxia-ischemia in rats. Exp Neurol 235:282–96.
Ostroumov K, Grandolfo M, Nistri A. 2007. The effects induced by the sulphonylurea glibenclamide on the neonatal rat spinal cord indicate a novel mechanism to control neuronal excitability and inhibitory neurotransmission. Br J Pharmacol 150:47–57.
Pompermayer K, Amaral F, Fagundes C, Vieira A, Cunha F, Teixeira M, Souza D. 2007. Effects of the treatment with glibenclamide, an ATP-sensitive potassium channel blocker, on intestinal ischemia and reperfusion injury. Eur J Pharmacol 556:215–222.
Popovich PG, Lemeshow S, Gensel JC, Tovar CA. 2012. Independent evaluation of the effects of glibenclamide on reducing progressive hemorrhagic necrosis after cervical spinal cord injury. Exp Neurol 233:615–22.
Popovich PG, Wei P, Stokes BT. 1997. Cellular inflammatory response after spinal cord injury in Sprague-Dawley and Lewis rats. J Comp Neurol 464:443–464.
Ramonet D, Rodriguez M, Pugliese M, Mahy N. 2004. ATP-sensitive potassium channels and glucokinase colocalize in activated microglia. Neurobiol Dis 17:1–9.
Rodriguez M, Martinez-Sánchez M, Bernal F, Mahy N. 2004. Heterogeneity between hippocampal and septal astroglia as a contributing factor to differential in vivo AMPA excitotoxicity. J Neurosci Res 77:344–353.

Sanagi T, Yuasa S, Nakamura Y, Suzuki E, Aoki M, Warita H, Itoyama Y, Uchino S, Kohsaka S, Ohsawa K. 2010. Appearance of phagocytic microglia adjacent to motoneurons in spinal cord tissue from a presymptomatic transgenic rat model of amyotrophic lateral sclerosis. J Neurosci Res 88:2736–46.

Santos-Nogueira E, Redondo-Castro E, Mancuso R, Navarro X 2011. Randall-Selitto Test: A new approach for the detection of neuropathic pain after spinal cord injury. J Neurotrauma 8:1–8.

Scholz J, Woolf CJ. 2007. The neuropathic pain triad: neurons, immune cells and glia. Nat Neurosci 10:1361–8.

Servitja JM, Masgrau R, Pardo R, Sarri E, Picatoste F. 2000. Effects of oxidative stress on phospholipid signaling in rat cultured astrocytes and brain slices. J Neurochem 75:788–94.

Da Silva-Santos J, Santos-Silva M, Cunha F, Assreuy J. 2002. The role of ATP-sensitive potassium channels in neutrophil migration and plasma exudation. J Pharmacol Exp Ther 300:946–951.

Simard JM, Chen M, Tarasov K, Bhatta S, Ivanova S, Melnitchenko L, Tsymbalyuk N, West G, Gerzanich V. 2006. Newly expressed SUR1-regulated NCCa-ATP channel mediates cerebral edema after ischemic stroke. Nat Med 12:433–440.

Simard JM, Tsymbalyuk O, Ivanov A, Ivanova S, Bhatta S, Geng Z, Woo SK, Gerzanich V. 2007. Endothelial sulfonylurea receptor 1 – regulated NC Ca-ATP channels mediate progressive hemorrhagic necrosis following spinal cord injury. J Clin Invest 117:2105–2113.

Simard JM, Woo SK, Bhatta S, Gerzanich V. 2008. Drugs acting on SUR1 to treat CNS ischemia and trauma. Curr Opin Pharmacol 8:42–9.

Simard JM, Yurovsky V, Tsymbalyuk N, Melnitchenko L, Ivanova S, Gerzanich V. 2009. Protective effect of delayed treatment with low-dose glibenclamide in three models of ischemic stroke. Stroke 40:604–609.

Sun X-L, Hu G. 2010. ATP-sensitive potassium channels: a promising target for protecting neurovascular unit function in stroke. Clin Exp Pharmacol Physiol 37:243–252.

Sweitzer SM, Schubert P, DeLeo JA. 2001. Propentofylline, a glial modulating agent, exhibits antiallodynic properties in a rat model of neuropathic pain. J Pharmacol Exp Ther 297:1210–7.

Tanga FY, Raghavendra V, DeLeo JA. 2004. Quantitative real-time RT-PCR assessment of spinal microglial and astrocytic activation markers in a rat model of neuropathic pain. Neurochem Int 45:397–407.

Tsuda M, Inoue K, Salter MW. 2005. Neuropathic pain and spinal microglia: a big problem from molecules in "small" glia. Trends Neurosci 28:101–7.

Valero-Cabré A, Forés J, Navarro X. 2004. Reorganization of reflex responses mediated by different afferent sensory fibers after spinal cord transection. J Neurophysiol 91:2838–48.

Vallejo R, Tilley DM, Vogel L, Benyamin R. 2010. The role of glia and the immune system in the development and maintenance of neuropathic pain. Pain Pract 10:167–84.

Virgili N, Espinosa-Parrilla J, Mancera P, Pastén-Zamorano A, Gimeno-Bayon J, Rodríguez MJ, Mahy N, Pugliese M. 2011. Oral administration of the K_{ATP} channel opener diazoxide ameliorates disease progression in a murine model of multiple sclerosis. J Neuroinflammation 8:149.

Watkins LR, Milligan ED, Maier SF. 2001. Glial activation: a driving force for pathological pain. Trends Neurosci 24:450–5.

Zarch A, Toroudi H, Soleimani M, Kateor M, Djahanguiri B. 2009. Neuroprotective effects of diazoxide and its antagonism by glibenclamide in pyramidal neurons of rat hippocampus subjected to ischemia-reperfusion-induced injury. Int J Neurosci 119:1346–61.

Zhao P, Waxman SG, Hains BC. 2007. Modulation of thalamic nociceptive processing after spinal cord injury through remote activation of thalamic microglia by cysteine cysteine chemokine ligand 21. J Neurosci 27:8893–902.

Publication

Positive and negative effects of ibuprofen treatment after spinal cord injury: especial focus on microglia

E.Redondo Castro, X.Navarro

Ready to be submitted

Positive and negative effects of ibuprofen treatment after spinal cord injury: especial focus on microglia

Elena Redondo-Castro, Xavier Navarro.

Group of Neuroplasticity and Regeneration, Institute of Neurosciences and Department of Cell Biology, Physiology and Immunology, Universitat Autònoma de Barcelona, and Centro de Investigación Biomédica en Red sobre Enfermedades Neurodegenerativas (CIBERNED), Bellaterra, Spain.

Corresponding author: Dr. Xavier Navarro, Unitat de Fisiologia Mèdica, Edif. M, Universitat Autònoma de Barcelona, E-08193 Bellaterra, Spain.
Tel: +34-935811966, Fax: +34-935812986, E-mail: xavier.navarro@uab.cat

ABSTRACT

Ibuprofen is commonly used as anti-inflammatory, analgesic and antipyretic drug, due to its high efficacy and few side effects. Its main effects are mediated by the non-specific inhibition of COX enzymes, but it can also exert some COX-independent effects, such as the inhibition of the RhoA signaling and the modulation of glial activity. These other effects have boosted the use of ibuprofen as a tool to promote axonal regeneration after neural injuries, as well as to increase functional recovery, with controversial results showing positive and negative outcomes of ibuprofen treatment in several experimental models. We have evaluated the effects of ibuprofen administered at 60mg/kg twice a day to rats subjected to a mild spinal cord contusion. Our results indicate that ibuprofen is highly effective reducing mechanical hyperalgesia in rats, but failed to produce locomotion and electrophysiological improvements. Such effects may be explained because ibuprofen reduces the phagocytic activity of microglia after the injury, when this action is essential to remove dead cell and myelin debris secondary to the trauma. These results highlight the importance to have into account the multiple activities of single drugs as well as the design of the treatment, in order to avoid unexpected detrimental effects.

Keywords: ibuprofen, neuropathic pain, spinal cord injury, microglia, functional recovery.
Running title: Ibuprofen after SCI

INTRODUCTION

Ibuprofen (2-(4-isobutylphenyl propionic acid)) is a non steroidal anti-inflammatory drug broadly used as anti-inflammatory, analgesic and antipyretic, because of its effectivity and few side effects (Adatia et al., 2012). Ibuprofen can exert actions on multiple cell targets in the central nervous system, such as astroglia, microglia and neurons. Regarding the molecular targets, the main actions are the inhibition of RhoA signaling and the unspecific inhibition of COX enzyme (Fu et al., 2007; Xing et al., 2011). The RhoA signaling pathway is important in regeneration, since its activation leads to axonal growth collapse and restriction of axonal growth as well as to neurite growth inhibition (Xing et al., 2011). Inhibition of RhoA signaling has been proposed as a mechanism contributing to functional recovery after different neural injuries (Dergham et al., 2002; Hiraga et al., 2006; Kubo et al., 2007). Ibuprofen can also exert some COX-independent effects, such as the inhibition of neutrophil attraction and activation, and the disruption of G protein activity, thereby altering several signaling processes (Adatia et al., 2012).

Despite not being a first-line drug for the treatment of neuropathic pain, several authors have reported beneficial effects of the use of ibuprofen, a drug with a short half-life but long lasting effects (Adatia et al., 2012). Among them, some highlight its powerful analgesic effects (Guindon and Beaulieu, 2006; Ortega-Álvaro et al., 2012), and others have also reported positive effects after spinal cord injury (SCI), such as enhanced tissue preservation and regeneration of descending serotoninergic and corticospinal fibers, leading to functional improvements (Dergham et al., 2002; Fu et al., 2007; Wang et al., 2009; Kopp et al., 2012). Ibuprofen has also been tested in other models with different results: positive results were achieved in stroke and ischemia models (Park et al., 2005) and in Alzheimer disease models (Blasko et al., 2001), but negative outcomes were detected in traumatic brain injury models (Browne et al., 2006).

In this work we assessed if administration of ibuprofen after a mild thoracic spinal cord contusion in rats was able to reduce neuropathic pain signs and to promote functional recovery. Our results confirm the analgesic efficacy of ibuprofen, although functional improvements were not

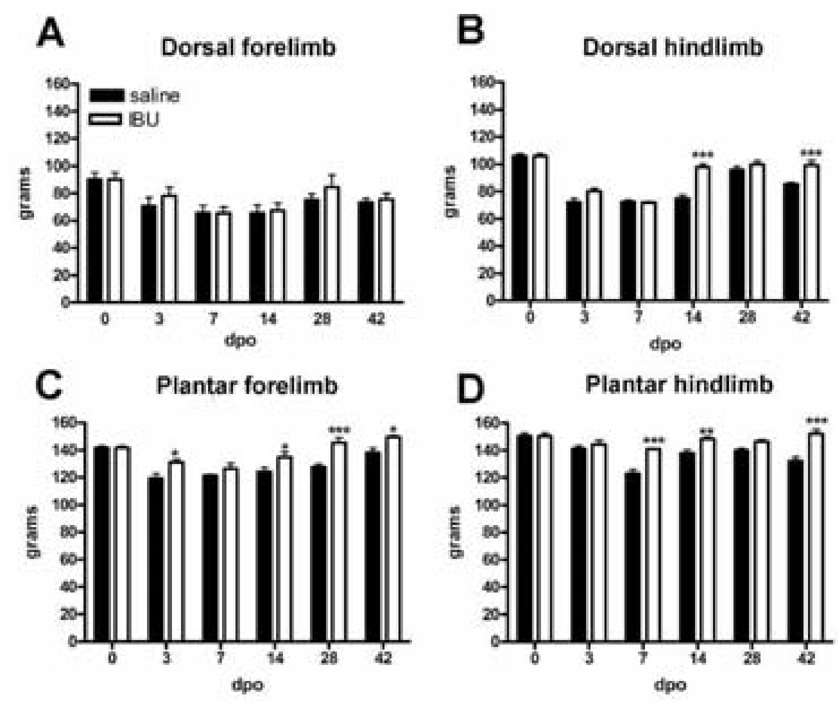

*Figure 1. Neuropathic pain. Randall-Selitto test results revealed a significant reduction of mechanical hyperalgesia in ibuprofen treated animals. dpo: days post operation. * p<0.05; ** p<0.01; *** p<0.001 vs. saline group.*

observed. We hypothesize that ibuprofen may have different effects on astroglia and microglia, that would explain the absence of functional and histological improvements but the amelioration of pain.

MATERIALS AND METHODS

Laboratory animals

Adult female Sprague Dawley rats (8 weeks old; 250-300 grams) were housed with free access to food and water at room temperature of 22±2°C under a 12:12 light-dark cycles. All experimental procedures were approved by the Ethics Committee of our institution, and followed the European Communities Council Directive 86/609/EEC. Researchers testing the animals were blinded regarding the treatments received.

Surgical procedures

Rats were operated under ketamine/xylacine anesthesia (90/10 mg/kg i.p.), and after subcutaneous injection of buprenorphine (0.05 mg/kg) at the incision site. In two groups of rats, the spinal cord was contused at T8 vertebral level after T8-T9 dorsal laminectomy, by using the Infinite Horizon impactor device (Precision Scientific Instruments, Lexington, UK). The force applied was 100 kilodynes, and data of displacement and force applied was recorded for each contusion. After the lesion, the muscular plane was sutured with 5/0 silk and the skin closed with small surgical clips and disinfected with povidone iodine solution. Animals were randomly divided in two experimental groups of 8 rats each: IBU group (administered ibuprofen, Sigma Aldrich, 60 mg/kg s.c. twice daily, starting 30 minutes after the SCI), and control group (received saline solution following the same administration time and volume). Animals were kept in a warm environment until full recovery from anesthesia. Bladders were expressed twice a day until the animals regained reflex voiding of the bladder. Amoxicillin was given in the drinking water for 1 week to prevent postoperative infections. No additional analgesics were administered after the surgery.

Functional evaluation

Neuropathic pain: the Randall Selitto test for mechanical hyperalgesia (IITC 2500 Digital Paw Pressure Meter, IITC Life Science, Woodland Hills, CA) was performed in all the animals before the surgery and at 3, 7, 14, 28 and 42 days after the SCI. Before the test, each animal received 5 min of handling to get used to manipulation; then it was placed into a soft cotton cloth and carefully immobilized. The tip of the device was applied onto the medial portion of the plantar or the dorsal surfaces of both fore and hind paws inducing an increasing mechanical force until a withdrawal response resulted (Santos-Nogueira et al., 2012). The maximum force applied was limited to 250g to avoid skin damage.

Voluntary locomotion: Locomotor hind limb function was assessed using the Basso, Beattie and Bresnahan (BBB) rating scale (Basso et al., 1995). Briefly, the BBB scale consists of an ordinal scale from 0 points (no discernable hindlimb movement) to 21 points (consistent, coordinated gait with parallel paw placement of the hindlimb and consistent trunk stability). One rat at a time was allowed to move freely inside a circular plastic tray (90 cm diameter x 24 cm wall height) for 5 minutes, and two examiners observed the hindlimbs movements of the rat. The score of each animal was the mean value of both examiners. Locomotion was tested weekly during the follow-up.

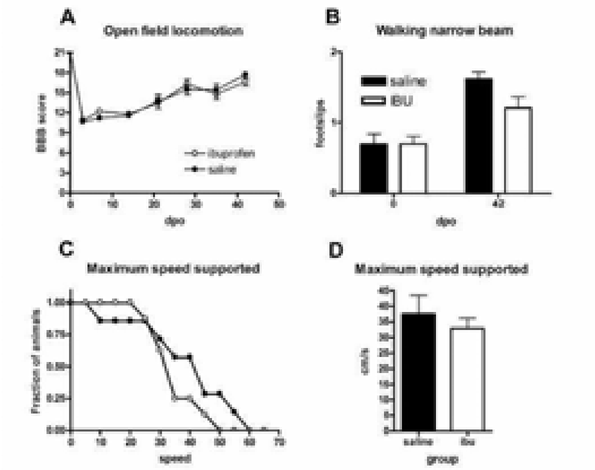

Figure 2. *Functional results. Results from functional tests indicate that the outcome is similar for both groups in the open field locomotion test (A) and the walking narrow beam test (B). The maximum speed supported in a treadmill was slightly lower in the ibuprofen group, although without significant differences (C-D).*

Narrow beam test: It is used to assess fine locomotor coordination. Animals had to walk inside a dark tunnel (7 cm width, 13 cm height, 40 cm length) along an elevated beam (2.5 cm width, 2 cm height, 2 mm separated from the ground to place a paper sheet). The hindpaw plantar surfaces were inked and the rats were allowed to walk along the beam, so the missteps were recorded with ink in the paper sheet placed under the beam. Three runs were performed, and only the left and right missteps done in the first 30 cm were counted in each run. The mean of these values were considered as the final result for each testing day.

Treadmill running: The animals were acclimated to the belt compartment of a DigiGait system (Mouse Specifics Inc., Boston, MA) for some minutes before starting the test. The treadmill speed was progressively increased to force the rat to walk, with some resting periods between trials. The maximum speed supported was recorded from 3-4 trials for each animal, preoperatively and at the end of the follow-up period.

Electrophysiological tests

Animals were anesthetized with pentobarbital (30 mg/kg, i.p.) and placed prone over a warmed flat coil controlled by a hot water circulating pump to maintain body temperature. Electrophysiological tests were performed preoperatively and at the end of the follow-up period.

Peripheral nerve conduction tests: Single electrical pulses (100 µs) were delivered by monopolar needles inserted at the sciatic notch at increasing intensity until the maximal amplitude of the response was reached. The compound muscle action potentials (CMAP) were recorded from the tibialis anterior and the interossei plantar muscles, by means of an active electrode inserted on the belly of the muscle and the reference electrode at the fourth toe (Valero-Cabré et al., 2004). Values from both hindlimbs of each animal were averaged. The latency and the amplitude of the direct muscle response (M wave) and the monosynaptic reflex response (H wave) were measured. The potentials with the highest amplitude were selected and used for analysis.

Motor evoked potentials (MEPs): They were elicited by transcranial electrical stimulation, using two needle electrodes placed subcutaneously over the skull, the anode over the sensorimotor cortex and the cathode at the hard palate, and recorded from the tibialis anterior muscle (García-Alías et al., 2006). Single pulses of 25 mA and 100 µs duration were delivered at 1 or 9 Hz, the adequate pulse rates for eliciting the brainstem component (bs-MEP) and the cortical component (c-MEP), respectively. The muscle responses were displayed in the oscilloscope to measure the amplitude and latency of each component.

Somatosensory evoked potentials (SSEPs): They were evoked by electrical stimuli of 6 mA and 100 µs delivered at

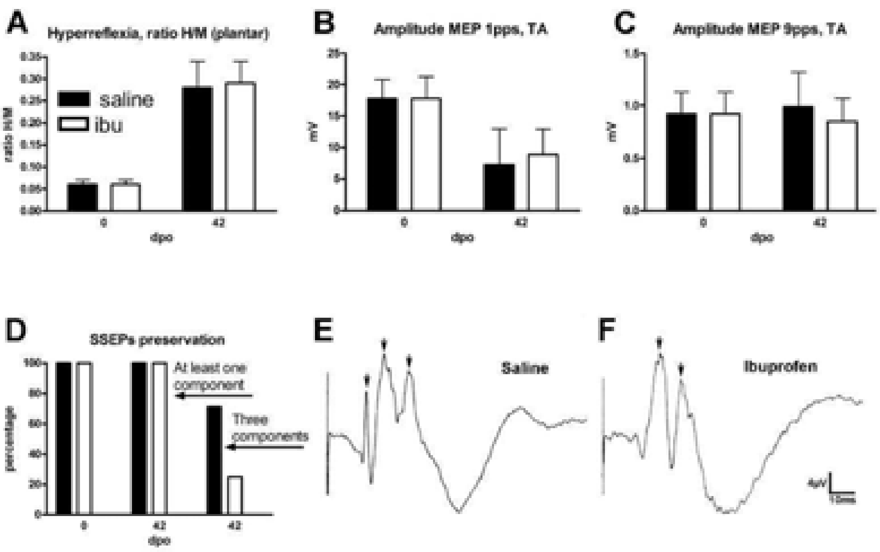

Figure 3. *Electrophysiology. Hyperreflexia measured as the H/M ratio was similarly increased in the two groups after spinal cord injury (A). The bs-MEP amplitude (B) was reduced at 6 weeks, but the c-MEP amplitude was similar to controls in both groups (C). A higher proportion of saline treated rats had the three components of the SSEPs preserved than the ibuprofen treated rats (D). Representative recordings of SSEPs are shown in E and F. dpo: days post operation.*

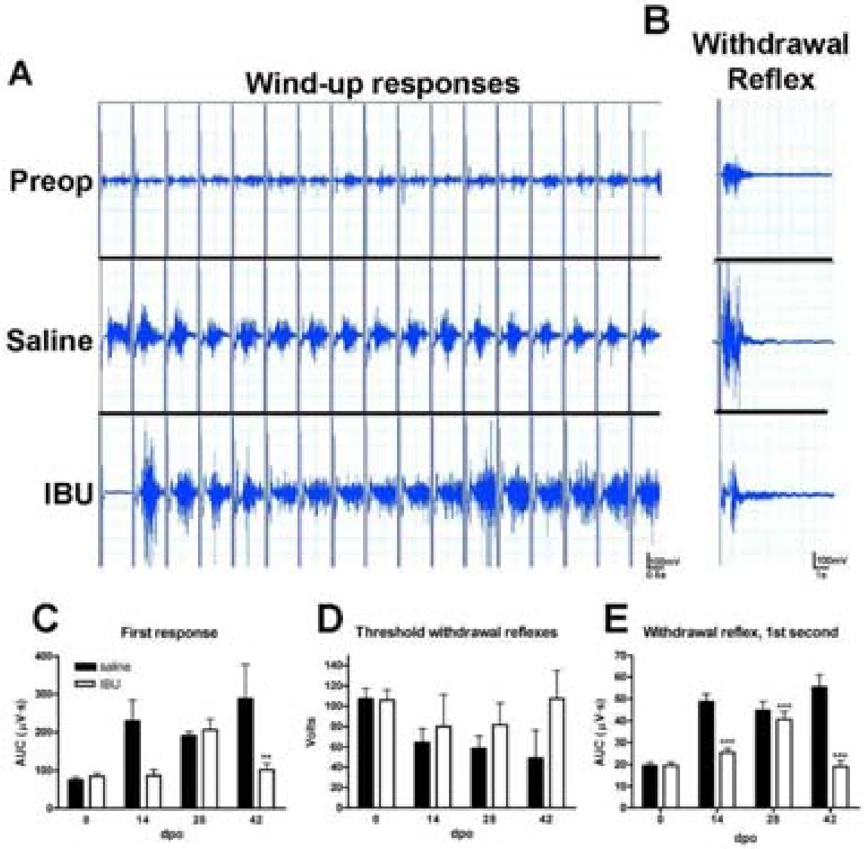

Figure 4. *Spinal reflexes. Representative recordings of wind-up responses (A) and of withdrawal reflexes (B) in intact rats and in rats subjected to spinal cord contusion and treated with saline or ibuprofen. The intensity of the first response of wind-up recordings tended to be lower in ibuprofen than in saline group (C), indicating reduced central basal hyperexcitability. The withdrawal spinal reflexes were evoked at higher threshold (D) and presented lower activity during the first second of the response (E) in the ibuprofen group compared to the saline group. ** p<0.01; *** p<0.001 vs. saline group.*

6 Hz to the tibial nerve at the ankle, and recorded by needle electrodes placed subcutaneously on the skull. Up to 256 responses were averaged on-line; the peak latency and the peak-to-peak amplitude were measured for N15, N20 and N30 waves (Valero-Cabré et al., 2004), referred here as N1, N2 and N3 components. SSEPs were repeated three times with minutes between trials, and the responses with the highest amplitude were selected and used for analysis.

Wind-up and withdrawal reflexes: Spinal reflexes were measured by delivering single stimuli (50mA, 1ms) by means of monopolar needle electrodes, the cathode inserted near the medial plantar nerve in the right paw, and the anode between the fourth and fifth toes of the same paw. The active recording needle electrode was placed in the tibialis anterior muscle, the reference electrode at the ankle, and a ground electrode at the base of the tail. In each session, withdrawal reflexes were first assessed by delivering single pulses (Valero-Cabré et al., 2004). Then, wind-up responses were obtained by applying a train of 16 stimuli at 1Hz and intensity ~0.7x threshold. Electromyographic responses were recorded and analyzed to measure the area under the curve (AUC) of each response, using Chart software and the RMS and Noise extension (ADInstruments) that determines the power content of a signal. Measurements of the AUC of the C-fiber mediated response during the first second were made to assess the intensity of the withdrawal reflex responses. Similarly, wind-up responses were measured and results expressed as the AUC of the first response (Valero-Cabré et al., 2004; Redondo-Castro et al., 2011).

Histological studies

Transcardiac perfusion with 4% paraformaldehyde in phosphate-buffered saline was carried out in anesthetized rats at 42 days after SCI. T7-T10 and L1-L6 spinal cord segments were removed, post-fixed overnight and cryoprotected in 30% sucrose.

The thoracic spinal cord segments were embedded in TissueTek and serially cut (30 µm thickness) in the transverse plane in a cryostat. Sections were immunostained with primary antibodies against glial fibrillary acidic protein (GFAP, 1:1000, Sigma-Aldrich) to visualize the cavity formed around the lesion, and NeuN (1:200, Millipore) to detect the neuronal nuclei. Conventional Luxol Fast Blue (LFB) staining was used to visualize myelin in samples from the lesion site. Sections 30µm thick and separated from the next 450µm were used to measure the total myelinated area as well as the myelination of the dorsal funiculus. In order to discard non functional myelin, additional measurements were done on sections immunolabeled against myelin basic protein (MBP, 1:50, Ultraclone) and neurofilament (NF, 1:200, Millipore). This combined labeling permits to differentiate functional fibers as a dot of neurofilament surrounded by MBP labelling, forming a dense and organized pattern.

Lumbar segments L4-L5 were embedded, cut at 20 µm thickness, and subjected to immunohistochemical detection of different proteins. Glial reactivity was assessed using antibodies for GFAP and Iba1 (1:1000, Wako). Measurements of integrated density were done using a ROI (region of interest) placed in the dorsal horn, and comprising the medial part of laminae I to IV. In ventral horn measurements, a ROI was placed around lamina IX. Cy3 conjugated secondary antibodies were used for single

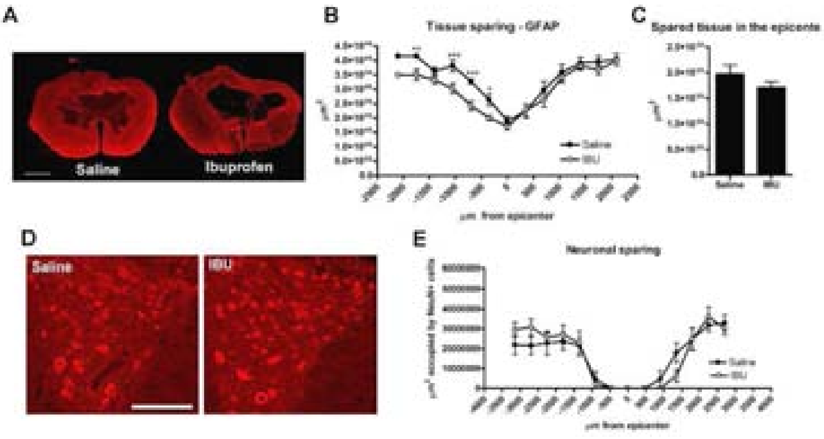

*Figure 5. Tissue and neuronal sparing. Sections of the injury site, stained for GFAP (A), showed a large central cavity and destruction of the dorsal half of the spinal cord. Measurements of the spared tissue revealed higher loss of tissue in the rostral areas of the injury in the ibuprofen than in the saline injected group (B), as well as in the epicenter (C). Images of ventral horns stained for NeuN to label surviving neurons (D). There were no significant differences in neuronal loss between the two groups (E). * p<0.05; ** p<0.01; *** p<0.001 vs. saline vs. ibuprofen group. Scale bar: 500µm in A, 200µm in D.*

immunohistochemistry (Jackson Immunoresearch, UK; dilution 1:200), and Alexa Fluor secondary antibodies for double immunohistochemistry. Five sections from each animal were used in all measurements, expressed as the percentage with respect to the integrated density measured in the saline group.

An additional batch of animals was injured (100kdyn lesion, n=3 per group) and sacrificed at 3 days in order to see the effects of ibuprofen administration at an early time. Injured segments were harvested after perfusion, cut longitudinally at 30 µm thickness, and immunolabeled against Iba1 (1:1000). ROIs for analysis were placed in the lesion epicenter and in regions rostral and caudal to the epicenter.

Microglial cell culture

Glial cell cultures were prepared from 1 day-old Sprague Dawley rats as previously described (Servitja et al., 2000). Rats were decapitated and cortices immediately dissected out. Meninges and blood vessels were removed, and the tissue was minced and incubated for 10 min at 37°C in Ca^{2+}-free Krebs-Ringer buffer containing 0.0025% trypsin. Cells were then mechanically triturated with a glass pipette and filtered through a 40-µm nylon mesh in the presence of 0.52 mg/ml soybean trypsin inhibitor and 170 IU/ml DNAse. After centrifugation (500g), the cells were stained with Trypan Blue exclusion dye, counted in a Neubauer chamber, and then resuspended (300,000 cells/ml) in 90% DMEM, 10% FBS, 20 U/ml penicillin and 20 mg/ml streptomycin. Cells were incubated at 37°C in a humidified atmosphere of 5% CO_2 and 95% air and used after 9-11 days in vitro; media was replaced every 5-7 days. Microglial cells were obtained by shaking the flasks during 3-4 hours at 300 rpm. Floating cells were pelleted and subcultured at 100,000 cells/ml on mixed glial-conditioned medium.

LPS (10ng/ml) or a spinal cord lesion extract (100µg protein/ml) were added in order to activate microglial cells. In both cases, ibuprofen (200mM) was added 24 hours later. Lesion extracts were obtained from injured spinal cords harvested 7 days after a 100kdyn contusion. Samples were rinsed with liquid nitrogen while being mechanically triturated. Then the frozen particles were resuspended in DMEM supplemented with a diluted cocktail of protease inhibitors (1/1000) and disgregated again. Finally samples were sonicated for 5 minutes and centrifuged (15000 rcf, 5 minutes). Protein content was measured by the BCA method.

Cells were fixed with 4% paraformaldehyde (25 min, room temperature). Samples were subjected to immunocytochemistry to detect Iba1 (1:500) and ED1 proteins (1:200, Serotec), used as a markers of microglia and phagocytic activity, respectively.

Data analysis

Data are shown as the mean ± SEM. Statistical comparisons between groups were made using two way ANOVA for repeated measures with Bonferroni *post hoc* tests or t-tests analyses (GraphPad Prism software). Differences between groups were considered statistically significant if $p<0.05$.

RESULTS

Neuropathic pain: mechanical hyperalgesia

Hyperalgesia to mechanical stimulus was tested in plantar and dorsal surfaces of hindpaws and forepaws. In dorsal forepaws (Fig. 1A) there was a general decrease of thresholds in both groups, with no difference between them. Contrarily, measurements in the dorsal surface of hindlimbs evidenced a reversion of the hyperalgesia in the ibuprofen treated group, starting at 14 days and maintained until the end of the follow-up period (Fig. 1B). Tests on plantar surfaces showed that ibuprofen reduced the hyperalgesia in both forelimbs and hindlimbs (Fig. 1C, D). This effect was especially evident in the hindpaws, since thresholds remained similar to preoperative values during all the follow-up period, being significantly higher than in the control injured group at several time points.

Recovery of locomotion

Scores obtained in the open field locomotion test did not differ between the two injured groups during the follow up (Fig. 2A). In the walking narrow beam test group IBU showed a slight reduction in the number of footslips, although without reaching statistical significance (Fig. 2B). In contrary, IBU treated animals had slightly worse results in the

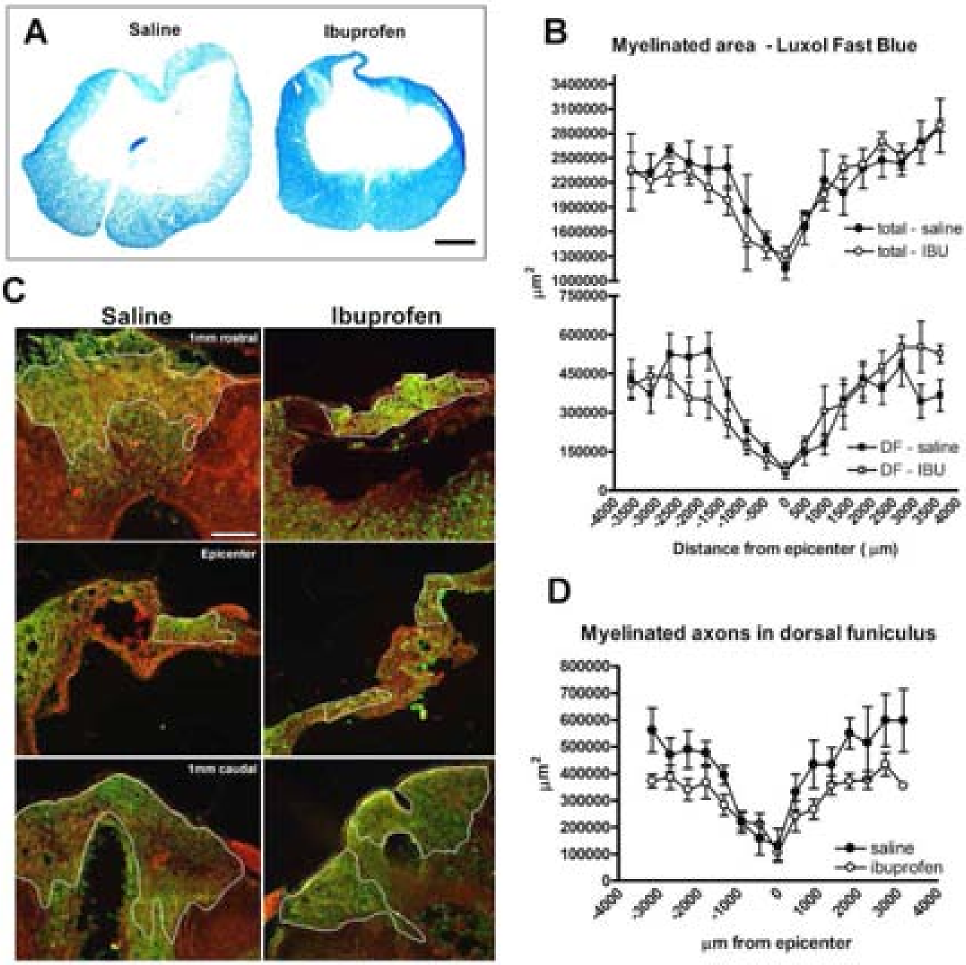

Figure 6. Myelination. Representative images of the spinal cord injured epicenter stained with Luxol Fast Blue (A). Measurements in the whole injury sections and in the dorsal funiculus (DF) indicated a similar loss of myelinated tissue in the two injured groups (B). Representative images (C) from 1mm rostral, epicentar and 1mm caudal cord sections immunostained for neurofilament and MBP, with white lines indicating the area with an organizated pattern of myelinated fibers. Myelinated axons were slightly more spared in the saline group than in the ibuprofen group (D). Scale bar: 500μm in A and 200μm in C.

maximum speed supported on the treadmill (Fig. 2C,D). Gait parameters were also measured and did not display any significant difference between the two injured groups (data not shown).

Electrophysiological results: Modulation of spinal reflexes

Hyperreflexia, measured as the ratio between the M wave amplitude and the H wave amplitude (ratio H/M, Fig. 3A) was similarly increased in both groups (~0.05 in preoperative values, ~0.3 in both treated groups).

The brainstem MEPs, evoked at 1Hz stimulation, were reduced in amplitude in both groups (intact rats: ~18mV, saline: ~7.3mV, ibuprofen: ~8.9mV; Fig. 3B), and present in a similar proportion of rats in both groups (25-30%). The cortical MEPs, evoked at 9Hz stimulation, were recorded with similar amplitudes (Fig. 3C), and in the same proportion of animals in both groups (~75-85%). Regarding SSEPs, the saline group had a higher proportion of animals with the three components recorded (~70%) than the ibuprofen treated group (25%) (Fig. 3 D-H).

Wind-up responses were increased after spinal cord contusion compared to intact animals (Fig. 4A). The first response, indicative of basal excitability, was more markedly increased in saline rats than in ibuprofen treated rats (Fig. 4C). This difference was more obvious at the end of the follow-up period, when ibuprofen animals had a first response similar to preoperative values and significantly lower than saline animals ($p<0.01$). Wind-up responses were similar in saline and IBU groups (quantification not shown).

Ibuprofen treated rats had a higher threshold to evoke the withdrawal reflexes than control injured rats, indicating lower excitability (Fig. 4D). In addition, the withdrawal reflex response (Fig. 4B, E) was of lower intensity

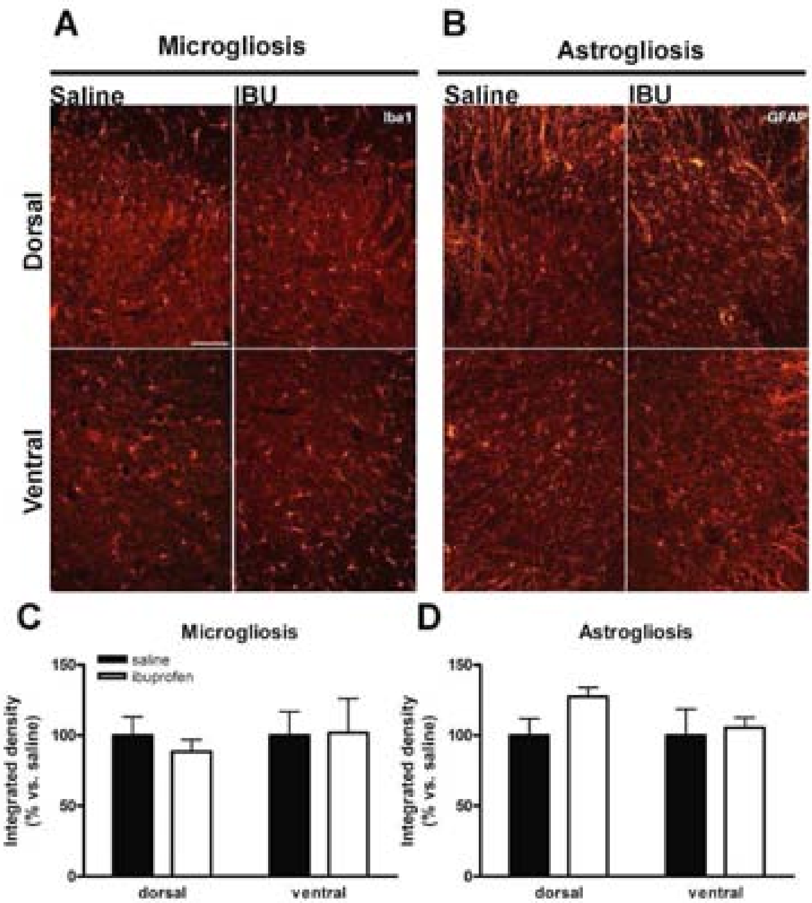

***Figure 7.** Microgliosis (A) and astrogliosis (B) were measured in dorsal and ventral horns of lumbar cord segments at 42 dpo. Measurements of integrated density did not reveal significant changes in microgliosis (C) and in astrogliosis (D) between the two injured groups. Scale bar: 100µm.*

in the IBU group at all time points, returning to almost normal values at the end of the follow-up period.

Histology in the lesion site

The amount of tissue spared after spinal cord contusion (Fig. 5A) was similar at the epicenter and caudal segments in the two groups, but in the rostral segments the IBU group presented larger tissue loss than the saline group (Fig. 5B). The area occupied by NeuN labeling, as well as the absolute neuronal counts, did not reveal any significant difference when comparing both groups (Fig. 5C,D). In both groups there was total loss of neurons in ventral horn at the epicenter and near sections (Fig. 5E).

Myelination was assessed in the injury site by two different techniques. Luxol Fast Blue stained sections (Fig. 6A) showed a similar profile of myelination in the epicenter and surrounding areas (Fig. 6B). An additional measurement of the myelinated fibers was done by combining neurofilament and MBP protein immunodetection in the dorsal funiculus (Fig. 6C). Although not reaching statistical significance, ibuprofen animals displayed a lower area occupied by myelinated axons (Fig. 6D).

Glial reactivity in lumbar cord segments

Both microglial and astroglial reactivity was assessed in the lumbar segments at the end of the follow up period (Fig. 7A,B). Measurements of integrated density (Fig. 7C,D) did not reveal any significant change in both populations between the groups, although in both cells displayed a clear activated phenotype.

Ibuprofen effects on microglia: cell cultures and early time effects

In order to unravel if ibuprofen was doing a direct effect on microglial activity, cultured microglial cells were activated by a classical activator (LPS), and by using a lysate obtained from injured spinal cords, in order to mimic the environment of a spinal cord injury. Phase contrast microscopy (images not shown) revealed activation of microglia after the two activators according to morphological criteria. The expression of ED1, used as an indirect marker of phagocytic activity, was increased by both activators. The addition of ibuprofen to the LPS and extract conditions induced a reduction in microglial signs of activation and phagocytic activity, especially in the extract condition (Fig. 8A).

In order to confirm this action in vivo, microglial reactivity was assessed in different areas of the spinal cord at 3 days after contusion and of ibuprofen administration (Fig. 8B). Results indicated that ibuprofen was able to attenuate microglial reactivity in the epicenter and more markedly in rostral and caudal regions to the lesion ($p<0.05$ vs saline) (Fig. 8C).

DISCUSSION

The results of this study indicate that ibuprofen offers good results regarding neuropathic pain after spinal cord contusion, since two daily injections of ibuprofen were able to significantly ameliorate mechanical hyperalgesia in rats. This effect was detectable in both forelimbs and hindlimbs, reflecting reduced pain responses above and below the level of the lesion. These positive results related to pain amelioration are coincident with others previously found (Guindon and Beaulieu, 2006; Ortega-Álvaro et al., 2012). Contrarily, administration of ibuprofen did not provide any improvement in terms of functional locomotion, electrophysiological results and histological measurements in our study. These results are contrary to those of authors which previously reported some functional and histological improvement with ibuprofen treatments in models of spinal cord injury (Fu et al., 2007; Wang et al., 2009), but coincident with results obtained in models of traumatic brain injury, in which worsening of cognitive outcomes and no histological improvement were detected (Browne et al., 2006), and of epilepsy, in which the edema was larger in the treated animals (Régnier et al., 2010).

Even though, our negative functional results are coincident with our electrophysiological data, which highlight a reduction in hyperreflexia, as can be seen in the wind-up responses and in the withdrawal reflexes. Peripheral elements were fully functional, and they permitted an almost perfect locomotion. Although hyperreflexia is normally considered as a negative outcome after spinal cord injury, in fact it is necessary to recover some functions below the injury site, since an additional afferent input is needed to compensate the loss of functionality of some elements (Lee et al., 2005). On the other hand, this reduction in the spinal excitability may account, at least partially, for the reduction in hyperalgesia detected in the Randall-Selitto test.

Regarding the lack of histological improvement in our model, it is important to take into account that the anti-inflammatory actions of ibuprofen, placed just after the injury, may have a dual effect on the secondary injury. Although an inadequately controlled inflammation can be harmful, some inflammation is needed to limit the expansion of the secondary injury as well as to scavenge all the cell and myelin debris originated in the initial phase of the spinal cord injury. For this reason, an early treatment with an anti-inflammatory drug as ibuprofen could reduce the beneficial inflammation occurring after the trauma. Maybe for these actions, the spared tissue in the epicenter is slightly minor in the epicenter in our model, as well as the area occupied for myelinated axons. This set of results is discordant with some other works that reported better tissue preservation as well as a better preservation of some spinal tracts (Fu et al., 2007; Wang et al., 2009; Xing et al., 2011). Fortunately, our model did not induce a major loss of neurons in the injury site, although it can not be defined as a clear neuroprotection, as some authors have reported (Park et al., 2005; Wang et al., 2009).

Since the involvement of glial actions in the appearance and maintenance of NP pain after SCI are widely known (Watkins et al., 2001; Hains and Waxman, 2006; Gwak et al., 2012), we decided to assess changes in glial reactivity after a 6 weeks of ibuprofen treatment. Effects of ibuprofen on astroglia have been extensively studied, and it is known to act on its migration, plasticity and functionality (Lichtenstein et al., 2010). On the other hand, effects aimed to microglia are not so well-studied, and are limited to some studies regarding the phagocytic properties (Jin et al., 2008;

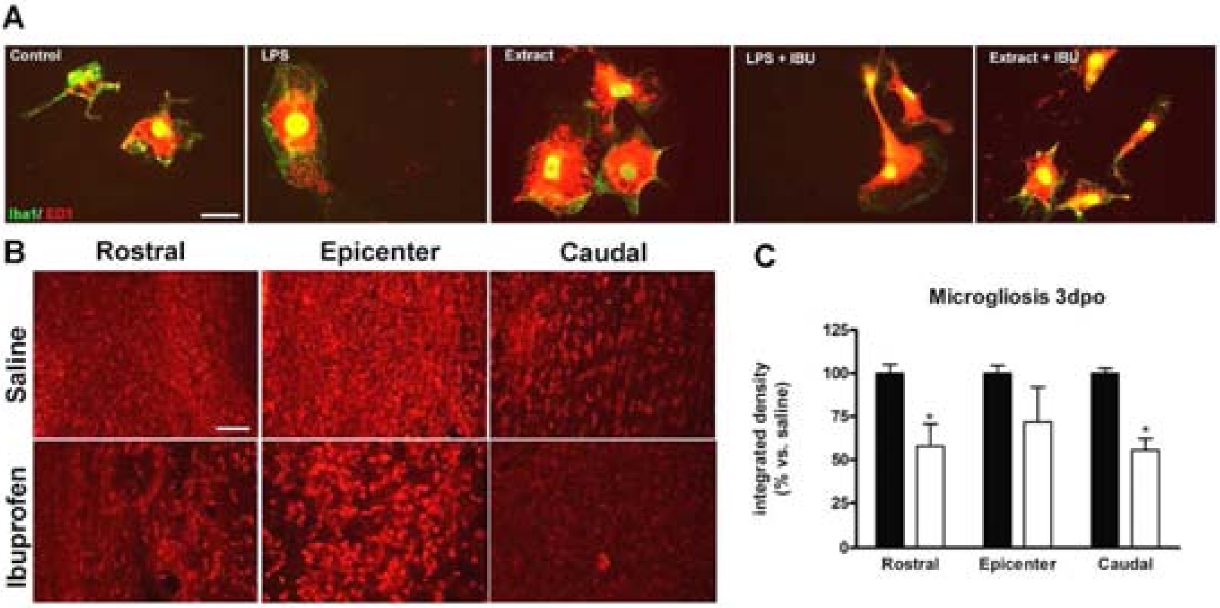

*Figure 8. Microglial cultures showed evidence of activation after the addition of LPS or a lesion extract (A). The addition of ibuprofen to both conditions induced morphological changes and reduced ED1 labeling, indicating a reduction in the phagocytic activity of microglia. Microgliosis was reduced by ibuprofen treatment in samples of spinal cords harvested at 3 days after operation (dpo) (B, C), especially around the epicenter. Scale bar: 20μm in A, 200μm in B. * p<0.05 vs. saline condition.*

Nagano et al., 2010) or modulation of cytokines related to the inflammatory response (Park et al., 2005; Heneka et al., 2005).

In our work we hypothesize than ibuprofen could have a strong effect on the early inflammation, concretely on the activation of microglia, and that it could obstruct the initial beneficial actions of microglia as a scavenger after a SCI.

The effects of ibuprofen in the glial reactivity at the end of the treatment seemed to be mild. Since treatment was started just after the injury, the initial action of ibuprofen was also assessed in samples harvested at three days after the injury, and they confirmed that ibuprofen was promoting an initial reduction of microgliosis in the injured spinal cord. To go a little bit deeper on this effect, we established microglial cell cultures, and our data suggest that ibuprofen may be modulating the phagocytic phenotype of microglia, as ED1 marker indicates. Then, we may hypothesize that anti-inflammatory actions of ibuprofen imply the reduction of the phagocytic abilities of microglia, therefore limiting their capacity or removing cell death and myelin debris. This could contribute to a worse resolution of the initial phase of SCI, and consequently promote a longer and more detrimental secondary phase of injury. This is translated in our model into a worse histological outcome and into a worse performance in functional tests. Something similar may have occurred in some works that obtained similar negative results (Browne et al., 2006). For this reason, it would be necessary to delay anti-inflammatory treatments after SCI, in order to generate a time window in which the early and beneficial inflammation can take place.

In conclusion, ibuprofen is able to ameliorate NP symptoms after SCI, but this beneficial effect is accompanied by a worst functional and histological outcome. Although further experiments may be addressed, our data indicate that this effect might be mediated by microglia. Ibuprofen reduces the phagocytic activity of microglia, therefore limiting their beneficial actions just after the SCI. For this reason it is important to consider the different phases of neuroinflammation after a SCI, in order to decide the best time window for each treatment. Results like this must be taken into account when designing therapies, since beneficial effects are usually sided by detrimental outcomes that really limit their effectivity and usefulness.

Acknowledgements

This work was supported by grants from the Fundació MaratóTV3 (grant 070210), the Ministerio de Ciencia y Innovación (grant SAF2009-12495), and funds from Red de Terapia Celular (TERCEL) of Spain. We thank the technical assistance of Monica Espejo, Jessica Jaramillo and Marta Morell, the surgical help of Abel Torres-Espín and the advice of Dr. Francisco J Rodríguez.

Conflict of interest statement

The authors declare no conflicts of interest.

References:

Adatia A, Rainsford KD, Kean WF (2012) Osteoarthritis of the knee and hip. Part II: therapy with ibuprofen and a review of clinical trials. The Journal of pharmacy and pharmacology 64:626–36

Basso DM, Beattie MS, Bresnahan JC (1995) A sensitive and reliable locomotor rating scale for open field testing in rats. Journal of neurotrauma 12:1–21

Blasko I, Apochal a, Boeck G, Hartmann T, Grubeck-Loebenstein B, Ransmayr G (2001) Ibuprofen decreases cytokine-induced amyloid beta production in neuronal cells. Neurobiology of disease 8:1094–101

Browne KD, Iwata A, Putt ME, Smith DH (2006) Chronic ibuprofen administration worsens cognitive outcome following traumatic brain injury in rats. Experimental neurology 201:301–7

Dergham P, Ellezam B, Essagian C, Avedissian H, Lubell WD, Mckerracher L (2002) Rho Signaling Pathway Targeted to Promote Spinal Cord Repair. 22:6570–6577

Fu Q, Hue J, Li S (2007) Nonsteroidal anti-inflammatory drugs promote axon regeneration via RhoA inhibition. The Journal of neuroscience : the official journal of the Society for Neuroscience 27:4154–64

García-Alías G, Valero-Cabré A, López-Vales R, Forés J, Verdú E, Navarro X (2006) Differential motor and electrophysiological outcome in rats with mid-thoracic or high lumbar incomplete spinal cord injuries. Brain research 1108:195–204

Guindon J, Beaulieu P (2006) Antihyperalgesic effects of local injections of anandamide, ibuprofen, rofecoxib and their combinations in a model of neuropathic pain. Neuropharmacology 50:814–23

Gwak YS, Kang J, Unabia GC, Hulsebosch CE (2012) Spatial and temporal activation of spinal glial cells: Role of gliopathy in central neuropathic pain following spinal cord injury in rats. Experimental neurology 234:362–72

Hains BC, Waxman SG (2006) Activated microglia contribute to the maintenance of chronic pain after spinal cord injury. The Journal of neuroscience : the official journal of the Society for Neuroscience 26:4308–17

Heneka MT, Sastre M, Dumitrescu-Ozimek L, Hanke A, Dewachter I, Kuiperi C, O'Banion K, Klockgether T, Leuven F Van, Landreth GE (2005) Acute treatment with the PPARgamma agonist pioglitazone and ibuprofen reduces glial inflammation and Abeta1-42 levels in APPV717I transgenic mice. Brain : a journal of neurology 128:1442–53

Hiraga A, Kuwabara S, Doya H, Kanai K, Fujitani M, Taniguchi J, Arai K, Mori M, Hattori T, Yamashita T (2006) Rho-kinase inhibition enhances axonal regeneration after peripheral nerve injury. Journal of the peripheral nervous system : JPNS 11:217–24

Jin D-Q, Sung J-Y, Hwang YK, Kwon KJ, Han S-H, Min SS, Han J-S (2008) Dexibuprofen (S(+)-isomer ibuprofen) reduces microglial activation and impairments of spatial working memory induced by chronic lipopolysaccharide infusion. Pharmacology, biochemistry, and behavior 89:404–11

Kopp M a, Liebscher T, Niedeggen A, Laufer S, Brommer B, Jungehulsing GJ, Strittmatter SM, Dirnagl U, Schwab JM (2012) Small-molecule-induced Rho-inhibition: NSAIDs after spinal cord injury. Cell and tissue research 349:119–32

Kubo T, Hata K, Yamaguchi A, Yamashita T (2007) Rho-ROCK inhibitors as emerging strategies to promote nerve regeneration. Curr Pharm Des 13:2493–9

Lee JK, Emch GS, Johnson CS, Wrathall JR (2005) Effect of spinal cord injury severity on alterations of the H-reflex. Experimental neurology 196:430–40
Lichtenstein MP, Carriba P, Baltrons MA, Wojciak-Stothard B, Peterson JR, García A, Galea E (2010) Secretase-independent and RhoGTPase/PAK/ERK-dependent regulation of cytoskeleton dynamics in astrocytes by NSAIDs and derivatives. Journal of Alzheimer's disease : JAD 22:1135–55
Nagano T, Kimura SH, Takemura M (2010) Prostaglandin E2 reduces amyloid beta-induced phagocytosis in cultured rat microglia. Brain research 1323:11–7
Ortega-Álvaro A, Berrocoso E, Rey-Brea R, Leza JC, Mico J a (2012) Comparison of the antinociceptive effects of ibuprofen arginate and ibuprofen in rat models of inflammatory and neuropathic pain. Life sciences 90:13–20
Park E-M, Cho B-P, Volpe BT, Cruz MO, Joh TH, Cho S (2005) Ibuprofen protects ischemia-induced neuronal injury via up-regulating interleukin-1 receptor antagonist expression. Neuroscience 132:625–31
Redondo Castro E, Udina E, Verdú E, Navarro X (2011) Longitudinal study of wind-up responses after graded spinal cord injuries in the adult rat. Restorative neurology and neuroscience 29:115–26
Régnier A, Vicaut E, Mraovitch S (2010) Aggravation of seizure-associated microvascular injuries by ibuprofen may involve multiple pathways. Epilepsia 51:2412–22
Santos-Nogueira E, Redondo Castro E, Mancuso R, Navarro X (2012) Randall-Selitto test: a new approach for the detection of neuropathic pain after spinal cord injury. Journal of neurotrauma 29:898–904
Servitja JM, Masgrau R, Pardo R, Sarri E, Picatoste F (2000) Effects of oxidative stress on phospholipid signaling in rat cultured astrocytes and brain slices. Journal of neurochemistry 75:788–94
Valero-Cabré A, Forés J, Navarro X (2004) Reorganization of reflex responses mediated by different afferent sensory fibers after spinal cord transection. Journal of neurophysiology 91:2838–48
Wang X, Budel S, Baughman K, Gould G, Song K-H, Strittmatter SM (2009) Ibuprofen enhances recovery from spinal cord injury by limiting tissue loss and stimulating axonal growth. Journal of neurotrauma 26:81–95
Watkins LR, Milligan ED, Maier SF (2001) Glial activation: a driving force for pathological pain. Trends in neurosciences 24:450–5
Xing B, Li H, Wang H, Mukhopadhyay D, Fisher D, Gilpin CJ, Li S (2011) RhoA-inhibiting NSAIDs promote axonal myelination after spinal cord injury. Experimental neurology 231:247–60

Effects of the combined treatment with glibenclamide and ibuprofen after spinal cord injury

As shown in the previous studies, a single dose of glibenclamide (GB) injected just after the SCI was enough to provide a consistent and long lasting functional improvement, observable in different functional tests. Unfortunately, this positive effect was accompanied by a more marked hyperalgesia in front of mechanical stimuli. On the other hand, chronic treatment with ibuprofen (IBU) was effective in ameliorating neuropathic pain signs occurring after the SCI, although without providing any functional improvement.

Since these two individual treatments provide good results in different aspects, we aimed to obtain synergistic effects by combining the two drugs. A group of rats was subjected to spinal cord contusion (group GB+IBU, n=8): GB was injected just after the injury in the spinal parenchyma (1µg divided in 2 injection points), and one week later a daily treatment with ibuprofen was started (60mg/kg, every 12 hours). In this way, GB may have a time window enough to exert its effects on microglia without being interfered by the anti-inflammatory effects of ibuprofen.

The methodology used for the functional, electrophysiological and morphological evaluation was the same explained in the two previous studies. The results are exposed below for the group receiving the combined treatment, compared with the previous groups treated with only GB or IBU, and the vehicle control groups.

Functional results

Contusion parameters were similar in all groups, independently of the later treatment received, so any effect cannot be attributed to differences in the contusion severity. Control conditions were set for both drugs, with saline solution injected subcutaneously (IBU-) or intraparenchimally (GB-). Since both control groups showed very similar outcomes in all the tests, both groups have been pooled and are represented as the *saline group* for convenience, and some of the values of the treated groups are represented as normalized values (normalized versus its own control in each case).

The assessment of the open field locomotion revealed an important improvement of voluntary locomotion only in the GB group (Fig.21). The rest of the groups presented similar evolution after the injury.

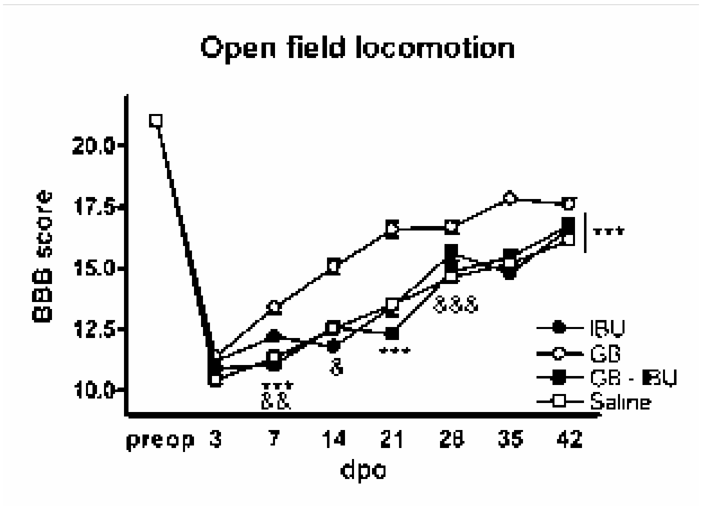

Fig. 21: scores obtained by the different groups in the open field locomotion test.. GB group displayed significantly better scores (***, p<0.001) than all the other groups during all the follow up period. The combined group achieved worst scores than IBU and saline group at 7 and 21 dpo (***, p<0.001). Saline and IBU groups followed a similar tendency during all the follow up, although some statistical differences were achieved at some time points (&; 7, 14 and 28dpo).

Other functional tests revealed a similar tendency, indicating that the combination of the two drugs was not affecting the final outcome compared to the controls. Glibenclamide treatment was the most effective treatment, promoting better locomotion results. In the walking narrow beam, assessing fine coordination, all the treated groups displayed similar results, which were significantly better than the saline controls, returning to almost normal values (Fig. 22). In the inclined plane, all treated groups also supported angles near the preoperative values, significantly better than the saline condition. In both tests, both treatments have a beneficial effect by themselves, but the combination does not result in any additional effect.

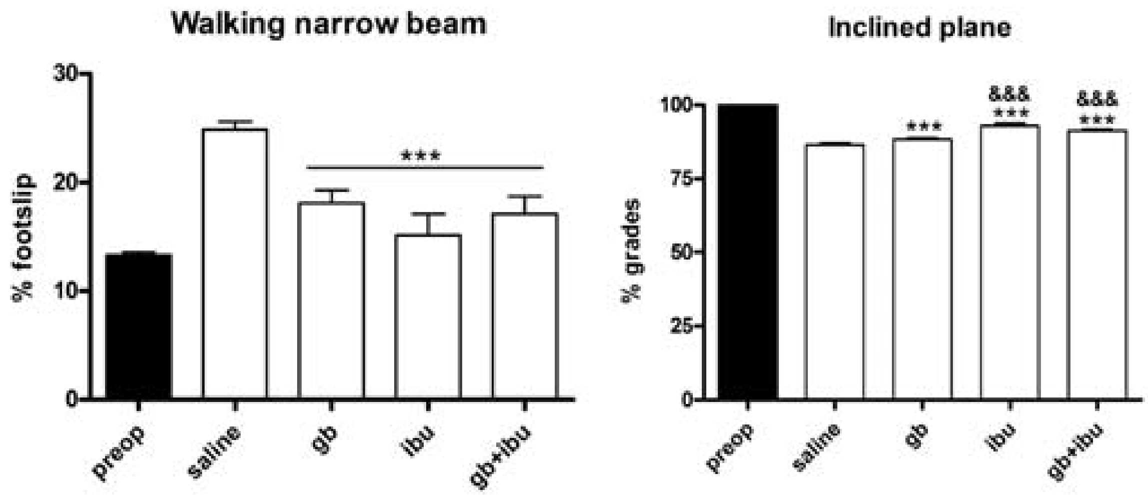

Fig. 22: Left, walking narrow beam: all treated groups had better result than the saline group, but no differences were detected between treatments. Right, the inclined plane test show similar results, with slight but significant improvement in the outcome compared to saline controls. In this case, IBU and GB+IBU results were significantly different from GB. Statistical significance: *** p<0.001 vs. saline condition; &&& p<0.001 vs. GB group.

Neuropathic pain

Good results were obtained by administering ibuprofen to SCI rats, as it consistently reduced mechanical hyperalgesia. Contrarily, GB seemed to increase it. The combination of both drugs did not provide additional effects in mechanical and thermal algesimetry tests. When all the groups were compared, no statistical significance was found in any of the comparisons (Fig. 23).

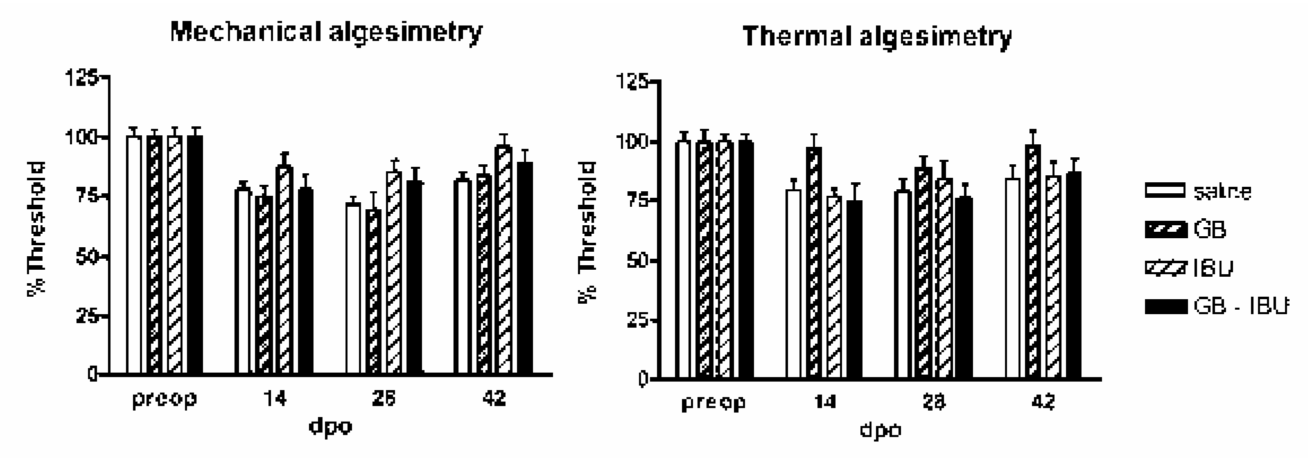

Fig. 23: Results of the customary algesimetric tests, expressed as the percentage of the preoperative threshold value.

A more precise test, the Randall-Selitto test, allowed the detection of differences in mechanical nociceptive thresholds. With this test we detected a worsening in the mechanical hyperalgesia in the GB group, but amelioration in the IBU group. The combined treatment did not provide improvement of the neuropathic pain signs. Only at some time points the combined treatment was better than the ibuprofen alone treatment, and only in the plantar surface (Fig. 24).

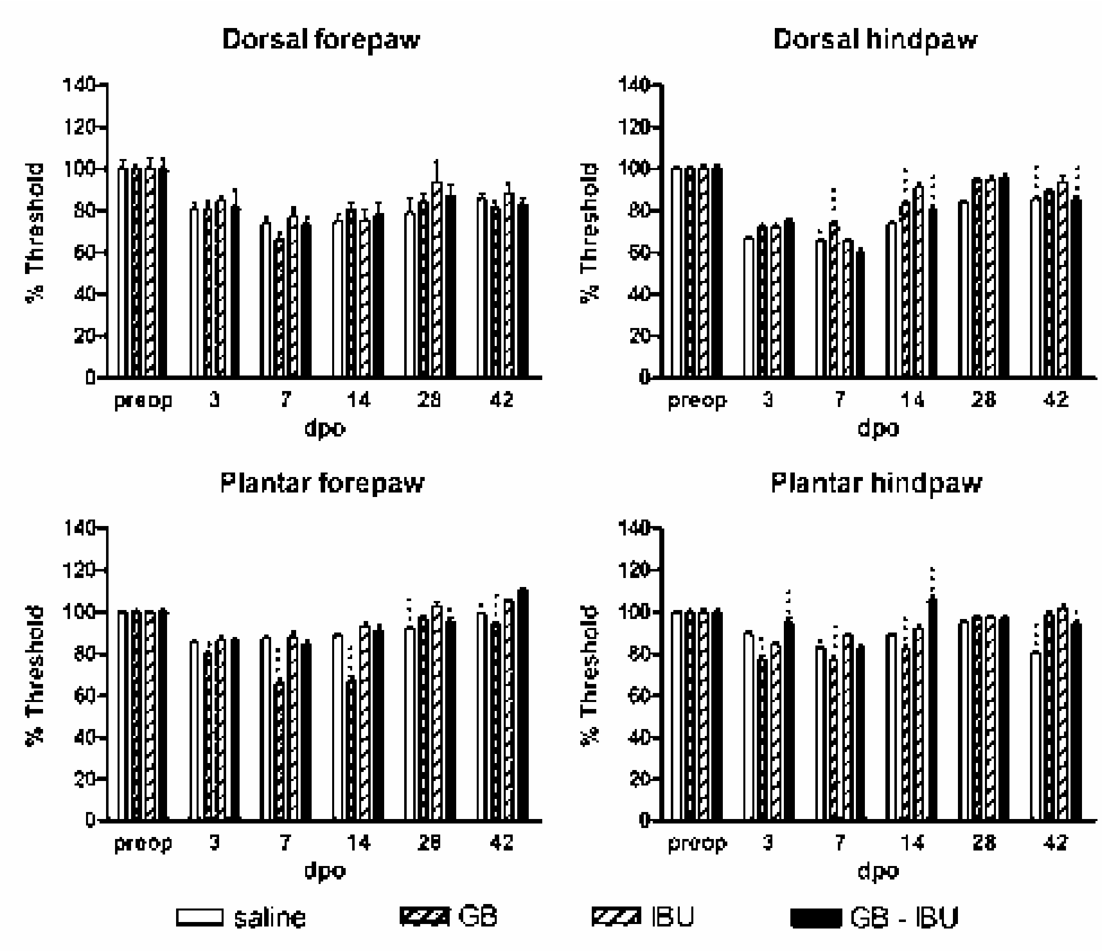

Fig.24: Randal-Selitto test results in plantar and dorsal surfaces of hindpaws and forepaws. The combined treatment only provides better results than ibuprofen treatment in the plantar hindpaw at two time points (3 and 14dpo).
* p<0.05; ** p<0.01; *** p<0.001 vs. IBU group.

Electrophysiology: peripheral and central conduction

Several electrophysiological measurements were performed in order to see any possible effect of the combined treatment. Unfortunately, none of the outcomes provided a clear improvement.

The peripheral nerve conduction tests were normal after the SCI. A few changes were detected in the amplitude and latency of CMAP of the tibialis anterior muscle. Similarly, the hyperreflexia (measured as the H/M ratio recorded in the plantar muscle) was similar in all the groups, and the combined group showed very similar results to the IBU group (Fig. 25).

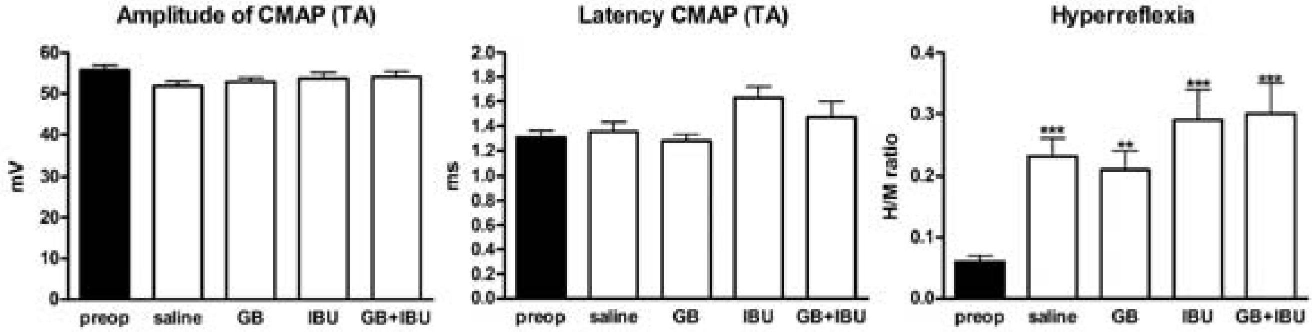

Fig. 26: Results of amplitude and latency of the CMAP in the tibialis anterior muscle. The H/M ratio was similarly increased in all experimental groups.

Regarding central conductions, MEPs and SSEPs were evaluated. Motor central conduction was severely affected after the spinal cord contusion, and the amplitude of bs-MEP became greatly reduced. In fact, only some animals had a preserved response, as indicated in figure 27. The cortical component appeared less affected, but its amplitude was also reduced in all the injured groups. For both components, the combined group was the one with the lowest mean amplitude, and also the group with the lowest percentage of animals preserving bs-MEP.

On the other hand, the preservation of SSEPS was present in a similar proportion of rats in the GB+IBU group than in the IBU group, and slightly lower than in the GB group, when only the preservation of at least one component was considered. However, when the three components were considered, all the groups displayed a reduced preservation, especially the groups treated with ibuprofen and with the combination of drugs.

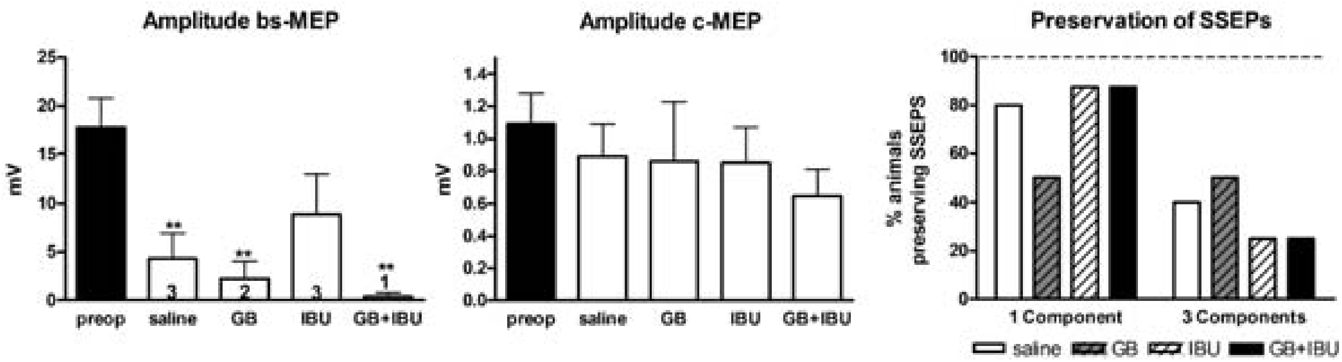

Fig. 27: Left panel, amplitude of the bs-MEP, elicited at 1Hz. Numbers indicate the number of rats preserving the MEP. Middle panel, amplitude of the c-MEP; all the rats presented the cortical component. Right panel, preservation of at least one component, or of the three components of SSEPs. ** p<0.01 vs. preoperative value.

Spinal reflexes

Spinal lumbar reflexes were assessed during all the follow-up, but the main differences were noticed at the end of the follow-up (Fig. 28). The intensity of the stimulus required to elicit the withdrawal reflex was higher in the IBU group, indicating a lower spinal hyperexcitability. The combined group required a threshold similar to the GB group. When the intensity of the response was measured, the combined group also reverted the effect obtained with the IBU treatment, as it presented a higher response. Something similar was detected in the wind-up responses. Treatment with ibuprofen alone reduced parameters related to central hyperexcitability, such as the first response intensity, but the combined group did not have better effects than the group with only GB. Similarly, when the total activity accumulated in the 16 responses was measured, the reduction found in the IBU group was not observed in the GB+IBU group. Thus, only treatment with ibuprofen alone had effects on reducing central hyperexcitability and hyperreflexia.

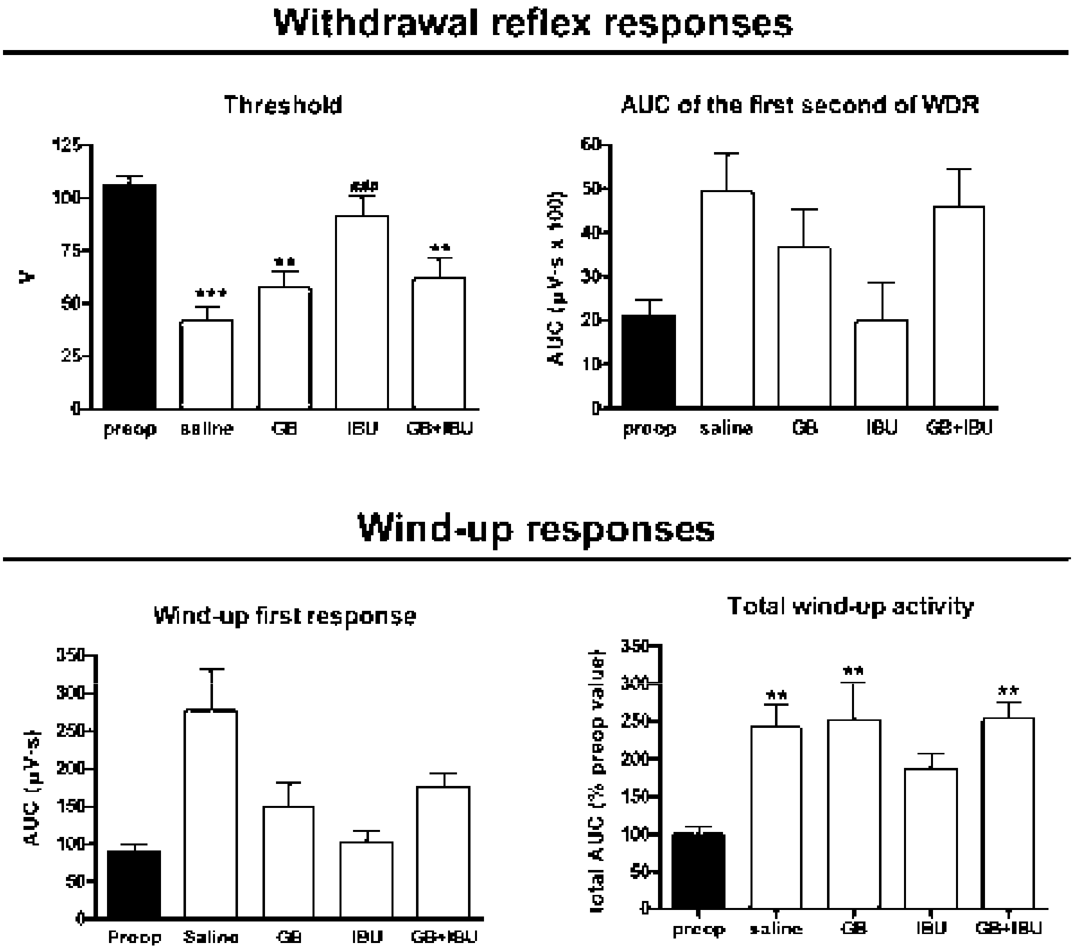

Fig. 28: Threshold needed to elicit the withdrawal response is reduced after injury. The intensity of the reflex response increased after injury, except in the IBU group, indicating a reduction in hyperreflexia. Similarly, wind-up responses tended to increase after the injury, and were partially reduced with all the treatments, but especially in the IBU group. The total wind-up activity was also increased in all the groups, and partially reduced in IBU animals. ** p<0.01¸*** p<0.001 vs. preoperative values; ### p<0.001 vs. saline group.

Histological analyses

Typical markers were assessed by immunohistochemistry to assess tissue sparing, gliosis, myelination and neuronal survival, and none of them revealed any significant improvement in the combined group (Fig. 29).

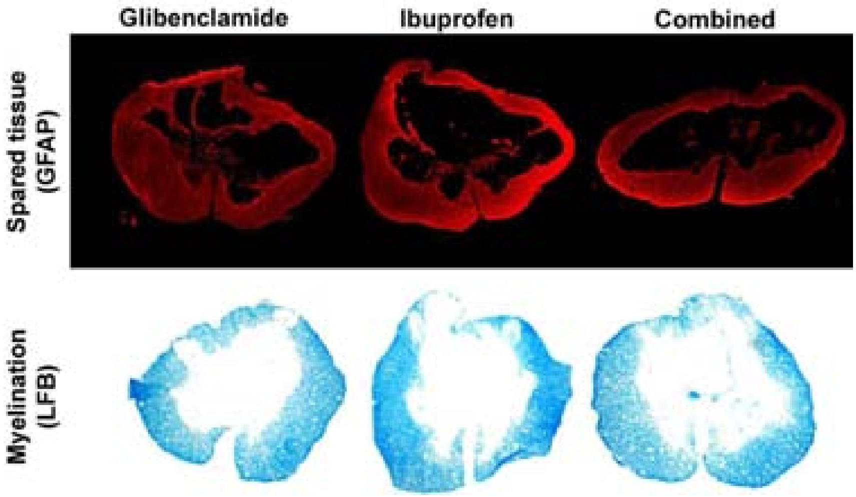

Fig 29. Representative images depicting the lack of effect of the combined treatment on tissue preservation and on demyelination.

Glial cell cultures

All the results obtained until this point lead us to the idea that although both drugs were supposed to act on different targets, they may be converging at some point, and probably cancelling the effects of the other drug. For this reason we used glial cultures in order to unravel if both drugs were counteracting their effects on astroglia or microglia.

In culture, GB did not seem to exert any clear effect on astroglia, as morphological changes were not visible, despite the fact that astroglia also possess SUR receptors (Simard et al., 2006). On the other hand, activated astroglia showed a change in morphology (concretely estelation, Lichtenstein et al., 2010) clearly visible in the cells supplemented with ibuprofen (Fig. 30).

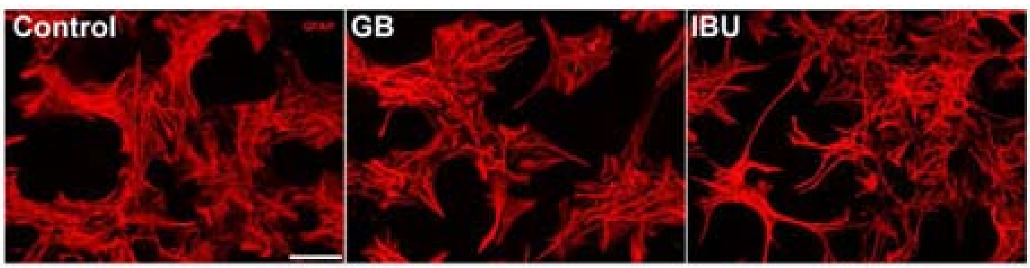

Fig. 30: Astroglial cells cultured in presence of GB or IBU. Note the morphological change only occurring in IBU treated cells. Scale bar 50µm.

Microglial features were studied in resting and activated conditions, using two different activators. The first was LPS, classically used to activate microglia through the TLR receptors pathway. With the intention to mimic as much as possible the environment of a recent spinal cord injury, we used protein lysates obtained from injured spinal cords that were added to the culture medium. Animals receiving a 100kdyn contusion (the same severity that was used in the treatment groups) were sacrificed and their cords were harvested at 7dpo, assuming that this time point is considered a peak of inflammation. In this case, we expected to activate microglia through the pathways that would act in the injury environment, such as lypidic mediators, interleukins, cytokines and myelin debris. This activation profile might be different from the activation in response to an infection, as mimicked by LPS.

A first approach was the observation of morphological changes, as depicted in figure 31. Both activators produced a morphological change in microglial cells consistent with a reactive phenotype, as they become hypertrophic and emitted thick prolongations. Interestingly, both activators produced slightly different morphological changes, and in the case of the activation for the lysate, they also promote the presence of refringent vacuoles inside the cells. These vacuoles may correspond to phagocytic vacuoles. This feature was even more evident when GB was also added, therefore confirming our initial hypothesis that GB may act boosting the phagocytic activities of microglia after a SCI.

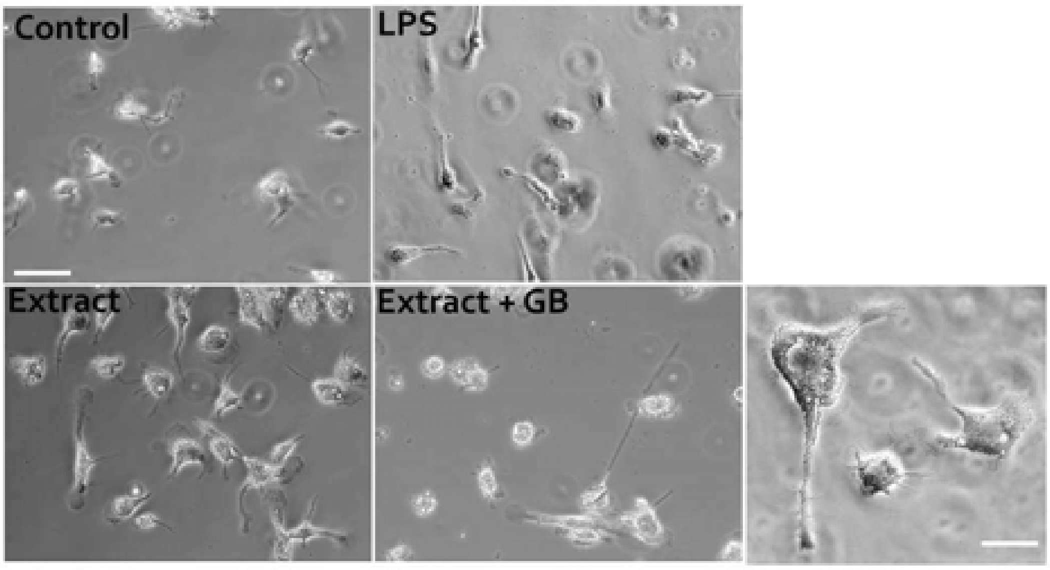

Fig. 31: Morphological changes in microglia after LPS or lysate activation. The last picture in the right is a detail from Extract+GB condition. Note the huge amount of vacuoles inside the cytoplasm of activated microglial cells. Scale bars: 200µm and 100µm in the detail.

Since the morphological changes can not be directly correlated with the activation profile, we assessed the expression of ED1 as a marker of phagocytic activity. ED1 is a glycoprotein placed in the lysosomal membranes and in the plama membrane, and their presence is increased in phagocytic phenotypes. Immunocytochemistry against this protein revealed a diffuse pattern in resting microglial cells, but its presence was greatly increased in activated conditions (Fig. 32).

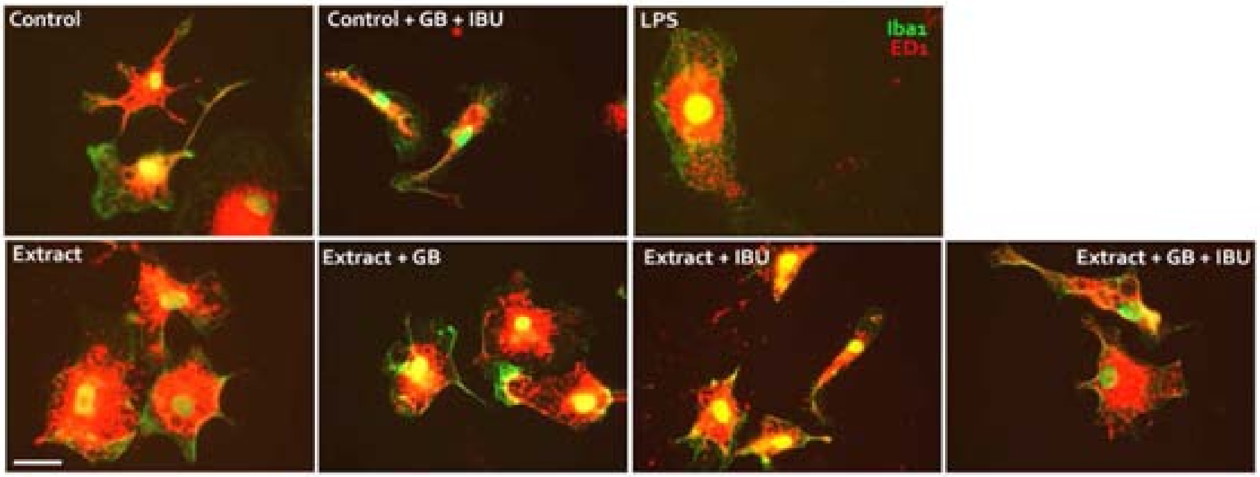

Fig. 32: Immunohistochemistry against Iba1 (in green) and ED1 (in red). Drugs did not exert a clear action on phagocytosis by themselves, but promoted a more intense labeling in the activated conditions. The combined treatment reduced the activation of microglia and their phagocytic abilities. Scale bar: 20μm

The combined GB+IBU treatment seemed to reduce the activation of microglia, as morphologies were more similar to the resting cells. Moreover, the intensity and extension of ED1 labeling was also reduced, indicating that the combination of both drugs was somehow limiting the activation of microglia in culture.

The lack of effectivity of the combined treatment

The treatments used were partially effective when administered alone, but the combination of both drugs did not imply a synergistic nor an increased effect. In fact, the combined treatment was even worse in some outcomes than the individual treatments. Both treatments were originally focused to different targets; ideally glibenclamide must exert its actions on microglia, during the early phase, and ibuprofen on astroglia on a prolonged phase. Despite considering a time window for the activity of glibenclamide, the anti-inflammatory effects of ibuprofen may have reverted the initial positive effects of glibenclamide. This fact has to be taken into account when combining different drugs, also when they have well defined actions. It is also important to respect the optimal timing of each strategy, in order to avoid interferences and consequently the reduction of the effects.

The exact mechanism by which glibenclamide and ibuprofen concur in the modulation of the phagocytic activity of microglia remains unknown, so further experiment might be addressed to unravel this issue.

Discussion

General discussion

Spinal cord injury (SCI) patients report with high prevalence a moderate to severe pain that degrades quality of life and interferes with rehabilitation therapy (Widerstrom-Noga et al., 2001a, 2001b). Because of the multiple tissue damage that accompanies SCI, pain may be the consequence of a number of pathological processes arising from musculoskeletal, peripheral, and central nervous system tissues. Among them, the most disabling and dificult to manage is neuropathic pain (NP). Below-level NP occurs following SCI and, similarly to neuropathic peripheral nerve injury pain, is poorly responsive to common analgesics. In addition, the decreased mobility and changes in autonomic functions further limit the possible range of analgesic therapeutics that may be used.

Experimental model of neuropathic pain after spinal cord injury

The development of new therapies for any injury or disease generally requires extensive basic research including adequate preclinical *in vivo* models before the translation to clinical trials in human patients. Nonetheless, there are frequent failures in translational attempts from converting experimental results into successful clinical treatments. These failures may be due, at least in part, to the experimental model itself not reproducing exactly the pathogenetic mechanisms of the human disease, or to methodological problems in the techniques used for assessment. In this sense, the research on pain has considerable shortcomings, since animals lack the capability of expressing the subjective sensation regarding quantity and quality of pain.

It is essential for researchers to count on reliable and reproducible animal models, despite the intrinsic unpredictability of human SCI consequences. The most frequent type of spinal injury in humans is the contusive trauma, and therefore spinal cord contusion or compression models in rodents are the most used in the field, and they have became an essential tool also in NP research. The weight-drop and the impact devices developed during the last years are reported to result in reproducible anatomical and behavioral outcomes (Basso et al., 1996; Ghasemlou et al., 2005), with mild to severe locomotor deficits resulting from the trauma intensity applied.

The first step of our work was to set up the animal model of contusion, confirming that the lesions were accurate and reproducible, in terms of mechanical parameters as well as in functional and electrophysiological outcomes and pain responses (Yezierski, 2005; Cao et al., 2005). Histological assessments were also done, mainly the measurement of the spared tissue and the glial reactivity. We have used contusions of different severities, as well as section cord injury models (hemisection or complete transection). In this way, we made available a wide range of experimental conditions to study the appearance of several physiopathological features, in order to unravel which ones were directly related to the severity of the injury and which were intrinsic to the lesion itself.

The first chapter of this thesis is based on the study of the evaluation of pain responses following SCI of varying severity, emphasizing the utility of the Randall-Selitto test, previously used to assess the efficacy of analgesic treatments (Randall and Selitto, 1957) as well as inflammatory painful responses (Anseloni, 2003). In this thesis we have used this method to assess NP in animals with central injuries of different severities. Importantly, it allows testing in complete section and severe contusion animals, which cannot be tested in customary algesimetric tests that require body weight support. Another important advantage of this test is the possibility to test pain responses at early time points after the injury. This is especially useful when testing acute effects, independently of the motor recovery from the different injuries.

Our results from the algesimentry tests applied to detect hyperalgesia and allodynia suggest that pain is basically an *all-or-none* phenomenon, and all animals present a similar degree of NP signs independently of the severity of the injury. Although in some measurements there was some slight tendency, indicating that more severe injuries can present more marked signs of hyperalgesia, in any case these differences achieved statistical significance.

The relevance of segments distant to the injury

One of the main objectives in this thesis was the study of spinal cord segments distal from the injury epicenter. In fact, alterations after SCI have been described in distant cord segments (rostral and caudal), thalamus, brainstem and cortex (Zhang et al., 2005; Hains et al., 2005; Zhao et al., 2007; Detloff et al., 2008; Carlton et al., 2009; Baastrup et al., 2010; Yague et al., 2011). We focused on the lumbar cord segments, where the sensory inputs and motor outputs for the hindlimbs are gathered, as a relevant site for studying below-level NP, the most frequently reported by SCI patients. Particularly, spinal lumbar reflexes are an important circuit to assess the connectivity as well as the excitability of the spinal cord (Cervero, 2009; Hubli et al., 2011). By simulating a nociceptive input, we elicited neural responses integrated and transmitted to produce a muscular response. In this way we confirmed the increased excitability of the spinal circuits after SCI, and found that spared segments not directly affected by the lesion play an important role in the maintenance of NP signs.

We have reported for the first time the wind-up responses in SCI rats. Although it was described some decades ago (Mendell, 1966), wind-up has rarely been used systematically, so comparisons between works and laboratories are difficult. We characterized the appearance of these responses as a form of short-term plasticity in the lumbar cord segments. Especial attention was given to the different calculations to quantify the wind-up responses, despite its inherent variability (Svendsen, 1999). Although the repetitive stimulation used in wind-up recording is not exactly the stimulation found in normal conditions, it can be used as a tool to activate nociceptive circuits, and as an indirect way to mimic features occurring in the spinal nociceptive circuits after SCI. In addition, it is also an easy way to demonstrate that the spinal system is able to amplify a nociceptive input, and this phenomenon is likely to occur in spinal cord injury patients. Despite wind-up cannot be considered as a direct measurement of pain, it gives essential information about the spinal function regarding the integration and modulation of sensory and nociceptive signals. More importantly, it demonstrates the ability of the spinal pain system to amplify signals, and this feature is extremely important in a neuropathic pain context.

The putative mechanisms underlying this increased spinal excitability have been widely discussed; among them the postlesional reactivity of glial cell populations seems to play an important role (Zhang et al., 2005; Hulsebosch, 2008; Cervero, 2009; Gwak et al., 2012). We assessed glial reactivity at different chronic time points (from 1 to 3 months), and observed a persistent activation of both astroglia and microglia populations. Such chronic activation has to be considered as pathological, since it should have been resolved in a shorter time. This fact also highlights the importance of remote regions not directly affected by the contusion itself. We observed that measurements of glial reactivity where quite similar between injuries of different severities, suggesting once more the existence of *all-or-none* phenomenona related with the presence of NP. In summary, once the spinal cord is injured, hyperexcitability develops and signs of pain appear, and the exacerbated glial reactivity participates in their maintenance; the lack of a direct relationship with the gradation of the injury may be due to the amplificatory nature of neuroinflammatory and excitability processes.

Functional deficits are dependent on the injury severity

Apart from sensory disturbances, locomotion and functional performance are also affected after SCIs. A good functional study provides important and useful information about the state of spinal circuits and pathways, as well as of the effectiveness of pharmacological treatments and physical therapies (Basso et al., 1995; Kuerzi et al., 2010). The BBB scale is probably the most frequently used when assessing functional recovery, mainly because it is a fast and easy method to obtain general information about the locomotion capabilities of the animal. Unfortunately, this scale is highly qualitative, especially in its upper part. Coordination is the most difficult parameter to assess in this test, and is in this part where many treatments can be discarded for not showing a clear efficacy (Basso, 2004; Ferguson et al., 2004; Koopmans et al., 2005). We strongly believed that we were missing a lot of information from a certain point of the scale. As an example, a 100kdyn contusion and a hemisection injury are clearly different lesions, but they obtained a similar score in the BBB scale. Therefore, we performed a battery of functional tests in order to obtain more detailed information, including gross and fine coordination, and general balance. Despite its versatility and low time consuming properties, tests such as the walking narrow beam, the walking track analysis or the graded plane did not provide enough quantitative data on coordination and alternation. Hence, we used the treadmill of the Digigait System to force the locomotion by increasing the speed. Adding difficulty to the functional tests permitted us to distinguish more clearly between different severities of functional deficits. That is, by increasing the difficulty of the locomotion task, the sensitivity increases (Collazos-Castro et al., 2006). Compensation and plasticity must be taken into account when assessing functional recovery, since once damaged, locomotion systems may readapt themselves to a new circuitry that can permit locomotion, although it can imply a variation in the normal features. It is also important not to expect complete reversion to normal features and parameters, so recovery can imply new motion characteristics (Gulino et al., 2007; Majczyński and Sławińska, 2007; Curt et al., 2008).

We analyzed gait parameters, coordination and alternation patterns by designing simple Excel macro programs, in order to add objectivity and quantify parameters that can hardly be observed in an open field locomotion test. The main advantage of this method is the reduction in time used when compared to other kinematics analysis made by other authors, and the fact that researchers do not need any specialized training to analyze most of the obtained results (Hamers et al., 2001; Beare et al., 2009).

Complementarily, we performed a study on peripheral axon preservation, in order to confirm that the functional deficits observed after SCI were depending on the lesion itself. Our results indicated that, although there was an increased number of structural abnormalities in the myelinated fibers of SCI animals, the total number of axons was maintained, and the functional conduction properties of the sciatic nerve were not significantly altered. These findings imply, firstly, that the peripheral nervous system is affected after the SCI, despite that it is not primarily affected by the lesion. Second, that peripheral axonal damage can be discarded as the basis of the functional deficits occurring after the spinal cord contusion. The alterations reported in paraplegic human nerves are more marked and include evidences of axonal degeneration (Berman et al., 1996; Nogajski et al., 2006; Lin et al., 2007; Van De Meent et al., 2010), but it does not occur in rats. Therefore, apart from the mild damage caused by SCI, most of the axonal alterations are likely attributable to immobilization and nerve compressions in disabled people. It is important to emphasize that efforts should be devoted to maintain the peripheral systems as normal and functional as possible during the recovery of SCI, in order to take the most possible from therapies and rehabilitation.

Plasticity of the spinal cord after injury: the importance of disinhibition

Circuits implicated in locomotion become remodeled after SCI, and the same occurs in sensory circuits participating in the processing of pain. We made a novel analysis focused on the plastic changes of the nociceptive spinal circuit occurring in the lumbar segments, caudal to the thoracic SCI. Although many publications have dealed with single alterations (Floyd et al., 1998; Tillakaratne et al., 2000; Hains and Waxman, 2006; Hasbargen et al., 2010; Lin et al., 2011; Kong et al., 2011), we detected a lack of integrative studies in the literature since one simple system can not explain most of the physiopathological features of NP detected after the injury. In our case, we studied the spinal circuitry of nociception, based on the withdrawal reflex response. Starting from the periphery and the nociceptive afferences, we moved into the spinal cord, where the information is integrated, modulated and conveyed to other areas, and to the motor output.

We assessed several key elements of pain signal processing in animals with SCIs of different severities. One of the main findings was a boost in some inhibitory features, such as an increase of the synthesis of GABA and of inhibitory synapses on motoneurons. The obvious lack of efficacy of this increase has to be seen not as a failure but as a compensatory mechanism, or, in the case of GAD enzyme, as a strategy to promote plastic changes. Thus an increase of excitability does not simply imply a compensatory increase in inhibition, but also the remodeling of circuits, in order to generate new connectivity and a new environment in the spinal cord.

In addition, the increased presence of nociceptive afferents, combined with an increased glial reactivity in the dorsal horn and the reduction of descending inhibition, contribute to the amplification of nociceptive inputs arriving to the spinal cord. Lumbar motoneurons are also surrounded by reactive glia, and despite the increase in inhibitory synapses, the lack of descending serotonin inputs can imply an additional point of amplification.

Once more, although some of the analyzed elements seem to change in a lesion severity-dependent manner, the NP signs were similar after contusion of varying intensity and transection of the spinal cord. This fact is probably explained because SCIs are accompanied by important inflammatory and excitotoxic responses that result in central hyperexcitability, so linearity is not kept in graded injuries (Gozariu et al., 1997; Costigan and Woolf, 2000; Mackie, 2003; Valero-Cabré et al., 2004; Ma and Quirion, 2008; Hulsebosch, 2008; Gwak and Hulsebosch, 2009).

The findings of our study in the chapter 3 give support to the view that the balance between excitation and inhibition is clearly inclined towards the excitation side following SCIs, despite that inhibitory elements are also clearly enhanced. It is important to note the importance of the remote changes in areas (lumbar segments) that are not directly affected by the injury (made at thoracic T8 segment), but undergo plastic adaptative changes to the new environment and interruption of descending inputs. This point of view is gaining interest in recent years for the design of new treatments and therapies, since plasticity might sometimes be underestimated (Ding et al., 2005; Dietz, 2011). Attempts for restoring lost functions do not necessarily imply the return to initial features. At the end, the unbalance between excitation and inhibition leads to the appearance of hyperreflexia, spasticity and neuropathic pain, independently of the severity of the injury.

Pharmacological treatments after SCI: modulating glial reactivity

Glial cells are the most abundant cell type in the central nervous system. The consideration of glial cells has evolved from a simple supportive role of neurons to presenting a predominant role in inflammatory, synaptic and plastic phenomena (Scholz and Woolf, 2007; Hulsebosch, 2008; Milligan and Watkins, 2009; McMahon and Malcangio, 2009; Pirttimaki et al., 2011; Gwak et al., 2012). After an important injury such as a contusion to the central nervous system, microglia and astroglia shift from their normal homeostatic and defensive actions to new phenotypes and functions. Microglia becomes quickly activated in the injury site and contributes to a fast and exacerbated neuroinflammatory reaction. There it contributes to limit the loss of tissue and reduce as much as possible the injured parenchyma, through the acquisition of a phagocytic and proinflammatory phenotype. Microglia and macrophages scavenge dead cells and myelin debris from disrupted axons (Popovich et al., 1997; Hains and Waxman, 2006; David and Kroner, 2011). Secondarily, astrocytes perform homeostatic functions, such as buffering the increased concentrations of glutamate and other excitatory amino acids, blood-barrier maintenance, and neurotransmitter regulation (Scholz and Woolf, 2007; Fitch and Silver, 2008). They also secrete extracellular matrix molecules and form the glial scar in order to limit the injured tissue and preserve surrounding tissues, although this can imply a regeneration barrier difficult to overcome.

After this primary phase, a secondary phase occurs in which there are endogenous attempts for reestablishing the lost connections (if possible) or for creating new ones. Inflammation events usually resolve after a few days/weeks, but unfortunately after a spinal cord injury the resolution of inflammation is quite longer and innefficient. Inflammation mediators diffuse from the injury epicenter and reach distant areas, and the inflammation becomes chronically and pathologically activated, instead of being progressively resolved. The persistent inflammation promotes feedback processes that contribute to maintain this situation. Simultaneously, as the environment of the SCI remains unhealthy, glial populations also remain activated. This unremitting activation can last for months after the injury, and contribute to the maintenance and perpetuation of abnormalities occurring after the SCI, such as hyperexcitability and central sensitization, and eventually NP states (Watkins et al., 2001; Milligan and Watkins, 2009).

This abnormal activation and chronic inflammation should be somehow modulated with anti-inflammatory drugs. However, it is important to highlight that NP include also non inflammatory features that anti-inflammatory drugs can not really modulate. Therefore, the reality is that NP is still refractory to most analgesic treatments (Finnerup et al., 2007). It is important to note that neuroinflammation is needed in the healing process after the SCI, but it requires certain control. For this reason we designed two different treatments based on the modulation of the glial component of neuroinflammation.

On one hand, we chose glibenclamide as a powerful drug aimed to boost initial actions of microglia, considered as beneficial. The main hypothesis was that promoting a more effective removal of degenerating debris from the lesion would result in a better resolution of neuroinflammation, and a less detrimental secondary phase of injury. On the other hand, ibuprofen is widely used as an anti-inflammatory agent, and administered some time after the SCI it may act helping in the resolution of neuroinflammation. It is important to consider an initial time window in which inflammation is required, so acute treatments with anti-inflammatory drugs might be counterproductive. When considered independently, both drugs offered good results in mild contusion injuries.

Glibenclamide provided functional improvement, probably through a microglia mediated effect that implies a stronger phagocytic phenotype and a reduced infiltration in the cord parenchyma, contributing to less tissue damage. Our hypothesis seemed to be right, as an intraspinal injection of glibenclamide promoted sparing of tissue and myelinated axons. Functional recovery was also significantly improved. Electrophysiological data was not so conclusive but suggested a slight improvement in central conduction.

Regarding the ibuprofen treatment, if started just after the injury, it was detrimental in terms of central conduction and functional outcomes, probably because the treatment limited the initial inflammatory response, so the damage became more extended and the tissular preservation was hampered. However, the reduction in inflammation partially reduced the mechanical hyperalgesia detected in forelimbs and hindlimbs.

Thus, we achieved partial efficacy with these two treatments, but mainly restricted to pain or to functional recovery. The combination of both treatments implied the delay of the start of ibuprofen administration, in order to permit the initial effects of glibenclamide. Unfortunately, we found an unexpected convergence of effects in the phagocytic ability of microglia after the SCI, and the interference gave even worse results in some outcomes when compared to the individual treatments. Interactions between drugs apparently working on different mechanisms or pathways must be carefully assessed, as many indirect effects can play unexpected roles. This probably increases the difficulties that researchers face when designing new treatments and strategies to ameliorate NP.

Conclusions

Conclusions

Chapter 1:

- The animal model of spinal cord contusion is reproducible and implies the appearance and maintenance of neuropathic pain signs, such as mechanical and thermal hyperalgesia.

- Hyperalgesia develops to a similar extent independently of the severity of the spinal cord injury.

- Wind-up responses are enhanced after SCI, and may be used as a good indicator of the spinal excitability after a SCI.

Chapter 2:

- SCI causes functional deficits that correlate with the severity of the lesion.

- Quantitative methods to assess functional deficits and recovery are essential to assess the effectivity of new treatments and therapies.

- Automatized analysis of locomotion using video recordings in a running belt increase the objectivity in measurements of general coordination and locomotion, when compared to customary functional tests.

Chapter 3:

- Distant cord segments are also affected by the SCI, and greatly contribute to the development of NP features.

- Lumbar cord segments show a wide variety of plastic changes in several sites of the nociceptive pathway. These changes imply a general disinhibition state, despite the boost of some inhibitory elements.

- The hyperexcitability resulting from the unbalance between excitatory and inhibitory systems is reflected in hyperalgesia and hyperreflexia.

- Peripheral axons are fully preserved three months after a thoracic SCI, but with some minor alterations. These alterations are more frequent as the severity of the injury is increased.

Chapter 4:

- Glibenclamide produces an enhancement of phagocytic actions of microglia just after the SCI. One single dose promotes a long-lasting functional recovery accompanied by a more marked mechanical hyperalgesia.

- Daily treatment with ibuprofen attenuates the inflammatory processes in the injured spinal cord. It ameliorates neuropathic pain symptoms but does not provide any functional, electrophysiological and histological improvement.

- The combination of both drugs did not provide additional beneficial effects because glibenclamide and ibuprofen present contrary effects on a common target, the phagocytic activity of microglia.

References

Afifi AK, Bergman RA (2005) Neuroanatomía funcional 2nd ed. McGraw-Hill, ed. Mexico DF.

Agrawal G, Kerr C, Thakor N V, All AH (2010) Characterization of graded multicenter animal spinal cord injury study contusion spinal cord injury using somatosensory-evoked potentials. Spine 35:1122–7

Alstermark B, Isa T (2012) Circuits for skilled reaching and grasping. Annual review of neuroscience 35:559–78

Amemori T, Jendelová P, Růzicková K, Arboleda D, Syková E (2010) Co-transplantation of olfactory ensheathing glia and mesenchymal stromal cells does not have synergistic effects after spinal cord injury in the rat. Cytotherapy 12:212–25

Anderson C, Ashwell K, Collewijn H, Conta A, Harvey A, Heise C, Hodgetts S, Holstege G, Kayalioglu G, Keast J, McHanwell S, McLachlan E, Paxinos G, Plant G, Scremin O, Sidhu A, Stelzner D, Watson C (2009) The Spinal Cord 1st ed. C. Watson, G. Paxinos, & G. Kayalioglu, eds. Lonson: Elsevier.

Anseloni V (2003) Optimization of the mechanical nociceptive threshold testing with the Randall–Selitto assay. Journal of Neuroscience Methods 131:93–97

Baastrup C, Maersk-Moller CC, Nyengaard JR, Jensen TS, Finnerup NB (2010) Spinal-, brainstem- and cerebrally mediated responses at- and below-level of a spinal cord contusion in rats: Evaluation of pain-like behavior. Pain 151:670–679

Baranauskas G, Nistri a (1998) Sensitization of pain pathways in the spinal cord: cellular mechanisms. Progress in neurobiology 54:349–65

Basso DM (2004) Behavioral Testing After Spinal Cord Injury : Congruities, Complexities, and Controversies. Journal Of Neurotrauma 21:395–404

Basso DM, Beattie MS, Bresnahan JC (1995) A sensitive and reliable locomotor rating scale for open field testing in rats. Journal of neurotrauma 12:1–21

Basso DM, Beattie MS, Bresnahan JC (1996) Graded histological and locomotor outcomes after spinal cord contusion using the NYU weight-drop device versus transection. Experimental neurology 139:244–56

Beare JE, Morehouse JR, Devries WH, Enzmann GU, Burke DA, Magnuson DSK, Whittemore SR (2009) Gait Analysis in Normal and Spinal Contused Mice Using the TreadScan System. Journal of Neurotrauma 26:2045–56

Berman SA, Young RR, Sarkarati M, Sherfner J. (1996) Injury zone denervation in traumatic quadriplegia in humans. Muscle & Nerve 19:701–6

Cao Q, Zhang YP, Iannotti C, DeVries WH, Xu X-M, Shields CB, Whittemore SR (2005) Functional and electrophysiological changes after graded traumatic spinal cord injury in adult rat. Experimental neurology 191 Suppl :S3–S16

Carlton SM, Du J, Tan HY, Nesic O, Hargett GL, Bopp AC, Yamani A, Lin Q, Willis WD, Hulsebosch CE (2009) Peripheral and central sensitization in remote spinal cord regions contribute to central neuropathic pain after spinal cord injury. Pain 147:265–76

Cervero F (2006) Pain and the spinal cord. 81

Cervero F (2009) Spinal cord hyperexcitability and its role in pain and hyperalgesia. Experimental brain research 196:129–37

Clark AK, Yip PK, Malcangio M (2009) The liberation of fractalkine in the dorsal horn requires microglial cathepsin S. The Journal of neuroscience : the official journal of the Society for Neuroscience 29:6945–54

Clarke RW, Harris J (2004) The organization of motor responses to noxious stimuli. Brain research. Brain research reviews 46:163–72

Collazos-Castro JE, López-Dolado E, Nieto-Sampedro M (2006) Locomotor deficits and adaptive mechanisms after thoracic spinal cord contusion in the adult rat. Journal of neurotrauma 23:1–17

Costigan M, Scholz J, Woolf CJ (2009) Neuropathic pain: a maladaptive response of the nervous system to damage. Annual review of neuroscience 32:1–32

Costigan M, Woolf C. (2000) Pain: Molecular mechanisms*1. The Journal of Pain 1:35–44

Curt A, Hedel HJ a Van, Klaus D, Dietz V (2008) Recovery from a spinal cord injury: significance of compensation, neural plasticity, and repair. Journal of neurotrauma 25:677–85

David S, Kroner A (2011) Repertoire of microglial and macrophage responses after spinal cord injury. Nature reviews. Neuroscience 12:388–99

David S, Lacroix S (2003) Molecular approaches to spinal cord repair. Annual review of neuroscience 26:411–40

Deng L-X, Hu J, Liu N, Wang X, Smith GM, Wen X, Xu X-M (2011) GDNF modifies reactive astrogliosis allowing robust axonal regeneration through Schwann cell-seeded guidance channels after spinal cord injury. Experimental neurology 229:238–50

Densmore VS, Kalous A, Keast JR, Osborne PB (2010) Above-level mechanical hyperalgesia in rats develops after incomplete spinal cord injury but not after cord transection, and is reversed by amitriptyline, morphine and gabapentin. Pain 151:184–93

Detloff MR, Fisher LC, McGaughy V, Longbrake EE, Popovich PG, Basso DM (2008) Remote activation of microglia and pro-inflammatory cytokines predict the onset and severity of below-level neuropathic pain after spinal cord injury in rats. Experimental neurology 212:337–47

Dietz V (2011) Neuronal plasticity after a human spinal cord injury: Positive and negative effects. Experimental neurology 235:110–115

Ding Y, Kastin AJ, Weihong P (2005) Neural plasticity after spinal cord injury. Current Pharmaceutical Design 11:1381–6128

Edgerton VR, Courtine G, Gerasimenko YP, Lavrov I, Ichiyama RM, Fong AJ, Cai LL, Otoshi CK, Tillakaratne NJK, Burdick JW, Roy RR (2008) Training locomotor networks. Brain research reviews 57:241–54

Esposito E, Rinaldi B, Mazzon E, Donniacuo M, Impellizzeri D, Paterniti I, Capuano A, Bramanti P, Cuzzocrea S (2012) Anti-inflammatory effect of simvastatin in an experimental model of spinal cord trauma: involvement of PPAR-α. Journal of neuroinflammation 9:81

Ferguson AR, Hook M a, Garcia G, Bresnahan JC, Beattie MS, Grau JW (2004) A simple post hoc transformation that improves the metric properties of the BBB scale for rats with moderate to severe spinal cord injury. Journal of neurotrauma 21:1601–13

Finnerup NB, Sindrup SH, Jensen TS (2007) Chronic neuropathic pain: mechanisms, drug targets and measurement. Fundamental & clinical pharmacology 21:129–36

Finnerup NB, Sindrup SH, Jensen TS (2010)(a) The evidence for pharmacological treatment of neuropathic pain. Pain 150:573–81

Finnerup NB, Sindrup SH, Jensen TS (2010)(b) Recent advances in pharmacological treatment of neuropathic pain. F1000 medicine reports 2:52

Fitch MT, Silver J (2008) CNS injury, glial scars, and inflammation: Inhibitory extracellular matrices and regeneration failure. Experimental neurology 209:294–301

Fleming JC, Norenberg MD, Ramsay D a, Dekaban G a, Marcillo AE, Saenz AD, Pasquale-Styles M, Dietrich WD, Weaver LC (2006) The cellular inflammatory response in human spinal cords after injury. Brain : a journal of neurology 129:3249–69

Floyd J, Parmer R, Reier PJ (1998) Alteration in rate modulation of reflexes to lumbar motoneurons after midthoracic spinal cord injury in the rat. I. Contusion Injury. Journal of neurotrauma 15:495–508

Fouad K, Tetzlaff W (2011) Rehabilitative training and plasticity following spinal cord injury. Experimental neurology 235:91–99

Gao Y-J, Zhang L, Samad OA, Suter MR, Yasuhiko K, Xu Z-Z, Park J-Y, Lind A-L, Ma Q, Ji R-R (2009) JNK-induced MCP-1 production in spinal cord astrocytes contributes to central sensitization and neuropathic pain. The Journal of neuroscience : the official journal of the Society for Neuroscience 29:4096–108

García-Alías G, Barkhuysen S, Buckle M, Fawcett JW (2009) Chondroitinase ABC treatment opens a window of opportunity for task-specific rehabilitation. Nature neuroscience 12:1145–51

García-Alías G, Torres-Espín A, Vallejo C, Navarro X (2010) Functional involvement of the lumbar spinal cord after contusion to T8 spinal segment of the rat. Restorative neurology and neuroscience 28:781–92

García-Alías G, Valero-Cabré A, López-Vales R, Forés J, Verdú E, Navarro X (2006) Differential motor and electrophysiological outcome in rats with mid-thoracic or high lumbar incomplete spinal cord injuries. Brain research 1108:195–204

Ghasemlou N, Kerr BJ, David S (2005) Tissue displacement and impact force are important contributors to outcome after spinal cord contusion injury. Experimental neurology 196:9–17

Gozariu M, Bragard D, Willer JC, Bars D Le (1997) Temporal summation of C-fiber afferent inputs: competition between facilitatory and inhibitory effects on C-fiber reflex in the rat. Journal of neurophysiology 78:3165–79

Graeber MB, Christie MJ (2012) Multiple mechanisms of microglia: A gatekeeper's contribution to pain states. Experimental neurology 234:255–61

Gulino R, Dimartino M, Casabona A, Lombardo SA, Perciavalle V (2007) Synaptic plasticity modulates the spontaneous recovery of locomotion after spinal cord hemisection. Neuroscience research 57:148–56

Guízar-sahagún G, Velasco-hernández L, Martínez-cruz A, Castañeda-hernández G, Bravo G, Rojas G, Hong E (2004) Systemic Microcirculation after Complete High and Low Thoracic Spinal Cord Section in Rats. 21:1614–1623

Gwak YS, Hulsebosch CE (2009) Remote astrocytic and microglial activation modulates neuronal hyperexcitability and below-level neuropathic pain after spinal injury in rat. Neuroscience 161:895–903

Gwak YS, Kang J, Unabia GC, Hulsebosch CE (2012) Spatial and temporal activation of spinal glial cells: Role of gliopathy in central neuropathic pain following spinal cord injury in rats. Experimental neurology 234:362–72

Hains BC, Saab CY, Waxman SG (2005) Changes in electrophysiological properties and sodium channel Nav1.3 expression in thalamic neurons after spinal cord injury. Brain : a journal of neurology 128:2359–71

Hains BC, Waxman SG (2006) Activated microglia contribute to the maintenance of chronic pain after spinal cord injury. The Journal of neuroscience : the official journal of the Society for Neuroscience 26:4308–17

Hama A, Sagen J (2007) Behavioral characterization and effect of clinical drugs in a rat model of pain following spinal cord compression. Brain research 1185:117–28

Hamers FPT, Lankhorst AJ, Laar TJANVAN, Veldhuis WB, Gispen WH, Laar TJ van (2001) Automated quantitative gait analysis during overground locomotion in the rat: its application to spinal cord contusion and transection injuries. Journal of neurotrauma 18:187–201

Hargreaves K, Dubner R, Brown F, Flores C, Joris J (1988) A new and sensitive method for measuring thermal nociception in cutaneous hyperalgesia. Pain 32:77–88

Hasbargen T, Ahmed MM, Miranpuri G, Li L, Kahle KT, Resnick D, Sun D (2010) Role of NKCC1 and KCC2 in the development of chronic neuropathic pain following spinal cord injury. Annals of the New York Academy of Sciences 1198:168–72

Herrero JF, Laird JM, López-García J a (2000) Wind-up of spinal cord neurones and pain sensation: much ado about something? Progress in neurobiology 61:169–203

Herruzo- Cabrera R, García- Reneses J, Vizcaino-Alcaide M, Madero R, Gil-Miguel A, Rey-Calero J (1993) The descriptive and analytical epidemiology of traumatic spinal cord lesions occurring in Spain during 1984 and 1985. Rev Clin Esp 192:217–222

Hubli M, Dietz V, Bolliger M (2011) Spinal Reflex Activity: A Marker for Neuronal Functionality After Spinal Cord Injury. Neurorehabilitation and neural repair

Hulsebosch CE (2008) Gliopathy ensures persistent inflammation and chronic pain after spinal cord injury. Experimental neurology 214:6–9

Hulsebosch CE, Hains BC, Crown ED, Carlton SM (2009) Mechanisms of chronic central neuropathic pain after spinal cord injury. Brain research reviews 60:202–13

Iannotti C a., Clark M, Horn KP, Rooijen N van, Silver J, Steinmetz MP (2011) A combination immunomodulatory treatment promotes neuroprotection and locomotor recovery after contusion SCI. Experimental Neurology 230:3–15

Inoue K, Tsuda M (2009) Microglia and neuropathic pain. Glia 57:1469–79

Inoue K, Tsuda M (2012) Purinergic systems, neuropathic pain and the role of microglia. Experimental Neurology 234:293–301

Jain KK (2008) Current challenges and future prospects in management of neuropathic pain. Expert review of neurotherapeutics 8:1743–56

Ji R-R, Suter MR (2007) p38 MAPK, microglial signaling, and neuropathic pain. Molecular pain 3:33

Kalous A, Osborne PB, Keast JR (2009) Spinal cord compression injury in adult rats initiates changes in dorsal horn remodeling that may correlate with development of neuropathic pain. The Journal of comparative neurology 513:668–84

Karimi-Abdolrezaee S, Eftekharpour E, Wang J, Schut D, Fehlings MG (2010) Synergistic effects of transplanted adult neural stem/progenitor cells, chondroitinase, and growth factors promote functional repair and plasticity of the chronically injured spinal cord. The Journal of neuroscience : the official journal of the Society for Neuroscience 30:1657–76

Kerr CL, Letzen BS, Hill CM, Agrawal G, Thakor N V, Sterneckert JL, Gearhart JD, All AH (2010) Efficient differentiation of human embryonic stem cells into oligodendrocyte progenitors for application in a rat contusion model of spinal cord injury. The International journal of neuroscience 120:305–13

Kim J (2003) Cold and mechanical allodynia in both hindpaws and tail following thoracic spinal cord hemisection in rats: time courses and their correlates. Neuroscience Letters 343:200–204

Kim J, Back SK, Yoon YW, Hong SK, Na HS (2005) Dorsal column lesion reduces mechanical allodynia in the induction, but not the maintenance, phase in spinal hemisected rats. Neuroscience letters 379:218–22

Koerber HR, Mirnics K, Lawson JJ (2006) Synaptic plasticity in the adult spinal dorsal horn: the appearance of new functional connections following peripheral nerve regeneration. Experimental neurology 200:468–79

Kong X-Y, Wienecke J, Chen M, Hultborn H, Zhang M (2011) The time course of serotonin 2A receptor expression after spinal transection of rats: an immunohistochemical study. Neuroscience 177:114–26

Koopmans GC, Deumens R, Honig WMM, Hamers FPT, Steinbusch HWM, Joosten E a J (2005) The assessment of locomotor function in spinal cord injured rats: the importance of objective analysis of coordination. Journal of neurotrauma 22:214–25

Kuerzi J, Brown EH, Shum-Siu a, Siu a, Burke D, Morehouse J, Smith RR, Magnuson DSK (2010) Task-specificity vs. ceiling effect: step-training in shallow water after spinal cord injury. Experimental neurology 224:178–87

Lane M a (2011) Spinal respiratory motoneurons and interneurons. Respiratory physiology & neurobiology 179:3–13

Lichtenstein MP, Carriba P, Baltrons MA, Wojciak-Stothard B, Peterson JR, García A, Galea E (2010) Secretase-independent and RhoGTPase/PAK/ERK-dependent regulation of cytoskeleton dynamics in astrocytes by NSAIDs and derivatives. Journal of Alzheimer's disease : JAD 22:1135–55

Lin CS-Y, Macefield VG, Elam M, Wallin BG, Engel S, Kiernan MC (2007) Axonal changes in spinal cord injured patients distal to the site of injury. Brain : a journal of neurology 130:985–94

Lin S-Y, Chang W-J, Lin C-S, Huang C-Y, Wang H-F, Sun W-H (2011) Serotonin receptor 5-HT2B mediates serotonin-induced mechanical hyperalgesia. The Journal of neuroscience : the official journal of the Society for Neuroscience 31:1410–8

Lindia J a, McGowan E, Jochnowitz N, Abbadie C (2005) Induction of CX3CL1 expression in astrocytes and CX3CR1 in microglia in the spinal cord of a rat model of neuropathic pain. The journal of pain : official journal of the American Pain Society 6:434–8

Lonjon N, Kouyoumdjian P, Prieto M, Bauchet L, Haton H, Gaviria M, Privat A, Perrin FE (2010) Early functional outcomes and histological analysis after spinal cord compression injury in rats. Journal of neurosurgery. Spine 12:106–13

Ma W, Quirion R (2008) Does COX2-dependent PGE2 play a role in neuropathic pain? Neuroscience letters 437:165–9

Mackie M (2003) Distribution and colocalisation of glutamate decarboxylase isoforms in the rat spinal cord. Neuroscience 119:461–472

Majczyński H, Sławińska U (2007) Locomotor recovery after thoracic spinal cord lesions in cats, rats and humans. Acta neurobiologiae experimentalis 67:235–257

Marino R, Barros T, Biering-Sorensen F (2003) ASIA Neurological Standards Committee 2002. International standards for neurological classification of spinal cord injury. Journal of Spinal Cord Medicine 26:468–479

McMahon SB, Malcangio M (2009) Current challenges in glia-pain biology. Neuron 64:46–54

Meent H Van De, Hosman AJ, Hendriks J, Zwarts M, Schubert M (2010) Severe degeneration of peripheral motor axons after spinal cord injury: a European multicenter study in 345 patients. Neurorehabilitation and neural repair 24:657–65

Meisner JG, Marsh AD, Marsh DR (2010) Loss of GABAergic interneurons in laminae I-III of the spinal cord dorsal horn contributes to reduced GABAergic tone and neuropathic pain after spinal cord injury. Journal of neurotrauma 27:729–37

Melzack R, Wall PD (1965) Pain Mechanisms: A new theory. Science 150:971–979

Mendell L (1966) Physiological properties of unmyelinated fiber projection to the spinal cord. Exp Neurol 16:316–332

Michaelis LS (1970) The problem of pain in paraplegia and tetraplegia. Bulletin of the New York Academy of Medicine 46:88–96

Milligan ED, Watkins LR (2009) Pathological and protective roles of glia in chronic pain. Nature reviews. Neuroscience 10:23–36

Moalem G, Tracey DJ (2006) Immune and inflammatory mechanisms in neuropathic pain. Brain research reviews 51:240–64

Nogajski J., Engel S, Kiernan MC (2006) Focal and generalized peripheral nerve dysfunction in spinal cord-injured patients. Journal of Clinical Neurophysiology 23:273–9

Ossipov MH, Lai J, Malan TP, Porreca F (2000) Spinal and supraspinal mechanisms of neuropathic pain. Annals of the New York Academy of Sciences 909:12–24

Pezet S, McMahon SB (2006) Neurotrophins: mediators and modulators of pain. Annual review of neuroscience 29:507–38

Pinzón A, Marcillo A, Pabon D, Bramlett HM, Bunge MB, Dietrich WD (2008) A Re-assessment of Erythropoietin as a Neuroprotective Agent Following Rat Spinal Cord Compression or Contusion Injury. Experimental Neurology 213:129–136

Pirttimaki TM, Hall SD, Parri HR (2011) Sustained neuronal activity generated by glial plasticity. The Journal of neuroscience : the official journal of the Society for Neuroscience 31:7637–47

Pitcher MH, Cervero F (2010) Role of the NKCC1 co-transporter in sensitization of spinal nociceptive neurons. Pain 151:756–62

Popovich PG, Wei P, Stokes BT (1997) Cellular Inflammatory Response After Spinal Cord Injury in Sprague-Dawley and Lewis Rats. Journal of Comparative Neurology 464:443–464

Purves D, Augustine G, Hall W, LaMantia A-S, McNamara J, Mooney R, Platt M, Simon S, White L, SM W (2008) Neuroscience 4th ed. D. Purves, G. J. Augustine, D. Fitzpatrick, W. C. Hall, A.-S. La Mantia, & J. O. McNamara, eds. Sunderland, USA: Sinauer.

Raffa RB, Friderichs E, Reimann W, Shank RP, Codd EE, Vaught JL (1992) Opioid and nonopioid components independently contribute to the mechanism of action of tramadol, an "atypical" opioid analgesic. The Journal of pharmacology and experimental therapeutics 260:275–85

Randall L, Selitto J (1957) A method for measurement of analgesic activity on inflamed tissue. Arch Int Pharmacodyn ther 111:409–19

Rao SD, Yin HZ, Weiss JH (2003) Disruption of glial glutamate transport by reactive oxygen species produced in motor neurons. The Journal of neuroscience : the official journal of the Society for Neuroscience 23:2627–33

Redondo Castro E, Udina E, Verdú E, Navarro X (2011) Longitudinal study of wind-up responses after graded spinal cord injuries in the adult rat. Restorative neurology and neuroscience 29:115–26

Ronsyn M., Berneman Z., Tendeloo V. Van, Jorens P., Ponsaerts P (2008) Can cell therapy heal a spinal cord injury? Spinal Cord 46:532–539

Santos-Nogueira E, Redondo Castro E, Mancuso R, Navarro X (2011) Randall-Selitto Test: A New Approach for the Detection of Neuropathic Pain after Spinal Cord Injury. Journal of neurotrauma 29:898–904

Scholz J, Woolf CJ (2007) The neuropathic pain triad: neurons, immune cells and glia. Nature neuroscience 10:1361–8

Semler J, Wellmann K, Wirth F, Stein G, Angelova S, Ashrafi M, Schempf G, Ankerne J, Ozsoy O, Ozsoy U, Schönau E, Angelov DN, Irintchev A (2011) Objective measures of motor dysfunction after compression spinal cord injury in adult rats: correlations with locomotor rating scores. Journal of neurotrauma 28:1247–58

Siddall PJ, Finnerup NB (2006) Pain following spinal cord injury In F. Cervero & T. S. Jensen, eds. Handbook of clinical neurology Elsevier B.V.

Siddall PJ, Taylor D a, Cousins MJ (1997) Classification of pain following spinal cord injury. Spinal Cord 35:69–75

Simard JM, Chen M, Tarasov K, Bhatta S, Ivanova S, Melnitchenko L, Tsymbalyuk N, West G, Gerzanich V (2006) Newly expressed SUR1-regulated NC(Ca-ATP) channel mediates cerebral edema after ischemic stroke. Nature Medicine 12:433–440

Sindrup SH, Finnerup NB, Otto M, Jensen TS (2006) Principles of pharmacological treatment. 81

Solano R, Mazario J, Orellana JM, Herrero JF (2003) Male Wistar rats show uniform wind-up responses in carrageenan-induced inflammation but not in the normal situation. Laboratory animals 37:207–14

Soler MD, Sauri-Ruiz J, Curcoll-Gallemi ML, Benito-Penalva J, Opisso-Salleras E, Chamarro-Lusar A, Vidal-Samso J (2007) Characteristics of chronic neuropathic pain and their relationship with psychological well-being in spinal cord injury patients. Rev Neurol 44(1):3–9

Sprenger C, Bingel U, Büchel C (2011) Treating pain with pain: Supraspinal mechanisms of endogenous analgesia elicited by heterotopic noxious conditioning stimulation. Pain 152:428–39

Svendsen F (1999) Some problems with wind-up and its calculation. Pain 83:109–114

Swartz KR, Scheff NN, Roberts KN, Fee DB (2009) Exacerbation of spinal cord injury due to static compression occurring early after onset. Journal of neurosurgery. Spine 11:570–4

Tarlov IM, Klinger H (1954) Spinal cord compression studies. II. Time limits for recovery after acute compression in dogs. A M A archives of neurology and psychiatry 71:271–290

Tator, C.H., Fehlings MG (1991) Review of the secondary injury theory of acute spinal cord trauma with emphasis on vascular mechanisms. Journal of Neurosurgery 75:15–26

Thacker M, AK C, Bishop T, J G, Yip P, Moon L, Thompson S, Marchand F, McMahon S (2009) CCL2 is a key mediator of microglia activation in neuropathic pain states. Eur J Pain 13:263–72

Tillakaratne NJ, Mouria M, Ziv NB, Roy RR, Edgerton VR, Tobin a J (2000) Increased expression of glutamate decarboxylase (GAD(67)) in feline lumbar spinal cord after complete thoracic spinal cord transection. Journal of neuroscience research 60:219–30

Valero-Cabré A, Forés J, Navarro X (2004) Reorganization of reflex responses mediated by different afferent sensory fibers after spinal cord transection. Journal of neurophysiology 91:2838–48

Valero-Cabré A, Navarro X (2001) H reflex restitution and facilitation after different types of peripheral nerve injury and repair. Brain research 919:302–12

Vallejo R, Tilley DM, Vogel L, Benyamin R (2010) The role of glia and the immune system in the development and maintenance of neuropathic pain. Pain practice : the official journal of World Institute of Pain 10:167–84

Wagner R, Janjigian M, Myers RR (1998) Anti-inflammatory interleukin-10 therapy in CCI neuropathy decreases thermal hyperalgesia, macrophage recruitment, and endoneurial TNF-α expression. Pain 74:35–42

Watkins LR, Milligan ED, Maier SF (2001) Glial activation: a driving force for pathological pain. Trends in neurosciences 24:450–5

White F a, Bhangoo SK, Miller RJ (2005) Chemokines: integrators of pain and inflammation. Nature reviews. Drug discovery 4:834–44

Widerstrom-Noga EG, Felipe-Cuervo E, Yezierski RP (2001)(a) Relationships among clinical characteristics of chronic pain after spinal cord injury. Archives of Physical Medicine and Rehabilitation 82:1191–1197

Widerstrom-Noga EG, Felipe-Cuervo E, Yezierski RP (2001)(b) Chronic pain after spinal injury: Interference with sleep and daily activities. Archives of Physical Medicine and Rehabilitation 82:1571–1577

Wijk G van, Veldhuijzen DS (2010) Perspective on diffuse noxious inhibitory controls as a model of endogenous pain modulation in clinical pain syndromes. The journal of pain : official journal of the American Pain Society 11:408–19

Woolf CJ (1983) Evidence for a central component of post-injury pain hypersensitivity. Nature 306:686 – 688

Xia Y, Zhao T, Li J, Li L, Hu R, Hu S, Feng H, Lin J (2008) Antisense vimentin cDNA combined with chondroitinase ABC reduces glial scar and cystic cavity formation following spinal cord injury in rats. Biochemical and biophysical research communications 377:562–6

Yague JG, Foffani G, Aguilar J (2011) Cortical hyperexcitability in response to preserved spinothalamic inputs immediately after spinal cord hemisection. Experimental neurology 227:252–63

Yang L, Blumbergs PC, Jones NR, Manavis J, Sarvestani GT, Ghabriel MN (2004) Early Expression and Cellular Localization of Interleukin-6 , and Tumor Necrosis Factor- ⎵ in Human Traumatic Spinal Cord Injury. 29:966–971

Yazdani SO, Pedram M, Hafizi M, Kabiri M, Soleimani M, Dehghan M-M, Jahanzad I, Gheisari Y, Hashemi SM (2012) A comparison between neurally induced bone marrow derived mesenchymal stem cells and olfactory ensheathing glial cells to repair spinal cord injuries in rat. Tissue & cell 44:205–13

Yezierski RP (2005) Spinal cord injury: a model of central neuropathic pain. Neuro-Signals 14:182–93

Zhang H, Xie W, Xie Y (2005) Spinal cord injury triggers sensitization of wide dynamic range dorsal horn neurons in segments rostral to the injury. Brain research 1055:103–10

Zhang J, Koninck Y De (2006) Spatial and temporal relationship between monocyte chemoattractant protein-1 expression and spinal glial activation following peripheral nerve injury. Journal of neurochemistry 97:772–83

Zhang YP, Burke D a, Shields LBE, Chekmenev SY, Dincman T, Zhang Y, Zheng Y, Smith RR, Benton RL, DeVries WH, Hu X, Magnuson DSK, Whittemore SR, Shields CB (2008) Spinal cord contusion based on precise vertebral stabilization and tissue displacement measured by combined assessment to discriminate small functional differences. Journal of neurotrauma 25:1227–40

Zhao P, Waxman SG, Hains BC (2007) Modulation of thalamic nociceptive processing after spinal cord injury through remote activation of thalamic microglia by cysteine cysteine chemokine ligand 21. The Journal of neuroscience : the official journal of the Society for Neuroscience 27:8893–902

Zigmond M, Bloom F, Landis S, Roberts J, Squire L eds. (1999) Fundamental Neuroscience 1st ed. San Diego: Academic Press.

Abbreviations

AMPA: Α-Amino-3-Hydroxy-5-Methyl-4-Isoxazolepropionic Acid
BDNF: Brain Derived Neurotrophic Factor
CamkII: Calmoduline Kinase II
CBR: Cannabinoid Receptor
CMAP: Compound Muscle Action Potential
CNS: Central Nervous System
COX2: Cyclooxygenase 2
CRPS: Complex Regional Pain Syndrome
CST: Corticospinal Tract
DNIC: Difusse Noxious Inhibitory Control
Erk: Extracellular Signal-Regulated Kinases
GABA: γ-Aminobutyric Acid
RMN: Raphe Magnocellular Nucleus
GB: Glibenclamide
HCNS: Heterotopic Noxious Conditioning Stimulation
IASP: International Association for the Study of Pain
IBU: Ibuprofen
IHC: immunohistochemistry
KCC: K-Cl Cotransporter
LFB: Luxol Fast Blue
LPS: Lipopolysaccharide
LTP: Long Term Potentiation
MAPK: Mitogen-Activated Protein Kinases
MCP1: Monocyte Chemoatractant Protein-1
MEP: Motor Evoked Potential
bs-MEP: Brainstem Component of Motor Evoked Potential
c-MEP: Cortical Component of Motor Evoked Potential
NFKB: Nuclear Factor Kappa
NK1: Neurokinin 1
NKCC: Na-K-Cl Cotransporter
NMDA: *N*-Methyl-D-Aspartate
NP: Neuropathic Pain
PAG: Periaqueductal Gray Matter
PGE2: Prostaglandin E2
PKA: Protein Kinase A
PKC: Protein Kinase C
RT: Room Temperature
SCI: Spinal Cord Injury
SSEP: Somatosensory Evoked Potential
STT: Spinothalamic Tract
SUR: Sulfonylurea Receptor
TCA: Tricyclic Antidepressant
TLR4: Toll-Like Receptor 4
TNFα: Tumor Necrosis Factor α
WDR: Wide Dynamic Range